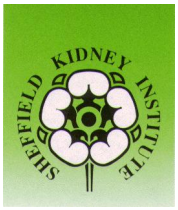

The mechanism of transglutaminase 2 externalisation in renal tubular epithelial cells

Chou, Che-Yi

Academic Nephrology Unit & Sheffield Kidney Institute, Faulty of Medicine and Dentistry, University of Sheffield

Student Registration number: 80116525

PhD Thesis

December 2011

Abstract

Transglutaminase type 2 (TG2) catalyses the formation of an ε-(γ-glutamyl)-lysine isopeptide bonds between adjacent peptides or proteins including those of the extracellular matrix (ECM). ECM crosslinking has been associated with both the acceleration of collagen deposition while conferring the ECM with resistance to proteolytic degradation. Subsequently the cellular secretion of TG2 has been associated with wound healing and aberrant wound healing leading to kidney, lung, liver and heart fibrosis as well as atherosclerosis. TG2 has no signal peptide and cannot be transported classically. It is unknown how TG2 is targeted to the cell surface and secreted into ECM. Understanding TG2 transport may help to develop specific mechanisms to interfere with TG2 action in the scarring process.

In this study, we identified that amino acids 88-106 in N-terminal β-sandwich domain of TG2 molecule is crucial for TG2 externalisation using deletion and mutation analysis in three renal tubular epithelial cells (TEC). Of interest, this TG2 export motif (aa88-106) itself appeared to be able to target other proteins for extracellular secretion. Yeast-two-hybrid studies were then performed to identify what the TG2 export motif would bind to and thus give clues as to the downstream mechanism of trafficking. Large T antigen (LTA) and tapasin were identified as binding partners. The interaction between LTA or tapasin and TG2 was confirmed by co-immunoprecipitation using endogenous protein from wild-type cells. TG2 externalisation was significantly decreased when LTA and tapasin were knockdown using siRNA suggesting that large T antigen and tapasin is involved in TG2 externalisation process.

The possible TG2 externalisation pathway was explored further using fluorescent imaging including co-localisation analysis and live cell imaging. TG2 was predominantly co-localised with endoplasmic reticulum (ER) around the cell nucleus, but not localised with Golgi apparatus and lysosomes. We observed plasma membrane blebbing in the cells transfected with wild-type TG2 but not in the cells transfected withTG2 carrying a mutation in the export motif. Plasma membrane blebbing or a direct molecular trap is the most likely mechanism for TG2 externalisation based on the data generated.

In conclusion, the amino acid sequence 88-106 in β-sandwich domain of TG2 is critical to TG2 externalisation in TEC. This export motif binds to large T antigen and tapasin. Large T antigen and tapasin is involved in TG2 externalisation possibly through plasma membrane blebbing or direct molecular trap in TEC.

Presentations and results from this study

Papers

1. Che-Yi Chou, Andrew J Streets, Philip F Watson, Linghong Huang, Elisabetta Verderio-Edwards & Timothy S. Johnson. A crucial sequence for transglutaminase type 2 extracellular trafficking in renal tubular epithelial cells lies in its N-terminal β-sandwich domain. J. Biol. Chem. 2011 jbc.M111.226340.
2. Che-Yi Chou, Andrew J Streets, Philip F Watson, Linghong Huang, Elisabetta Verderio-Edwards & Timothy S. Johnson. Two potential pathways for transglutaminase type 2 (TG2) extracellular trafficking in renal tubular epithelial cells. J. Biol. Chem (submitted)

Poster presentation

1. Che-Yi Chou, TS Johnson. A crucial sequence for tissue transglutaminase transport in its N-terminal β-sandwich domain. BRS/RA conference 2010
2. Che-Yi Chou, TS Johnson. A crucial sequence for tissue transglutaminase transport in its N-terminal β-sandwich domain. Gordon Research Conference 2010: Transglutaminases In Human Disease Processes
3. Che-Yi Chou, TS Johnson. The binding of large tumour antigen and transglutaminase 2 (TG2) is linked to TG2 externalisation in tubular epithelial. RA/BRS joint conference 2011, Birmingham.
4. Che-Yi Chou, TS Johnson. The binding of large tumour antigen and transglutaminase 2 (TG2) is linked to TG2 externalisation in tubular epithelial. The Medical School Research meeting 2011.

Oral presentation

1. Faculty of Medicine and Dentistry PhD 3rd year students presentation day 2011, Best presentation award
2. Che-Yi Chou, TS Johnson. Determining the extracellular trafficking pathway for transglutaminase type 2 (TG2). Yorkshire and Humber Renal Research Day 2010.
3. Che-Yi Chou, TS Johnson. A crucial sequence for tissue transglutaminase transport in its N-terminal β-sandwich domain. Department of Infection & Immunity Research Day 2009
4. Che-Yi Chou, TS Johnson. The mechanism of transglutaminase 2 externalisation in renal epithelial cells. Yorkshire and Humber Renal Research Day 2009.

ACKNOWLEDGEMENTS

Dr. Tim Johnson: For offering me the chance to undertake a PhD at the University of Sheffield; for allowing me to attend numerous national and international conferences and for his excellent supervision throughout the project and writing this thesis.

Dr. Elisabetta Verderio-Edwards. For providing one of the transglutaminase vectors used in this study and critical suggestions regarding the project.

Dr LingHong Huang. For helping me with the transglutaminase assays and laboratory work in general.

Dr. Andy Streets. For helping me with many aspects of molecular biology .

Dr. Philip Watson. For teaching me how to use pymol software that was so crucial for this project.

Dr Shuang Feng. For providing valuable suggestions regarding the yeast two hybrid work.

Professor Chiu-Ching Huang. For giving me the chance to study for a PhD in England and the application of financial support from China Medical University Hospital.

Miss Peiling Tsai. For her full support during my PhD and taking care of our children allowing me to focus on my project.

Abbreviations

ACBP	Acyl-coenzyme (Co) A binding protein
BCA	Bicinchoninic acid
BLAST	Basic local alignment search tool
BM	Basement membrane
BSA	Bovine serum albumin
CKD	Chronic kidney disease
CO-IP	Co-immunoprecipitation
DAPI	4’, 6 diamidino-2-Phenylindole
DMEM	Dulbecco's modified eagle medium
ECM	Extracellular matrix
EDTA	Ethylenediaminetetraacetic acid
ELISA	Enzyme-linked immunosorbent assay
EMT	Epithelial/endothelial mesenchymal transition
ER	Endoplasmic reticulum
eGFR	Estimated glomerular filtration rate
EGF	Epidermal growth factor
FGF	Fibroblast growth factor
FITC	Fluorescein isothiocyanate
HSPGs	Heparan sulphate proteoglycans
HRP	Extravidin horse radish peroxidase
IL	Interleukin
Ist2	Increased sodium tolerance protein 2
LAP	Latency associated peptide
LTBP	Latent TGF-β binding protein
LTA	Large tumour antigen
MMP	Matrix metalloproteinase
MPs	Microparticles
MVBs	Multivesicular bodies
MDCK II	Madin-Darby canine kidney strain II cells
NHANES	National health and nutritional examination survey
NRK52E	Normal rat kidney epithelial cells
OD	Optical density
OK	Opossum kidney epithelial cells
OFP	Orange fluorescent protein
PBS	Phosphate buffered saline
PFA	Paraformaldehyde

PMSF	Phenylmethylsulphonylfluoride
PSF	Point-spread function
PCR	Polymerase chain reaction
SNARE	Soluble NSF attachment protein receptor
SDS-PAGE	Sodium dodecyl sulfate polyacrylamide gel electrophoresis
RT-PCR	Reverse transcription polymerase chain reaction
TAP	Tapasin, TAP-associated glycoprotein, TAPBP, TAP transporter associated with antigen processing
TIMP	Tissue inhibitor of matrix metalloproteinases
TG2	Transglutaminase type 2 or tissue transglutaminase
TGF-β	Transforming growth factor-β
TEMED	N,N,N’,N’-tetramethylethylenediamine
TMB	3,3’,5,5’ tetramethyl benzidine
TRITC	Tetramethylrhodamine isothiocyanate
TRAP-γ	Translocon associated protein γ
TEC	Tubular epithelial cells
Y2H	Yeast two hybrid
YPDA	Yeast extract peptone dextrose adenine
USRDS	The United States renal data system
VEGF	Vascular endothelial growth factor
WB	Western blot
wt	Wild type

Table of Contents

Figures

Tables

Chapter 1

Introduction

1.1 Chronic Kidney Disease

Chronic kidney disease (CKD) is defined as functional or structural abnormalities of the kidney for at least 3 months (2002). Stage 1 is defined by an estimated glomerular filtration rate (eGFR) of >90 ml/min/1.73 m^2 and either >20 mg/dl of albumin in the urine, an albumin/creatinine ratio ≥30 mg/g, or other evidence of structural damage to the kidney. Stage 2 has a similar definition, but an eGFR of 60–89. Stages 3, 4, and 5 are defined solely by an eGFR of 30–59, 15–29, and less than 15, respectively (Table 1). The five-stage classification was developed through analysis of data from the National Health and Nutritional Examination Survey (NHANES), and is based on an eGFR (calculated from the serum creatinine level) and level of proteinuria.

Criteria

1. Kidney damage for ≥3 months, as defined by structural or functional abnormalities of the kidney, with or without decreased GFR, manifest by *either*:
   - Pathological abnormalities; or
   - Markers of kidney damage, including abnormalities in the composition of the blood or urine, or abnormalities in imaging tests
2. GFR <60 mL/min/1.73 m^2 for ≥3 months, with or without kidney damage

Stage	Description	GFR (mL/min/1.73 m^2)
1	Kidney damage with normal or ↑ GFR	≥90
2	Kidney damage with mild ↓ GFR	60–89
3	Moderate ↓ GFR	30–59
4	Severe ↓ GFR	15–29
5	Kidney failure	<15 (or dialysis)

Figure 1.1-1 Definition and stages of chronic kidney disease (CKD)

(Modified from KDOQI CKD guideline 2002)

End-stage renal disease (ESRD) or Stage 5 CKD has reached epidemic proportion with over 1 million individuals affected worldwide. The ESRD population is projected to reach 650,000 by 2010, but the rising ESRD population is just a small tip of the large CKD iceberg. For each patient with ESRD, there are more than 100 with various stages of CKD (reviewed in 2002). Based on the definitions of CKD, it is estimated that 13-16% of U.S. individuals

and 11.9% of the general population in Taiwan have CKD, however only half of the patients are aware of their kidney disease (Wen *et al.* 2008). According to the annual report of United States Renal Data System (USRDS), end-stage renal disease (ESRD) patients account for 0.16% of the population covered by health insurance in the USA, however, they consumed up to 6.9% of the total medical cost. The importance of CKD as a public health problem and an economic burden in every country can't be over emphasised (USRDS 2009).

In the previous century, infectious disease was the major cause of death and disability (Beaglehole *et al.* 2003). However, non-infectious diseases and non-communicable diseases such as diabetes, hypertension, metabolic syndrome, cardiovascular disease, and cancer have become the leading cause of death and morbidity during the 20th century (Beaglehole *et al.* 2003; Atkins 2005). The prevalence of diabetes is increasing worldwide and 30% of patients with diabetic nephropathy eventually enter ESRD. Diabetes has become the major cause of ESRD as a result of a global pandemic of type 2 diabetes (USRDS 2009). In general diabetes, hypertension, and glomerulonephritis accounts for 90% of individual with ESRD (USRDS 2009). Although the etiology of CKD varies, renal fibrosis is the final pathway for every types of CKD (Meguid El Nahas *et al.* 2005; Liu 2006).

1.1.1 Renal fibrosis and CKD

Stage V CKD or ESRD was defined as a GFR less than 15 ml/min/1.73m^2 when dialysis treatment or kidney transplantation is needed. Despite the large variations in the underlying diseases that cause ESRD, they all lead to an indistinguishable scared and fibrotic kidney (Klahr *et al.* 1988; Bohle *et al.* 1989; Strutz *et al.* 1995; Remuzzi *et al.* 1998). The fibrotic kidney or end-stage kidney is characterised by nephron loss, glomerulosclerosis, tubulointerstitial fibrosis, increased mesangial volume, expansion of extracellular matrix and capillary collapse (Melk *et al.* 2001; Hill *et al.* 2003). As the development of renal fibrosis is independent of the underlying diseases, this leads to speculation that there must be a common pathogenic pathway for renal fibrosis. More attractively, treatment targeted against renal fibrosis may stop the disease progression regardless of the underlying disease.

1.1.2 The mechanism of renal fibrosis

Renal fibrosis is characterised by glomerular and interstitial fibrosis that leads to an excessive accumulation of extra-cellular matrix (ECM) components, renal parenchyma destruction, and a decrease of functional nephrons. Renal interstitial fibrosis is considered the hallmark of progressive renal disease. The cellular events and signalling mediators in renal fibrosis are summarized in Figure 1.1-2. The cellular events include mesangial and fibroblast activation, tubular epithelial to mesenchymal transition, monocyte/macrophage & T-cell infiltration, and cell apoptosis (Liu 2004). Transforming growth factor-β (TGF-β) and its downstream Smad signalling play an essential role in kidney fibrosis (Hirschberg 2005; Liu 2006). TGF-β correlates with increasing renal fibrosis and the progress of kidney disease (Miyazaki *et al.* 1997; Spurgeon *et al.* 2005; van de Wetering *et al.* 2006). The inhibition of TGF-β may decrease renal fibrosis and preserve renal function (Petersen *et al.* 2008). Transfection of the TGF-β gene into rat glomeruli results in progressive glomerulosclerosis (Isaka *et al.* 1993) and mice transgenic to TGF-β develop spontaneous glomerulosclerosis (Kopp *et al.* 1996). Under the influence of TGF-β, renal tubular epithelial cells may transit into an embryonic phenotype. The process is called epithelial/endothelial mesenchymal transition (EMT). The tubular epithelial cells or glomerular endothelial cells acquire mesenchymal properties similar to those of fibroblasts and myofibroblasts (Fan *et al.* 1999; Lan 2003). Myofibroblast can also come from interstitial fibroblast or mesangial cells through TGF-β activation. Myofibroblasts synthesise large amounts of fibrillar collagens such as type I& III, but can also produce increased amounts of collagen IV, proteoglycans and fibronectin (Tomasek *et al.* 2002; Qi *et al.* 2006). The activated renal cells produce chemotactic cytokines, which guide inflammatory monocyte/macrophages and T cells to the injury site and result in infiltration of inflammatory cells.

Smad refers to a large family of proteins which also includes Smad transcriptional corepressors such as SnoN (Ski-related novel gene, non Alu-containing), Ski (Sloan-Kettering Institute proto-oncogene), and TGIF (TG-interacting factor). The Smad signalling pathway can protect tissue from unwanted TGF-β reaction (Yang *et al.* 2003). The Smad signalling pathway is a critical pathway for TGF-β and angiotensin II to induce tubular epithelial-myofibroblast transdifferentiation *in vitro* (Fan *et al.* 1999; Lan 2003).

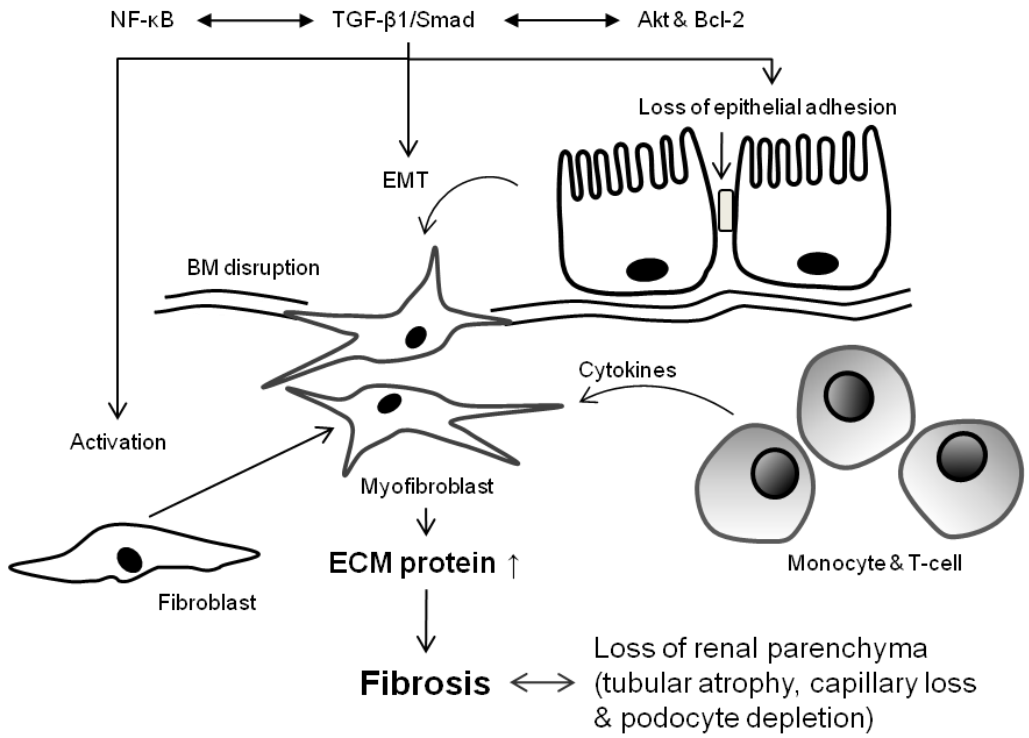

Figure 1.1-2 The major cellular events and key signalling mediators in renal fibrosis

Multiple cellular events and mediators interact in concert in renal fibrogenesis, often in a mutually stimulating manner. A stress on the cell results in the activation of TGF-β1/Smad activation that interacts with NF-κB and Akt & Bcl-2 signalling pathway. The activation of TGF-β1/Smad pathway initiates epithelial/endothelial-mesenchymal-transition (EMT) of epithelial cells into myofibroblasts. Loss of epithelial adhesion and interrupt of basement membrane (BM) are characteristics of EMT. Myofibroblast can be also transformed from in situ fibroblasts through the activation of cytokines released from monocyte & T-cell. These lead to the increase of extracellular matrix (ECM) protein accumulation/deposition and thus result in fibrosis formation. The final events of kidney fibrosis include loss of renal parenchyma tubular atrophy, loss of capillary and depletion of podocytes (Liu 2006).

1.1.3 Transforming growth factor-β (TGF-β) and TG2

TG2 plays a role in the activation of TGF-β. TGF-β also actives the PI3K-Akt pathway and thus increases TG2 expression in human subconjunctival fibroblasts (Jung *et al.* 2007). TGF-β can be activated through the crossslinking of TG2, large latent TGFb1 complex and ECM proteins (Figure 1.1-3). TGF-β is produced as dimeric precursors (Pro-TGF-β) and is intracellularly cleaved by furin into mature TGF-β (25 kDa)(Koli *et al.* 2001). The mature TGF-β is associated with latent associated peptide (LAP) to form the small latent complex that is biologically inactive. Latent TGF-β binding protein (LTBP) facilitates the extracellular secretion of the small latent TGF-β complex (Mangasser-Stephan *et al.* 1999) forming a large latent complex. One activation route for TGF-β is the crosslinking of the LTBP in this large latent complex into the extracellular matrix (ECM) by a TG2 dependent mechanism (Nunes *et al.* 1997). The large latent TGF-β complex is then cleaved by ECM proteinases such as plasminogen and the small latent TGF-β is released from the large latent complex (Godar *et al.* 1999). The small latent TGF-β then binds to Manossue 6 phosphate or IGF-II receptors on the cell surface where cell surface associated plasmin can cleave the LAP to release the active TGF-β1 dimer. The active TGF-β1 dimer binds to TGF receptors on cell surface and up regulates TGF-β synthesis that result in a positive feedback loop (Annes *et al.* 2003). These result in the activation of TGF-β and Smad pathway and thus initiate fibrogenic events including epithelial/endothelial-mesenchymal-transition, activation of myofibroblast, and an increase of ECM protein production as described in Section 1.1.2.

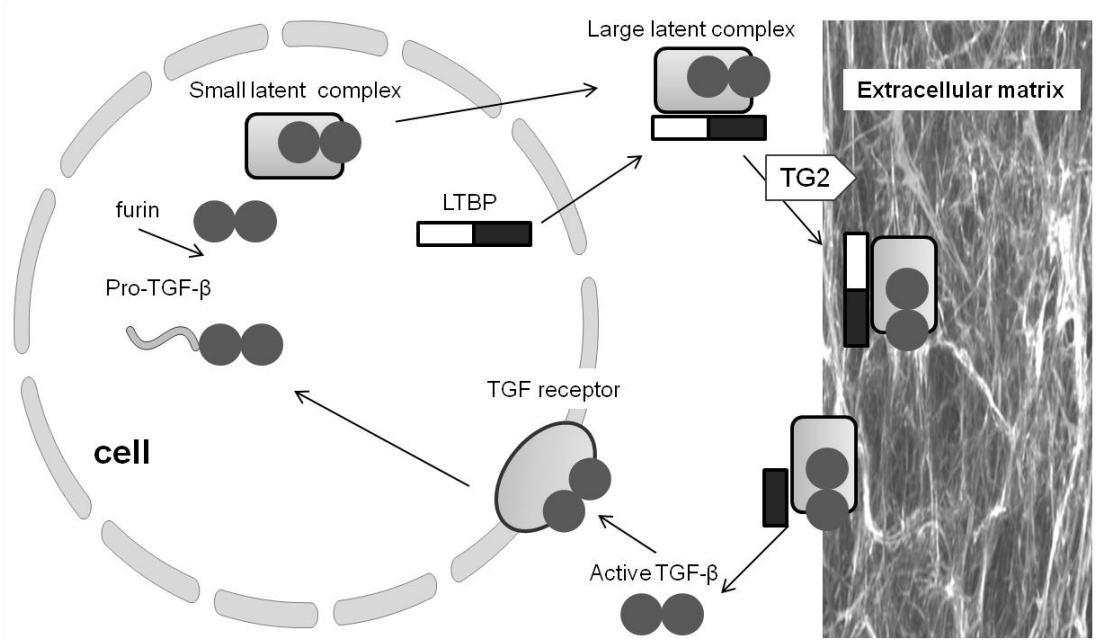

Figure 1.1-3 Extracellular processing of transforming growth factor beta (TGF-β)

TGF-β is produced as dimeric precursors (Pro-TGF-β) and is cleaved by furin into mature TGF-β (25 kDa). The mature TGF-β associates with latency associated peptide (LAP) to form the small latent complex that is biologically inactive. Latent TGF-β binding protein (LTBP) facilitates the extracellular secretion of small latent TGF-β complex forming the large latent complex. The large latent complexes crosslinked to the extracellular matrix (ECM) by TG2 dependent linkage of LTBP to fibronectin and other ECM proteins. The large latent TGF-β complex is cleaved by ECM proteinases to release the small latent complex. This is able to bind to mannose 6 phosphate and ILGF-2 receptors on the cell surface. One bound cell surface plasmin can cleave the LAP to release the active dimer. The active TGF-β binds to TGF receptor on cell surface. This not only up regulate TGF-β but also activate Smad pathway causing a range of fibrogenic responses such as epithelial/endothelial-mesenchymal-transition, increase the production of ECM proteins by fibroblasts (Gressner et al. 2002).

1.1.4 Mechanism for renal fibrosis - the role of extracellular matrix

In response to renal damage, kidney tissue generates a series of repair and recovery processes to accelerate recover. Glomerular or interstitial inflammatory cells are activated and produce inflammatory and fibrotic cytokines. Thereafter, the mesangial cells, fibroblasts, and tubular epithelial cells undergo phenotypic activation or transition that result in extra cellular matrix (ECM) accumulation (Liu 2006). ECM in normal tissues is balanced by matrix production and degradation. The excessive ECM accumulation in renal fibrosis is caused by over production of ECM proteins and decreased degradation of ECM proteins. Plasminogen/plasmin and matrix metalloproteinase systems are proteolytic enzymes that able to degrade ECM. Plasminogen activator inhibitors and tissue inhibitor of matrix metalloproteinases (TIMP) inhibit these proteolytic enzymes, therefore increasing ECM accumulation. Excess accumulation of ECM leads to fibrous scars, distortions of normal kidney tissue, and a decrease in viable nephrons. The outcome for glomerular and tubular injury is dependent on whether healing or scarring occurs. The resolution of inflammatory infiltrate, prevention of excess ECM formation, and the removal of deposited ECM favour recovery from damage (El Nahas 2005).

1.1.5 Renal fibrosis and tissue transglutaminase (TG2)

The accumulation of ECM is central to the development of glomerulosclerosis and tubulointerstitial fibrosis (El Nahas 2005). The association between TG2 and renal fibrosis is linked to its role in ECM accumulation. TG2 crosslinks ECM proteins such as fibronectin, fibrinogen/fibrin, von Willebrand factor, vitronectin, dermatane sulfate proteoglycans, collagen I, III, IV, V, osteonectin, laminin, nidogen and osteopontin in the ECM (Aeschlimann *et al.* 2000). TG2 crosslinking of the ECM renders it resistant to degradation by MMPs (Fisher *et al.* 2009). Further TG2 accelerates the rate of ECM deposition by providing a none conventional deposition and stabilisation route. Together this causes increased accumulation of ECM (Fisher *et al.* 2009).

In the rat 5/6 subtotal nephrectomy model of renal scarring, cells in areas showing fibrotic changes have higher TG2 activity while levels of TG2 and its

protein crosslink product, ε(γ-glutamyl) lysine, correlate with scar tissue formation suggesting the association between TG2 activity and the development of renal fibrosis (Johnson *et al.* 1997). The inhibition of TG2 activity decreased the ECM accumulation and preserved renal function (Johnson *et al.* 2007). In CKD patients, TG2 activity is robustly associated with the development of kidney fibrosis regardless of the underlying renal disease (Johnson *et al.* 2003). In the rat streptozotocin model of diabetic nephropathy, the development of diabetic nephropathy is associated with the activation of TG2 and the inhibition of TG2 decreases the ECM accumulation (Skill *et al.* 2001; Huang *et al.* 2009).

1.2 Transglutaminase

1.2.1 Transglutaminase family

Transglutaminases (TGs) were first found by Clarke et al in 1957 in guinea-pig liver (Sarkar *et al.* 1957). Ten years later, Pisano et al found a ε-(γ-glutamyl)lysine isopeptide bond in stable fibrin during blood clotting. This bond is characterized by an acyl transfer reaction between the γ-carboxamide group of peptide-bound glutamine and the ε-amino group of peptide-bound lysine (Pisano *et al.* 1968). The catalytic function of TGs is achieved through the cysteine active site to form an acyl-enzyme thioester intermediate with polypeptide-bound glutamine (Folk *et al.* 1977). As TGs have similar catalytic triad to papain, and papain-like cysteine protease, they are in the same structural classification in the protein database (Fesus *et al.* 2002). So far nine types of transglutaminase have been identified and the characteristics of them are shown in Table 2 (Lorand *et al.* 2003).

Blood-coagulation factor XIII is essential for blood coagulation and mutations of the encoding gene results in bleeding disorder (Haemophilia). TG1 is important in cell envelope formation in the differentiation of keratinocytes and erythrocyte membrane formation. The mutation of TG1 gene is linked to ichthyosis (Laiho *et al.* 1997) and inhibition of TG1 results in severe skin disease such as parakeratosis (Harrison *et al.* 2007). The TG3 has a similar function to TG1 in skin maturation and integrity. The prostate secretary TG4 is essential for fertility in rodents (Dubbink *et al.* 1998). TG5 is associated with cornified envelope in the keratinocyte (Aeschlimann *et al.* 1998; Candi *et al.* 2001). The physiological function for TG6 & 7 is unknown. Band 4.2 is an ATP-binding protein and may have a role in maintaining the shape of red blood cells. In

Table 1.2-1 Characteristics of Transglutaminases Family (Lorand et al. 2003)

Protein	Synonyms	MW	Tissue expression	Localisation	Function
Factor XIIIA	Fibrin-stabilizing factor, Laki-Lorand factor, Pro-fibrinoligase, plasma pro-TG	83	Platelets, astrocytes, dermal dendritic cells, chondrocytes, placenta, plasma, synovial fluid	Cytosolic, extracellular	Blood coagulation, bone growth
TG1	TG_K, kerationcyte TG, particulate TG	90	Keratinocytes, brain	Membrane, cytosolic	Cell-envelope formation
TG2	TG_C, tissue TG	80	Ubiquitous	Cytosolic, nuclear, membrane, cell surface, extracellular	Multiple
TG3	TG_E, epidermal TG, callus TG, hair follicle TG, bovine snout TG	77	Squamous epithelium, brain	Cytosolic	Cell-envelope formation
TG4	TG_P, prostate TG, vesiculase dorsal prostate protein 1 (DP1), major androgen-regulated prostate secretory protein	77	prostate	Unknown	Semen coagulation in rodents
TG5	TG_X	81	Ubiquitous except for the CNS and lymphatic system	Unknown	Unknown
TG6	TG_Y	Unknown	Unknown	Unknown	Unknown
TG7	TG_Z	81	Ubiquitous	Unknown	Unknown
Band 4.2	B4.2; ATP-binding erythrocyte membrane protein band 4.2	72	Red blood cells, bone marrow, fetal liver& spleen	Membrane	Membrane skeletal component

MW: molecule weight

comparison to other TGs, TG2 has a diverse range of functions.

1.2.2 Transglutaminase Type 2 / Tissue transglutaminase (TG2)

TG2 is a 76-kDa protein consisting of 686 amino acids and has peliotrophic function according to the location of cells. TG2 has four distinct domains (Figure 1.2-1): an N-terminal β-sandwich (with fibronectin and integrin binding sites), a catalytic core (containing the catalytic triad for the acyltransfer reaction and a conserved Trp277 essential for this catalytic activity (Murthy *et al.* 2002) and two C-terminal β-barrel domains (the second contains a phospholipase C binding sequence (Hwang *et al.* 1995). In cells with a relatively high intracellular calcium environment, TG2 can crosslink cellular proteins, modify proteins by amine incorporation, cause protein deamidation, and act as an isopeptidase (reviewed in Fesus *et al.* 2002). At the plasma membrane, TG2 can bind to and hydrolyse guanosine triphosphate (GTP) with an affinity similar to those of the α subunits of large heterodimeric G proteins and small Ras-type G proteins (Iismaa *et al.* 2000; Martinez-Salgado *et al.* 2008). TG2/Gh is involved in coupling the α1b- and α1d- beta adrenoreceptors, thromboxane, and oxytocin receptors to phospholipase C, thereby mediating inositol phosphate production in response to agonistic activation (Mehta *et al.* 2006). When TG2 binds to GTP/GDP, TG2 cannot catalyze protein cross-linking reactions, but calcium can reverse this inhibition and regulate the transamindation functions of the TG2

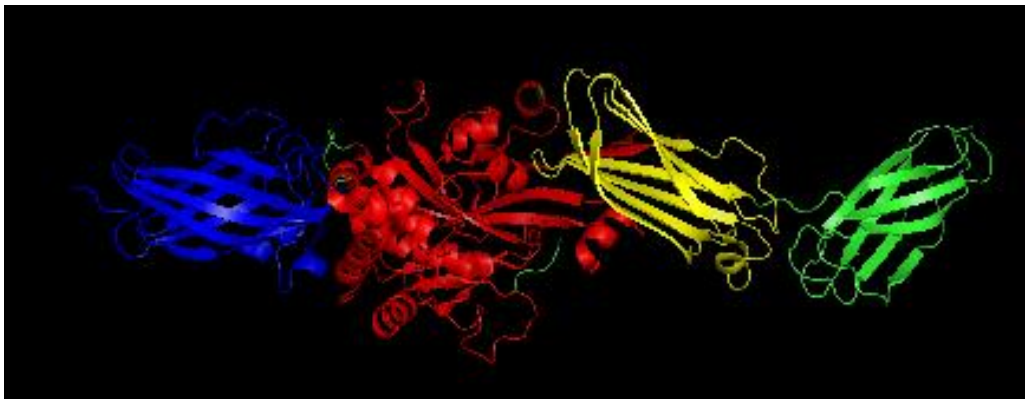

Figure 1.2-1 Three-dimensional structure of TG2 (PDB ID:2Q3Z)

The four structural domains are indicated by different colour: blue for the β-sandwich, red for catalytic core, yellow for β-barrel1 and green for β-barrel2 domain. TG2 is in its linear calcium activated shape (Pinkas et al. 2007).

(reviewed in Fesus *et al.* 2002). Such calcium-dependent activation of TG2 has been implicated in diverse biologic functions, such as differentiation, receptor-mediated endocytosis, cell adhesion, and induction of apoptosis (Mehta *et al.* 2006). Importin-3 may be an important transporter for the translocation of TG2 into the nucleus that is associated with cell apoptosis (Peng *et al.* 1999; Milakovic *et al.* 2004). As TG2 is majorly distributed in the cytosol fraction of the cells (Campisi *et al.* 2003; Shin *et al.* 2004) containing ribosomes and mitochondria, it is likely that TG2 is synthesised in the cytosolic free ribosomes of the cell. Glycosylation and disulfide bond are important process of post-translational protein modification for classical protein synthesised and transported through the Golgi/ER network. Although six potential glycosylation site were identified in TG2, TG2 is not glycosylated (Ikura *et al.* 1988). TG2 has a disulfide bond between two surface cysteine residues, C370 and C371, which causes the intervening peptide bond to assume a cis configuration of TG2 (Pinkas *et al.* 2007). TG2 can be inactivated by the formation of a intra-molecular disulfide bond that is not related to the active cysteine (Connellan *et al.* 1969; Chung *et al.* 1970) and can be related to a redox features of TG2 (Begg *et al.* 2006). As disulfide bond can be formed in free ribosomes (Yin *et al.* 2004) and blocking Golgi/ER network did not stop TG2 synthesis and externalisation (Zemskov *et al.* 2011), the intra-molecular disulfide bond of TG2 does not suggested that TG2 is synthesised in rough ER and modified in Golgi network. It is possible that TG2 is synthesised in cytosolic ribosomes and externalised through an non-classical protein transport pathway. The activation of TG2 required a high calcium and low GTP environment (Achyuthan *et al.* 1987), thus most of TG2 is inactive in the cells where the calcium is low and the GTP is high. TG2 became active in extracellular environment where the calcium is high and GTP is low. Extracellular TG2 is more likely to be associated with fibrosis formation in human disease.

1.2.3 TG2 externalisation and wound healing

The externalisation of TG2 in epithelial cells is essential for ECM stabilisation, cell adhesion, migration, and remodelling. The major characteristics of wound

healing are inflammation, tissue formation / stabilisation, and remodelling (Verderio *et al.* 2004). In a broad definition, organ repair after injury is a form of wound healing and kidney fibrosis is faulty wound healing. The migration of cells into open wounds is dependent on transglutaminase-mediated (factor XIIIa) cross-linked fibrin with incorporated plasma fibronectin (Hoffner *et al.*). Fibronectin acts as a provisional matrix for cell migration and cell adhesion by interaction of its epitopes with transmembrane receptors such as syndecan-4. Cells within the thrombus, predominantly activated platelets, release many wound healing mediators (such as platelet-derived growth factor, PDGF) leading to the activation of macrophages and fibroblasts (Nunes *et al.* 1997). Macrophages continuously play an important role in phagocytosis of microorganisms and remnants of the ECM as well as in the secretion of wound healing cytokines such as PDGF, vascular endothelial growth factor (VEGF) (Isaka *et al.* 1993), transforming growth factor (TGF-β) and basic and acidic fibroblast growth factor (FGF), which all mediate the transition between inflammation and tissue repair. Fibroblasts migrate into the wound area and synthesise new ECM replacing the provisional matrix with a collagen matrix (Verderio *et al.* 2004). Matrix metalloproteases (MMPs) and tissue inhibitors of matrix metalloproteases (TIMPs) are responsible for matrix remodelling and create a path for cell migration in wound healing (Stetler-Stevenson 1999).

As TG2 modulates cell-matrix interaction, ECM stability, and a variety of cell functions, TG2 also plays an important role in wound healing. Activation of TGs is directly associated with wound healing and angiogenesis (Bowness *et al.* 1988; Haroon *et al.* 1999) and the activation of the TG1 gene may facilitate skin repair (Inada *et al.* 2000). TG2 is able to bind fibronectin through a gelatin-binding domain (Turner *et al.* 1989; Jeong *et al.* 1995) and modify fibronectin matrix by calcium-dependent transamindation (Belkin *et al.* 2001; Gross *et al.* 2003). Many of TG2's roles in wound healing are related to its binding to fibronectin. Another important pathway that TG2 is involved in during wound healing is through the activation of cytokines such as TGFβ1 related to cell inflammation, repair, proliferation, matrix formation, and neovascularisation (reviewed in Verderio *et al.* 2004). The role of TG2 in human disease is associated with its externalisation.

1.2.4 TG2 externalisation and atherosclerosis

TG2 is expressed in endothelial cells, smooth muscle cells, fibroblasts and monocytes-macrophages (Thomazy *et al.* 1989). TG2 is increased in neointimal tissue of atherosclerotic coronary arteries with atherosclerosis progression. (Cho *et al.* 2008). Calcification lesions indicate the presence of atherosclerotic plaque and the calcification lesions are well co-localised with ε-(γ-glutamyl) lysine cross-link in the atherosclerotic lesion of the carotid artery (Matlung *et al.* 2009). This suggests that TG2 is directly involved in the formation of atherosclerotic plaque. TG2 is involved in several steps in the pathogenesis of atherosclerosis including the response of endothelial cells to disturbed blood flow, monocyte attachment, vascular remodeling and plaque stability. TG2 was up-regulated by turbulent shear stress in the coronary artery endothelial cells (Ohura *et al.* 2003). Cell surface TG2 associates with integrins and is important for monocyte adhesion (Akimov *et al.* 2000) and transmigration (Thomas-Ecker *et al.* 2007). An arteries exposure to TG2 results in arterial remodelling. The induced arteries remodelling can be blocked by TG2 inhibitor (Bakker *et al.* 2005). The cross-linking of extracellular proteins by TG2 is important for atherosclerotic plaque stability (Haroon *et al.* 2001). TG2 must be transported to extracellular space to play its key role in atherosclerosis.

1.2.5 TG2 externalisation and liver fibrosis

In liver fibrosis, TG2 accumulates in the cells adjacent to fibrotic tissue with most of the TG2 from dying cells released into ECM (Piacentini *et al.* 1999). TG2 cross-linking plays an important role in the accumulation of ECM in liver cirrhosis (Grenard *et al.* 2001). Resolution of fibrotic tissue is dependent on TG2 cross-linking, hepatic satellite cells and protein accumulation in the ECM (Issa *et al.* 2004). Cell surface TG2 binds to integrin and provides a high binding affinity to fibronectin (Akimov *et al.* 2000). The fibronectin-TG2 complex binds to collagen in the extracellular matrix and the crosslinking of ECM proteins by TG2 causes the ECM to become resistant to degradation by MMP (Johnson *et al.* 1999). The fibronectin-TG2 complex is also important to cell migration, adhesion, and growth (Verderio *et al.* 2004). The externalised TG2

activates cytokines such as TGF-β, interleukin-6, and tumour necrosis factor-α that further induces the expression of TG2 and further increases fibrosis formation (Fesus *et al.* 2002). The role of TG2 in liver cirrhosis (fibrosis) is closely related to extracellular TG2. Therapy specific to TG2 externalisation therefore can be a potential treatment for liver cirrhosis.

1.2.6 TG2 externalisation and Coeliac disease

TG2 on the surface of intestine mucosa cells plays an important role in the pathogenesis of Coeliac disease (Dieterich *et al.* 1997; Molberg *et al.* 1998). Coeliac disease is a malabsorbtion syndrome and characterised by small intestine villi atrophy due to ingestion of dietary glutens. Individuals with HLA DQ2 (majority) and DQ8 (minority) are predisposed to the development of Coeliac disease. TG2 is involved in generating T cell stimulatory gluten peptides through deamidation of specific glutamines. , TG2 catalyses the transamindation (crosslinking) or deamidation of specific glutamine residues in proteins or polypeptides (Figure 1.2-2). At lower pH and a higher concentration ratio of glutamine/polyamines, TG2 tends to deamidation rather than transamindation (Sollid 2002). TG2 is located mainly extracellularly in the subepithelial region and is also found in the brush border (Halstensen *et al.* 1993).

Coeliac disease patients on a gluten-containing diet produce immunoglobin A and G autoantibodies that are specific to TG2 binding gliadin. Gluten with resistance to luminal and brush-border enzymes is transported across the mucosal epithelium as polypeptides. Gluten peptides are deamidated by extracellular TG2 and recognised by CD4+ T cells in the lamina propria. The deamidated gluten peptides are presented to CD4+ T cells by HLA-DQ2 or -DQ8 molecules on the cell surface of antigen-presenting cells (Sollid 2002). The presence of immunoglobin A auto-antibodies against TG2 can be a screening and diagnostic tool for Coeliac disease in clinical practice (Dieterich *et al.* 1997). In cultured T cells from adult human Coeliac lesions, T cells predominantly recognise deamidated gliadin epitopes that are formed *in situ* by endogenous TG2 and inhibition of TG2 activity with cyst amine can reduce T-cell proliferative responses to deamidated gluten digests (Molberg *et al.*

2001). The TG2 inhibitor, 2-[(2-oxopropyl)thio]imidazolium inhibitor L682777, can prevent T-cell activation *in vitro* by keeping gluten peptides in the non-deamidated state (Maiuri *et al.* 2005) . So far the only clinical effective treatment for Coeliac disease is gluten-free diet. This is typically bland and not well accepted by patients. Treatments that target TG2 externalisation may decrease TG2 related deamidation of gluten and prevent the serious autoimmune response that leads to Coeliac disease.

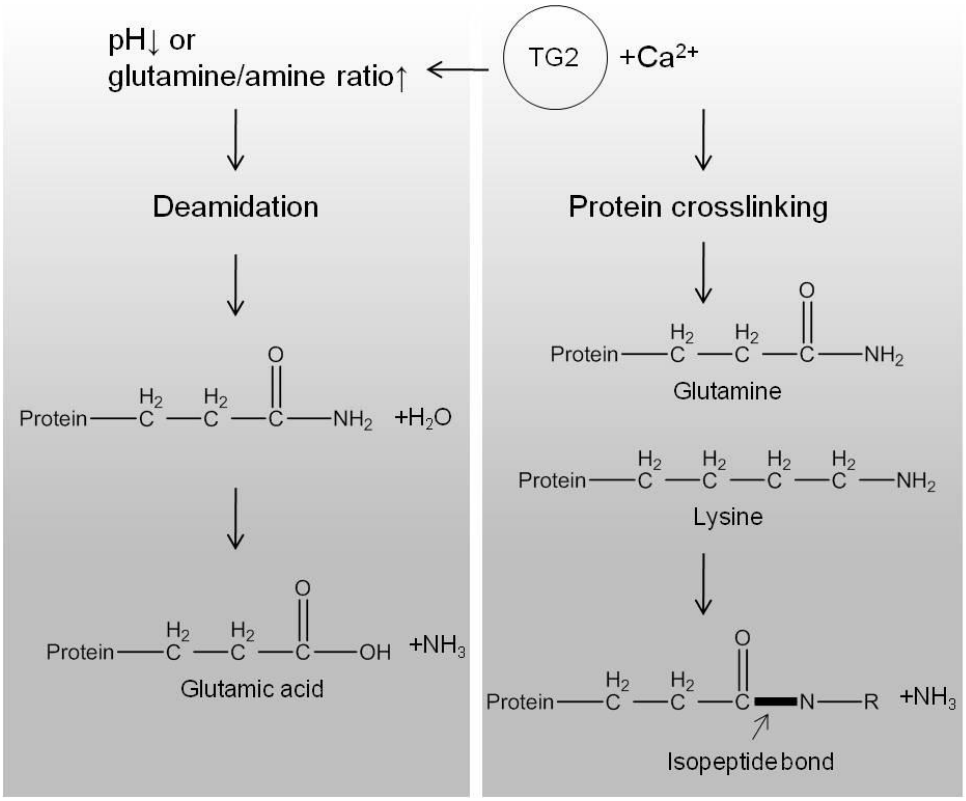

Figure 1.2-2 Enzymatic action of TG2 in Coeliac disease

TG2 catalyses the transamindation (crosslinking) or deamidation of specific glutamine residues in proteins or polypeptides. In lowering the pH and by increasing the concentration ratio of glutamine substrates to polyamines, the propensity for deamidation compared with transamindation is increased. (Sollid 2002)

1.2.7 TG2 externalisation and cancer

Cancer cells are characterised by an insensitivity to growth signals and evasion of apoptosis. These are critical for cancer cells to proliferate and infiltrate the surrounding tissue (Hanahan *et al.* 2000). Anti-cancer drugs such as adriamycin, actinomycin D, mithrimycin and bleomycin are the major treatment choices for cancer as these cytotoxic agents can induce apoptosis in cancer cells. Drug resistance is critical for cancer cells to survive during cytotoxic drug treatment and thus allow metastasise to distance sites. TG2 has been reported as a pro-apoptotic and anti-apoptotic protein (Melino *et al.* 1994; Boehm *et al.* 2002; Piacentini *et al.* 2002). The anti-apoptotic function of TG2 might be related to drug resistance of cancer cells. TG2 is linked to an increase of cytotoxic drug resistance in some types of cancer cells including ovarian cancer (Cao *et al.* 2008), melanoma (Fok *et al.* 2006), glioblastoma (Yuan *et al.* 2005) and pancreatic ductal adenocarcinoma (Verma *et al.* 2006). In breast cancer cells, increased TG2 is linked to an increase in drug resistance (Mehta 1994) with inhibition of TG2 reversing the drug resistance of breast cancer cells (Kim *et al.* 2006). Metastatic cancer cells can expressed high levels of TG2 (Fok *et al.* 2006; Verma *et al.* 2006) and thus TG2 can be a prognostic markers in some cancers. TG2's anti-apoptotic role can be explained by the activation of prosurvival signal transduction pathways mediated by Ras-ERK (Antonyak *et al.* 2003), phosphoinositide-3-kinase (PI3K/Akt) (Antonyak *et al.* 2002) and nuclear factor-kappa B (NF-κB) (Mann *et al.* 2006) through the binding of TG2 and integrin (Gaudry *et al.* 1999; Janiak *et al.* 2006; Song *et al.* 2007). Extracellular TG2 is critical for cell adhesion through the binding of integrin, fibronectin and syndecans (Jones *et al.* 1997; Verderio *et al.* 2003; Thomas-Ecker *et al.* 2007). TG2 related adhesion may also contribute to the anti-apoptotic role of TG2. Anoikis is a programmed cell death induced by cells detaching from the ECM. Expression of TG2 protects cells from anoikis by increasing cellular adhesion (Verderio *et al.* 2003). This suggests that TG2 externalisation may be important for the anti-apoptotic role of TG2. As some anticancer drugs contain amines such as adriamycin, and bleomycin can be substrates for TG2 (Russell *et al.* 1982), it is possible that extracellular TG2 consumes the anti-cancer drugs by crosslinking the drug

with ECM protein and thus decrease the anti-cancers potency.

However, other studies suggested that increasing TG2 expression is associated with an increase of apoptosis (TG2 as a pro-apoptotic protein) in some types of cell such as cervix adenocarcinoma, neuroblastoma cells (Piacentini *et al.* 1991) and hepatoma (Fukuda *et al.* 1994). The pro-apoptotic role of TG2 can be explained by the activation of Bax protein signalling pathway (Yoo *et al.* 2012). It was suspected that the pro-apoptotic role of TG2 may be dependent on the location of TG2 in the cell *i.e.* cytosolic TG2 (Fesus *et al.* 2005; Gundemir *et al.* 2009; Piacentini *et al.* 2011).

Angiogenesis is also an important step in the development of cancer as it prerequisite to vascularise the primary tumour and migration into blood which is the first step in metastasis. Angiogenesis involves vascular endothelial cell migration, proliferation, interaction with smooth muscle cells and fibroblasts (reviewed in Kotsakis *et al.* 2007). The increase of TG2 externalisation in fibrosarcomas stabilised the ECM and lead to inhibition of angiogenesis and tumour growth (Johnson *et al.* 1994; Jones *et al.* 2006). Targeting TG2 externalisation therefore might be a potential treatment for cancer metastasis.

1.2.8 TG2 externalisation and neurodegenerative disease

Neurodegenerative diseases including Alzheimer's disease, Parkinson's disease and Huntington's disease, are characterised by the accumulation and deposition of neurotoxic protein aggregates in the brain parenchyma or neurons. In Alzheimer's disease, the protein aggregates are composed of primarily amyloid-beta protein that deposits in the brain parenchyma as senile plaques. In Huntington’s disease, the accumulated protein aggregates as neurofibrillary tangles in neurons and is called cerebral amyloid angiopathy or tau protein (Selkoe 1991). In Parkinson's disease, the characteristic intracellular Lewy bodies and Lewy neurites are aggregates of α-synuclein protein aggregates (Polymeropoulos *et al.* 1997). In Huntington's disease, the aggregates of protein are huntingtin protein in the neuron (Leavitt *et al.* 2001).

TG2 externalisation seems particularly relevant to the formation of senile plaques in Alzheimer’s disease. Senile plaques and cerebrovascular amyloid angiopathy are pathological features of brain parenchyma for Alzheimer’s

disease. Both senile plaques and cerebrovascular amyloid angiopathy are formed by extracellular deposition of aggregated amyloid-beta (Selkoe 1991). Amyloid-beta protein is a 4 kDa proteolytic cleavage product (Glenner *et al.* 1984) of the amyloid-beta precursor protein. Amyloid-beta may play a role in neuronal outgrowth in normal brain; however, amyloid-beta interacts with itself, forms neurotoxic, insoluble aggregates in the brain parenchyma as senile plaques and accumulates in vessel wall as cerebrovascular amyloid angiopathy in Alzheimer's disease (Selkoe 1991; Selkoe 2000). Amyloid-beta is a good substrate for TG2 (Ho *et al.* 1994) and TG2 can catalyse the formation of amyloid-beta polymers (Dudek *et al.* 1994) in vitro. This suggests that TG2 may initiate the aggregation of amyloid-beta in Alzheimer's disease.

TG2 is linked to the development and pathology of Alzheimer's disease. TG2 level and TG2 activity are elevated in the brain cortex of individuals with Alzheimer's disease compared to normal individuals (Johnson *et al.* 1997). In the brain of patients with Alzheimer's disease, staining for TG2 and TG-catalyzed cross-links demonstrates co-localisation with amyloid-beta in senile plaques and cerebrovascular amyloid angiopathy lesions (Zhang *et al.* 1998; Wilhelmus *et al.* 2009). In an *in vitro* cell model of Alzheimer's disease, amyloid-beta toxicity towards neuroblastoma cells was reduced by inhibiting TG2 activity using TG inhibitor monodansyl cadaverine (Wakshlag *et al.* 2006). Taken together, inhibition of TG2 externalisation may provide a novel therapeutic target for Alzheimer's disease.

1.2.9 TG2 externalisation pathway

Inhibition of TG2 activity could be a novel treatment in fibrosis. The major disadvantage of existing chemical TG inhibitors is the lack of specificity for TG2 that has limited the clinical usefulness of these compounds (Siegel *et al.* 2007). Nine transglutaminases have identified so far. Chemicals that inhibit TG2 also inhibit other transglutaminase such as Factor XIII and TG1. Inhibition of factor XIII leads to a tendency to bleed and haemophilia like syndrome (Nijenhuis *et al.* 2004; Ishida *et al.* 2010). Inhibition of TG1 may result in parakeratosis and skin disease (Harrison *et al.* 2007). The activity of all TGs relies on the core domain. TGs have a 70-80% similarity across the

transglutaminase family (Grenard *et al.* 2001) and as such small molecule inhibitors that specifically target 1 family member may be impossible to find.

TG2 is a protein without a leader sequence (Grundmann *et al.* 1986; Ichinose *et al.* 1986). Other proteins without a leader sequence, however, still can be secreted to extracellular space include interleukin-1β, fibroblast growth factor (FGF-2), etc (Nickel *et al.* 2008). As mentioned above, the development of specific inhibitors for TG2 is difficult because of the sequence similarity between transglutaminases in the catalytic core region. Therefore, another possible way to interfere with TG2 activity in fibrosis may be to prevent TG2 externalisation by interfering with its extracellular trafficking mechanism. However, the mechanism of TG2 externalisation is unknown. Understanding of TG2 externalisation pathway is the first step for any treatment that targets TG2 externalisation.

1.3 Protein synthesis and targeting

Proteins are organic molecules made of amino acids in a linear chain joined by peptide bonds (Lodish 2007). The default pathway for proteins without any sorting sequence is staying in the cytosol and waiting for a targeting signal. For proteins with a leader sequence such as MMSFVSL in the N terminal domain, the default pathway is through ER, Golgi, plasma membrane, and extracellular environment (Berg 2002) (Figure 1.3-1). The leader sequence is removed from the mature proteins in the ER lumen (Rothman 1994). Vesicles formed on the surface of rough ER carry these proteins, bud off from the rough ER, and enter the Golgi complex where protein glycosylation and phosphylation is completed. Specific vesicles carry proteins and bud off the Golgi complex forming lysosomes, peroxisomes, or travel to the plasma membrane secreting into extracellular space (Pfeffer *et al.* 1987). TG2 has no leader sequence and cannot be transported classically through this route (Grundmann *et al.* 1986; Ichinose *et al.* 1986).

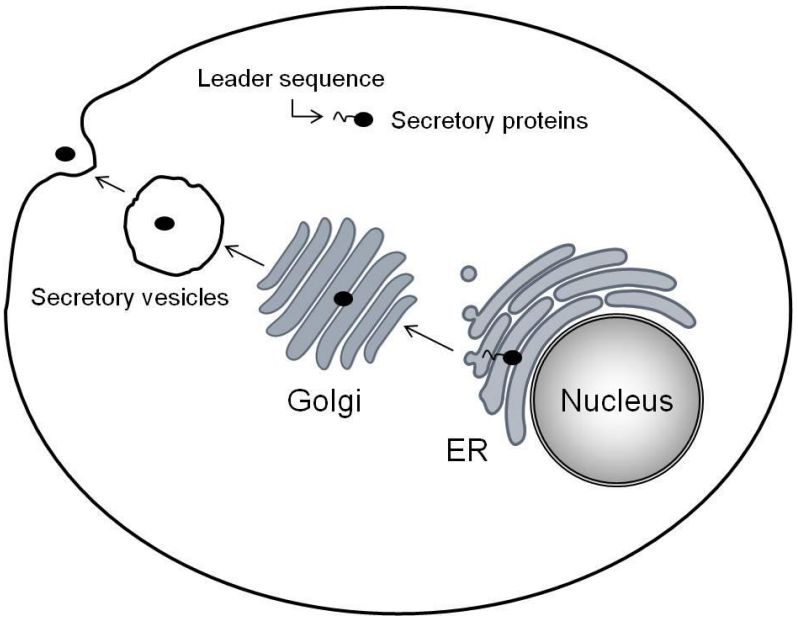

Figure 1.3-1 Traditional protein cell externalisation through endoplasmic reticulum (ER) and Golgi apparatus

Proteins with a leader sequence that target extracellular environment are synthesised at ribosomes on the endoplasmic reticulum (ER) membrane. The secretory protein enters the ER lumen due to leader sequence targeting. The leader sequence is then removed & the secretory protein matured before entering the Golgi apparatus where protein modifications such as glycosylation and phosphorylation are completed. The secretory protein is transported into secretory vesicles and the proteins are released to extracellular space following the fusion of secretory vesicles and plasma membrane.

1.3.1 Non-traditional protein transport pathways

Initially, it was thought that cells released unconventional secretary proteins following exposure to either stress or mechanical injury only (reviewed in McNeil *et al.* 1989). However, later studies clearly showed that unconventional protein secretion occurs not only during inflammation and angiogenesis but is a temperature-sensitive and energy-consuming process (Hughes 1999; Nickel 2003). Interleukin-1β was one of the first identified extracellular proteins that did not contain a leading signal peptide (Rubartelli *et al.* 1990), although it is ultimately secreted via a lysosome route.

Blocking the ER/Golgi-dependent secretary pathway does not inhibit secretion of unconventional secretary proteins (Nickel 2003; Nickel *et al.* 2008). Four possible mechanisms for unconventional secretory pathways have been proposed (Figure 1.3-2) (Nickel 2005). 1. Lysosomes secretion, 2. Exosomes secretion, 3. Plasma membrane blebbing, and 4. Direct molecular trap.

In terms of cell morphology, the first two pathways may also involve a vesicle formation in the protein externalisation process. Some of the extensively studied unconventional secretory proteins such as interleukin-1β (IL-1β) and fibroblast growth factor 2 (FGF-2) can be involved in more than one secretory pathways based on the organelles involved in extracellular trafficking.

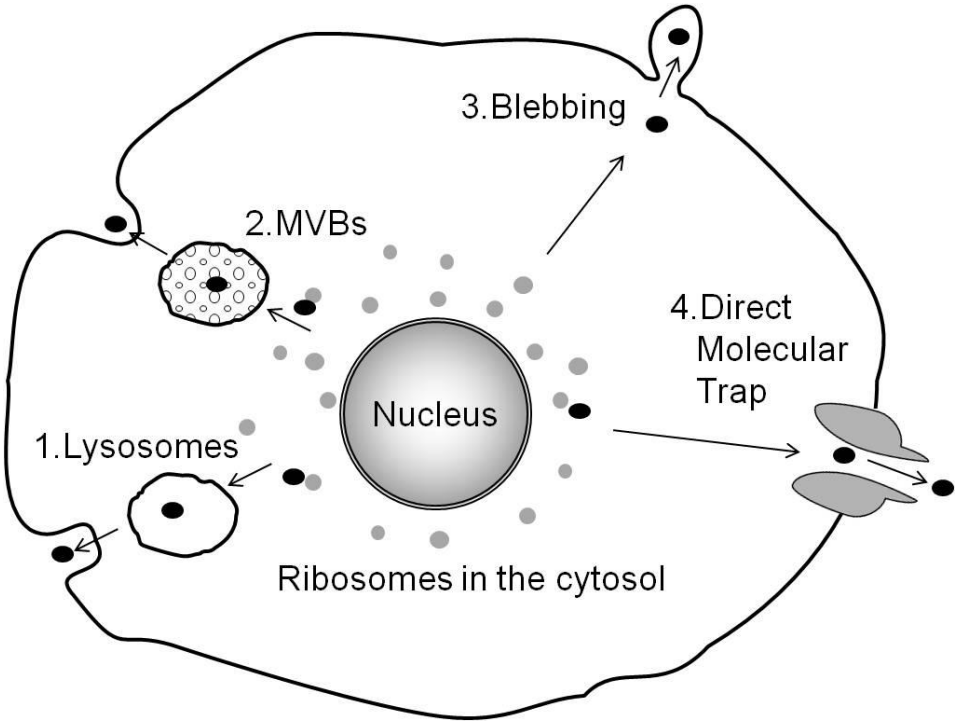

Figure 1.3-2 Possible unconventional protein secretary processes

Proteins were synthesised by the ribosomes in the cytosol and externalised through 1) Lysosomes 2) Multivesicular bodies (MVBs). MVBs (also known as late endosomes) are part of endocytic membrane transport pathway in which early endosomes matured into late endosomes. The membrane of MVBs comes from plasma membrane or endoplasmic reticulum during endocytosis. MVBs and endosomes can direct fuse with plasma membrane and release the secretary protein into extracellular space. 3) Plasma membrane blebbing. Proteins are transported to and associate with the plasma membrane. The plasma membrane then protrudes outside of the cell and proteins are secreted when the protruding plasma membrane where by it separates from the cell. 4) Direct molecular trap by plasma membrane-resident transporters. Plasma membrane-resident transporters may "grip" the secretory proteins and move it through the membrane either by a conformational change in the transporter. (Nickel 2005)

1.3.1.1 Lysosomes secretion

The major function for conventional lysosomes is degradation of proteins. The unconventional secretory lysosomes are similar to conventional lysosomes in that they are acidic and contain degradative proteins that degrade other proteins (Blott *et al.* 2002). Secretory lysosomes can directly fuse with plasma membrane and release the containing protein into the ECM such as the secretory lysosomes from cytotoxic T lymphocytes and melanosomes of melanocytes (Stinchcombe *et al.* 2004). This process can be involved in traditional protein secretion and unconventional protein secretion such as interleukin-1β (IL-1 β). IL-1 β is one of the most well-known secretory protein without a leader sequence and has been suggested it can be externalised both through lysosomes (Rubartelli *et al.* 1990; Andrei *et al.* 1999) and plasma membrane blebbing (MacKenzie *et al.* 2001). The IL-1β positive vesicles in the cytoplasm are positive for cathepsin D (a classical marker for late endosomes) and Lamp-1 (a classical marker for lysosomes) (Andrei *et al.* 1999). IL-1β has no signal sequences and is modified by adding a mannose 6-phosphate moiety during biosynthesis in the trans-Golgi network (Andrei *et al.* 2004). The mannose 6-phosphate moiety is recognized by mannose 6-phosphate receptor on lysosomes and imports proteins into secretary lysosomes. The mannose 6-phosphate receptors cycle between Golgi apparatus and lysosomes (Seelenmeyer *et al.* 2008). Mannose 6-phosphate receptor on lysosomes therefore can continuously import IL-1β from the trans-Golgi network.

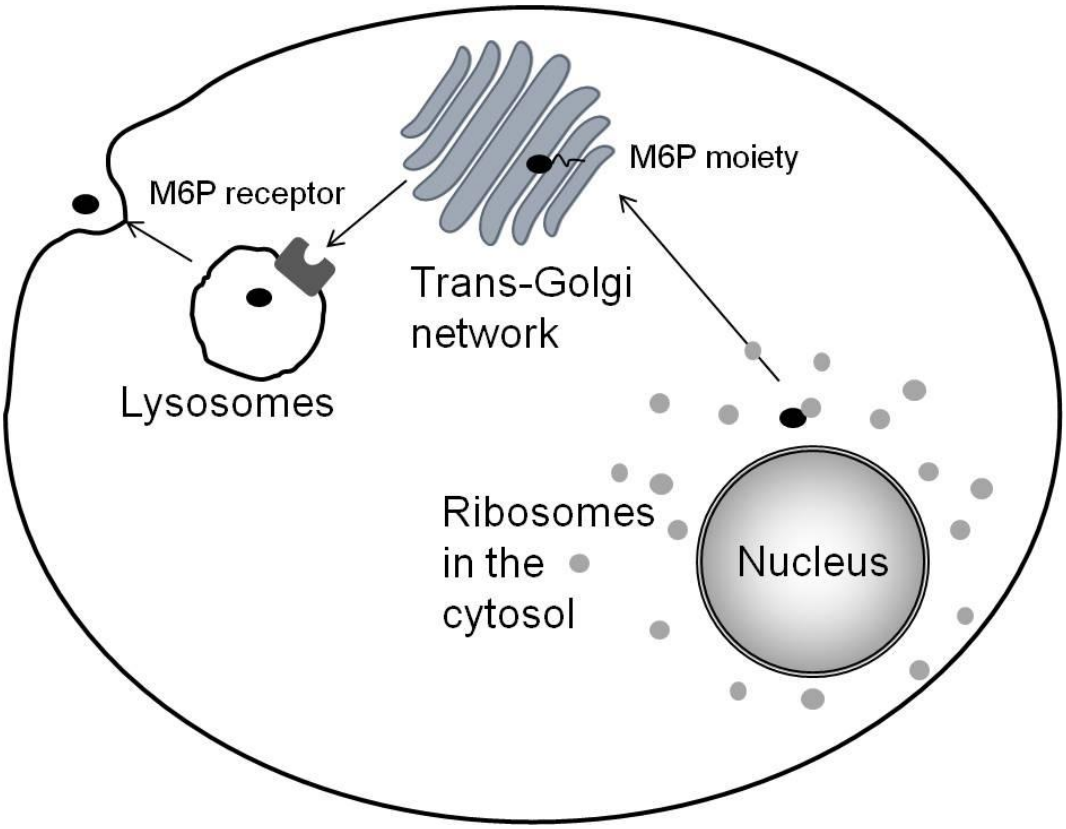

Figure 1.3-3 Lysosomes secretion of interleukin 1 beta (IL-1β)

After being synthesised at the ribosome, IL-1β enters trans-Golgi network where mannose 6-phosphate moiety (M6P moiety) is added. M6P moiety binds to mannose 6-phosphate receptor (M6P receptor) on the lysosomes membrane. IL-1β therefore enters lysosomes and secreted to extracellular space after lysosomes fuse with the plasma membrane.

1.3.1.2 Exosomes secretion

Exosomes derived from cortical ER

Exosomes are released from the cell by fusion with the plasma membrane allowing the secretion protein within the exosome to be released into the extracellular space. Examples of proteins secreted through this mechanism include increased sodium tolerance protein 2 (Ist2) (Aronov *et al.* 2007) and Galectin-3 (Brian Henderson 2005). Ist2 can be directly transported from cortical ER to plasma membrane through an exosome that is formed by the membrane of cortical ER or a direction fusion of ER membrane and plasma membrane (McNew *et al.* 2000). The cortical ER is different from the rough ER where synthesis of proteins occurs. It is located in the peripheral area of the

cytosol. Ist2 is synthesised by ribosomes in the cytosol and then recruited by the COPI coat on the cortical ER membrane which will subsequently bud vesicles from the cortical ER (Bednarek *et al.* 1995). The ER-located v-SNARE and plasma membrane coated t-SNARE (McNew *et al.* 2000) mediate the fusion of cortical ER membrane and plasma membrane.

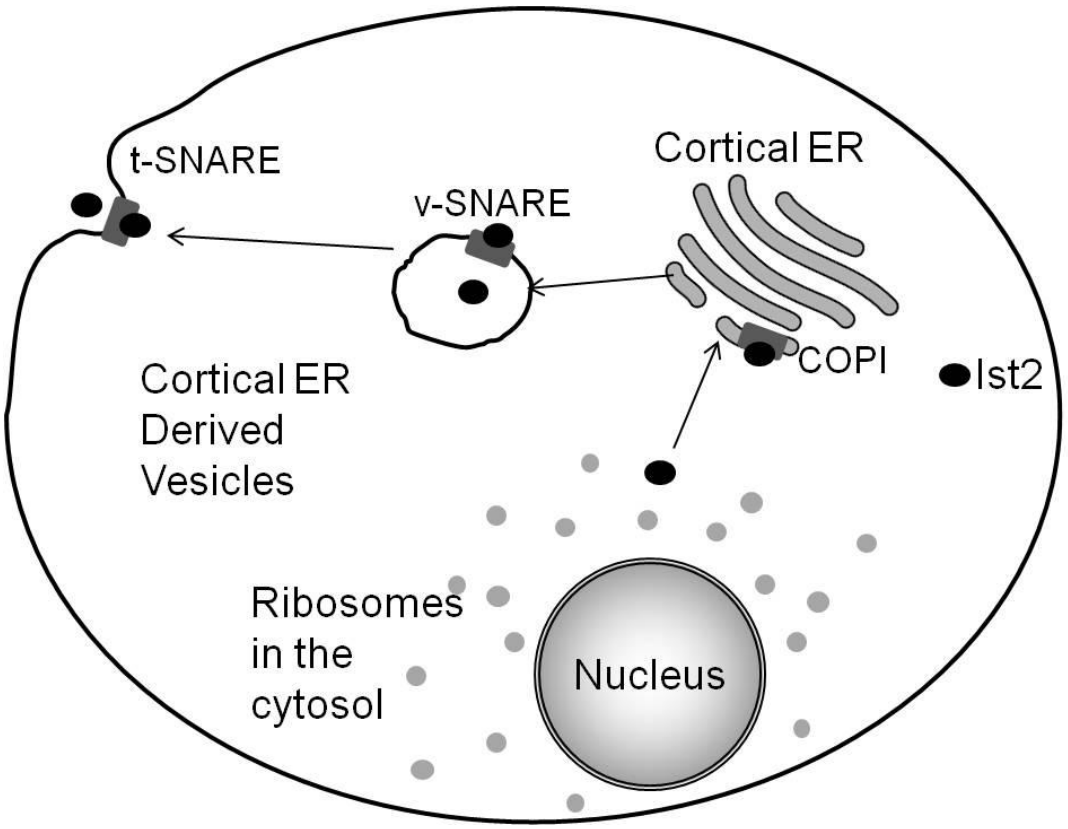

Figure 1.3-4 Exosomes derived from cortical ER

After being synthesised in ribosomes, Ist2 is recruited by COPI on cortical ER membrane. The cortical ER membrane budding forms an Ist2 containing exosome. The exosome fuses with plasma membrane through v-SNARE on exosome membrane and t-SNARE on plasma membrane. Ist2 is therefore released in extracellular space.(Nickel et al. 2008)

Exosomes derived from multivesicular bodies (MVBs)

MVBs are involved in cell autophagy; a cellular self-eating process in a basal and an activated state induced by starvation. Traditionally, autophagy is associated with packaging damaged cell components into double-membrane vesicles (autophagosomes) and the contents of autophagosomes are

degraded by fusion with lysosomes. Recent research has suggested a novel role of autophagy in unconventional protein secretion by extracellular delivery (reviewed in Manjithaya *et al.* 2010). Acyl-coenzyme (Co) A binding protein (ACBP) is an example for protein secreted through autophagy (Duran *et al.* 2010). ACBP enters autophagosome after being synthesised at ribosomes in the cytosol and the ACBP enters MVBs after autophagosomes fuse with MVBs (Figure 1.3-5). ACBP is secreted into extracellular space following MVBs fusion with the plasma membrane. The same process can be involved in endocytosis which is a process where cells absorb molecules such as protein. In endocytosis, the absorbed protein was uptaken by the plasma membrane and form endosomes that are intracellular vesicles containing the absorbed protein. Endosomes can be divided into early and late endosomes in the process of endocytosis. Endosomes are fused with lysosomes normally in the process of endocytosis. Late endosomes are also known as MVBs and the secretory proteins in MVBs can be secreted extracellularly while the MVBs fuse with the plasma membrane (Russell *et al.* 2006).

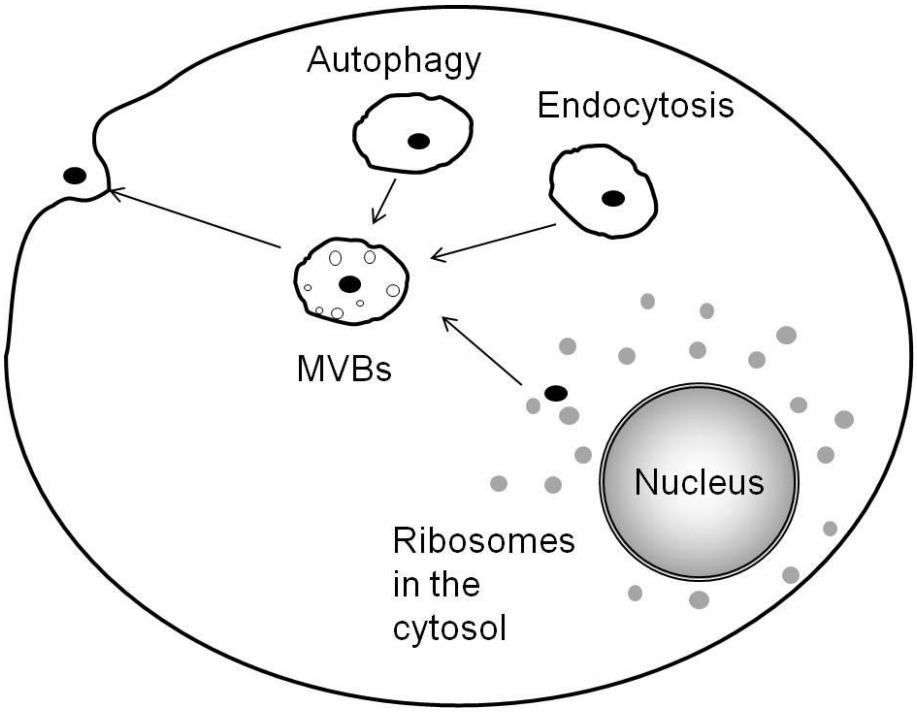

Figure 1.3-5 Exosomes derived from multivesicular bodies (MVBs) or endosomes

Exosomes can be derived from MVBs in autophagy. The secretory protein enters or is packed by autophagosome. The autophagosome fuses with MVBs and forms exosomes. The exosomes fuse with plasma membrane and released the secretory protein in to the extracellular space.

Exosomes can also be derived from endosomes that is part of endocytosis. The protein is taken up by endosomes which mature into early endosomes. The early endosomes subsequently develop into late endosomes that also known as MVBs.

1.3.1.3 Plasma membrane blebbing

A bleb is an irregular bulge of plasma membrane on the cell surface. The formation of a bleb is caused by localised decoupling of the cytoskeleton from the plasma membrane (Charras *et al.* 2008). Plasma membrane blebbing is a result of an imbalance between the inner leaflet and outer leaflet of membrane phospholipids (Sims *et al.* 2001). Blebbing and subsequent shedding can occur in all cell types under stress conditions or apoptosis (Freyssinet 2003; Martinez *et al.* 2005). During apoptosis the cells cytoskeleton breaks up which results in the plasma membrane bulging upward (Charras *et al.* 2006).

It has been suggested that Galectin-3 and FGF-2 can be externalised through plasma membrane blebbing. Galectin-3 aggregates underneath the plasma membrane (Figure 1.3-6) using an N-terminal acylation motif and is released by membrane blebbing (Mehul *et al.* 1997). FGF-2 can also be released from cells through microparticles that are vesicles released from plasma membrane blebbing (Taverna *et al.* 2003). The microparticles from the plasma membrane contain the secretory proteins and other markers from the origin cells (Mallat *et al.* 2000). Plasma membrane blebbing from the cells with a high level of transglutaminase expression has been observed in fibroblasts (Gentile *et al.* 1992), but the association between plasma membrane blebbing and TG2 externalisation is unknown.

Microparticles are plasma membrane vesicles released into the ECM by plasma membrane blebbing. Microparticles are usually smaller than one micron and express a panel of phospholipids and proteins specific to the original cells (reviewed in Leroyer et al. 2008). Microparticles in circulation have a prognostic role in clinical conditions. For example the use of leukocyte-derived microparticles to predict arthrosclerosis (Chironi et al. 2006) and endothelial cell original microparticles to predict to acute coronary syndrome (Mallat et al. 2000). These microparticles bear tissue factor and can be captured by thrombus associated platelets, which in turn initiate coagulation and fibrin formation (Furie et al. 2004). Factor XIII is a member of the transglutaminase family which like TG2 does not have a leader sequence. Factor XIII can be found in the platelet derived microparticles (Garcia *et al.* 2005) but it is not clear if this indicates that Factor XIII is externalised through plasma membrane blebbing and microparticles.

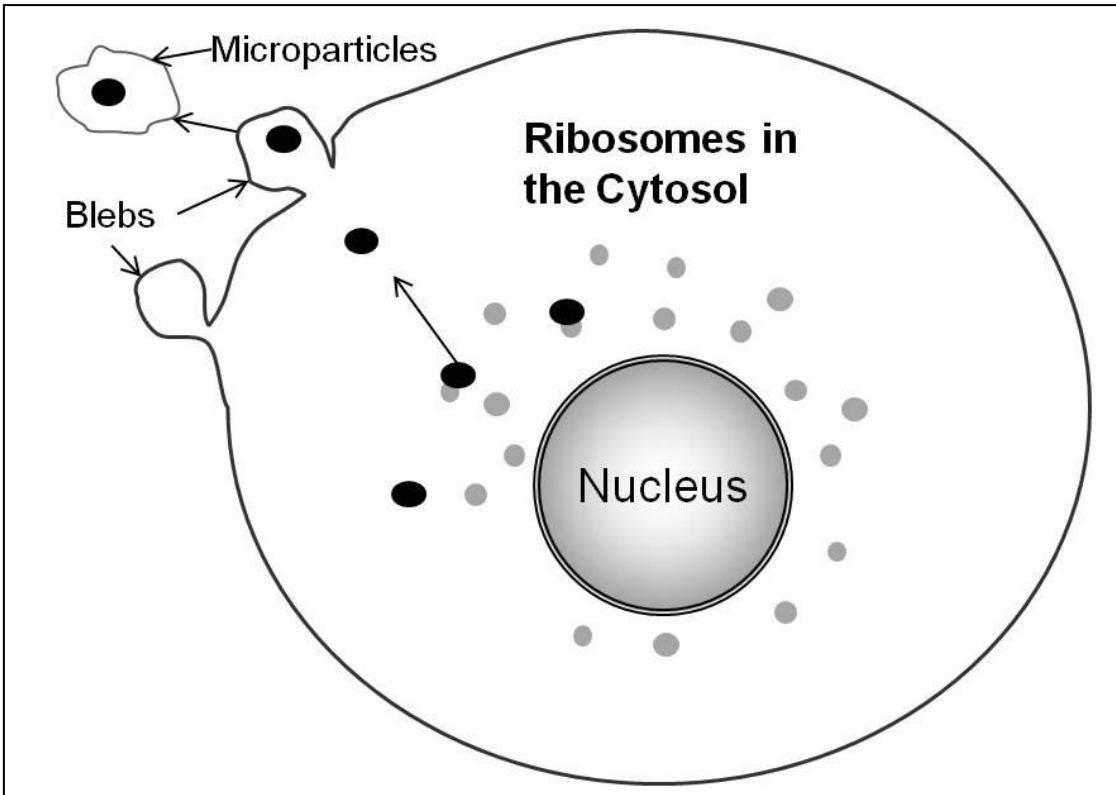

Figure 1.3-6 Protein secretion by plasma membrane blebbing

Secretory proteins in the cytosol are accumulated in the sub-plasma membrane area due to interaction with a specific plasma membrane binding protein. The secretory proteins enter blebs in the plasma membrane. The bulging plasma membrane is separated from plasma membrane of the cells and forms microparticles. The secretory proteins then released to extracellular space.

1.3.1.4 Direction molecule trap

Some complexes on the plasma membrane can directly bind proteins near the membrane and transport these proteins out of the cell. Fibroblast growth factor 2 (FGF-2) is one example of a protein that is directly transported to the cell surface (Nickel *et al.* 2008). Three hypothesis mechanisms of FGF-2 translocation was proposed in the later works by Nickel *et al* (2008) (Figure 1.3-7). (a) Cytoplasmic FGF-2 is recruited to the inner leaflet by binding to phosphatidylinositol 4,5 bisphosphate [$PI(4,5)P_2$]. Heparan sulfate proteoglycans (HSPGs) on the cell surface and FGF-2 receptors inside the cell surface form a molecular trap that can bind FGF-2 and drive FGF-2 translocation cross plasma membrane. In model (b) and (c), no specific receptor is needed for FGF-2 translocation. The interaction between FGF-2 and $PI(4,5)P_2$ generates a cholesterol-dependent lipid microdomain that opens

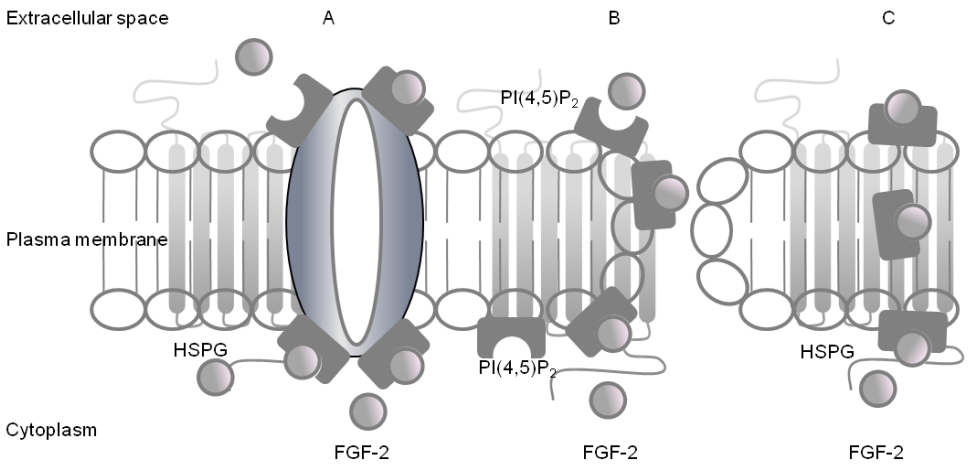

Figure 1.3-7 Possible mechanism for direct molecular trap

A specific protein transport channel (A) is located on the plasma membrane. Phosphatidylinositol 4,5 bisphosphate [$PI(4,5)P_2$] recruit FGF-2 to the sub-plasma membrane area. Heparin sulphate proteoglycans (HSPG) grapes FGF-2 accumulated at the sub-plasma membrane area and FGF-2 is pulled through the plasma membrane by HSPG. $PI(4,5)P_2$ formed a hydrophilic pore on the plasma membrane (B) that allows FGF-2 to pass through the plasma membrane and HSPG is responsible for the net extracellular trafficking of FGF-2. $PI(4,5)P_2$ binds FGF-2 and guide FGF-2 translocation through the plasam membrane (C). HSPG also responsible for the net extracellular trafficking of FGF-2. (Nickel et al. 2008)

the plasma membrane (Temmerman *et al.* 2008) or results in penetration through the lipid bilayer (Milburn *et al.* 2003). In model (b) and (c) HSPG ensure the net extracellular transport of TG2. HSPG is essential for these three proposed possible mechanisms of FGF-2 transport because the deletion of the C-terminus of FGF-2 prevents FGF-2 from binding to HSPGs and subsequently translocation cross plasma membrane. (Zehe *et al.* 2006). Although a direct molecular trap has been suggested as a potential unconventional protein secretion pathway; however, no direct visualisation of a direct molecular trap had been reported in the literature.

1.3.1.5 Transport binding partners

In the possible unconventional protein transport mechanisms mentioned above, binding partners play an important role in the transport of protein secreted. For example, FGF2 is recruited by $PI(4,5)P_2$ on the inner side of the plasma membrane and exported through a direct molecular trap or a transport channel. Ist2 is recruited by the COPI coat on the cortical ER membrane and secreted to extracellular space by the fusion of ER membrane and plasma membrane. A mannose 6-phosphate moiety is added to IL-1β such that it can be recognized by mannose 6-phosphate receptor on lysosomes and imported into secretary lysosomes. TG2 may also have binding partners that lead to its externalisation, but the binding partners for TG2 have not been identified.

1.3.2 Possible pathways for TG2 extra-cellular trafficking

The mechanism for TG2 trafficking out of cells is unknown. As TG2 does not have a leader signal peptide, it can't proceed via ER/Golgi dependent N-glycosylation (Gentile *et al.* 1991) and inhibition of ER/Golgi pathway did not prevent TG2 extracellular trafficking (Zemskov *et al.* 2011). So far, several possible routes have been hypothesised in the literature, but there remains no conclusive evidence for these.

1.3.2.1 TG2 extracellular trafficking by fibronectin co-transport

Fibronectin is one of the better substrates for TG2 crosslinking in the extracellular matrix. Evidence suggesting TG2 is co-transported with fibronectin came from two studies. Cell surface localisation of TG2 is

dependent on fibronectin and the deletion of fibronectin binding site (the first 6 amino acids) of TG2 in the N-terminal β-Sandwich domain has been shown to decrease TG2 expressed on cell surface (Gaudry *et al.* 1999). These two studies both measured TG2 on the cell surface. It is not clear if the cell surface TG2 can represent TG2 extracellular externalisation. It is possible that fibronectin retained TG2 on the plasma membrane, but not TG2 in the ECM. As fibronectin is transported through the conventional pathway, it is possible that TG2 binds to fibronectin and is co-transported with fibronectin though the ER/Golgi pathway. However, considerably more evidence is needed to support this hypothesis such as the co-localisation of TG2/fibronectin with Golgi apparatus. TG2 is not always secreted with fibronectin and is not activated by the same factors as fibronectin. Therefore, co-transport with fibronectin does not completely explain TG2 externalisation.

1.3.2.2 TG2 extracellular trafficking using Syndecan and heparan sulfate proteoglycans as co-receptors for TG2

The heparan sulfate proteoglycans (HSPGs) on the cell surface modulates a wide range of extracellular protein ligands which affect angiogenesis, blood coagulation, and tumour metastasis. Several families of cell surface HSPGs including transmembrane syndecans and the glycosylphosphoinositide-linked glypicans bind extracellular ligands and enhance formation of their receptor-signalling complexes (Bernfield *et al.* 1999). TG2 has some affinity for heparin sulphate and heparin that is an analogue of the chains of HSPGs (Scarpellini *et al.* 2009). In addition, the binding of TG2 to heparin does not affect the catalytic activity of TG2, but protects TG2 from thermal unfolding and proteolytic degradation (Verderio *et al.* 2008). Heparitinase digestion of cell-surface heparin sulfate impairs both RGD-independent cell spreading and actin assembly mediated by fibronectin-bound TG2 (Verderio *et al.* 2003). As FGF-2 may externalise through molecular trapping formed by HSPGs complex, it is possible that TG2 may also be transported through similar HSPGs complexes given its affinity to heparin. The association between fibronectin and TG2 in previous studies (Gaudry *et al.* 1999) may be explained by the peptide similarity of heparin sulphate proteoglycans and fibronectin (Nickel *et al.* 2008;

Verderio *et al.* 2008).

HSPGs belong to the syndecan family of cell-surface receptors. There are three main subclasses that may potentially interact with TG2 (Bishop *et al.* 2007). Syndecans' can activate cell growth and survival factors such as FGF-2, heparin-binding epidermal growth factor (EGF)-like growth factor (Kleeff *et al.* 1998) and transforming growth factor-β (TGF-β) (Filmus *et al.* 2001). This may explain to role of HSPGs in cancer. Syndecan-4 (S4), in particular is involved in controlling adhesive function and the regulation of cell behaviour in response to the external environment (Morgan *et al.* 2007) and has been postulated as a co-receptor for TG2 (Telci *et al.* 2008; Scarpellini *et al.* 2009). The S4 cytoplasmic domain binds phosphatidylinositol 4,5, biphosphate and directly activates protein kinase Ca (PKCa) to promote cellular spreading.

1.3.2.3 TG2 extracellular trafficking via Autophagy

So far no study has demonstrated that TG2 can be externalised through exosomes or lysosome secretion pathways. However, exosomes and lysosome secretion can be linked together through autophagy to potentially define a TG2 externalisation pathway. Cell surface TG2 can be internalised through the endocytic receptor, low-density lipoprotein receptor-related protein 1, and degraded in lysosomes (Zemskov *et al.* 2007). Endocytosis is a different direction of protein transport from protein externalisation. Autophagy can turn endocytosis into a protein externalisation process through the fusion of lysosomes and MVBs. It is possible that lysosomes that contain undegraded TG2 fuse with plasma membrane and release TG2 into extracellular space. Endocytosis related late endosomes are involved in TG2 externalisation through a phospholipid delivery system (Zemskov *et al.* 2011). However, the overall process seems to be related to TG2 recycling rather than TG2 externalisation per se. As cell surface TG2 must be externalised first before endocytosis, the primary pathway for TG2 externalisation remains unknown. TG2 has been associated with autophagy because over-expression of TG2 is related to drug resistance in cancer cells through the inhibition of TG2 on cell autophagy in pancreatic cancer cells (Akar *et al.* 2007). The ablation of TG2 results in an increase of immature autophagosomes formation (D'Eletto *et al.*

2009). However, it is unknown if TG2 can be externalised through autophagy. If TG2 is externalised through autophagy, it is expected that the over-expression of TG2 should increase autophagy and ablation of TG2 should result in a decrease of autophagy. Therefore, TG2 seems to be a regulator for autophagy rather than being externalised through this process.

1.3.2.4 TG2 extracellular trafficking via plasma membrane blebbing and microparticles

Plasma membrane blebbing from the cells with a high level of transglutaminase expressed has been observed in fibroblasts (Gentile *et al.* 1992), but the association between plasma membrane blebbing and TG2 externalisation is unclear. Other transglutaminase such as TG4 do not have a leader sequence (Grant *et al.* 1994) and can be externalised in rodent prostate through bleb-like structures (Seitz *et al.* 1990). Another member of transglutaminase without a leader sequence, Factor XIII, can be found in the platelet derived microparticles formed by plasma membrane blebbing (Garcia *et al.* 2005). Could plasma membrane blebbing and microparticles can be a potential externalisation pathway for TG2?

1.3.3 Concluding remarks

In summary, it is likely that TG2 is externalised through an unconventional protein externalisation pathway. Being able to target such a pathway could provide a highly specific means of lowering TG2 extracellular activity through locking TG2 in the cells. Such an approach could be a potential treatment for CKD and fibrosis.

To target TG2 externalisation, we must understand the externalisation pathway. Most of the research regarding TG2 cell export and extracellular function has been performed in fibroblasts; however, numerous studies on tissue Sections have shown that fibroblasts produce less TG2 than epithelial cells especially in diseased states. Pilot studies from our own lab have clearly shown that fibroblasts fail to release transfected TG2, withTG2 simply accumulating in the cytosol until export is induced by cell stress (Fisher 1973). Fibroblasts therefore may not be an ideal cell in which to study TG2 externalisation as a clean system can never be achieved due to the need to stress cells for release.

In contrast, the extracellular TG activity is usually positively correlated to intracellular TG activity in renal tubular epithelial cells (Fisher *et al.* 2009) where TG2 is known to be elevated in CKD. Previous studies on unconventional cell export routes suggest TG2 may have a specific sequence within the TG2 molecule that is essential for its externalisation. In most of the unconventional secretory proteins, another binding protein is subsequently needed to recruit the protein to be exported from the cell into the sub-plasma membrane area for plasma membrane blebbing, cortical ER for exosomes, lysosomes and MVBs.

It is therefore highly likely that TG2 has a similar motif within it that is essential for its export and this motif binds to a protein or other type of molecule that forms the start of an externalisation pathway which may or may not dip into either the conventional export pathway or one of the described unconventional export pathways.

The purpose of this thesis is therefore to try and identify which parts of TG2 are needed for its export, what this sequence may interact with and subsequently try and visualise how TG2 is moved out of the cell to ultimately provide early clues as to the TG2 extracellular trafficking pathway in tubular epithelial cells

Chapter 2

Aims

Hypothesis I

TG2 is trafficked to the cell surface by a novel mechanism that relies on specific amino acid motifs within the TG2 molecule.

To test this hypothesis we aim to

1. Use deletion and point mutation analysis of transfected TG2 into renal tubular epithelial cells and asses TG2 externalisation by measurement of intracellular and extracellular TG activity and TG2 antigen in 3 Tubular epithelial cell lines.
2. Initially identify which domain of TG2 any export sequence resides in by generating domain deletion mutants of TG2 by systematically removing each domain.
3. Once a domain is highlighted use point mutation analysis to ascertain the specific sequence involved for TG2 to be exported.

Hypothesis II

TG2 externalisation is dependent on another intracellular protein that can bind to the specific export sequence in TG2.

To test this hypothesis we aim to

1. Apply a yeast two hybrid screen to identified candidate proteins that bind to the amino acid sequence that is critical to TG2 externalisation.
2. Confirm interaction between candidate proteins and TG2 by co-immunoprecipitation from cells endogenous proteins.
3. Establish if the candidate proteins binding to the TG2 export sequence are critical to TG2 externalisation by knockdown of the candidate proteins with siRNA.

Hypothesis III

TG2 externalisation followed one of the four possible unconventional protein secretion pathways.

To test this hypothesis we aim to

1: Generate constructs of TG2 that carry a tetracysteine tag that can be visualised using FlAsH and ReAsH staining.

2: Use chronological imaging to track TG2s movement with time post transfection and combine with co-localisation analysis of various cell organelles to provide clues as to the export mechanism.

3: Apply a combination of fixed and live cell imaging techniques to generate 3 dimensional cell maps to show TG2 cellular movement and extracellular trafficking. This will be undertaken using deconvolution microscopy with 3D image rendering software.

Chapter 3 Materials and Methods

List of buffer

10x PBS	2 g KCl, 2.4 g KH_2PO_4, 80 g NaCl, 21.6 g Na_2HPO_4 ($7H_2O$) to 1000 ml
^3H putrescine incorporation assay reaction buffer	25 mM $CaCl_2$, 38.5 mM Dithiothreitol, 12.2mM ^3H Putrescine, 25 mg/ml N N'-Dimethylcasein
BCA solution A	1% (w/v) bicinchoninic acid, 2% (w/v) sodium carbonate, 0.16% (w/v) sodium tartrate, 0.4% (w/v) sodium hydroxide, 0.95% (w/v) sodium hydrogen carbonate
BCA solution B	4% (w/v) copper sulphate
Colorimetric assay reaction buffer	13.3 mM dithiothreitol, 6.7 mM $CaCl_2$, and 10 µM biotin-TVQQEL in 100mM Tris-HCl
Halotag binding buffer	100mM Tris-HCl, 150mM NaCl, 0.01% IGEPAL® CA-630, pH 7.6
LB medium	10 g tryptone, 5 g yeast extract, 10 g NaCl in 950 ml ddH_2O, pH 7.0
NP-40 cell lysis buffer	50 mM Tris-HCl, 150 mM NaCl, 1% (v/v) NP-40, pH 8.0
Protease inhibitors	1 mM leupeptin, 1 mM benzamidine, 1 mM phenylmethylsulphonylfluoride (PMSF) in STE buffer
SOC medium	20 g tryptone,5 g yeast extract, 0.5 g NaCl, 0.186 g KCl, 0.952 g $MgCl_2$ in ddH_2O to 1000 ml pH 7.4
STE buffer	0.32 M sucrose, 5 mM Tris, 2 mM EDTA
TBST	20 mM Tris, 150 mM Sodium Chloride, 0.1% (v/v) Tween 20, pH 7.6
TE buffer	10 mM Tris-HCl, pH 8.0, 1 mM EDTA
WB Reducing buffer	10 mM Tris (pH 6.8), 2.5% (w/v) SDS, 10% (v/v) glycerol, 0.02% (w/v) bromophen blue, 5% (v/v) β-mercaptoethanol
WB Transfer buffer	39 mM glycine, 48 mM Tris, 20% (v/v) methanol

3.1 Molecular Biology techniques

3.1.1 Plasmids and plasmid Systems

3.1.1.1 TOPO Plasmids

The TOPO group of vectors are designed to allow high speed, correct orientation insertion of cDNA into plasmids that then facilitate rapid switching of that sequence into other vectors based on using Gateway® Cloning Technology (Figure 3.1-1). This provides a fast, room temperature cloning reaction with a high efficiency deliver the clone and maintains orientation. The insert DNA can be shuttled from one expression vector to another expression vector as needed. The pENTR/D-TOPO plasmid (Figure 3.1-2) (Invitrogen, UK) utilise a highly efficient, 5-minute cloning strategy ("TOPO® Cloning") to

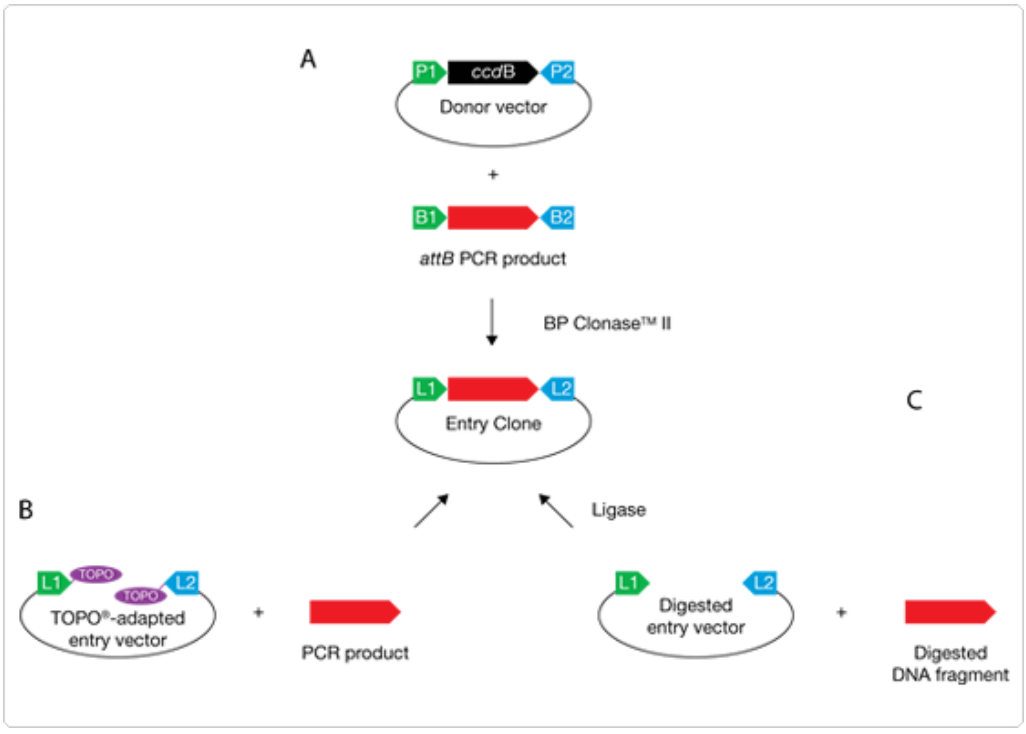

Figure 3.1-1 Schematics of Gateway® Cloning Technology

Vectors contain attL (L1 & L2) sequences for recombination into any destination vector. The PCR products containing attB sequences (A) can be cloned into the pENTR/D-TOPO vector in the correct orientation. The PCR insert can also be cloned into any TOPO-adapted entry vector (B) or a traditional ligase reaction (C). Adapted from Invitrogen user manual.

directionally clone a blunt-end PCR product into a vector for entry into the Gateway® System or the MultiSite Gateway® System. Blunt-end PCR products clone directionally at greater than 90% efficiency, with no ligase, post-PCR procedures, or restriction enzymes required. The sequence of proteins can be cloned into this entry vector and transfer to other expression vectors using Gateway® system.

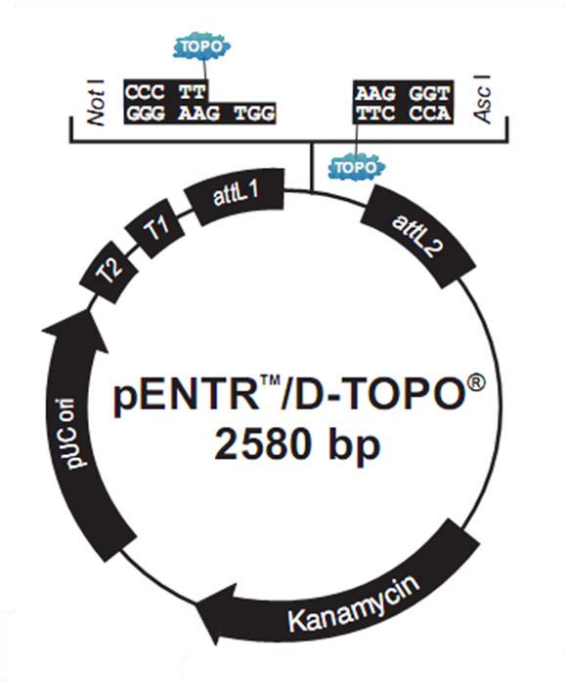

Figure 3.1-2 DNA map of pENTR/D-topo vector

attL1 and attL2 sites: bacteriophage λ-derived recombination sequences that allow recombinational cloning of a gene of interest in the entry construct with a Gateway destination vector (Landy, 1989). TOPO cloning site allows rapid, directional cloning of the PCR product. The insert DNA sequence can be checked using T7 promoter and M13 reverse primer. Kanamycin resistance gene allows selection of the plasmid in E. coli. pUC origin of replication allows high-copy replication and maintenance in E. coli.

3.1.1.2 Tetra cysteine tagging mammalian expression plasmids

Two vectors that add a 4 cysteine residues (ie a tetra cysteine tag) to the protein to be expressed have been used in this study. pcDNA6.2/nTC-Tag-DEST for N-terminal tagging and pcDNA6.2/cTC-Tag-DEST for C-terminal tagging (Figure 3.1-3) (Invitrogen, UK) with a tetracysteine tag (CCPGCC) were used in this study. Both vectors can be labelled with the green-fluorescent FlAsH-EDT2 reagent or the red-fluorescent ReAsH-EDT2 reagent. The main advantages of tetracysteine tag is that it is very small will have little effect on protein externalisation or movement through the cell and that FlAsH and ReAsH reagents can be used in live cells. Double staining with FlAsH and ReAsH can be used for tracking TG2 externalisation chronologically as once 1 die has bound to the tag, the other can not. Therefore for example a protein synthesised in 24 hours can be labelled green with FlAsH, so that any new protein synthesised say between 24 to 48 hours can be labelled with ReAsH – thus older protein appears green and newer red.

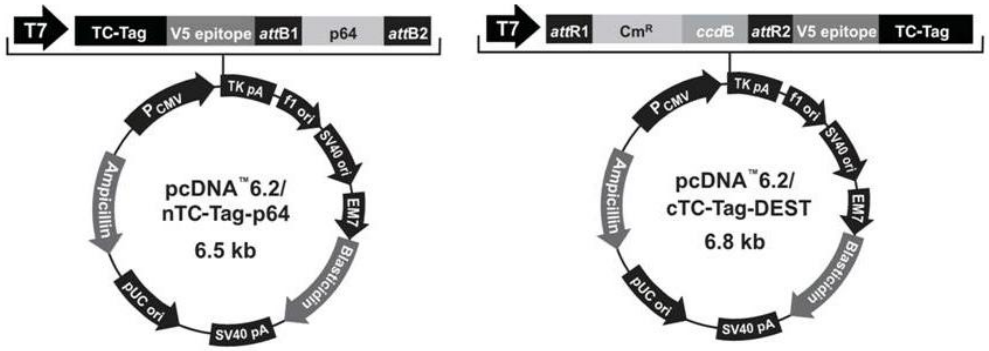

Figure 3.1-3 DNA map of N- and C-terminal tetracysteine tag vectors

Human cytomegalovirus (CMV) allows efficient, high-level expression of the recombinant protein. The gene of interest was cloned into attR1 and attR2 site that can be transcripted using T7 promoter. A V5 epitope was also fused with protein of interest and tetracysteine tag can be detected using FlAsH (green) and/or ReAsH reagent. Cells with stable expression of proteins can be selected using blasticidin resistance gene.

3.1.1.3 HaloTag Mammalian expression vector

pFC14K HaloTag® CMV Flexi® Vector is a HaloTag fusion vector. HaloTag can be used to immobilise the protein of interest using resin or magnetic beads.

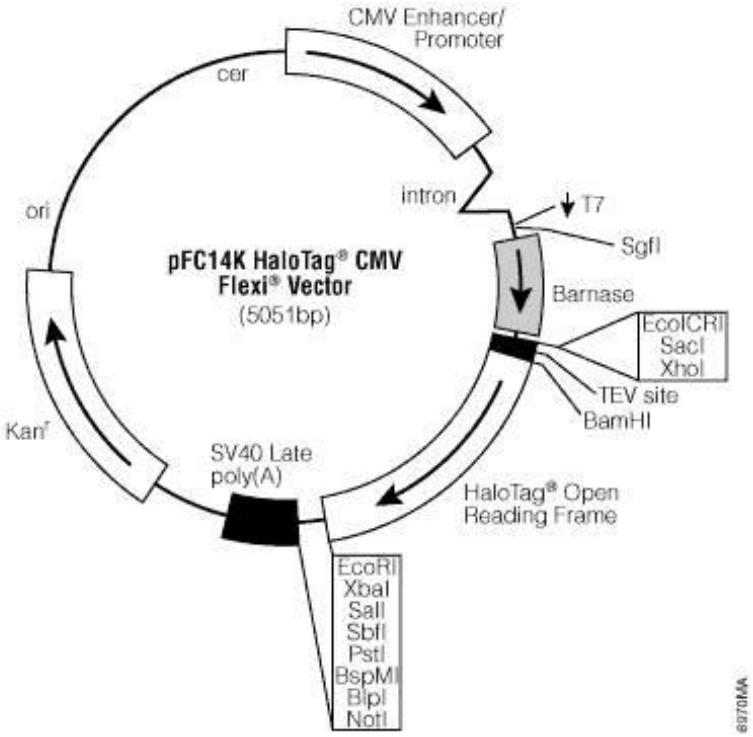

Figure 3.1-4 DNA Map of pFC14K HaloTag® CMV Flexi® Vector

expression of C-terminal-tagged HaloTag® fusion proteins in mammalian cells. Once expressed, the HaloTag® fusion protein may be used for cell imaging of protein localization or trafficking in conjunction with the fluorescent HaloTag® Ligands. In addition, the HaloTag® fusion protein can be purified or pulled down as a complex with its protein partners such as TG2.

3.1.2 Polymerase Chain Reaction (PCR)

3.1.2.1 Basics of PCR

The polymerase chain reaction is a technique that amplify a single or a few copies of a piece of DNA across several orders of magnitude and generate thousands to millions of copies of a particular DNA sequence (Bartlett *et al.* 2003).

3.1.2.2 PCR general protocol

Phusion high-fidelity DNA polymerase (Finnzymes, Finland) was used for all PCR reactions. 50 µl of a PCR reaction mix was made by mixing the following in order: 35.5 µl distilled water, 10 µl of 5x Phusion HF buffer, 1 µl of 10 mM dNTPs, 0.5 µl of 50 µM forward primer, 0.5 µl of 50 µM reverse primer, 10 ng of template DNA, 1.5 µl of DMSO, and 0.5 µl of Phusion DNA polymerase and making up to 50 µl with ultrapure endonuclease free water. The PCR reaction was run using a thermocycler (gene cycler, Bio-rad, UK) with the following settings: 1 cycle of 98ºC for 30 seconds, 35 cycles of (98ºC for 10 seconds, 55ºC for 30 seconds, and 72ºC for 30 seconds), and 72ºC for 10 minutes.

3.1.3 Insertion of PCR products into vector

All PCR products was purified using a PCR clean-up system (A9281, Promega) and cloned into an entry vector (pENTR™/D-TOPO®) using the pENTR™/D-TOPO® Cloning kit (K2400-20, Invitrogen). 2 µl of PCR product obtained from the PCR reaction was mixed with 1 µl salt solution, 1µl pENTR™/D-TOPO vector (15 ng/µl), 4 µl sterile water and incubated for 5 minutes at room temperature. 2 µl of this cloning reaction was then mixed with competent TOP10 *E. coli* (C4040-03, Invitrogen) and incubated on ice for 30 minutes followed by 30 seconds of heat-shock at 42ºC, 250 µl of SOC (Super Optimal Broth) medium (20 g tryptone,5 g yeast extract, 0.5 g NaCl, 0.186 g KCl, 0.952 g $MgCl_2$ in ddH_2O to 1000 ml pH 7.4) was added to the E. coli and the tube was shaken horizontally (200 rpm) at 37ºC for 1 hour on an orbital shaker (Kika Labortechnik KS250 basic). 100 µl of the transformation was spread on a LB plate containing 50 µg/ml kanamycin and incubated overnight

at 37ºC. Colonies forming (ie containing the kanamycin resistance gene) were picked the next day and grow in 10 ml LB medium containing 50 µg/ml kanamycin overnight at 37°C on an orbital shaker. 850 µl of this culture was added to 150 µl of sterile glycerol, mixed by vortexing and stored at -80°C. The remainder of the culture was used to prepare a small scale plasmid preparation (Section 3.1.9) to verify successful transformation.

3.1.4 Preparation of Competent Cells

A glycerol stock of the JM109 strain of E.coli was streaked on a LB [1% (w/v) bactotryptone, 0.5% (w/v) yeast extract, 1% (w/v) sodium chloride, pH 7.0] agar plate and the plate incubated at 37°C overnight. A colony was transferred to 5 ml of LB media and the culture incubated at 37°C with shaking at 250 rpm for 3 hours on an orbital shaker (Kika Labortechnik KS250 basic). The culture was transferred to 200 ml LB media and incubated overnight with shaking at 300 rpm until an absorbance of 0.6 at 600 nm. The culture was kept on ice for 15 minutes, divided into four 50 mL sterile centrifuge tubes, and centrifuged at 2,500 *g* for 10 minutes in 4°C. The cells were resuspended in 15 ml pre-cooled 0.1 M calcium chloride by gentle pipetting, left on ice 15 minutes, and centrifuged at 2,500 *g* for 10 minutes in 4°C. The cells were suspended in 4 ml pre-cooled 0.1 M calcium chloride/15% (v/v) glycerol, and left on ice for 4 hours. The cells were dispensed in 50 µL aliquots and frozen at -80°C.

3.1.5 LR Recombination for the transfer of sequences in D-TOPO vectors to expression vectors

The LR Recombination reaction was used to transfer the cDNA insert (Gentile *et al.* 1991) from the entry vector to the expression vector. Gateway® LR Clonase® enzyme mix contains a proprietary blend of Int (Integrase), IHF (Integration Host Factor) and Xis (Excisionase) enzymes that catalyze the *in vitro* recombination between an entry clone (pENTR/D-TOPO containing TG2 or TG2 mutants flanked by attL sites) (Figure 3.1-5) and a destination vector (containing attR sites, pcDNA6.2/nTC-Tag-DEST or pcDNA6.2/cTC-Tag-DEST) to generate the expression clone (Figure 3.1-6).

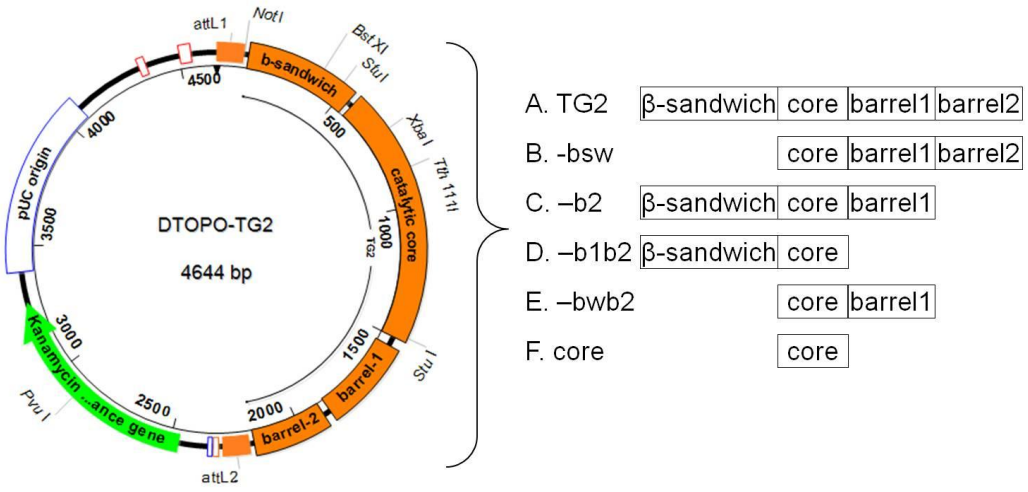

Figure 3.1-5 DNA map for D-TOPO entry vector with different TG2 constructs

D-TOPO entry vector containing full length human TG2 (TG2), TG2 with the β-sandwich domain deleted (-bsw), TG2 with β-barrel 2 domain deleted (-b2), TG2 with both β-barrels removed (-b1b2),TG2 with the β-sandwich domain and β-barrel 2 removed (-bwb2) and the core domain of TG2 (core).

LR recombination reaction was performed using LR clonase II enzyme mix (11791-020, Invitrogen). 100 ng of the vector obtained from the previous section in entry vector: pENTR/D-TOPO (Figure 3.1-5) was mixed with 100 ng of expression vector (pcDNA6.2/nTC-Tag-DEST or pcDNA6.2/cTC-Tag-DEST) (Figure 3.1-6), 6 µl TE buffer, pH 8.0 and incubated at 25ºC for 1 hour. 1 µl of Proteinase K solution (to degrade native proteins) was added to each reaction and the reaction was incubated for 10 minutes at 37ºC. 1 µl LR recombination reaction was then transferred to 50 µl of competent JM109 E. coli and incubated on ice for 30 minutes followed by a 45 seconds of heat-shock at 42ºC and then placed on ice for 2 minutes, 250 µl of SOC medium was added to the *E*. coli and the tube was shaken horizontally (200 rpm) at 37ºC for 1 hour on an orbital shaker (Kika Labortechnik KS250 basic). 100 µl of the transformation was spread on a LB plate containing 100 µg/ml ampicillin and incubated overnight at 37ºC. The ampicillin resistant colonies were picked the next day and grown in 10 ml LB medium containing 100 µg/ml ampicillin overnight at 37°C on an orbital shaker with shaking at 200 rpm. 850 µl of this

culture was added to 150 µl of sterile glycerol mixed by vortexing and stored at -80°C. The remainder of the culture was used to prepare a small scale plasmid preparation (Section 3.1.9) to verify successful transformation.

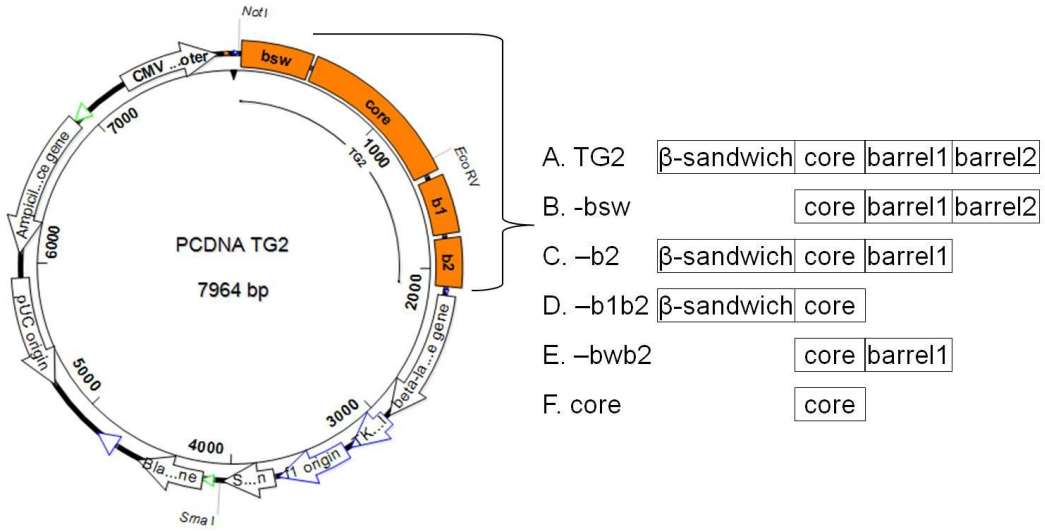

Figure 3.1-6 DNA map for pcDNA6.2/cTC-Tag dest with different TG2 constructs

pcDNA6.2/cTC –tag-dest vector containing full length human TG2 (TG2), TG2 with the β-sandwich domain deleted (-bsw), TG2 with β-barrel 2 domain deleted (-b2), TG2 with both β-barrels removed (-b1b2),TG2 with the β-sandwich domain and β-barrel 2 removed (-bwb2) and the core domain of TG2 (core).

3.1.6 Site-directed mutagenesis

The QuickChange Site-Directed Mutagenesis kit with Pfu turbo polymerase (Stratagene, UK) was used as per manufacturer's instructions. The reaction was prepared by mixing 5 µl 10× reaction buffer, 20ng pcDNA6.2/ cTC-Tag-DEST containing full length TG2, 125 ng forward primer, 125ng reverse primer (Chapter 5.3), 1 µl dNTP mix and ddH_2O to a final volume of 50 µl. Then 1 µl PfuTurbo DNA polymerase (Stratagene, UK) was added to the mix. The PCR reaction was run using a thermocycler (gene cycler, Bio-rad, UK) with the following settings: segment 1: 1 cycle of 95ºC for 30 seconds, segment 2: 12 cycles of (95ºC for 30 seconds, 55ºC for 1min and 68ºC for 16minutes). Segment 2 was adjusted according to the type of point mutations: 12 cycles were used for 1 point mutation and 18 cycles for two point mutations. The

reaction was placed on ice for 2 minutes. 1 µl of *Dpn* I restriction enzyme was added in each PCR reaction and mixed by pipetting. After spin down the reaction mix, the reaction was incubated at 37°C for 1 hour to digest the parental supercoiled dsDNA. 1 µl of the *Dpn* I-treated DNA was added to 50 µl JM109 E. coli and incubated on ice for 30 minutes followed by a 90 seconds of heat-shock at 42ºC and then placed on ice for 2 minutes, 250 µl of SOC medium was added to the E. coli and the tube was shaken horizontally (200 rpm) at 37ºC for 1 hour on an orbital shaker (Kika Labortechnik KS250 basic). 100 µl of the transformation was spread on a LB plate containing 100 µg/ml ampicillin and incubated overnight at 37ºC. The colonies were picked on the next days and grown in 10 ml LB medium containing 100 µg/ml ampicillin overnight at 37°C on an orbital shaker with shaking at 200 rpm. 850 µl of this culture was added to 150 µl of sterile glycerol mixed by vortexing and stored at -80°C. The remainder of the culture was used to prepare a small scale plasmid preparation (Section 3.1.9) to verify successful transformation. As β-sandwich domain is critical for TG2 externalisation (Section 4.3), point mutation of amino acid Asp^{94} and/or Asp^{97} to Ala (Hang *et al.* 2005) was used to determine to effect of aa 88-106 (2^{nd} fibronectin binding site in β-sandwich domain) on TG2 externalisation (Section 5.3).

Table 3.1-1 Primers for deletion and point mutations

	Constructs	Forward primer	Reverse primer
-7a	Remove first 7 aa of β-sandwich domain	CACCGAGAGGTGTGATCTGGAGCT	AAATCCGCCCCGGTTACTACTGT
f1	^{88}WTATVVAQQDCTLSLQLTT^{106}	CAGCCACCGTGGTGGCCCAGAAAGACTGCAC	GTGCAGTCTTGCTGGGCCACCACGGTGGCTG
f2	^{88}WTATVVDQQACTLSLQLTT^{106}	TGGTGGACCAGCAAGCCTGCACCCTCTCGCT	AGCGAGAGGGTGCAGGCTTGCTGGTCCACCA
f3	^{88}WTATVVAQQACTLSLQLTT^{106}	CAGCCACCGTGGTGGCCCAGCAAGCCTGCACCCTCTCGCT	AGCGAGAGGGTGCAGGCTTGCTGGGCCACCACGGTGGCTG

f1: single point mutation of Asp^{94} to Ala, f2: single point mutation of Asp^{97} to Ala , f3: a two point mutation of TG2 at Asp^{94}& Asp^{97} to Ala

3.1.7 Construction of pFC14K vector containing TG2 fragments

In results (Chapter 5.3) a TG2 export amino acid export sequence was identified. To generate a protein of this export sequence that can be immobilised a HaloTag label was used. HaloTag labelled proteins can then be pulled out by using HaloTag magnetic beads separated using SDS-PAGE and then examined by western blotting, silver staining or mass spectrometry. Here the β-sandwich domain, the TG2 export motif spanning amino acids 88-106 within the β-sandwich domain identified in Chapter 5.3 and the TG catalytic core were placed into a HaloTag vector.

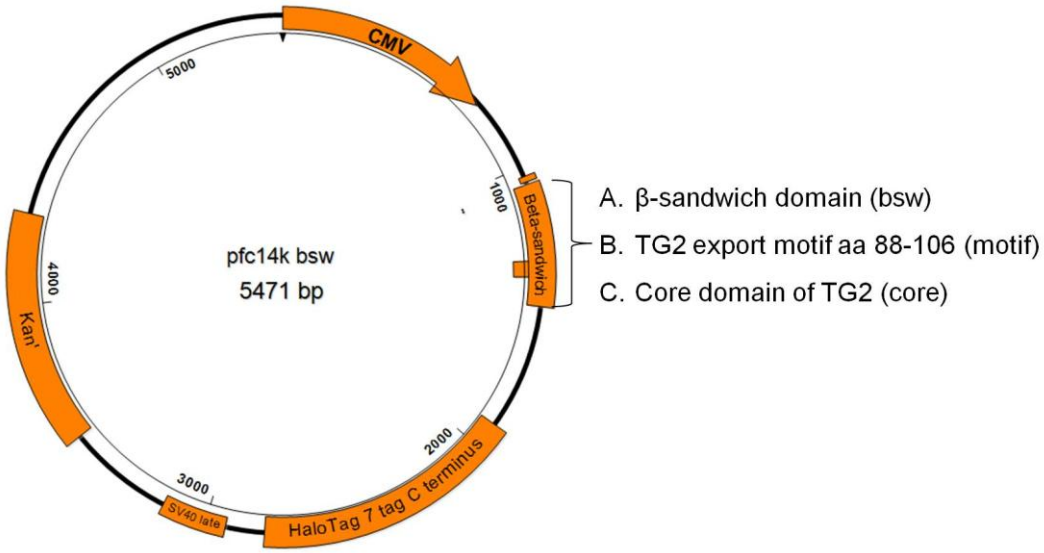

Figure 3.1-7 DNA map for pFC14K HaloTag® CMV Flexi® Vector

pFC14K HaloTag CMV Flexi vector containing the β-sandwich domain (bsw), the TG2 export motif aa 88-106 (motif) or the core domain of TG2 (core)

Constructs using TG2 cDNA (Gentile *et al.* 1991) were generated by PCR (Section 3.1) using suitable primer pairs. The PCR products were inserted into the HaloTag plasmids using the Flexi enzyme blend system (SgfI and PmeI, R1851, Promega). 250 ng of PCR product was digested with 4 µl Flexi enzyme blend and 4 µl 5X Flexi digest buffer at 37ºC for 30 minutes. Meanwhile, 2 µl pFC14K (HaloTag 7) CMV flex (G9661, Promega, UK) vector (Figure 3.1-7) was digested with 2 µl Flexi enzyme blend and 2 µl 5X Flexi digest buffer in 12 µl nuclease-free water at 37ºC for 30 minutes. The enzyme was inactivated by 20 minutes incubation at 65ºC. The ligation of PCR product and pFC14K

vector was performed by mixing 10 µl 2X Flexi ligase buffer, 5 µl digested vector, 100 ng of digested PCR product & 1 µl T4 DNA ligase. The reaction was incubated at room temperature for 1 hour and 1 µl reaction mix was transferred to JM109 competent cells. The JM109 E. Coli was incubated on ice for 30 minutes followed by a 45 seconds of heat-shock at 42ºC and then placed on ice for 2 minutes, 250 µl of SOC medium was added to the E. coli and the tube was shaken horizontally (200 rpm) at 37ºC for 1 hour on an orbital shaker (Kika Labortechnik KS250 basic). 100µl of the transformation was spread on a LB plate containing 50 µg/ml kanamycin and incubated overnight at 37ºC. Discrete colonies were picked the next day and grown in 10 ml LB medium containing 100 µg/ml kanamycin overnight at 37°C on an orbital shaker at 200 rpm. 850 µl of this culture was added to 150 µl of sterile glycerol mixed by vortexing and stored at -80°C. The remainder of the culture was used for a small scale plasmid preparation (Section 3.1.9) to verify successful transformation.

3.1.8 Sub cloning and propagation of bacterial colonies

A single colony of transformed bacteria was picked from agar plates and used to inoculate 10 ml of LB medium containing 50 µg/ml of ampicillin or kanamycin depending on the resistance carried by the transforming vectors. The culture was incubated at 37°C overnight with shaking at 250 rpm. 850 µl of this culture was added to 150 µl of sterile glycerol, mixed by vortexing and stored at -80°C. The remainder of the culture was used in a small scale plasmid preparation to verify successful transformation. The identity of all cDNA constructs was confirmed by DNA sequencing (Core Genomic Facility of the University of Sheffield) using a T7 Promoter primer following restriction mapping.

3.1.9 Small scale plasmid preparation

Small scale plasmid preparation was performed using the Wizard Miniprep DNA Purification System (Promega). 10 ml of cells were centrifuged at 2,500 *g* (Fisons MSE) for 15 minutes, supernatant removed and the cell pellet suspended in 250 µl cell resuspension solution by pipetting. Cells were lysed in 250 µl of cell lysis solution and mixed by inverting the tube 4 times. 10 µl of

alkaline protease solution was added in the lysate, mixed by inverting the tube 4 times, and incubated for 5 minutes at room temperature. The bacterial lysate was neutralised by 350 µl of neutralisation solution and centrifuged at 5,000 *g* for 10 minutes at room temperature. In the meantime, plasmid DNA purification units were prepared by inserting one spin column into one 2 ml collection tube for each sample. The cleared lysate was transferred to the prepared spin column by decanting and centrifuged for 1 minute. The spin column was washed twice, firstly with 750 µl then 250 µl of column wash solution and centrifuged at maximum speed for 1 minute. The spin column was transferred to a sterile 1.5 ml tube and the DNA was eluted by the addition of 100 µl nuclease-free water followed by centrifugation at 10,000 *g* for 1minute.

3.1.10 Large scale plasmid preparation

Large scale plasmid preparation was performed using the PureYield Plasmid Maxiprep System (Promega). 200 ml of bacterial cells culture overnight were centrifuged at 5,000 *g* (Beckman J25) at room temperature for 10 minutes. After removal of the supernatant, the cell pellets were completely resuspended in 12 ml cell resuspension solution. The cells were lysed in 12 ml cell lysis solution, neutralised using 12 ml neutralisation solution, and centrifuged at 5,000 *g* (Jouan A14) at room tempature for 15 minutes. A column stack was assembled by placing a blue PureYield™ clearing column on the top of a white PureYield™ maxi binding column. The assembled column stack was placed onto the vacuum manifold and the clarified supernatant applied to the DNA binding column after passage through a clearing column. The binding column was washed with 5 ml of endotoxin removal wash and 20 ml of column wash. After the membrane of the binding column was dry, the binding column was placed into a new 50 ml disposable centrifuge tube and the DNA was eluted by adding 1 ml nuclease-free water and centrifuging at 1500 *g* for 1 min.

3.1.11 Agarose gel electrophoresis

All DNA was separated on a 1% (w/v) agarose gel prepared in 1× TAE buffer [40 mM Tris, 0.1% (v/v) glacial acetic acid, 1 mM EDTA, pH8.0]. Ethidium bromide was added to the gel at a final concentration of 0.5 µg/ml prior to

pouring. 2 µg of DNA (5 µl) was mixed with 1 µl of 6X DNA loading dye (Promega) and the mixture was loaded onto the gel. 8µl of BenchTop 1 Kb DNA ladder (Promega) was loaded and the gel was electrophoresed at 100 V (Model 1000/500 Power Supply, Biorad) until the bromophenol blue front had run 3/4 of the length of the gel. The DNA was visualised on a transilluminator and the image was documented using Kodak EDAS 290 Electrophoresis Documentation System (Kodak DC 290 Zoom Digital Camera, light shroud, and Kodak_1D software).

3.1.12 Restriction Mapping of DNA Construct inserted into vectors

To confirm that the various TG2 constructs used were inserted in the correct orientation in vectors post ligation, restriction mapping of DNA construct was performed for every entry and expression vectors. The restriction site and the size of fragment after digestion were calculated for each construct in its correct orientation (Table 3.1-2 &
Table 3.1-3). 5 µg of plasmid DNA was digested with 6 units of restriction enzyme at 37°C for 2 hours and run on a 1% (w/v) agarose gel (Section 3.1.11). The identity of all cDNA constructs was confirmed by DNA sequencing (Core Genomic Facility of the University of Sheffield) using a T7 Promoter primer and TK poly A Reverse primer following restriction mapping.

Table 3.1-2 Restriction mapping of TG2 in TOPO and Entry plasmids

	D-TOPO		pcDNA6.2	
Construct	Enzyme/Buffer	Fragment (Reverse)	Enzyme/Buffer	Fragment (Reverse)
tg	NotI/XbaI/D	604/4040 (1483/3161)	NotI/EcoRV/D	1330/6634 (748/7216)
-bsw	PvuI/XbaI/D	2187/2028 (734/3481)	SmaI/EcoRV/M	2705/4830 (2061/5474)
-b2	PvuI/Tth111I/C	1748/2632 (1274/3106)	SmaI/EcoRV/M	1668/6076 (2516/5208)
-b1b2	PvuI/BstX1/D	1851/2145 (985/3011)	NotI/EcoRV/D	1330/5950 (68/7212)
-bwb2	NotI/StuI/D	962/2977 (420/3719)	NotI/EcoRV/D	913/6346 (421/6838)
core	PvuI/NaeI/M	1851/2145 (985/3011)	NotI/EcorV/D	901/5950 (68/6789)
-7a	NotI/XbaI/D	583/4040 (1483/3140)	NotI/EcoRV/D	1309/6634 (748/7195)

Restriction enzymes, buffers, and predicted DNA fragment sizes for restriction

mapping of the following TG2 sequences (Gentile *et al.* 1991) in TOPO and entry vectors *tg: full length of TG2 cDNA, -bsw: TG2 with β-sandwich domain missing, -b2: TG2 with β-barrel 2 missing, -b1b2: TG2 with both β-barrels missing, -bwb2: tg with β-sandwich and barrel 2 domains missing, core: tg core domain, M: multi-core buffer*

Table 3.1-3 Restriction mapping of TG2 in tagging plasmids

Construct	Enzyme/buffer	Fragment
Halotag7-bsw	BstX I/ Not I/ buffer D	1584/3880
Halotag7-core	EcoR V/ Not I/ buffer D	1541/4510
Halotag7-motif	BstX I/ Not I/ buffer D	1491/3619
pGBKT7-motif	BstX I, buffer D	2273/5071
LT-Myc	Hind III, buffer D	1182/5136
Motif-HA	Pst I, buffer H	1396/4082

Restriction enzymes, buffers, and predicted DNA fragment sizes for restriction mapping of the following TG2 sequences in various tag vectors. *Halotag7-bsw: β-sandwich domain with HaloTag, Halotag7-core: core domain with HaloTag, Halotag7-motif: motif 88-106 with HaloTag, pGBKT7-motif: pGBKT7 vector containing motif 88-106, LT-Myc: origin binding domain of large T antigen protein with Myc tag, Motif-HA: motif 88-106 with HA tag*

3.2 Cell Culture

3.2.1 Cell lines

Opossum proximal tubule cells (OK cells) (Malstrom *et al.* 1987) and NRK-52E tubular epithelial cells (de Larco *et al.* 1978) were obtained from the European Cell Culture Collection. MDCK II cells were a gift from N. Simmons (University of Newcastle, Newcastle, UK) and NRK-49F renal fibroblasts were a gift from Dr. Jill Norman (UCL, London).

3.2.1.1 Validate the renal tubular epithelial cell lines

To validate if the cells used in this study are tubular epithelial cells, electron microscopy images were obtained (With the assistance of Mr Bart Wagner, Histopathology, NGH) with classical characteristics of microvilli and microvesicles (Figure 3.2-1).

To confirm all cells used retained the characteristics of tubular epithelial cells (TECs), markers for tubular epithelial cells including β-catenin and E-cadherin

were used. OK, NRK52E and MDCKII cells were incubated with anti-β-catenin antibodies and anti-E-cadherin antibodies followed by FITC secondary antibodies (Section 3.4.14). NRK49F (fibroblast) cells were used as negative controls. β-catenin and E-cadherin were highly expressed in OK (Figure 3.2-2 A&B), NRK52E (Figure 3.2-2.C&D) and MDCKII (Figure 3.2-2 E&F) cells in a pericellular pattern. The green fluorescence is mainly found between cells because β-catenin and E-cadherin are markers for cell junctions. In contrast, β-catenin and E-cadherin green fluorescence was localised in the cytosol in NRK49F fibroblasts (Figure 3.2-2 G&H). This result confirmed that cell lines used in this study had the typical characteristics for tubule epithelial cell.

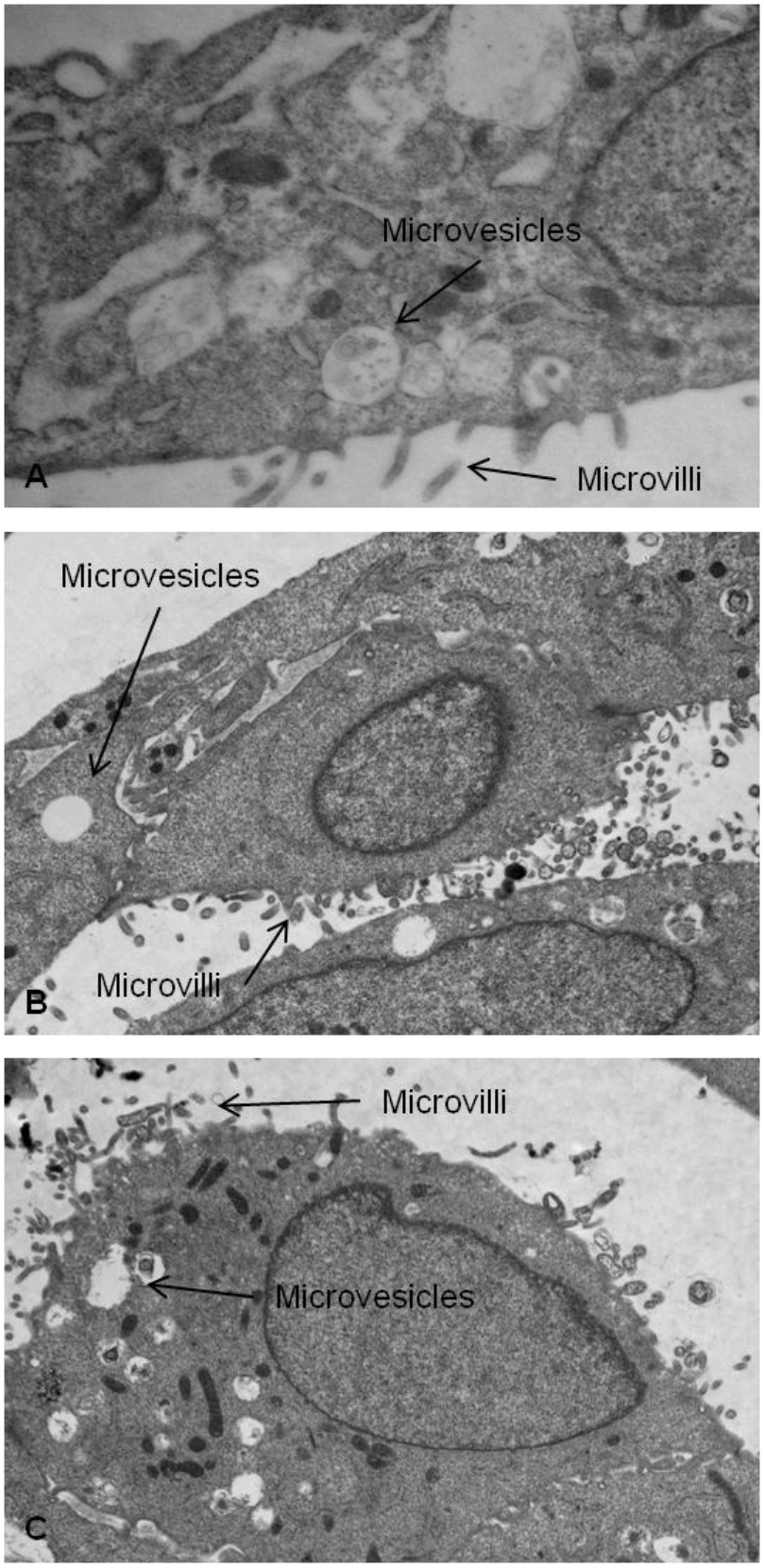

Figure 3.2-1 Electron microscopy images of tubular epithelial cells (TECs)

Transmission electron microscopy images for microvilli and microvesicles in TECs including OK (A), NRK52E (B) and MDCK II (C) cells

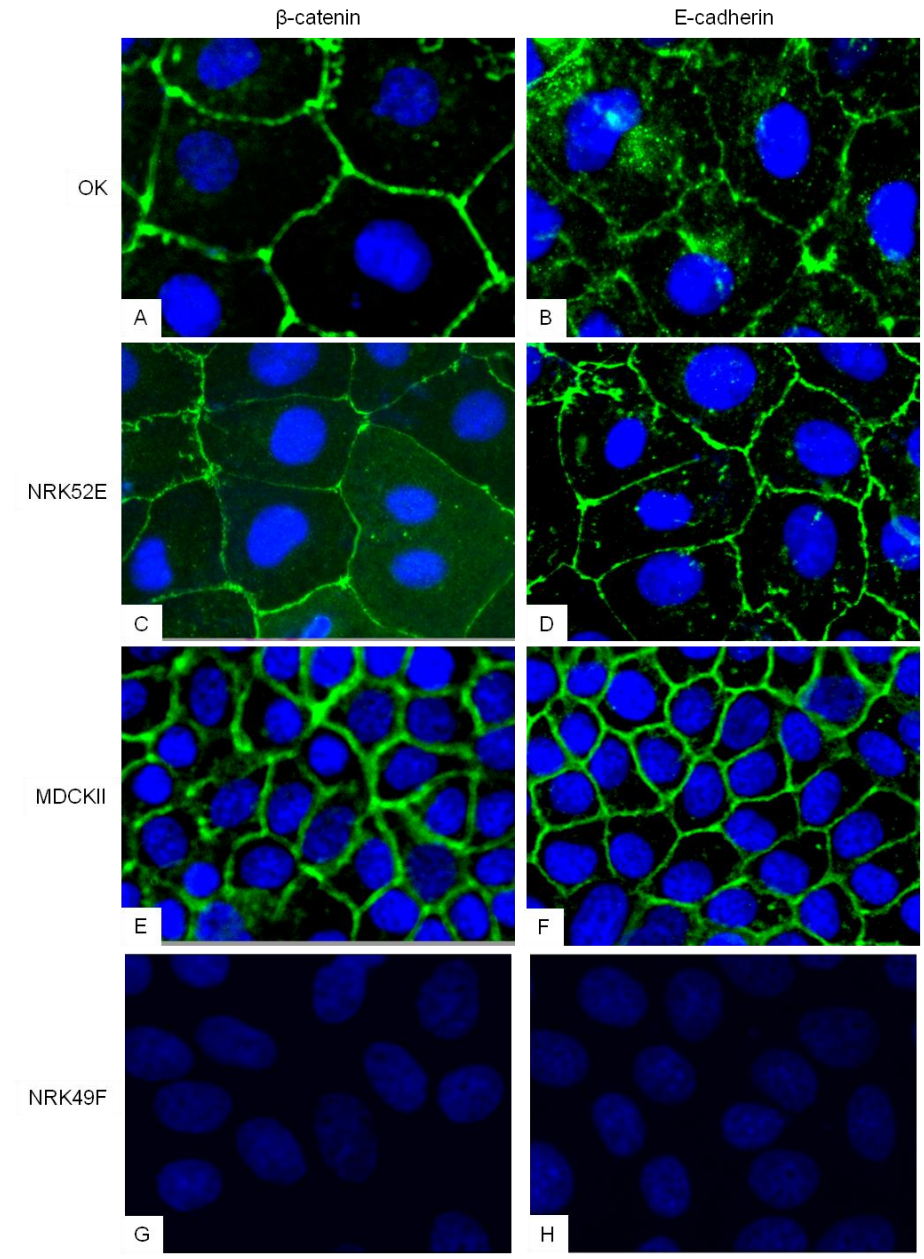

Figure 3.2-2 β-catenin and E-cadherin staining in renal tubular epithelial cells (TECs)

β-catenin and E-cadherin staining (green) in OK (A,B), NKR52E (C,D) and MDCKII cells (E, F) showed a peri-cellular distribution that is the cell junction. β-catenin and E-cadherin stains in NRK49F (G, H) fibroblast are localised in the cytosol. The cell nucleus was stained with DAPI in blue

3.2.2 Cell culture media

OK cells were cultured in Dulbecco's Modified Eagles Medium (DMEM) containing 584 mg/L L-glutamine, 5% (v/v) heat inactivated foetal calf serum, 100 IU/ml penicillin, and 100 µg/ml streptomycin.

NRK-52E, MDCKII, and NRK-49F cells were cultured in Dulbecco's Modified Eagles Medium (DMEM) containing 584 mg/L L-glutamine, 10% (v/v) heat inactivated foetal calf serum, 100 IU/ml penicillin, and 100 µg/ml streptomycin. All cultures were maintained at 37ºC and in a humidified atmosphere of 5% CO_2 in air.

3.3 Transfection of tubular epithelial cells (TEC)

3.3.1 Lipofectin

1×10^5 Cells were seeded into a 6-well plate and allowed to attach overnight at 37°C after which they reached about 60% confluency. 10 µl of lipofectin reagent (Invitrogen, UK) was diluted in 100 µl of Opti-MEM reduced serum medium (Invitrogen, UK) and incubated at room temperature for 45 minutes. 2 µg of vector was diluted in 100 µl of Opti-MEM medium. The lipofectin and DNA solutions were combined and incubated at room temperature for 15 minutes. Meanwhile, cells were washed once with 2 ml of Opti-MEM medium. 0.8 ml of Opti-MEM medium was added to the DNA and lipofectin complexes, and added to the cells. The cells were incubated at 37°C overnight. Media was removed and replaced with complete media. The cells were incubated at 37°C for a total of 48 hours before analysis.

3.3.2 Lipofectamine 2000 or LT1

2×10^5 Cells were seeded into a 6-well plate and allowed to attach overnight at 37°C after which they reached about 90% confluency. 4 µg of DNA and 10 µl of Lipofectamine 2000 (11668-027, Invitrogen, UK) or LT1 (MIR 2300, Geneflow, UK) was diluted in 50 µl of Opti-MEM reduced serum medium (Invitrogen, UK) separately with 5 minutes of incubation at room tempature. The Lipofectamine 2000/LT1 and DNA mix were combined and incubated at room temperature for 20 minutes. The DNA and Lipofectamine 2000/LT1 complexes were added to

the cells with 0.9 ml of Opti-MEM medium. The cells were incubated overnight. The Opti-MEM medium was replaced with complete media after a overnight incubation and the cells were incubated at 37°C for a total of 48 hours before analysis.

3.3.3 Transfection using nucleofection

1×10^6 harvested cells were resuspended in 100 µl Ingenio electroporation solution (Geneflow, UK) containing 5 µg of DNA (or with 8 µg of siRNA) and transferred to a 0.4 cm cuvette. The cuvette was inserted in nucleofector (Nucleofector I device, Amaxa, UK). The optimal programs were A-20 for OK cell, L-05 for MDCK II cell line and X-01 for the NRK-52E cell line. The cells were rinsed in complete culture media, transferred to 6-well culture plate and incubated at 37°C for 48 hours before analysis.

3.3.4 Optimise transfection protocols in renal epithelial cells

To determine the relative levels of transfection using different transfection methods (lipofectin, lipofectamine 2000, LT-1 & Amaxa Nucleofector), the transfection efficiency for each method in each cell line was determined by the measurements of both TG activity and the percentage of cells positive for fluorescently labelled TG2 following transfection of pcDNA6.2/cTC-Tag-dest vector containing full length TG2 cDNA (Gentile *et al.* 1991). The percentage of green fluorescent positive was calculated from the number of cells with FlAsH positive (see Section 3.4.14) compared to the total cell number in 10 randomly selected fields using a 10x objective lens. 50% of OK cells were positive for green fluorescent protein using lipofectin, lipofectamine 2000, LT1 reagent (Figure 3.3-1 A). The percentage of green fluorescent positive was slightly higher for OK cells transfected by nucleofection (program A-20) (Figure 3.3-1 A). There was no difference between with Amaxa solution V and Ingenio solution. The transfection efficiency for NRK52E and MDCK II cells using lipofectin was 20%. The transfection efficiency increased to 50% using lipofectamine and LT1 reagents ($p=0.01$, *t*-test). Nucleofector with amaxa solution V or Ingenio solution (program X-01 for NRK52E and L-05 for MDCKII cells) further increased the transfection efficiency to 60% ($p=0.03$ and 0.05)

compared to lipofectamine 2000 and LT1 (Figure 3.3-1 C&E).

A significantly increase in TG activity was found in OK cells transfected with TG2 tetracysteine tag vector using lipofectin, lipofectamine 2000, LT1 and nucleofector protocols. The TG activity increase 20 folds for OK cells transfected with nucleofector compared to the cells without transfection (Figure 3.3-1 *B*). For NRK52E (Figure 3.3-1 D) and MDCKII (Figure 3.3-1 F) cells transfected with TG2 tetracysteine tag vector using lipofectin reagent, no significant differences in TG activity compared to cells without transfection can be detected. This can be explained the endogenous TG2 of the cells or the expression of pcDNA6.2/cTC-Tag-dest vector in a protein level. Transfection with lipofectamine 2000 and LT1 reagent resulted in a 5 to 10 fold increase in TG activity ($p=0.02$). Transfection using nucleofector method resulted in a 10 to 15 fold increase of TG activity comparing to the cells without transfection ($p=0.05$ compared to LT1 and lipofectamine 2000).

As transfection using the nucleofector with the Ingenio solution showed similar transfection efficiency and TG activity to that of Amaxa solution V, nucleofection with Ingenio solution with program A-20 for OK, X-01 for NRK52E and L-05 for MDCKII cells was used in the study.

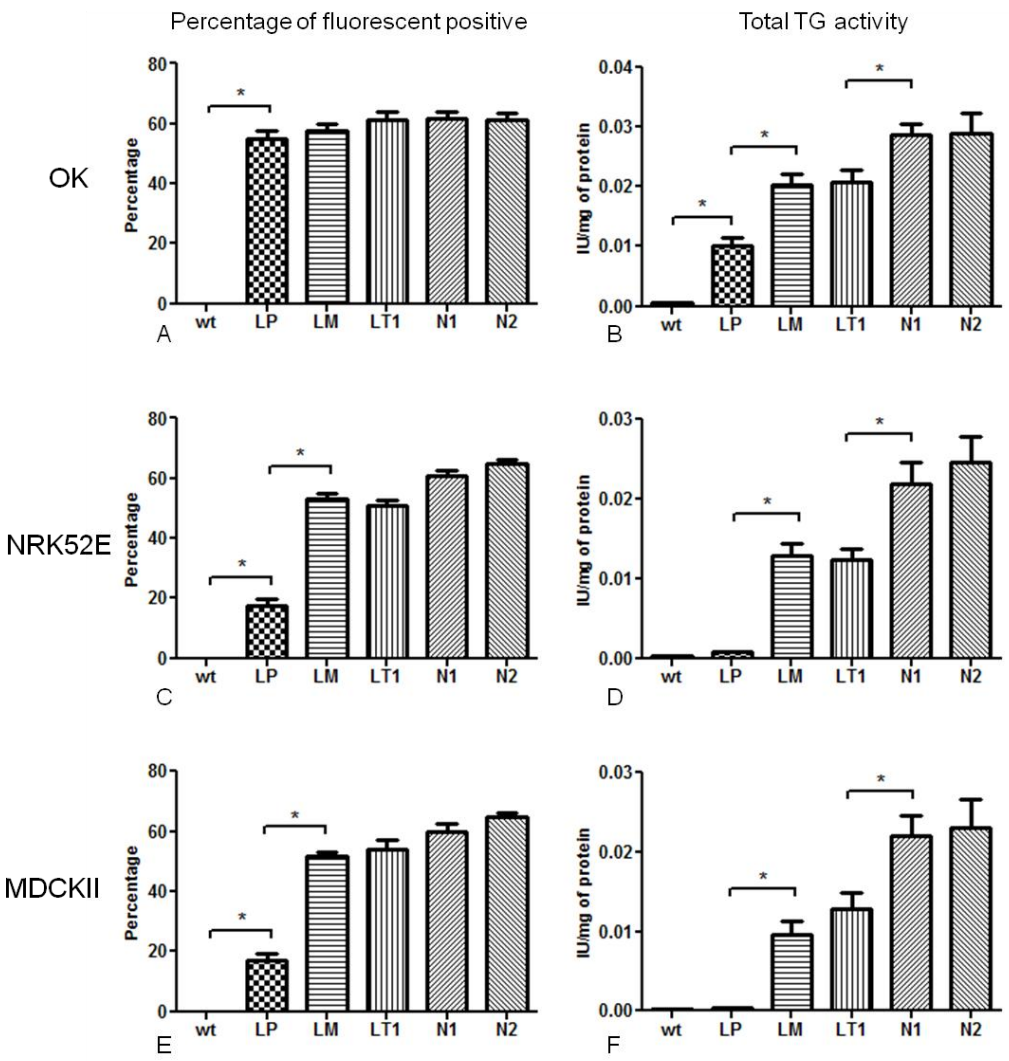

Figure 3.3-1 Comparison of Transfection efficiencies using different transfection reagents

*OK, NRK52E and MDCKII cells transfected with TG2 tetracysteine tag vectors pcDNA6.2/cTC-Tag-dest vector containing full length TG2 cDNA using different transfection methods were analysed 48 hours post transfection. The percentage of fluorescently positive cells in 10 random 100X fields was calculated in OK (A), NRK52E (C) and MDCKII (E) cells. Total TG activity (B) measured by ^{3}H putrescine incorporation assay (section 3.4.5) using different transfection methods was used to evaluate transfection efficiency in tubular epithelial cells. wt: cells without transfection, LP: lipofectin, LM: lipofectamine, LT1: LT1 reagent N1: Amaxa solution V, N2: Ingenio solution. Data represents mean ±SEM, n=5, *:p<0.05*

3.3.5 Stable transfection in NRK 52E cells

The vector we chose to use for stable expression of various TG2 constructs was the pcDNA 6.2 cTC-Tag vector. This contains the blasticidin resistance gene. Therefore to determine the dose of blasticidin required for the selection of stably transfected NRK52E cells, a blasticidin cell survival curve was generated against increasing does of blasticidin. No wild type NRK52E cells can survive in a 5 µg/ml blasticidin for more than 2 days or in 2 µg/ml blasticidin for more than 5 days (Figure 3.3-2). 5 µg/ml of blasticidin followed by 2 µg/ml blasticidin after 5 days was used for the selection of stably transfected cells.

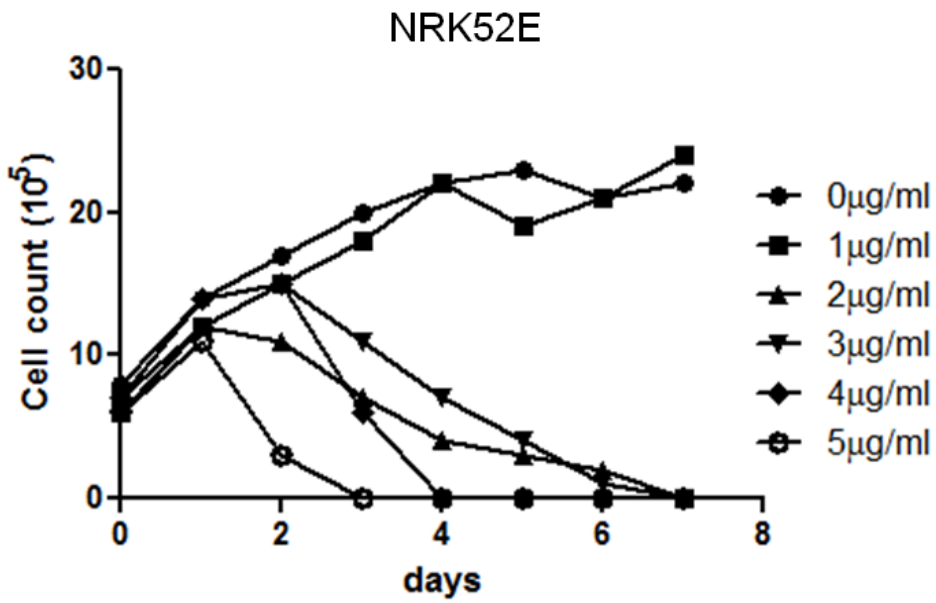

Figure 3.3-2 Cell survival curve according to blasticidin doses

Cells were trypsinised using 1x trypsin/EDTA, then resuspended in 10 ml of medium and counted using a hemocytometer. Cells counts according to 0-5 µg/ml of blasticidin in the media up to 7 days were recorded.

3.3.6 Selection of cell lines to study TG2 extracellular trafficking

To explorer the mechanism of TG2 externalisation, using a cell in which increasing intracellular TG2 has a direct effect on the amount of TG2 exported is highly preferable as it means no further stimulus (or confounding factor) is required. The total TG activity of the cell lysate (the amount of TG2 inside the cells) (Figure 3.3-3 A), extracellular TG activity (the amount of TG on cell surface) (Figure 3.3-3 B) and TG activity in the culture media (the amount of TG2 outside the cells) (Figure 3.3-3 C) were measured in response to increasing amounts (5, 10, 15, 20 µg) of tetracysteine tag vector with full length TG2 cDNA was transfected in 5 cell lines. The extracellular TG activity and TG activity in the medium showed no changes in NRK49F and 1097 cells according to the different levels of TG2 inside the cells (Figure 3.3-3). This suggested that TG2 transport in NRK49F and 1097 cells were not correlated to the amount of TG in the cells. OK, NRK52E and MDCKII cells had a clear correlation between of transported TG2 and the amount of TG2 in the cells. Therefore, OK, NRK52E and MDCKII cell lines were selected for studying TG2 externalisation.

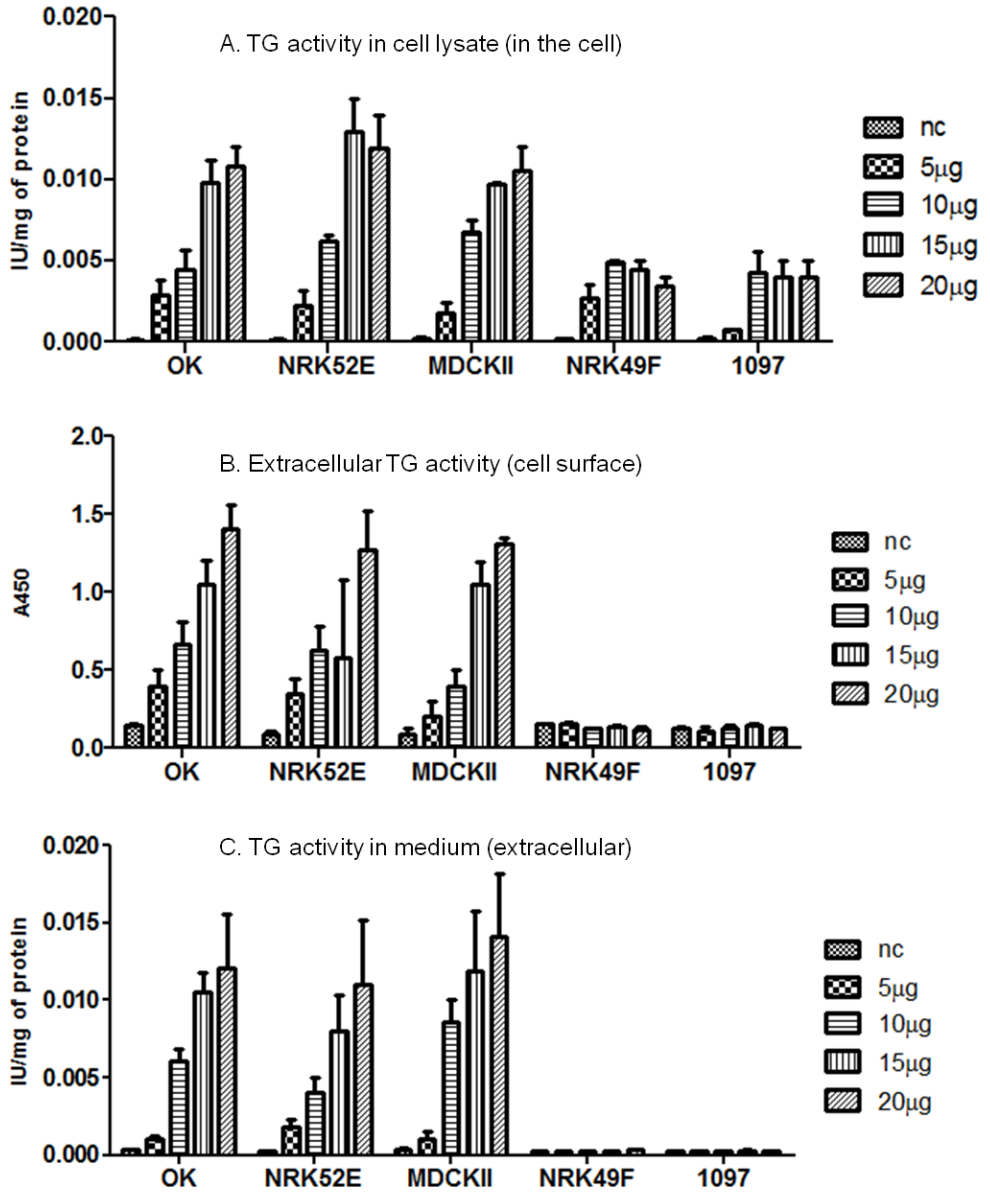

Figure 3.3-3 Select cell line for studying TG2 externalisation

TG activity in the cell lysate (A) (the amount of TG2 in the cells), extracellular TG activity (B) (the amount of TG2 on cell surface/ outside the cell) and TG activity in the medium (C) (the amount of TG2 outside of the cells) for OK, NRK52E, MDCKII, NRK49F, 1097 cells in response to transfection with a different amounts of tetracysteine tag TG2 expression vector pcDNA6.2/cTC-tag-DEST (0, 5, 10, 15 and 20 µg). Data represent mean±SEM, n=5

3.4 General and Biochemical Techniques

3.4.1 Preparation of cell lysates

Cells were trypsinised using 2x trypsin-EDTA solution (Invitrogen, UK) (2% v/v) for 5 minutes at 37ºC. These were resuspended in the same volume of complete media and centrifuged at 400 *g* (Fisons MSE) for 5 minutes at room temperature. The media was removed and cells centrifuged at 400 *g* (Jouan A14 microfuge) for 2 minutes to produce a cell pellet. After the removal of excess media, cells were resuspended in 100 µl of STE buffer (0.32M sucrose, 5mM Tris, 2mM EDTA) containing protease inhibitors [1 mM leupeptin, 1 mM benzamidine and 1 mM phenylmethylsulphonylfluoride (PMSF)] (Sigma, UK). A cell lysate was produced by sonicating (Qsonica sonicator 3000) the cells for 3×5 seconds at 40kHz, 25% amplitude on ice. For immunoprecipitation, the cells were lysed using NP-40 cell lysis buffer (50 mM Tris-HCl, 150 mM NaCl, 1% (v/v) NP-40, pH 8.0) with protease inhibitors added before use (11836170001, Roche, UK).

3.4.2 Preparation of media samples

Cells were grown to confluency, the media removed and replaced with 400µl of serum free culture medium into each well in a 6-well plate. The medium was collected and centrifuged at 10,000 *g* in a Jouan A14 microfuge for 10 minutes. The supernatant was used for analysis. To determine the time at which the most TG activity (measured as showed in section 3.4.4) was present in the medium once fresh medium is added, at 48 hours post transfection of a TG2 expression vector, serum free medium was added and incubated for 2, 4, 6, 8, 10, 12 and 16 hours at 48 hours post transfection. Peak TG activity is seen after 4 to 6 hours (Figure 3.4-1) that is consistent with the half-life of TG2 (Fesus *et al.* 1989) and thus 4 hours was used for all subsequent study.

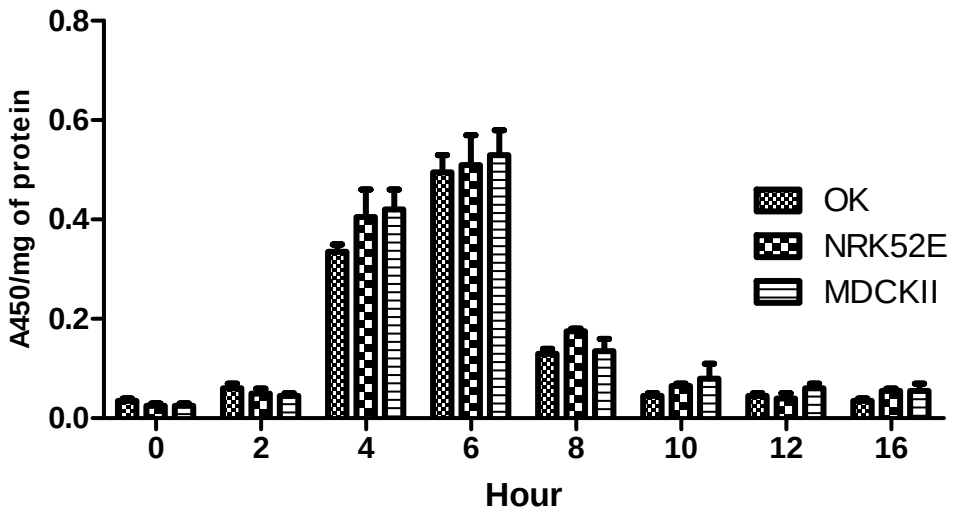

Figure 3.4-1 TG activity in serum free culture medium incubation for 0-16 hours

48 hours post transfection, the culture medium was replaced with 400µl of serum free medium and incubated for 0-16 hours. The TG activity of the culture medium was measured in OK, NRK52E and MDCKII cells. TG activity in culture medium can be measured in 4 & 6 hours of incubation. Data are expressed as mean±SEM, n=5

3.4.3 Protein knock-down by siRNA

The cells were co-transfected with 5 µg of plasmid DNA plus either 300 nM of nonsense siRNA or the selected siRNA with TG2 cDNA using the Amaxa Nucleofection using the optimised program for the expression vector. The siRNA used included anti-fibronectin 1 siRNA (s130401, Applied Biosystems, UK), anti-tapasin siRNA (sc42938, Santa Cruz biotechnology, UK), anti-translocon-associated proteins siRNA (sc63149, Santa Cruz biotechnology, UK) and anti-large T antigen siRNA (applied Biosystems, UK). The selected siRNA consist of five target-specific 19-25 nt siRNA.

The TG activity of the cell lysates, extracellular TG activity, antigen and TG activity in the culture medium were measured 48 hours after transfection. The knock down of fibronectin in the cell lysate was determined by fractionation of the cell lysate on a 7.5% (v/v) SDS-PAGE gel in reducing buffer followed by western blot analysis for fibronectin. The knock down of LTA, tapasin and

translocon-associated proteins in the cell lysate was also determined by western blot analysis but using 10% (v/v) SDS-PAGE gels.

3.4.4 Total transglutaminase activity by colorimetric assay

Total TG activity was measured by the incorporation of Biotinylated TVQQEL peptide into casein as described by Trigwell (Trigwell *et al.* 2004). A 96-well plate was pre-coated with casein at 1 mg/ml in 50mM sodium carbonate and kept overnight at room temperature. The next day, the casein solution was discarded and the wells were washed with distilled water. 250 µL of blocking solution [0.1% BSA (w/v) in 50 mM sodium carbonate] was added into every well and incubated at 37°C for 1 hour. After 3 wash of distilled water, 150 µL of reaction buffer (13.3 mM dithiothreitol, 6.7 mM $CaCl_2$, and 10 µM biotin-TVQQEL in 100 mM Tris-HCl) were added in each well. The reaction was started by adding 50 µL of cell lysates into each well and incubated for 1 hour at 37°C. After 3 wash of distilled water, 200 µl of 1 in 5000 diluted Extravidin-peroxidase in blocking solution was added into every well and incubated 1 hour at 37°C. After 3 wash of distilled water, the extravidin binding is revealed by adding 200 µl of 3,3',5,5' tetramethyl benzidine (TMB) solution to each well. The colour was developed after 5-15 minutes at room temperature and the colour development was stopped by adding 50 µl of 2.5 M H_2SO_4. The resulting colour was then read in an ELISA plate reader (Labsystems Multiskan Ascent) using Genesis Software (version 3.05) at 450 nm. A standard curve (Figure 3.4-2) was obtained using Guinea pig liver transglutaminase (T006. Zedria) (0.0001, 0.0025, 0.005, 0.01, 0.025 and 0.05 IU per well) showing a linear response between 0.0001 and 0.05 IU. The expression of total TG activity was calculated in unit of TG activity/mg of protein.

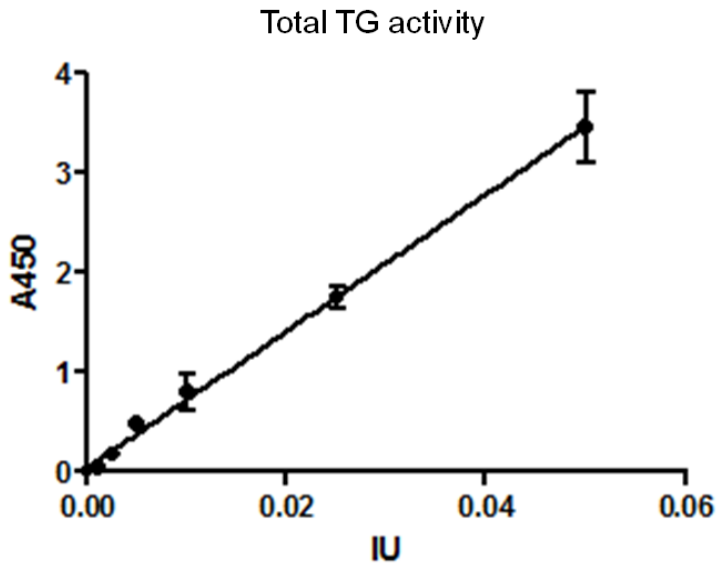

Figure 3.4-2 Standard curve for colorimetric assay

A standard curve of total TG activity measured by colorimetric assay using Guinea pig liver transglutaminase (T006, Zedria).The A450nm and TG2 activity data forms a linear correlation between 0.0001 to 0.05 IU.

3.4.5 Total transglutaminase activity by ^{3}H putrescine incorporation assay

In the presence of Ca^{2+}, active transglutaminase uniquely incorporates ^{3}H-putrescine into N'N-dimethylcasein forming a radioactive trichloroacetic acid (TCA)-insoluble material capable of being detected by scintillation counting.

50 µl of cell lysate was added to 50 µl of reaction solution (Table 3.4-1). A background control in which calcium was replaced with EDTA was used to determine non-enzymatic incorporation. Samples and controls were incubated at 37ºC for up to 60 minutes. At set time points (0, 20, 40, and 60 minutes) after initiation of the reaction, 10 µl aliquots in duplicate were removed from the tubes and dotted on to 1 cm^2 Whatman 3MM filter paper. The filter papers were immediately dropped into 10% (w/v) TCA to stop the reaction and precipitate protein. This was followed by a further wash with 10% (w/v) ice cold TCA for 10 minutes, 5% (w/v) ice cold TCA 3 times for 5 minutes, 100% (v/v) ethanol for 5 minutes and drying. To determine efficiency of counting, a 10 µl aliquot was

dotted on to two filter paper squares and not washed. These two filter papers represent the total counts in the samples. Filter papers were allowed to air dry before being placed in 2 ml of Ultima Gold Liquid scintillation fluid (Packard) and radioactive incorporation measured by scintillation counting on a Rack Beta liquid scintillation counter (Packard Instruments, UK). The gradient (change in cpm per hour) was calculated which was subsequently used to calculate TG activity. Values were corrected for protein and expressed as nmol of putrescine incorporated per hour (unit of activity per mg of protein: IU/mg protein). A cell lysate was prepared using sonicating in 100 µl of STE buffer (Section 3.4.1.)

Table 3.4-1 Constituents of a TG activity assay reaction solution

Per sample		Per control	
Reagent	Volume	Reagent	Volume
25 mM $CaCl_2$	5 µl	100 mM EDTA	5 µl
38.5 mM Dithiothreitol	5 µl	38.5 mM Dithiothreitol	5 µl
12.2 mM ^{3}H Putrescine	5 µl	^{3}H 12.2 mM Putrescine	5 µl
25 mg/ml N N'-Dimethylcasein	10 µl	25 mg/ml N N'-Dimethylcasein	10 µl
Total volume	25 µl	Total volume	25 µl

12.2mM ^{3}H Putrescine was made by mixing 1ml of 59.8mM Putrescine in 1.05M Tris-HCl pH 7.4 and 2ml ^{3}H putrescine (1:2), $CaCl_2$, N N'-Dimethylcasein and dithiothreitol were made in 50mM Tris-HCl pH 7.4, EDTA was made in 1.05M Tris-HCl pH 7.4.

3.4.6 Measurement of Total TG activity using ^{3}H putrescine incorporation assay and colorimetric assay

The ^{3}H putrescine incorporation assay is more sensitive and the gold standard assay for Total TG activity measurement; however, the ^{3}H putrescine incorporation assay is very expensive and is complicated by the need to use radioactive isotopes. To determine if the colorimetric assay can provide similar data and thus replace the ^{3}H putrescine incorporation assay, we measured total TG activity using both the ^{3}H putrescine and colorimetric assay of the cell lysates from OK, NRK52E and MDCKII cells transfected with 5 domain deletion mutants of TG2: TG2 lacking the β-sandwich domain (-bsw); the

β-barrel 2 domain (-b2); both β-barrel domains (-b1b2); the TG2 core domain (core). Total TG activity increased by 5-10 folds in transfected cells compared to wild type (non-transfected control) in both the ^{3}H putrescine (Figure 3.4-3A-C) and colorimetric assay (D-F). All the mutants of TG2 were equally active for TG activity in OK (Figure 3.4-3 A&D), NRK52E (B&E) and MDCKII cells (Figure 3.4-3 C&F) irrespective of the assay used. As both ^{3}H putrescine and colorimetric assay can detect baseline TG activity (wt) and distinguish the difference of TG activity between transfected cells and non-transfection control (wt), the colorimetric assay was used for all measurement for total TG activity in this study as cheaper, quicker and free of isotopes.

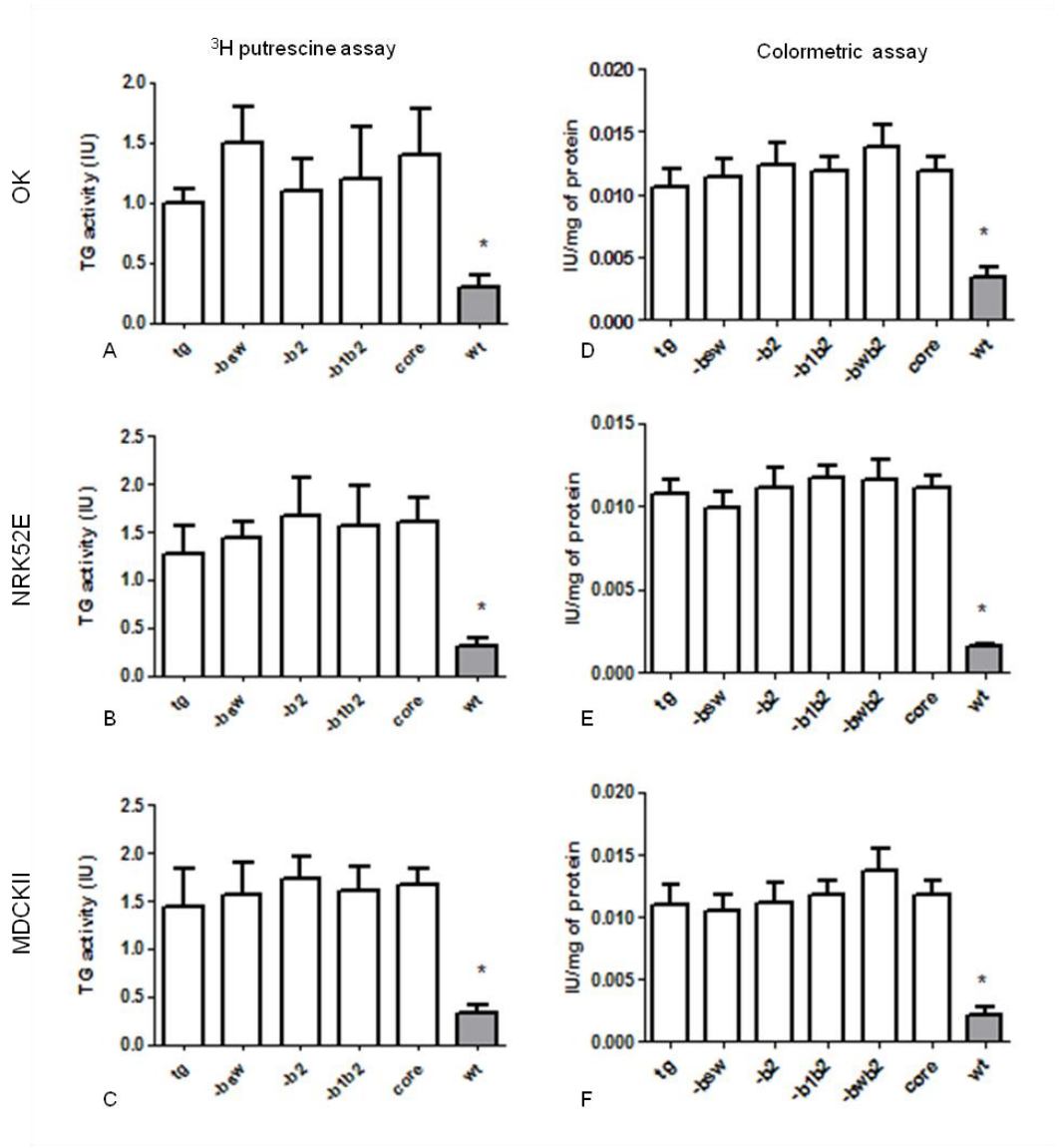

Figure 3.4-3 Total TG activity in the cell lysate using 3H putrescine and colorimetric assay

*Total TG activity in the cell lysate of OK, NRK52E and MDCK II cells was measured 48 hours post transfection with tetracysteine tag vectors containing TG2 constructs. tg: full length TG2 cDNA, -bsw: TG2 with β-sandwich domain missing, -b2: TG2 with barrel 2 domain missing, -b1b2: TG2 with barrel 1&2 missing, core: core domain only, wt: non-transfection control. Data represents mean values ±SEM. *: p<0.05, n=5*

3.4.7 Cell surface biotin-cadaverine incorporation

Extracellular TG activity was measured by the incorporation of biotinylated cadaverine into fibronectin described by Jones et al (Jones *et al.* 1997). A

96-well plate was pre-coated with 100 µl of 5 µg/ml plasma fibronectin (Sigma) in 50 mM Tris buffer (pH 7.4) and kept at 4°C overnight. The next day, the fibronectin solution was discarded and the wells were washed with PBS. Cells were harvested using 2 mM EDTA in PBS for 10 minutes at room temperature and pelleted by centrifugation at 400g (Fisons MSE) for 5 minutes. Cells were resuspended in 10 ml serum-free DMEM medium and counted using a haemocytometer.

8×10^4 cells in 100 µl serum-free DMEM containing 0.1 mM biotinylated cadaverine (Molecular Probes, Netherlands) per well were plated and incubated for 1 hour at 37°C. Negative controls were serum free culture medium with biotinylated cadaverine. The reaction was stopped by two washes of 5 mM EDTA in PBS. The cells were lysed using 100 µl of a detergent solution consisting of 0.1% (w/v) sodium deoxycholate in PBS & 5 mM EDTA with 20 minutes of incubation at room temperature. EDTA was added to inhibit any TG activity released from lysed cells. The supernatant was removed and used to determine the amount of cellular protein using the BCA assay (Section 3.4.13). The remaining fibronectin layer was washed three times with PBS. The wells were blocked with 3% (w/v) bovine serum albumin (BSA) in PBS for 30 minutes at 37°C and incubated with a 1:5000 dilution of extravidin horse radish peroxidase (HRP) conjugate (Sigma) for 1 hour at 37°C. Incorporated biotinylated cadaverine was revealed using 0.01% (w/v) 3,3',5,5'-tetramethylbenzidine (TMB) (Sigma) in 50 mM phosphate / citrate buffer (50 mM dibasic sodium phosphate, 25 mM citric acid, pH 5.0). The resulting colour was then read in an ELISA plate reader (Labsystems Multiskan Ascent) using Genesis Software (version 3.05) at 450 nm. The standard curve (Figure 3.4-4) was obtained using Guinea pig liver transglutaminase.

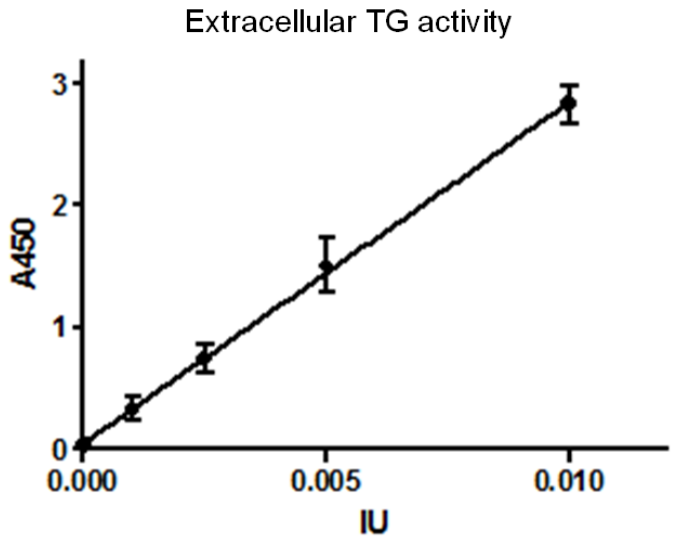

Figure 3.4-4 Standard curve for the extracellular TG activity assay

The standard curve was obtained using Guinea pig liver transglutaminase showing a linear response between A450 nm and 0.0001 to 0.01 IU of transglutaminase on cell surface.

3.4.8 Extracellular TG2 antigen measurement using the modified ELISA

The amount of extracellular TG2 antigen was quantified using a modified quantitative ELISA adapted from the one described by Achyuthan et al (Achyuthan *et al.* 1995). 8×10^4 cells per well were prepared as above and plated into a fibronectin coated 96-well plate as previously described. Cells were allowed to incubate in serum-free DMEM for 2 hours at 37°C before being washed twice with PBS and lysed using 100 µl per well of 0.1% (w/v) deoxycholate in PBS containing 5 mM EDTA at room temperature for 20 minutes. The supernatant was removed and used for quantification of cellular protein. The remaining fibronectin layer containing TG2 was washed three times with PBS. Wells were then blocked with 3% (w/v) BSA in PBS for 30 minutes at 37°C and incubated with a 1:500 dilution of anti-TG2 mouse monoclonal antibody cub 7402 (Neomarkers, USA) at 4°C overnight. Samples incubated without cub 7402 were used as negative controls. The wells were washed 3 times with PBS containing 0.1% (v/v) Tween 20 and incubated

with a 1:1000 dilution of HRP conjugated goat anti-mouse IgG (Dako, Denmark) at 37°C for 1 hour. Following 3 washes with PBS/Tween, TMB was added and the resulting colour was then read in an ELISA plate reader (Labsystems Multiskan Ascent) using Genesis Software (version 3.05) at 450nm. The standard curve (Figure 3.4-5) was obtained using Guinea pig liver transglutaminase.

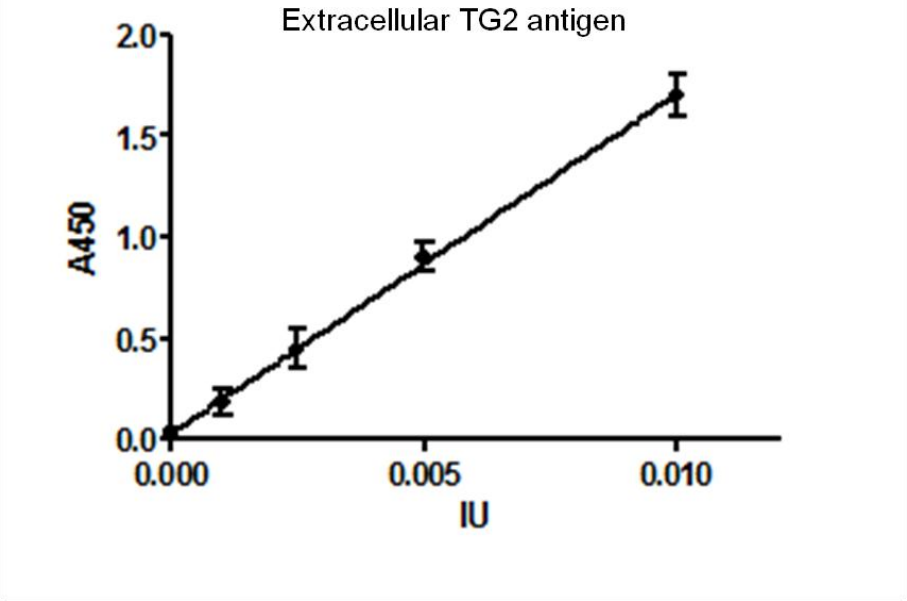

Figure 3.4-5 Standard curve for extracellular TG2 antigen assay

The standard curve was obtained using Guinea pig liver transglutaminase showing a linear response between A450 nm and 0.0001 to 0.01 IU of extracellular TG2 antigen.

3.4.9 HaloTag® protein measurements

HaloTag protein® was measured using ELISA according to manufacturer's instructions. 50µl of cell lysate or culture medium was plated into 96-well plate and incubated at 37°C for 1 hour. After three washes of 1% (w/v) of BSA, rabbit anti-HaloTag pAb (G9281, Promega, UK) at 1:500 was added in each well and incubated for 1 hour at 37°C. Following three washes of 1% (w/v) BSA, anti-rabbit immunoglobulins/HRP at 1:1000 was added and incubated for 1hr at

37°C. The anti-HaloTag protein pAb and anti-rabbit immunoglobulins/HRP binding was revealed by TMB and read at 450 nm.

3.4.10 Immunoblotting

SDS-Polyacrylamide Gel Electrophoresis (PAGE): Gel preparation

20 ml of a 10% (v/v) polyacrylamide resolving gel was made up by mixing 7.9 ml ddH_2O, 6.7 ml 30% (w/v) acrylamide mix (Geneflow, UK), 5 ml 1.5 M Tris (pH 8.8), 200 µl 10% (w/v) SDS and 200 µl of fresh 10% (w/v) ammonium persulfate, de gassing and then 8µl N,N,N',N'-tetramethylethylenediamine (TEMED) to initiate polymerisation. The mixture was poured into the assembled glass plates (Mini-PROTEAN II System, Biorad) and the gel allowed to set at room temperature. 10 ml of a 5% (v/v) polyacrylamide stacking gel was made up by mixing 6.8 ml ddH_2O, 1.7ml 30% (w/v) acrylamide solution, 1.25 ml 1M Tris (pH 6.8), 100 µl 10% (w/v) SDS, 100 µl 10% (w/v) ammonium persulfate and 10 µl TEMED. The mixture was poured on top of the set resolving gel and allowed to set for 30 minutes. 20 µg of cell lysate in no more than 10 µl was mixed with 10 µl reducing buffer [10 mM Tris (pH 6.8), 2.5% (w/v) SDS, 10% (v/v) glycerol, 0.02% (w/v) bromophen blue, 5% (v/v) β-mercaptoethanol] and boiled for 5 minutes. Samples were immediately loaded and separated by SDS-PAGE at 100 V till the blue dye reached the bottom of the gel.

Western blotting

The gel was removed from the gel tank and soaked in transfer buffer [39 mM glycine, 48 mM Tris, 20% (v/v) methanol] for 15 minutes. 8 pieces of 3 MM filter paper and 1 piece of Hybond C nitrocellulose membrane (Amersham Life Science) were cut to the same size as the gel and also socked in transfer buffer. Western blotting was performed using a Trans-Blot SD Semi-dry Transfer Cell (Biorad). 4 pieces of filter paper were placed on to the anode plate and bubbles removed. The nitrocellulose membrane was placed on the filter paper block and the gel was then positioned onto the membrane with bubbles removed again prior to the placement of the second block of 4 pieces of filter paper on the top to form a sandwich. The cathode plate was placed on the top of the gel and the electrode pins connected. Proteins in the gel were electroblotted onto the membrane for 30 minutes at 15V. Transfer of proteins from the gel to the

membrane was checked by staining the membrane with 0.1% (w/v) Ponceau S solution (Sigma). The western blot was blocked at room temperature for 1.5 hours with 5% (w/v) non-fat dry milk in TBST [20 mM Tris, 150 mM Sodium Chloride, 0.1% (v/v) Tween 20, pH 7.6] and probed overnight at 4°C with the primary antibody in TBST (Table 3.1-2). Following 3 washes with TBST, primary antibody was revealed with a secondary antibody. Protein bands were visualised using an ECL chemiluminescent detection system (Geneflow, UK). Blots were exposed to Kodak BioMax ML film for approximately 6 seconds, developed in GBX developer (Kodak) and fixed in GBX fixer (Kodak) for 2 minutes at room temperature. The appropriate length of exposure was assessed from the resulting films.

3.4.11 Immobilisation of HaloTag® fusion proteins on Halolink™ magnetic beads

HaloLink™ magnetic beads (G9311, Promega, UK) were used to immobilise and analyse HaloTag® fusion proteins including the β-sandwich domain, the TG2 export motif aa88-106 and the core domain (Section 3.1.7). To identify proteins that bind to the TG2 export motif aa88-106, cell lysates from NRK52E cells transfected with HaloTag® containing the TG2 export motif aa88-106, β-sandwich domain and core domain were immobilised using HaloLink™ magnetic beads. Proteins that bind to the TG2 export motif aa88-106 are also immobilised and can be visualised by SDS PAGE using silver staining. The bands present in cells transfected with the TG2 export motif aa88-106 and β-sandwich domain that also contains the export motif, but not on the core domain construct indicate proteins specifically binding to the TG2 export motif. These bands can be cut out and further analysed by mass spectrometry to identify amino acid sequences. of proteins that bind to the TG2 export motif aa88-106.

Cell lysates from NRK52E cells were prepared as described in Section 3.4.1 using NP-40 cell lysis buffer at 48 hours post transfection. HaloLink™ magnetic beads were equilibrated with 3 washes of 200µl binding buffer (100mM Tris-HCl, 150mM NaCl, 0.01% IGEPAL® CA-630 pH 7.6). 50µl of cell lysate was added to the equilibrated HaloLink™ magnetic beads and mixed by

inversion on a tube rotator at 4°C for 1 hour. The magnetic beads were captured by placing the tube on a magnetic stand and supernatant was removed. After 3 washes of 200 µl binding buffer, the “TG2 export motif 88-106-candidate protein complex” was released with 20 µl of Factor Xa Protease (V5581, Promega) buffer (5 µg Factor Xa Protease in 20 mM Tris-HCl, 0.1 M NaCl, pH 7.4) at room temperature for 1 hour. The magnetic beads were captured by placing the tube on a magnetic stand and supernatant was analysed by SDS-PAGE.

3.4.12 Silver stain

SDS-polyacrylamide gels were fixed with 40% (v/v) Methanol & 12% (v/v) glacial acetic acid at 4ºC overnight. After decanting off the fixing solution, the gels were washed with 30% (v/v) ethanol three times. The gels were sensitised in 0.02% (w/v) sodium thiosulphate for 90 seconds followed by three washes of deionised water. The gels were stained with 0.2% (w/v) silver nitrate & 0.02% (v/v) formalin for 20 minutes. After three washes of deionised water, the gels were developed in 3% (w/v) sodium carbonate, 0.05% formalin and 0.000005% (w/v) sodium thiosulphate until the stained protein band becoming clearly visible. After two washes with deionised water, the staining was stopped using 0.5% (v/v) glycine.

Table 3.4-2 List of antibodies used for immunoblotting

Primary antibodies	Dilution	Secondary antibodies	Dilution
Mouse anti-transglutaminase 2 antibodies cub7402 (ab2386, Abcam, UK)	1:750	Anti-mouse IgG-HRP (P0447, Dako, UK)	1:1000
Mouse anti-fibronectin antibodies (Ab6328, Abcam, UK)	1:1000	Anti-mouse IgG-HRP	1:1000
Rat anti-large T antigen (ab18187, Abcam, UK)	1:1000	Anti-rat IgG-HRP (ab7097, Abcam, UK)	1:5000
Goat anti-tapasin antibodies (sc11473, Santa Cruz biotechnology, UK)	1:1000	Anti-goat IgG-HRP (P0449, Dako, UK)	1:2000
Goat anti-translocon-associated proteins antibodies (sc54414, Santa Cruz biotechnology, UK)	1:1000	Anti-goat IgG-HRP	1:2000
Mouse anti-β-actin (ab8226, Abcam, UK)	1:1000	Anti-mouse IgG-HRP	1:1000

3.4.13 Quantitation of total protein by bicinchoninic acid assay

Total protein was determined in cell lysates using the bicinchoninic acid assay. A standard curve was prepared of 0, 0.4, 0.8, 1.2, 1.6, 2.0 mg/ml BSA in distilled water. A volume of 1ml of BCA working solution [25 parts solution A (1% (w/v) bicinchoninic acid, 2% (w/v) sodium carbonate, 0.16% (w/v) sodium tartrate, 0.4% (w/v) sodium hydroxide, 0.95% (w/v) sodium hydrogen carbonate): 1 part solution B (4% (w/v) copper sulphate)] was added to samples and standards. All tubes were vortexed prior to incubation at 37^{o}C for 30 minutes. 200 µl of standards and samples were pipetted in duplicate into a 96 well plate and the optical density read at 600 nm on a 96 well plate reader (Labsystems Multiskan Ascent).

3.4.14 Immunofluorescent staining

3.4.14.1 Optimisation of cell fixation

To optimise cell fixation of the subsequent procedures, cells were fixed using the following fixation solutions:

1. Ice cold methanol for 20 minutes (methanol)
2. Ice cold acetone for 20 minutes (acetone)
3. 50% (v/v) methanol and 50% (v/v) acetone for 20 minutes (M+A)
4. 4% (w/v) paraformaldehyde in PBS, pH 7.2 for 1 hour (PFA)

5. Bouin’s solution for 1 hour (Bouin)
6. 1% (v/v) glutaraldehyde in PBS pH 7.2 for 2 hours (Glutaraldehyde)
7. 50% (v/v) ethanol, 5% (v/v) glacial acetic acid, 4% (v) paraformaldehyde in ddH_2O for 20 minutes (FAA)

Cells were transfected with a pcDNA6.2/cTC-Tag-DEST plasmid containing full length TG2. 48 hours post transfection, the cells were stained with organelle light orange ER (red) (Section 3.4.14.7) and FlAsH (green) for the tagged TG2. The images for the cells fixed with methanol, acetone and 4% paraformaldehyde (PFA) were similar in the fluorescent signals intensity and coverage for ER and TG2 (Figure 3.4-6). The details for ER (red) and TG2 staining (green) can be observed. Some co-localisation of ER and TG2 staining was found around the cell nucleus (blue). The image for cells fixed with 1% (w/v) glutaraldehyde was associated with a higher background signal of FlAsH and Organelle light in the cytosol that makes it difficult to identify organelles from TG2 stains. The images for the cells fixed with Bouin’s solution and methanol+acetone (M+A) were similar and showed less detailed for the structure of the organelles compared to the image obtained from acetone, methanol and PFA fixation. ER should be visible as a membrane structure that runs round the cell nucleus and cytosol. However, most of the images obtained showed a dot pattern and more linear structure can be visualised in the cells fixed using PFA. PFA therefore was selected as standard fixation method in this study.

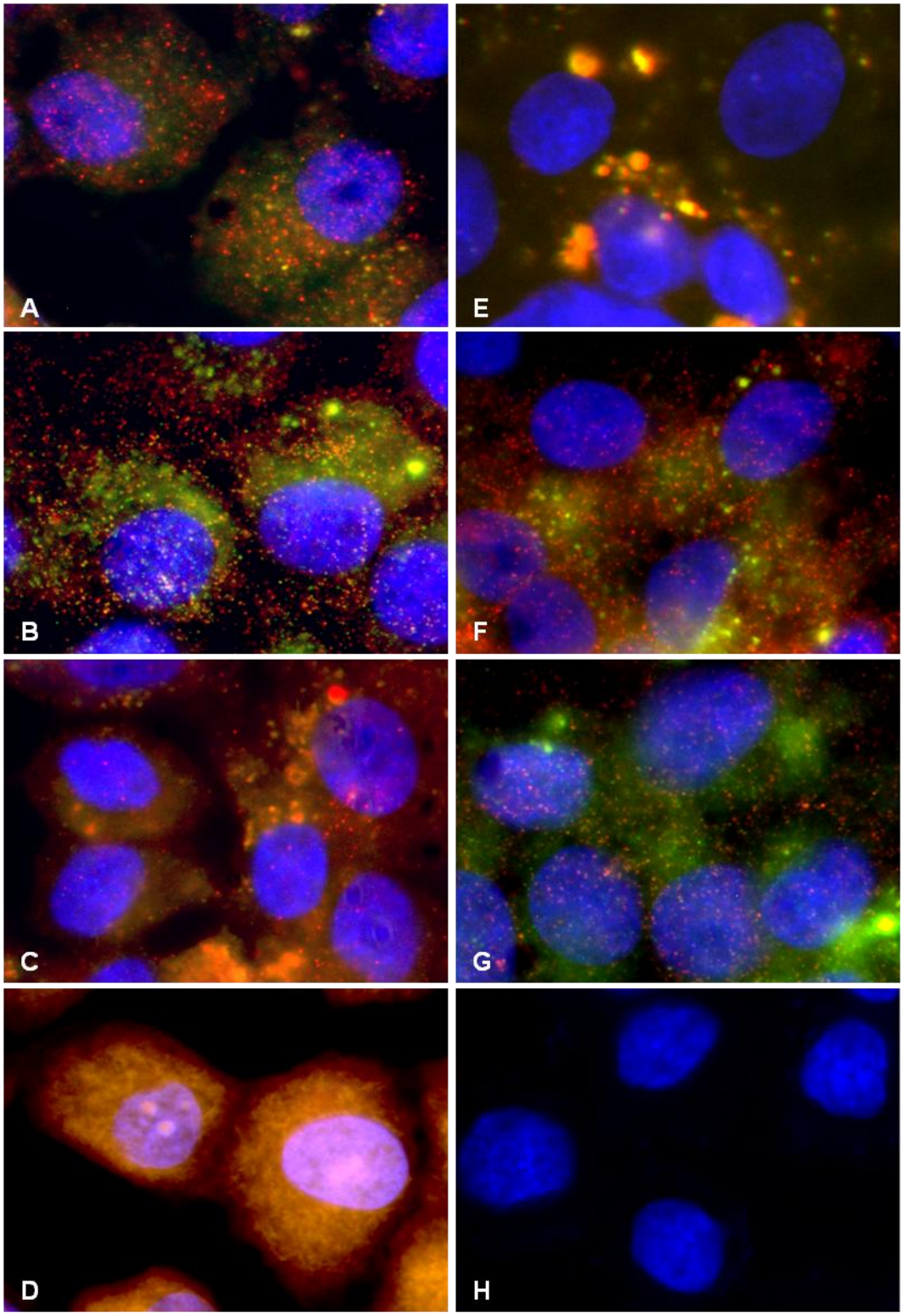

Figure 3.4-6 TG2 and ER fluorescent images of cells fixed using different solution

Cells stained with Organelle-light ER (red) and FlAsH-TG2 (green) fixed using A. pure methanol, B. acetone, C. Bouin's solution, D.1% (v/v) glutaraldehyde, E. 50%(v/v) methanol & 50% (v/v) acetone F. 4% (w/v) paraformaldehyde (PFA), G.50% (v/v) ethanol, 5% (v/v) glacial acetic acid, 4% (w/v) paraformaldehyde (FAA). H. Wild type NRK52E cells without ER and FlAsH stain

3.4.14.2 Mounting reagents

Mowiol mounting solution

2.4 g of Mowiol 4-88 (sigma) was mixed with 6 g of glycerol by stirring. 6 ml of ddH_2O was added and left stirring for 2 hours at room temperature. 12 ml of 0.2 M Tris-HCl (pH 8.5) and 4 mg of sodium azide was added into the mix. After incubation at 60°C for 10 minutes, the mix was centrifuged at 5,000 *g* for 15 minutes and undissolved solids were removed. 0.1% (w/v) p-phenylenediamine solution (prepared separately and protect from light) was added to the Mowiol solution before use (1:9).

Other mounting reagents used include ProLong® Gold antifade reagent (P36930, Invitrogen, UK) and VECTASHIELD HardSet Mounting Medium (H-1400, vector laboratories, UK).

3.4.14.3 Optimisation of mounting reagents

VECTASHIELD HardSet mounting medium with 4', 6 diamidino-2-Phenylindole (DAPI) was associated with a high blue background signal. ProLong® Gold antifade reagent (Invitrogen) and Mowiol mounting solution with DAPI (final concentration 0.5 µg/ml) provides a similar antifade effect on fluorescence. Mowiol mounting solution has the advantage of hardening at room temperature and is cheaper. Mowiol mounting solution with DAPI was used in this study.

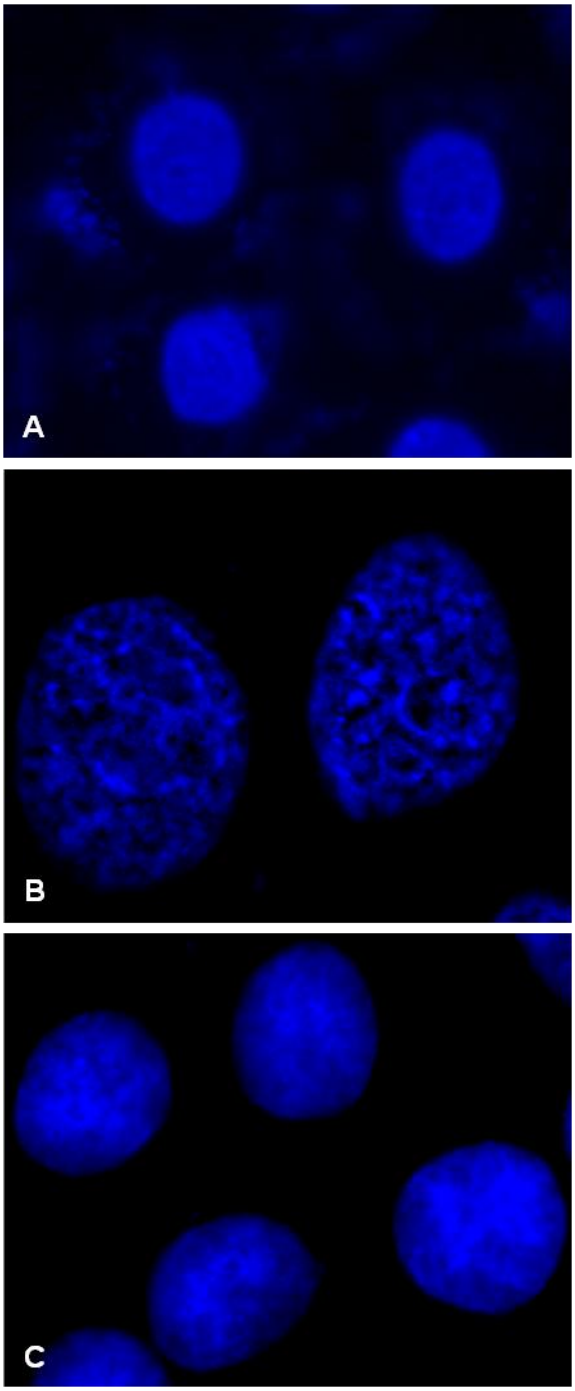

Figure 3.4-7 Fluorescent images using different mounting reagents

NRK52E cells VECTASHIELD HardSet mounting medium with DAPI (A) ProLong® Gold antifade reagent (B) and Mowiol mounting solution with DAPI (C). The cell nucleus was blue using DAPI.

3.4.14.4 FlAsH and ReAsH staining

The FlAsH and ReAsH-EDT2 staining was performed using the TC-FlAsH™ TC-ReAsH™ II In-cell Tetracysteine Tag Detection Kit (T34563, Invitrogen, UK).

After the removal of culture media, the cells were washed once with 2ml of Opti-MEM. 1ml of labelling solution (2.5 µM FlAsH-EDT2 or ReAsH-EDT2 reagent in Opti-MEM) was added in each well. The plate was incubated for 30 minutes at 37ºC while protected from light. For dual labelling the cells were washed once with BAL buffer, followed by the complete growth medium, and incubate at 37ºC for the desired amount of time. The labelling procedure was repeated with the second labelling solution.

3.4.14.5 Validation of FlAsH and ReAsH staining

To validate FlAsH and ReAsH staining, NRK52E cells were transfected with a suitable tetracysteine tag vector or non-tetracysteine tag vector such as, pCIneo-hTG (Huang *et al.* 2004). 48 hours post transfection the cells were incubated with either FlAsH or ReAsH reagents before visualisation. Clear green (FlAsH) and red (ReAsH) fluorescent signals were found in the cells transfected with tetracysteine tag vector (Figure 3.4-8) and little back ground fluorescent signals were found in the cells transfected with non-tetracysteine tag vector confirming that tetracysteine tag staining technology was suitable to these cells.

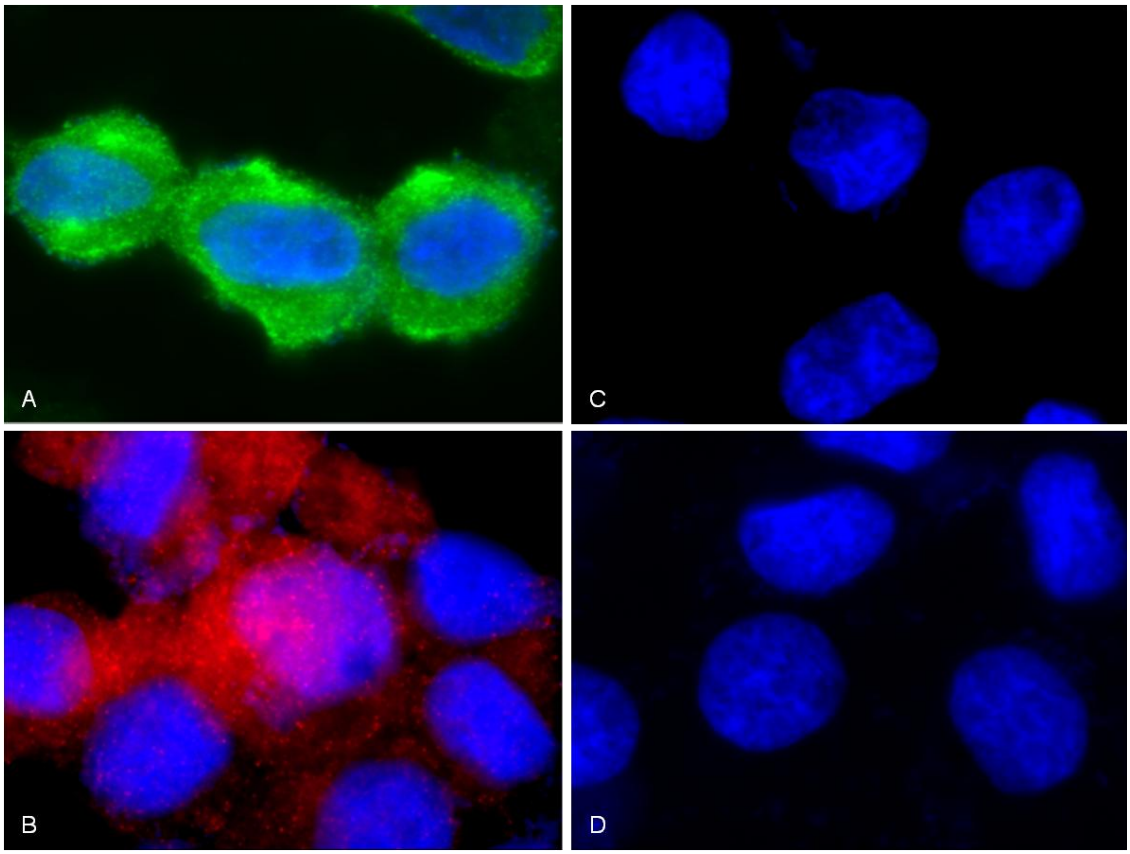

Figure 3.4-8 Validation of tetracysteine tag staining

NRK52E cells transfected with tetracysteine tag vector followed by incubation with FlAsH (A) or ReAsH (B) reagents 48 hours after transfection. Cells transfected with pCIneohTG that is a non-tetracysteine vector containing TG2 cDNA incubated with FlAsH (C) and ReAsH (D) reagent. The cell nucleus was stained with DAPI in blue.

3.4.14.6 Immunofluorescent staining

Cells were grown on sterilised microscopy glass cover slips to an optimal confluence and harvested after 3 washes of PBS. The cover slip was fixed with 4% (w/v) PFA and blocked with blocking buffer [3% (w/v) BSA, 0.1% (w/v) Tween 20 in PBS, pH 7.4] at room temperature for 1 hour. The cover slip was incubated with the selected primary antibody with an optimal dilution in blocking buffer at 4°C over night (Table 3.4-3). After 3 washes of blocking solution, the cover slip was incubated with the selected secondary antibody with an optimal dilution in blocking buffer at 37°C for 1.5 hours (Table 3.4-3). After three washes of PBS, the cover slip was mounted with MowioI mounting solution with or without with DAPI (0.5 µg/ml) (Vector Laboratories, UK) and allowed to set in the dark.

To visualise TG2 transport, NRK52E cells were grown on sterilised microscopy slide cover slips and incubated with 2.5 µM FlAsH-EDT2 reagent (Invitrogen, UK) for 30 minutes at 37°C to stain TG2. After this, the cover slip was rinsed in PBS and fixed with 4% (w/v) PFA. For co-localisation dual immunofluorescent staining was performed using the following antibodies at a 1:300 dilution; monoclonal anti-human collagen IV (C1926, Sigma, UK); rabbit polyclonal human calnexin (endoplasmic reticulum) (C4731, Sigma, UK); monoclonal anti-Golgi 58K protein (G2404, Sigma, UK) & monoclonal anti-LAMP2 (lysosomes) (SAB1402250, Sigma, UK). Secondary antibodies were polyclonal anti-rabbit IgG-TRITC (T5268, Sigma, UK) and anti-mouse IgG-TRITC at 1:500 (T5393, Sigma, UK). Cell organelle staining, cell markers and antibodies used in this study are listed in Table 3.4-3. Images were acquired on an Olympus BX-61 microscopy using Cell^F software. FlAsH, ReAsH, FITC, TRITC, DAPI, OFP (orange) filters were used according to the fluorochrome used.

Table 3.4-3 List of antibodies and reagents used for immunofluorescent staining

Primary antibody (dilution)	Dilution	Secondary antibody (dilution)	Dilution
Cell Junction			
Mouse anti-β-Catenin (610154, BD Transduction laboratories, UK)	1:300	Anti-mouse IgG-TRITC (T5393, Sigma, UK)	1:500
Mouse anti-E-Cadherin (610182, BD Transduction laboratories, UK)	1:300	Anti-mouse IgG-TRITC	1:500
Apical			
Texas Red-X phalloidin (T7471, Invitrogen, UK)	1:100		
Basolateral			
Mouse anti-collagen IV (C1926, Sigma, UK)	1:100	Anti-mouse IgG-TRITC	1:500
Endoplasmic reticulum			
Rabbit anti-calnexin (C4731, Sigma, UK)	1:100	Anti-rabbit IgG-TRITC (T5268, Sigma, UK)	1:500
Organelle Lights™ ER-OFP (O36223, Invitrogen, UK)			
Golgi apparatus			
Mouse anti-Golgi 58K (G2404, Sigma, UK)	1:300	Anti-mouse IgG-TRITC	1:500
Organelle Lights™ Golgi-OFP (O36224, Invitrogen, UK)			
Lysosome			
Mouse anti-LAMP2 (SAB1402250, Sigma, UK)	1:100	Anti-mouse IgG-TRITC	1:500
Plasma membrane			
Organelle Lights™ PM-CFP (O36216, Invitrogen, UK)			
CellMask™ Orange plasma membrane (C10045, Invitrogen, UK)	1:1000		
Proteins			
Mouse anti-transglutaminase 2 antibodies cub7402 (ab2386, Abcam, UK)	1:300	Anti-mouse IgG TRITC (T2402, Sigma, UK)	1:200
		Anti-mouse IgG FITC (F0257, Sigma, UK)	1:200
		Anti-mouse IgG FITC (ab7064, Abcam, UK)	
TG2 FlAsH-EDT2 or ReAsH-EDT2 reagent	1:1000		
Rat anti-large T antigen (ab18187, Abcam, UK)	1:300	Anti-rat IgG-TRITC (ab7094, Abcam, UK)	1:500
Goat anti-tapasin antibodies (sc11473, Santa Cruz biotechnology, UK)	1:100	Anti-goat IgG-TRITC (T7028, Sigma, UK)	1:300
Goat anti-translocon-associated proteins antibodies (sc54414, Santa Cruz biotechnology, UK)	1:100	Anti-goat IgG-TRITC (T7028, Sigma, UK)	1:300
Mouse anti-β-actin (ab8226, Abcam, UK)	1:300	Anti-mouse IgG-TRITC	1:500

3.4.14.7 Organelle light staining

Organelle light™ ER and Golgi stains were obtained from Invitrogen. Organelle light™ reagents contain baculovirus that upon entry into mammalian cells, directs the expression of autofluorescent proteins that are localized to specific organelles via a signal peptide. Organelle light™ ER targets calrecitulin and KDEL (ER retention signal). Organelle light™ Golgi targets Golgi-resident enzyme (N-acetylgalactosaminyltransferase 2). The advantages of using organelle lights to visualise cell structures include it can be used in live cell imaging and double labelling of organelles.

1×10^5 Cells were seeded into a 6-well plate and allowed to attach overnight at 37°C. Culture medium was removed and 550 µl of Organelle light solution (200 µL of Organelle Lights™ reagent mixed with 350 µL Dulbecco's Phosphate Buffered Saline (D-PBS) without Ca^{2+} or Mg^{2+}) was added in the well. The cells were incubated at room temperature in the dark for 3 hours with gentle rocking. The Organelle light solution was removed, replaced with culture medium containing 1x enhancer and the plate was incubated at 37°C for 2 hours. After the enhancer was removed, the cells were incubated at 37°C overnight and were ready for imaging.

3.4.14.8 Validation of organelle light fluorescent signal

To validate the fluorescent signals obtained from organelle light reagents, cells treated with organelle light reagents were compared to the stains obtained from anti-calnexin antibodies (C4731, Sigma) for ER and anti-Golgi 58K (O36224, Invitrogen) for Golgi apparatus. The fluorescent signals obtained from NRK52E cells stained with organelle light ER were predominately accumulated around the cell nucleus and some of the fluorescent signals in a reticular shape were found at the peripheral of the cytosol (Figure 3.4-9 A). Similar pattern of fluorescent signals distribution was found in the cells stained with anti-calnexin antibodies followed by anti-rabbit IgG-TRITC (B) confirming the Organelle light ER was picking up the ER.

Organelle light Golgi stained predominately around the cell nucleus with little fluorescent signals in the cytosol and followed a pattern consistent with Golgi apparatus sitting on ER. A similar distribution of Golgi apparatus was also

found in the cells stained with anti-Golgi 58K antibodies but with a slightly higher back ground fluorescent signals in the cytosol. This confirms that the organelle light stains for Golgi apparatus are fit for NRK52E cells. Organelle light ER and Golgi stains were selected because as an easy and fast option in this study.

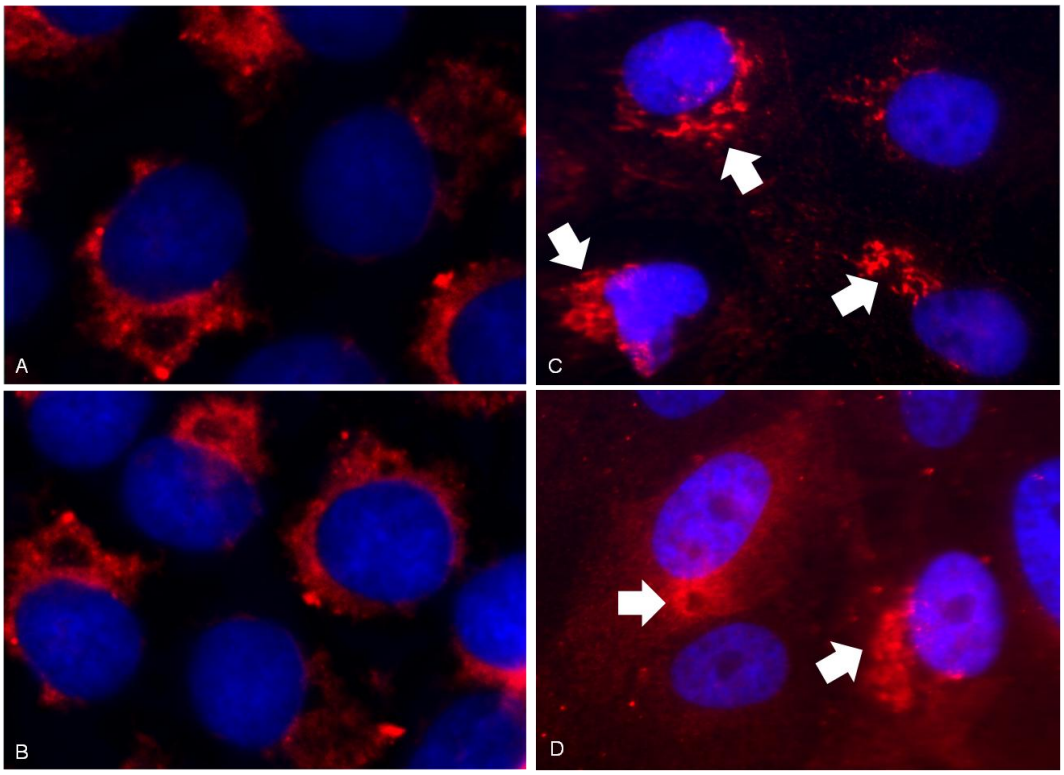

Figure 3.4-9 Comparison of organelle light stain for endoplasmic reticulum and Golgi apparatus with classical immunofluorescent staining of ER and Golgi markers

NRK52E cells were stained with organelle light ER (A) and anti-calnexin antibodies for ER (B) showing membrane like structure around the cell nucleus and in the cytosol. Organelle light Golgi apparatus (C) and anti-Golgi 58K antibodies for Golgi apparatus (D) showed a high density structure around the cell nucleus indicated by white arrows. The cell nucleus was stained with DAPI in blue

3.4.14.9 CellMask™ plasma membrane staining

Cells were grown on a cover slip or in a 6-well plate for an optimal time. After three washes of PBS the cover slip was incubated with CellMask™ plasma membrane stain (2.5 µg/ml) in PBS for 5 minutes at 37°C. The cover slip or plate can be visualised or fixed with PFA after three washes of PBS.

3.4.14.10 Optimisation of CellMask™ plasma membrane staining

Incubating CellMask™ plasma membrane reagent for 5minutes at 37ºC on live cells followed by 1-3 washes of PBS or medium was recommended in the instruction manual for CellMask™ plasma membrane reagent. However, the fluorescent signal was not only present on plasma membrane but was also found in the cytosol when applied to tubular epithelial cells (Figure 3.4-10 A). This makes it difficult to observe the position of intracellular components by co-localisation as well as determine when something is outside the cell membrane. We tested a series time of incubation times to try and optimise the procedure and found that 30 seconds of incubation with the CellMask™ reagent at room temperature followed by 3 washes of PBS showed the best fluorescent signal on plasma membrane with little background in the cytosol (Figure 3.4-10B) that is useful in observation of protein trafficking in 2D images.

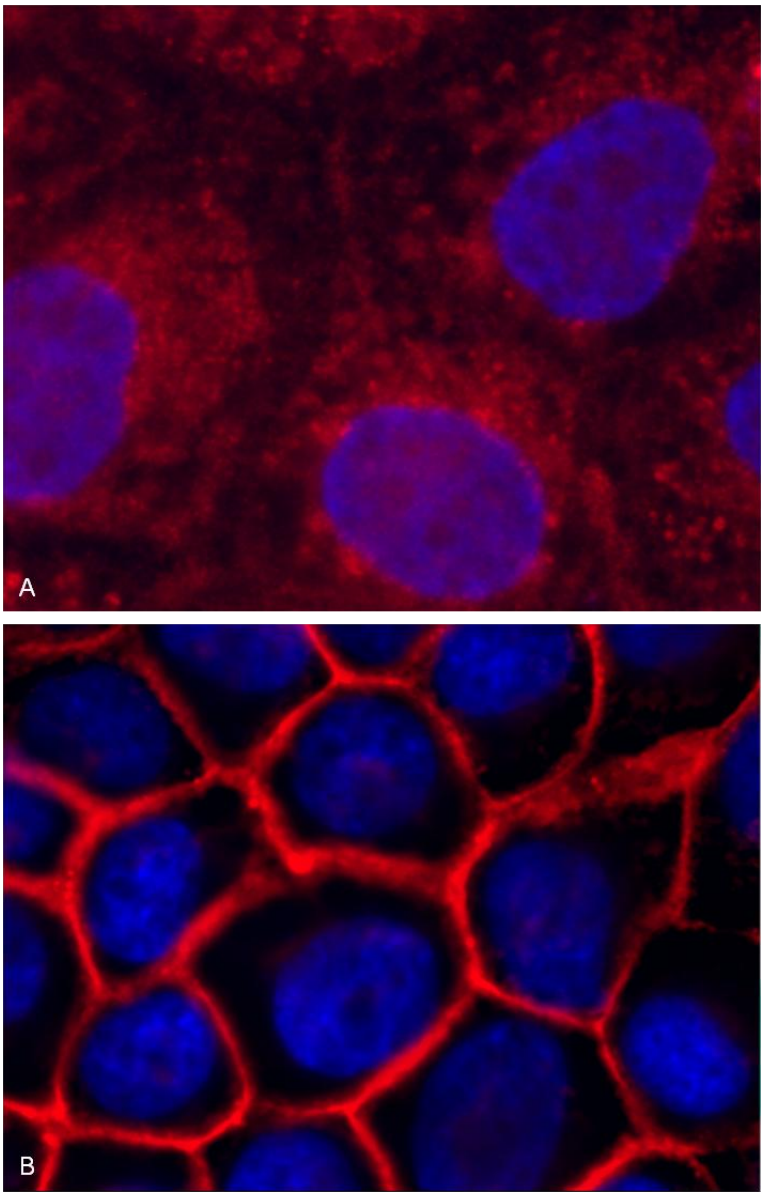

Figure 3.4-10 NRK52E cell stained with CellMask^{TM} plasma membrane

NRK52E cells were incubated with CellMask^{TM} plasma membrane reagent for 5 minutes at 37ºC followed by 1 wash of PBS (A) and 30 seconds at room temperature followed by 3 washes of PBS (B). A short incubation with more PBS washes provides a better observation of plasma membrane between cells in a 2D image. The cell nucleus was stained with DAPI in blue

3.4.15 Deconvolution microscopy

Deconvolution is a computational image processing technique for improving the contrast and resolution of digital images captured from the fluorescent microscopy. The image information like the size of each pixel and information about the particulars of the optics are given to the computer-based program, an algorithm excludes “out of focus” blur and reassigns “out of focus” light to its proper location. The characterisation of out-of-focus light is based on the 3D image of a point source of light called point-spread function (PSF). Each PSF can be localized using 3D coordinates (X, Y, Z; XY correspond to the focal-plane coordinates and Z corresponds to the direction of focal-plane axial coordinates). After mathematical calculation of the PSF results in a focused light source with a X,Y,Z coordinates that enable the generation of a 3D reconstruction image. Deconvolution microscopy has the advantages of generating clear image from multiple-focal plane and at very low light levels.

The 3D images generated by deconvolution microscope are crucial in this study. Many of the fluorescent signals were localised on top of or below the cell nucleus and many apparent co-localised proteins were actually not in the same focal plane. When one sees “green” TG2 around cell nucleus in conventional fluorescent microscopy, it is impossible to know if the TG2 is secreted in rough ER that is near the cell nucleus, translocated to sub-plasma membrane. We can visualise the exact location of TG2 using the tetracysteine tag in three-dimensional images using deconvolution microscopy and with 3D imaging rendering of the deconvolved data. Cells were grown on sterilised microscopy cover slips and visualised 48 hours post transfection or till an optimal confluence was reached. Plasma membrane, FlAsH and/or ReAsH reagents and organelle light staining were applied as described in Section 3.4.14.9 , Section 3.4.14.4 and Section 3.4.14.7 respectively. The cells were fixed after 3 washes of PBS and immunofluorescent staining (Section 3.4.14.6) applied as needed. Images were acquired on an Olympus BX-61 microscope using Cell^F software using a 100X objective lens with immersion oil (Numerical aperture 1.2). The Z-stock images were acquired every 0.2µm and the thickness of the cells were determined by the plasma membrane stains or DAPI for the cell nucleus (20-25 sections were taken). Where applicable

images were deconvolved using Autoquant X2 (Media Cybernetics, Silver Spring, MD, USA) with the specific setting to the acquired image stacks (X, Y, Z spacing, emission wavelength of the fluorescence, refractive index of the immersion oil and the point spread function (detailed in Section 3.4.16.1). Deconvolution algorithm settings were 20 iterations with a low noise level. The deconvoluted images were then 3D-rendered using Imaris (Bitplane AG, Zurich, Switzerland). A 3D blend model that shows the fluorescent signals or a 3D cartoon model that is the volume calculated from fluorescent signals obtained (Figure 3.4-11). The volume and the percentage of co-localisation of fluorescent signals can be also measured in the software as needed.

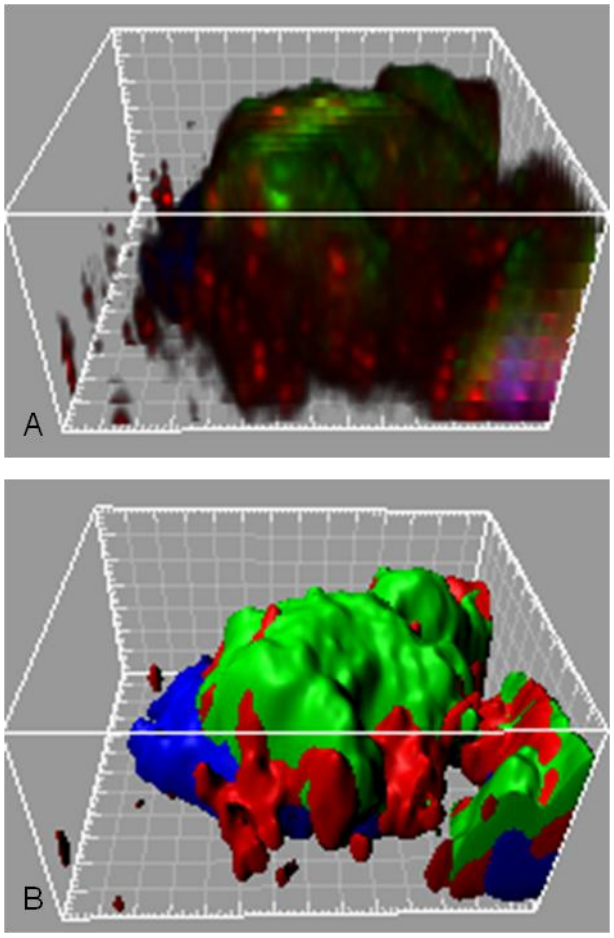

Figure 3.4-11 Three dimensional model generated using Imaris software

NRK52E cells transfected with pcDNA6.2/cTC-Tag-dest vector containing full length TG2 cDNA were stained green with FlAsH 24 hours post transfection and red with ReAsH 48 hours post transfection. The 3D blend image of fluorescent signals (A) and a cartoon image (B) based on the calculation of volume for each fluorescent signals. The volume of fluorescent signals less than the threshold intensity are not shown. The cartoon image (B) provides a better observation of the co-localisation of fluorescent signals. The image shows the basal side of the cell (basement membrane) upwards. TG2 synthesised in the last 24 hours (red) is located around the cell nucleus and where as TG2 synthesised in 24-48 hours (green) accumulates at basal side of the cells. The cell nucleus is stained with DAPI in blue.

3.4.16 Optimisation of image acquiring for deconvolution microscopy

3.4.16.1 Point spread function for different fluorescent

A point spread function (PSF) is a mathematical function that describes distortion in terms of the pathway a theoretical source of light takes through the observed samples. Such a light source contributes a small area of fuzziness to the final image. The PSF of the z-stack image obtained from 0.1 µm fluorescent beads is shown in Figure 3.4-12 A in XY, XZ and Y plane. By correcting such an image based on a theoretical PSF an undistorted image can be obtained (Figure 3.4-12 B), however because the 0.1 µm fluorescent beads used are smaller than the limitation of the objective lens and camera, the green and red fluorescence from the bead are refracted differently and thus appear separated and spread. A perfect objective lens would be able to focus all light (red, green and blue) in the same spot; however, it is impossible to make perfect objective lens. Therefore signals obtained from three colour channels overlap but not in the same spot and thus need to be further corrected for the properties of the lens to generate a true image (Figure 3.4-12 C). Therefore to properly generate a high resolution image a PSF must use an algorithm that determines both the source and path of light through a sample

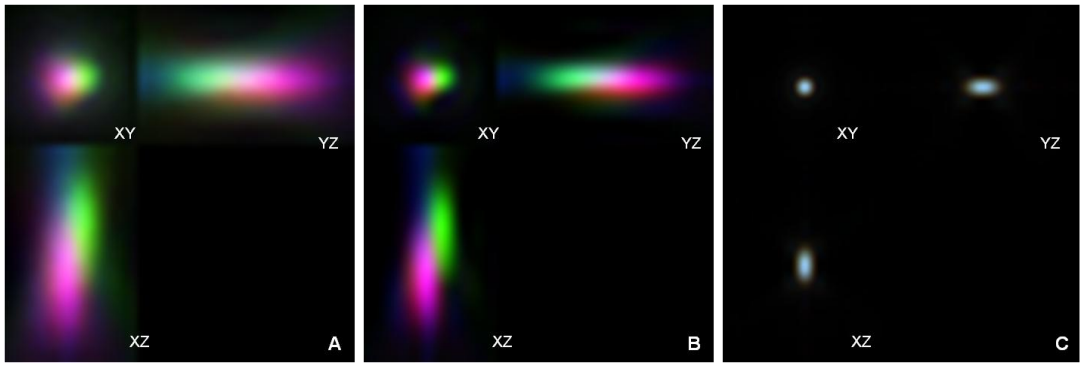

Figure 3.4-12 A point spread function for the objective lens

The point spread function was obtained from 0.1 µm fluorescent beads (A) and after correction for PSF (B). As the size of the beads is smaller than the limitation of the objective lens, the real 3D image of a bead should look like (C). The difference between (B) and (C) comes from the refraction of the different fluorescent wave lengths through the lens.

and have a objective lens correction. This allows an accurate deconvoluted image (Figure 3.4-12 C) allowing accurate co-localisation of three fluorescent colours (red, green and blue) in all 3 planes.

3.4.16.2 Nyquist rate

The image acquisition spacing in a Z-axis is another important factor in deconvolution microscopy. Too larger spacing (1 or 2 µm) may loose the detail of the fluorescent signals and thus not able to distinguish the location of two fluorescent signals. Equally too small spacing such as 0.1 µm means 20 to 30 images are required to cover the thickness of the cell and fluorescence is lost because of photobleaching at the end of image acquisition. The three fluorescent signals (red, green and blue) have different wavelengths and thus have different ideal acquisition spacing in Z-axis. The location of the fluorescent molecule in the Z-axis is not accurate in a large Z-axis spacing because the differences are caused by the differences of wavelengths.

Nyquist rate was used to determine the optimal spacing of Z-stack. Nyquist rate was calculated based on the type of microscopy, numerical aperture, excitation and emission wavelength of fluorescents and lens medium refractive index. A 0.2 µm acquisition space for Z-stock image for three fluorescents (red, green and blue) was used. A spacing less than 0.2 µm makes it impossible to distinguish the real Z-position of the fluorescence. The difference in Z-position can be caused by the different wave length of different fluorescents, for example a red and green fluorescent signal can be focused in different plane but are in fact on the same Z-position.

3.4.17 Live cell imaging

TG2 is mainly localised at the basal side of the cell where it attaches to the basement membrane. It is difficult to observe TG2 externalised through the plasma membrane using statics images and thus live cell imaging was used. Images were acquired on an Olympus IX81 inverted microscopy with a incubator chamber using a Hamamatsu Orca camera and SimplePCI (Hamamatsu) software. Cells were grown in a 6-well plate as described in Section 3.2. The culture medium was replaced with 1ml of serum free Dulbecco's Modified Eagle Medium (D-MEM) without phenol red (21063-029,

Invitrogen). The focus plane was sat using phase contrast images and the fluorescent signals obtained using the specific filter with an automatic acquisition every 1 minute for 200 minutes. The focus plane was automatically re-set after 10 images had been acquired. The images acquired were exported to AVI or WMV video files using Imaris as needed. The imaging was performed 48 hours after transfection at 37ºC for an optimal period of time.

3.4.17.1 Optimisation of live cell imaging acquisition

To visualise TG2 externalisation in TECs, the maximum duration of live cell imaging that can be acquired before cell apoptosis or any other morphological changes occur was determined using wild type NRK52E cells stained with CellMask^{TM} plasma membrane (red) (Section 3.4.14.9). Cells were placed on an Olympus IX81 microscopy with incubation at 37ºC for 4 hours. The images were acquired every 5 minutes with a maximum of 240 minutes. Images were displayed every 40 minutes from 0 minute to 200 minute (Figure 3.4-13 A-F) showing morphological changes over time.

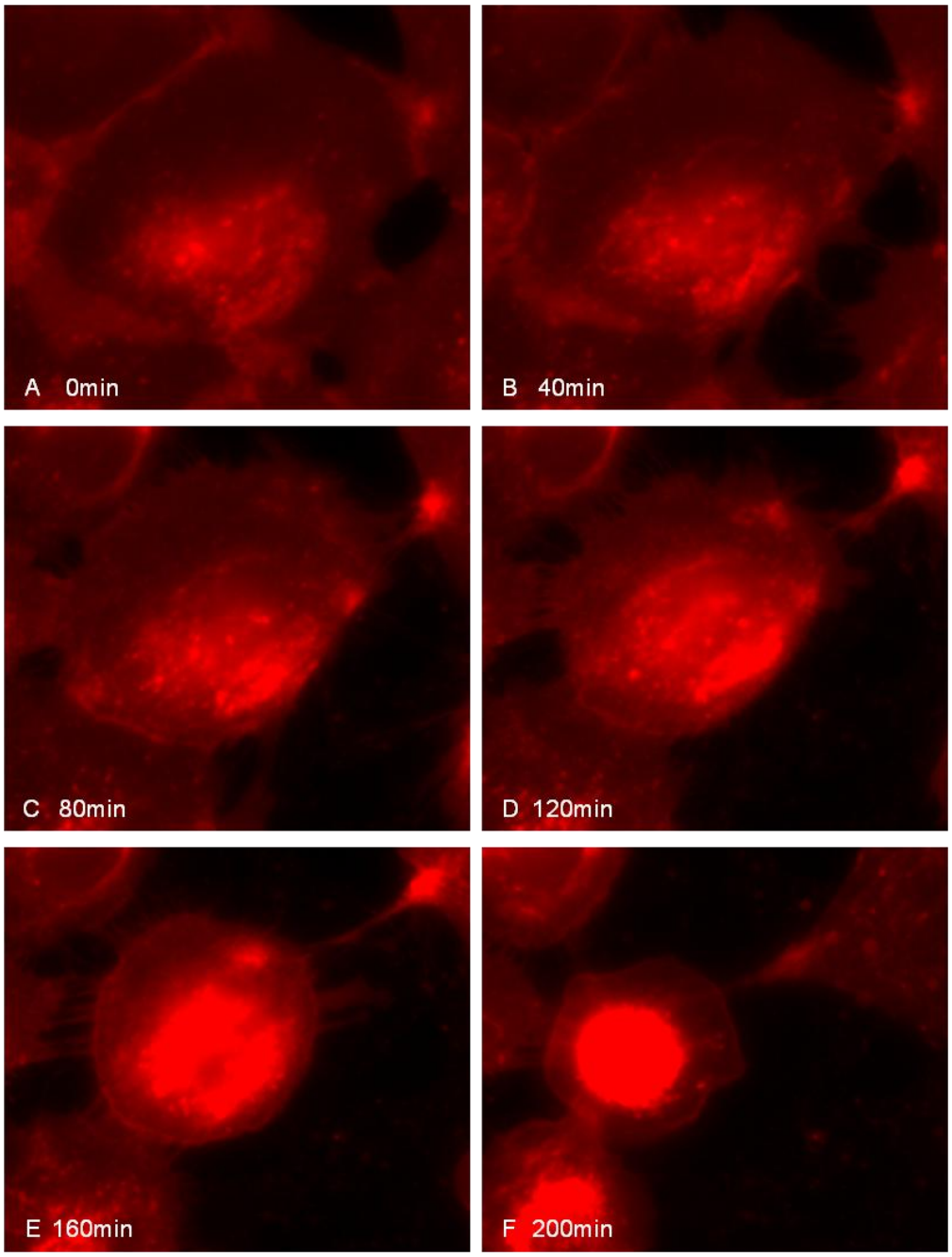

Figure 3.4-13 NRK52E cells with plasma membrane staining visualised for 200 minutes

To determine the maximum duration of live cell imaging, NRK52E cells with CellMask™ plasma membrane stains (images acquired every 20 seconds) were shown at 0 minute (A), 40 minutes (B), 80 minutes (C), 120 minutes (D), 160 minutes (E) and 200 minutes (F). The cell shrank with time and detached from the culture plate after 200 minutes.

3.4.17.2 Optimisation of fluorescent signals for live cell imaging

Antifade reagents such as sodium azide and p-phenylenediamine are toxic to cells and thus antifade reagents cannot be used in live imaging. To determine optimal duration for fluorescent imaging and total images before photobleaching of the fluorochrome, NRK52E cells were labelled with FlAsH reagent and visualised for a different interval and duration for example 1) every 10 seconds for 40 minutes, 2) every 20 seconds for 60 minutes, 3) every 1 minute for 40 minutes and 60 minutes, 4) every 2 minutes for 60 minutes, 120 minutes. The time of photobleaching was determined by the back ground fluorescent signals by an inability to distinguish the fluorescent signal in the cell and background (Figure 3.4-14).

The fluorescent signal can last for 80minutes using acquisition of one fluorochrome (green or red) with an interval of 20 seconds or 40minutes with an interval of 10 seconds.

To visualise TG2 externalisation using tetracysteine tag with FlAsH or ReAsH stain in live cell imaging, an acquisition time of 40 to 60 minutes with 20 seconds interval was used.

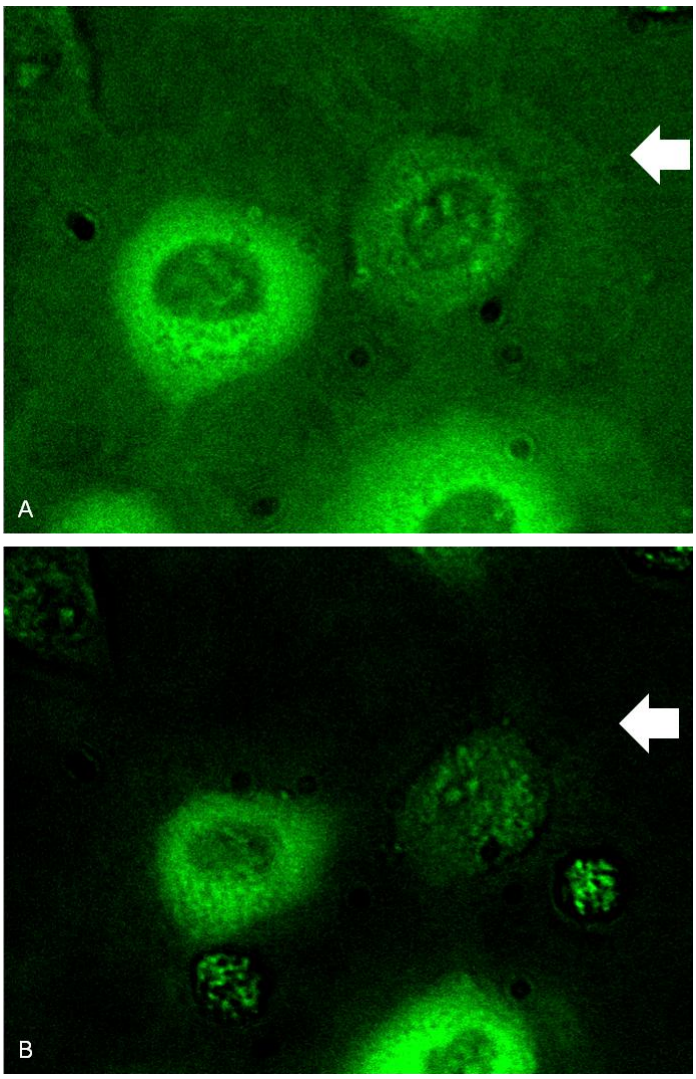

Figure 3.4-14 Live fluorescent signal fading with time

NRK52E cells were transfected with pcDNA6.2/cTC-Tag-dest vector containing full length TG2 cDNA (Gentile et al. 1991) & stained with FlAsH reagent before being visualised to determine the maximum time of live cell imaging. The time was determined using the differences of the cytosol and back ground fluorescent signals. The images are FITC merged with phase contrast at 0 minute (A) that cytosol fluorescent signal is different from back ground (white arrow). At 60 minutes (B) that the fluorescent signal at the peripheral of the cell was not different from back ground fluorescent (white arrow). 60 minutes is the maximum time for live cell imaging with phase contrast and FlAsH.

3.5 Yeast two hybrid screen

Yeast two hybrid (Y2H) screening was performed using Matchmaker Gold Yeast Two-hybrid System (Cat. No. 630489, Clontech, UK). In a Matchmaker GAL4-based two-hybrid assay (Figure 3.5-1), a bait protein is expressed as a fusion to the Gal4 DNA-binding domain (DNA-BD), while libraries of prey proteins are expressed as fusions to the Gal4 activation domain. As bait and library (prey) fusion proteins interact, the DNA-BD and AD are brought into proximity to activate transcription of four independent reporter genes (AUR1-C, ADE2, HIS3, and MEL1). AUR1-C is an antibiotics (Aureobasidin A) resistance gene in yeast. Y2H Gold is unable to synthesise histidine and adenine, the expression of ADE2 and HIS3 allow the cells to grow on histidine and/or adenine minimal medium. MEL1 encoded α-galactosidase that is an enzyme occurring naturally in many yeast strains and turn the yeast blue in the presence of the chromagenic substrate X-α-Gal. The yeast two hybrid assay can be used to identify novel protein interactions, confirm putative interactions and define interacting domains. In this study, we used Y2H library screen to indentify proteins that bind to the TG2 export motif aa88-106.

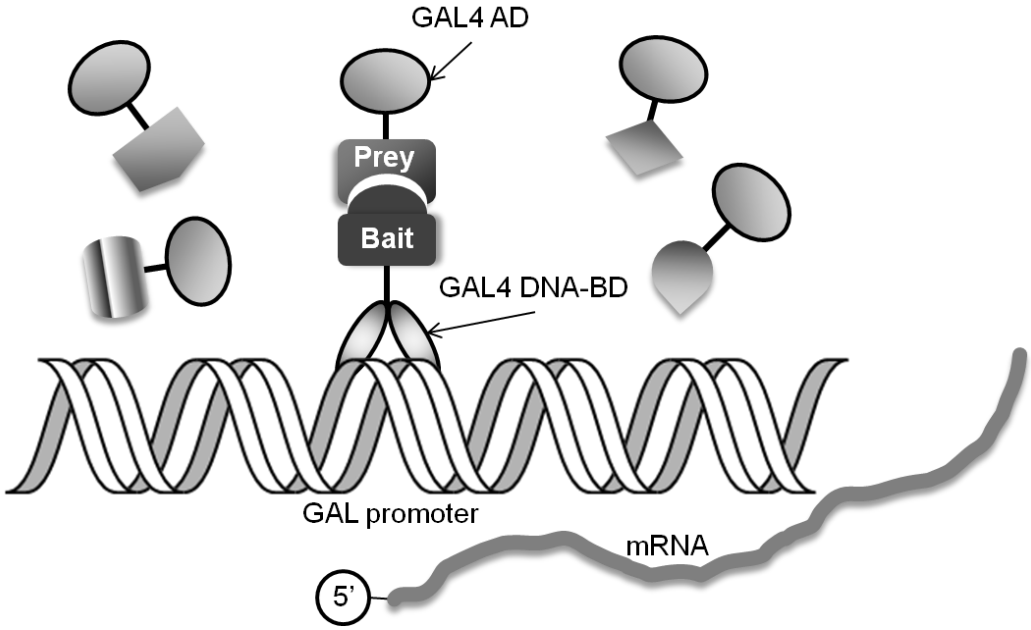

Figure 3.5-1 Principle of the two-hybrid principle

Two proteins are expressed separately, one (a bait protein) fused to the Gal4 DNA-binding domain (BD) and the other (a prey protein) fused to the Gal4 transciptional activation domain (AD). Thus activation of the reporters (AUR1-C, ADE2, HIS3, and MEL1) only occurs in a cell that contains proteins which interact and bind to the Gal4-responsive promoter in Y2HGold Yeast Strain.

3.5.1 Construct of pGBKT7 vector with motif 88-106

The TG2 export motif aa88-106 was cloned into the pGBKT7 DNA-BD vector (630443, Clontech, UK) (Figure 3.5-2) between Nde I and ECoRI restriction sites. The PCR products were generated with the primers as detailed (Table 3.5-1) using a standard PCR protocol (Section 0.). 50 ng pGBKT7 DNA-BD vector and 50 ng of PCR product was digested using Nde I (R6801, Promega, UK) and ECoRI restriction enzymes (R6017, Promega) in buffer D at 37°C for 1 hour followed by 10 minutes incubation at 65°C to inactive the restriction enzyme. DNA ligation was performed by combining 2µl 10X T4 DNA ligase buffer, the pGBKT7 DNA-BD vector, the PCR product, T4 DNA ligase (M0202, New England BioLabs, UK) with nuclease-free water to 20 µl. This was incubated at room temperature for 20 minutes. 5 µl of the reaction mix was used to transform 50 µl JM109 E. Coli (Section 3.1.8.). The identity of all cDNA

constructs was confirmed by DNA sequencing (Core Genomic Facility of the University of Sheffield) using a T7 Promoter primer following restriction mapping.

Table 3.5-1 Primers for pGBKT7 vector containing The TG2 export motif cDNA

	Forward primers	Reverse primers
Y2H-motif	CTCGTACATATGGGTGGTGAGC TGCAGCGA	CTCGTAGGATTCGGACAGCCA CCGTGGTGG

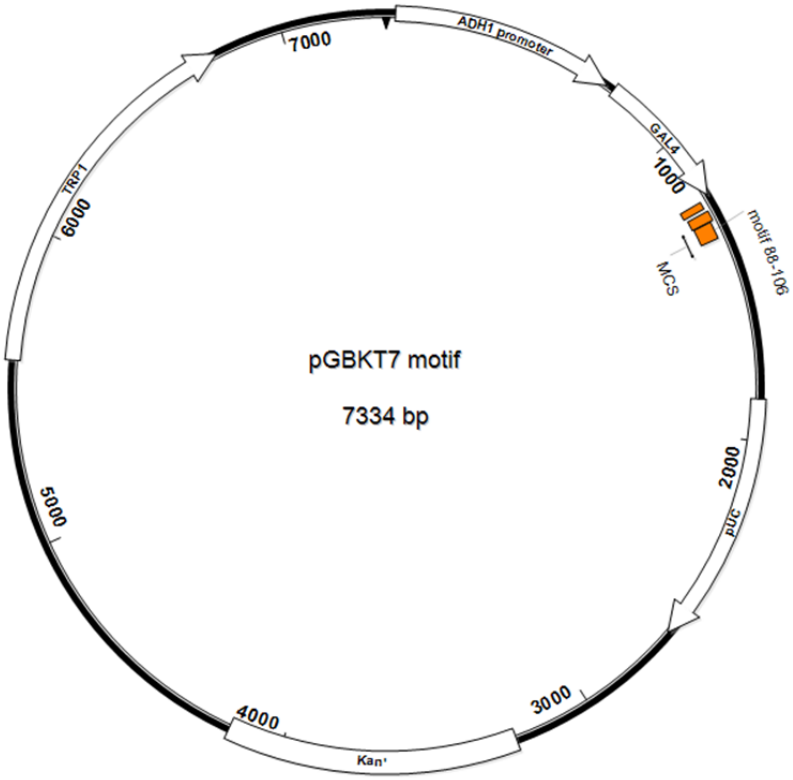

Figure 3.5-2 DNA map for pGBKT7 vector containing the TG2 export motif cDNA

pGBKT7 vector containing the transport motif amino acid sequence 88-106 of TG2

3.5.2 Preparation of competent yeast cells

Y2H Gold yeast and Y187 yeast was streaked on a Yeast Extract Peptone Dextrose Adenine (YPDA) agar plate with 3 days of incubation at 30ºC. A colony (diameter 2 mm) was inoculated into 3 ml YPDA medium. After

incubation at 30ºC with shaking at 250 rpm for 8 hours, 5 µl of the culture medium was transferred to 50 ml of fresh YPDA in a 250 ml flask. The flask was incubated with shaking for 16 hours until the OD 600 nm reached 0.2. The cells were then centrifuged at 700 *g* for 5 minutes at room temperature. The supernatant was discarded and the cell pellet was resuspended in 100 ml of fresh YPDA medium. The 100 ml of YPDA culture was incubated at 30ºC for 4 hours until the OD 600 nm reached 0.4 and was divided into two 50 ml sterile Falcon conical tubes. The cells were centrifuged at 700 *g* for 5 minutes at room temperature. The supernatant was discarded and the pellet was resuspended in 30 ml sterile deionised H_2O. The cells were centrifuged at 700 *g* for 5 minutes at room temperature and the supernatant was discarded. The cell pellets were resuspended 1.5ml of 1.1x TE/LiAc. The cells were transferred to two 1.5ml eppendorf tubes and centrifuged at 10,000 *g* for 15 seconds. The supernatant was discarded and the cell pellets were resuspended in 600 µl of 1.1xTE/LiAc.

3.5.3 Transformation of competent yeast cells

The followings were combined in a pre-chilled sterile 1.5ml tube for a small-scale experiment (control experiment and testing bait for autoactivation and toxicity) or a 15 ml tube for library screening.

Table 3.5-2 Constituents and Procedure for competent yeast cells transformation

	Small-Scale	Library-Scale
Pre-chilled, sterile tube	1.5 ml tube	15 ml tube
Plasmid DNA	100 ng	10 µg
Yeast maker carrier DNA	5 µl	20 µl
Competent cells and gently mix	50 µl	600 µl
PEG/LiAC and gently mix	500 µl	2.5 ml
Incubate at 30ºC	30 min	45 min
DMSO	20 µl	160 µl
Place the tube in a 42ºC water bath	15 min	20 min
Centrifuge to pellet yeast cells	10,000 *g* 15 sec	700 *g* 5 min
Remove the supernatant and resuspend the cells in YPD Plus Medium	1 ml	3 ml
Incubate at 30ºC with shaking (200 rpm)	30 min	90 min
Centrifuge to pellet yeast cells	10,000 *g* 15 sec	700 *g* 5 min
Discard the supernatant and resuspend the pellet in 0.9% (w/v) NaCl solution	1 ml	15 ml

3.5.3.1 Plating and determination of transformation efficiency

100 µl of cells were spread at a dilution of either 1/10 or 1/100 onto a 100 mm

selection medium plate containing the appropriate selection medium (SD/-Trp medium for pGBKT7 vector, SD/-Leu medium for pGADT7 vector and SD/-Leu/-Trp medium for co-transformations of pGBKT7 and pGADT7). The plates were incubated upside down at 30ºC for 3 days. The transformation efficiency was calculated as following:

Transformation efficiency=cfu x suspension volume (ml) / Volume plated (ml) x amount of DNA (µg). (Multiply by 10 and 100 for 1/10 and 1/100 dilutions respectively)

3.5.4 Two-Hybrid library screening with yeast mating

After testing for autoactivation and toxicity for the bait construct, a 2 mm colony of bait strain was inoculated into 50 ml of SD/-Trp liquid medium. The culture was incubated at 30ºC with shaking (200 rpm) for 20 hours until the OD 600 nm reached 0.8. After centrifugation to pellet the cells (1,000 *g* for 5 minutes at room temperature) and removal of the supernatant, the pellet was resuspended to a density of $1x10^8$ cells per ml in SD/-Trp medium (5ml). The library strain (630481, Clontech, UK) and the medium of bait strain were combined in a sterile 2L flask. 45 ml of 2x YPDA medium containing 50 µg/ml kanamycin was also added to the flask. The flask was incubated at 30ºC for 20 hours with slow shaking (40 rpm). A drop of the culture was checked under a phase contrast microscopy (40x) for the presence of the zygotes. The culture was centrifuged at 1,000 *g* for 10 minutes to pellet cells and resuspended in 10ml 0.5x YPDA (with 50 µg/ml kanamycin) medium. The final total volume of the cells with medium was 11.5 ml. To calculated the mating efficiency 100 µl of the 1/10, 1/100, 1/1000 and 1/10,000 dilutions of the mated culture medium was spread on 100 mm agar plates (SD/-Trp, SD/-Leu and SD/-Leu/-Trp) and incubated at 30ºC for 3 days. The remainder of the mated culture was spread 100 µl per 100 mm DDO/A plate (SD/-Leu/-Trp agar containing 125 ng/ml Aureobasidin A (630466, Clontech, UK)) and incubated at 30ºC for 3 days. The mating efficiency was calculated as followings:

The viability of the prey library (number of cfu/ml on SD/-Leu plate) and bait (number of cfu/ml on SD/-Trp plate) was measured. The strain (bait or prey) with the lower viability is the limiting partner. The viability of diploids was the

number of cfu/ml on SD/-Leu/-Trp plate. Mating efficiency= number of cfu/ml of diploids / number of cfu/ml of limiting partner x 100%. All colonies from the previous step was picked and grew on QDO/A (SD/-Ade/-His/-Leu/-Trp and 125ng/ml Aureobasidin A) agar plate.

3.5.5 Confirmation of positive interaction

3.5.5.1 Extracting yeast plasmids

E.Z.N.A. yeast plasmid kit (D3376-02, Omega Bio-Tek, UK) was used to extract yeast plasmid. A yeast colony from the previous section was inoculated in 5mL SD/-Leu liquid medium and incubated at 30°C overnight. The yeast culture was centrifuged at 5,000 *g* for 5 minutes at room temperature. The supernatant was discarded and the cells were resuspended in 480 µl buffer SE containing 2-mercaptoethanol and 40 µl lyticase solution by vortexing for 1 minute. After incubation at 30°C for 30 minutes, the cells were pelleted by centrifuging at 4,000 *g* for 5 minutes at room temperature. The cell pellet was resuspended with 250 µL buffer YP I, followed by 50 mg glass beads and vortex at for 5 minutes. The supernatant was transferred to a new 1.5 mL eppendorf tube, 250 µl YP II was added and gently mixed by inverting 5 times. After 5 minutes incubation at room temperature, 350 µl YP III was added to the lysate and gently mixed by inverting 5 times until a flocculent white precipitate formed. The cell lysate was centrifuged at 10,000 *g* for 10 minutes at room temperature. The clear supernatant was aspirated and added to a clean HiBind DNA mini column (treated with equilibration buffer) assembled in a 2 ml collection tube. The lysate passed through the column by centrifugation for 1 minute at 10,000g at room temperature. The flow-through liquid was discarded and the column was washed with 500 µl of buffer HB followed by centrifuge for 1 minute at 10,000 *g*. The flow-though was discarded and the column was washed with 700 µl DNA twice. The empty column was centrifuged at 13,000 *g* for 2 minutes to dry the column. The column was placed into a clean 1.5 ml eppendorf tube and 50 µl elution buffer (10 mM Tris, pH 8.5) added to the column. After incubation for 1 minute at room temperature, the DNA was eluted by centrifugation at 13,000 *g* for 1 minute. The plasmid was amplified by transforming JM109 E. Coli and selecting bacteria incorporating the vector with 100 µg/ml ampicillin LB plate.

3.5.5.2 Confirmation of genuine positive interactions

Genuine interactions were confirmed using a small-scale transformation procedure by co-transforming 100 ng of the paired vector pGBKT7/bait + prey/ pGADT7 or empty pGBKT7 + prey/pGADT7 into Y2H gold competent cells. 100 µl of 1/10 and 1/100 dilutions of the co-transformed cells were spread on DDO (Double dropout medium: SD/–Leu/–Trp) and QDO/A plates (Quadruple Dropout, SD/–Ade/–His/–Leu/–Trp with Aureobasidin A). The plates were incubated at 30°C for 3 days. A genuine positive interaction was seen by 2 mm colonies on DDO/A and QDO/A plate from pGBKT7/bait + prey/ pGADT7 mix and no colony on DDO/A and QDO/A plate from empty pGBKT7/bait + prey/ pGADT7.

The prey/pGADT7 vector was then sent for sequencing by Sheffield University Core Sequencing service to identify the protein of interest.

3.5.6 Reverse transcription Polymerase Chain Reaction (RT-PCR)

The results from Y2H library screen generated a list of candidate sequences that interacted with the TG2 export motif aa88-106. These candidate proteins were screened based on literature review to identify proteins that may have a profile that could possibly be involved in protein externalisation. Selected candidate proteins should also be expressed in TECs as TG2 externalisation in TECs was being studied (Section 7.3). RT-PCR was therefore used to identify the presence of the candidate proteins from yeast two hybrid screening.

3.5.6.1 RNA extraction

Tubular Epithelial Cells (TECs) were scraped from a confluent 100 mm petri dish in 1 ml trizol and disrupted by sheer stress induced by a 25-gauge hypodermic syringe needle. The trizol/cell lysate was transferred into a 1.5 ml eppendorf tube. After incubation for 5 minutes at room temperature, 250 µl of chloroform was added to the eppendorf tube and the eppendorf tube was shaken vigorously for 10 seconds. The eppendorf tube was incubated for a further 5 minutes at room temperature and then centrifuged at 10,000 *g* for 5 minutes. Three layers in the tube include top layer: clear aqueous, middle layer: white precipitated DNA & bottom layer: pink organic phase (protein). The aqueous phase was carefully aspirated and placed in a new 1.5 ml eppendorf

tube. 550 µl of isopropanol was added to the aqueous phase and mixed by pipetting. After 5 minutes of incubation at room temperature, the eppendorf tube was centrifuged 13,000 *g* for 20 minutes at 4°C. A barely visible pellet was left at the base of the eppendorf tube after the removal of isopropanol. 1 ml of 75% (v/v) EtOH in DEPC treated H_20 was added to the tube and mixed gently. After centrifugation at 10,000 *g* for 5 minutes, the pellet was left to air-dry after the EtOH was removed. 20 µl DEPC treated TE buffer was added to the RNA pellet. The RNA was diluted in 1/40 (1.2 µl in 48.8 µl of TE buffer) and the absorbance of RNA was measured at 260 nm. An absorbance of 1 unit at 260 nm corresponds to 40 µg of RNA per ml.

3.5.6.2 DNase treatment

2 µg of RNA from the previous section was mixed with 1 µl of RQ1 Rnase free DNase (M6101, Promega, UK), 2 µl of DNase 10x reaction buffer, 6 µl of DEPC-treated H_2O and 0.5 µl of Rnase inhibitor (N2111, Promega, UK). The mix was incubated at 37°C for 15 minutes, and then 65°C for 20 minutes to deactive the DNase in a thermal cycler before being placed on ice.

3.5.6.3 Reverse transcription of RNA

Reverse transcription was performed using RETROscript kit (AM1710, Ambion, UK). The DNase treated RNA from the previous step was mixed with 2 µl of random primer, 2 µl of 10x RT buffer, 4 µl of dNTP mix, 1 µl of RNase inhibitor, 1 µl of MMLV-RT and nuclease-free water to 20 µl. The reaction was incubated at 44°C for 1 hour and the reverse transcriptase was inactivated by heating at 92°C for 10 minutes. The DNA was amplified with PCR (Section 3.1) using designed primers (Table 3.5-3). The absorbance of PCR products was measured at 260 nm.

Table 3.5-3 Primers for reverse transcription polymerase chain reaction (RT-PCR)

Protein	Forward	Reverse	Size (BP)
Iduronate 2-sulfatase	GCTTGTTGCTAGGCTTCTT	TCAGAATCGACAAAATAGAGT	1458
large neutral amino acids transporter small subunit 1	CCCGAGGGCGAAGGCGTGAC	GCAGGATCCATTTGGGCTTGTTTT	1357
Neurobeachin-like protein 2	GTTGTGGCTGCTCTACTACG	GTTCAAGTGGAGGATATGTAGAGA	972
Voltage-dependent calcium channel subunit alpha-1A	ATGGCCCGCTTTGGAGA	GCCGTGCCCCGCGTAGTAACCATT	1035
Voltage-dependent L-type calcium channel subunit alpha-1C	GCCTTCGCTCAGCCATCCACA	CTGCAGTTCACAAAAGGTAA	1386
Tapasin	GCTTCTTCCCCTGCTCGTC	AGGCCCAAAAGGAGAAAAGCAGAC	1278
Translocon-associated protein gamma	CTTCAGGATTTCAGCCGCAACC	CCAGTAGACAAGAGGGCGATGAG	500

3.5.7 Co-immunoprecipitation

Cells were harvest from a confluent 100 mm petri dish and lysed in 100 µl cell lysis buffer (50 mM Tris-HCl, 150 mM NaCl, 1% IGEPAL, pH 8.0) after centrifuge at 80 *g* in room temperature. 1 µg of selected antibody was added to the cell lysates and the tube incubated with rotation for 1 hour at 4°C. 50 µl of Dynabeads protein G (100.04D, Promega, UK) was added into the tube and incubated with rotation for 10 minutes at room temperature. The tube was placed on the magnet and the supernatant was removed. After 3 washes of 200 µl PBS, the antigen complex was eluted using reducing buffer and electrophoresed on SDS-polyacrylamide gels. Gels were western blotted and immunoprobed for the protein suspected of binding the protein targeted by the pull down antibody (Table 3.5-4).

Table 3.5-4 List of antibodies use for co-immunoprecipitation studies

Primary antibodies	Dilution	Secondary antibodies	Dilution
Mouse anti-transglutaminase 2 antibodies cub7402 (ab2386, Abcam, UK)	1:750	Anti-mouse HRP (ab97040, Abcam,	1:5000

		UK)	
Rat anti-large T antigen (ab18187, Abcam, UK)	1:1000	Anti-rat HRP (ab7097, Abcam, UK)	1:5000
Goat anti-tapasin antibodies (sc11473, Santa Cruz biotechnology, UK)	1:1000	Anti-goat IgG-HRP (P0449, Dako, UK)	1:2000
Goat anti-translocon-associated proteins antibodies (sc54414, Santa Cruz biotechnology, UK)	1:1000	Anti-goat IgG-HRP	1:2000

3.6 Statistical Analyses

Data analyses were performed using unpaired Student's t-test or one-way ANOVA with a Bonferroni post hoc test as appropriate. A value of $p<0.05$ was considered as statistical significant. All analysis was performed with GraphPad Prism (GraphPad software Inc, California, USA).

Chapter 4 Determination of which TG2 domain is critical for its extracellular trafficking using deletion analysis

4.1 Introduction

While there is extensive evidence for TG2 export from the cell and its extracellular functions in TECs (Fisher 1973; Basile *et al.* 1998; Skill *et al.* 2004; Fisher *et al.* 2009), there is very little data detailing how TG2 is moved out of the cell or in fact which parts of TG2 are used in this process (Aeschlimann *et al.* 2000; Grenard *et al.* 2001; Skill *et al.* 2004; Jones RA 2005; Fisher *et al.* 2009). While the fibronectin binding domain of the β-sandwich has been reported to be involved in TG2 export from fibroblasts (Gaudry *et al.* 1999; Hang *et al.* 2005), it is unknown if this could be applicable to other cell types. Further, the nature of the previous studies does not fully confirm the role of this fibronectin domain and it remains a possibility the authors were simply measuring TG2 association at the cell surface from damaged cells rather than export per se.

To address this a series of deletion mutants of TG2 (Gentile *et al.* 1991) were prepared (Section 3.1.3) and inserted into the pCDNA6.2/cTC-Tag-DEST mammalian expression vector (Section 3.1.5) The constructed vectors were then transfected into OK, NRK52E and MDCK II cells renal tubular epithelial cells (TECs) using nucleofection with Ingenio solution (Section 3.3.3) with total TG activity & TG2 antigen of the cell lysate, extracellular TG activity, extracellular TG2 antigen and TG activity in culture medium measured 48 hours after transfection. Expression vectors containing the full length TG2 cDNA (tg), TG2 without β-sandwich domain (-bsw), TG2 without β-barrel 2 (-b2), TG2 without both β-barrels (-b1b2), TG2 with β-sandwich and barrel 2 domain missing (-bwb2) and the core domain of TG2 (core) (Figure 4.1-1) were used for this study to identify the TG2 domain required for TG2 export. The constructed vectors were transfected into OK, NRK52E and MDCK II cells renal tubular epithelial cells (TECs) using the nucleofection with Ingenio solution as described in section 3.3.3. Total TG activity and TG2 antigen of the cell lysate, extracellular TG activity, extracellular TG2 antigen and TG activity in culture medium were measured 48 hours after transfection.

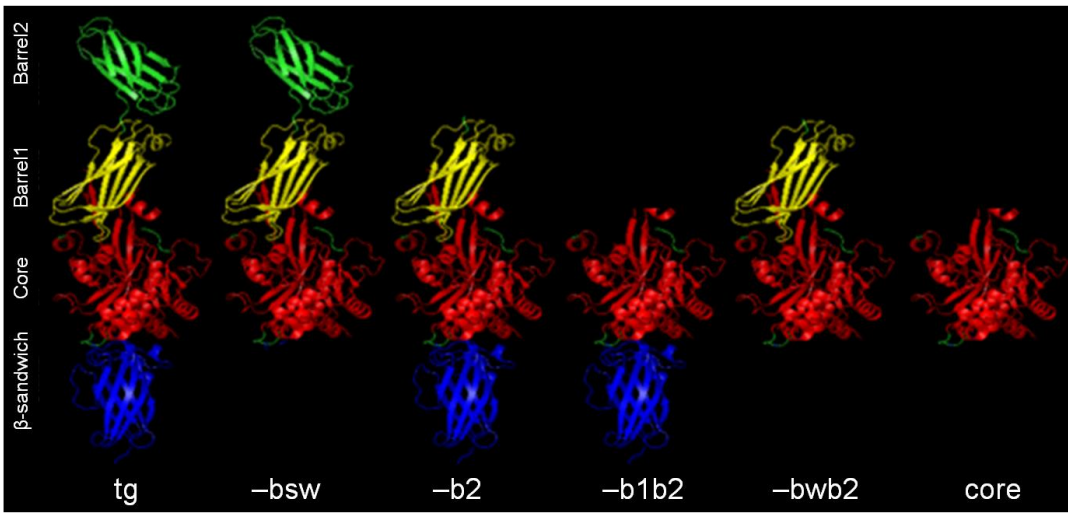

Figure 4.1-1 TG2 mutants for deletion analysis

Five TG2 mutants were constructed to determine which domain of TG2 is critical for TG2 externalisation. Full length TG2 (tg) (Gentile et al. 1991), TG2 with β-sandwich domain missing (-bsw), TG2 with β barrel 2 missing (-b2), TG2 with β-barrel 1 &2 missing (-b1b2), TG2 with β-sandwich & β barrel 2 domain missing (-bwb2) and TG2 with β-sandwich, β barrel 1 & 2 domains leaving just the core

4.2 Generation of TG2 Domain deletion cDNA by PCR

All constructs were prepared by PCR using the human TG2 cDNA as a template (Gentile *et al.* 1991) using the primers detailed in

Table 4.2-1. All TG2 constructs were transferred from pENTR/D-TOPO® vector to mammalian pcDNA6.2/cTC-Tag-dest and transfected into TECs as described in Section 3.1.5.

After having identified the domain that is essential for TG2 externalisation, a point mutation analysis was used to determine the sequences in the domain that is critical for TG2 externalisation.

Table 4.2-1 Primers for deletion analysis

	Forward primers	Reverse primers
tg	CACCATGGCCGAGGAGCTGGTCTT	AAATCCGCCCCGGTTACTACTGT
-bsw	CACCATGCTGTGTACCTGGACTCG	AAATCCGCCCCGGTTACTACTGT
-b2	CACCATGGCCGAGGAGCTGGTCTT	AAAGTAGAGGTCCCTCTCAGCCA
-b1b2	CACCATGGCCGAGGAGCTGGTCTT	AAAGTTCGCCCTTGTGAAGGCCT
-bwb2	CACCATGCTGTGTACCTGGACTCG	AAAGTAGAGGTCCCTCTCAGCCA
core	CACCATGCTGTGTACCTGGACTCG	AAAGTTCGCCCTTGTGAAGGCCT

Forward primers were designed by adding CCAC at 5-end of the insert sequences. Reverse primers were designed by adding AAA at the 5-end of the insert sequences. Full length TG2 (tg), TG2 with β-sandwich domain missing (-bsw), TG2 with β barrel 2 missing (-b2), TG2 with β-barrel 1 &2 missing (-b1b2), TG2 with β-sandwich & β barrel 2 domain missing (-bwb2) and TG2 with β-sandwich, β barrel 1 & 2 domains leaving just the core domain (core), removal of first 7 amino acid of N-terminal β-sandwich domain (-7a).

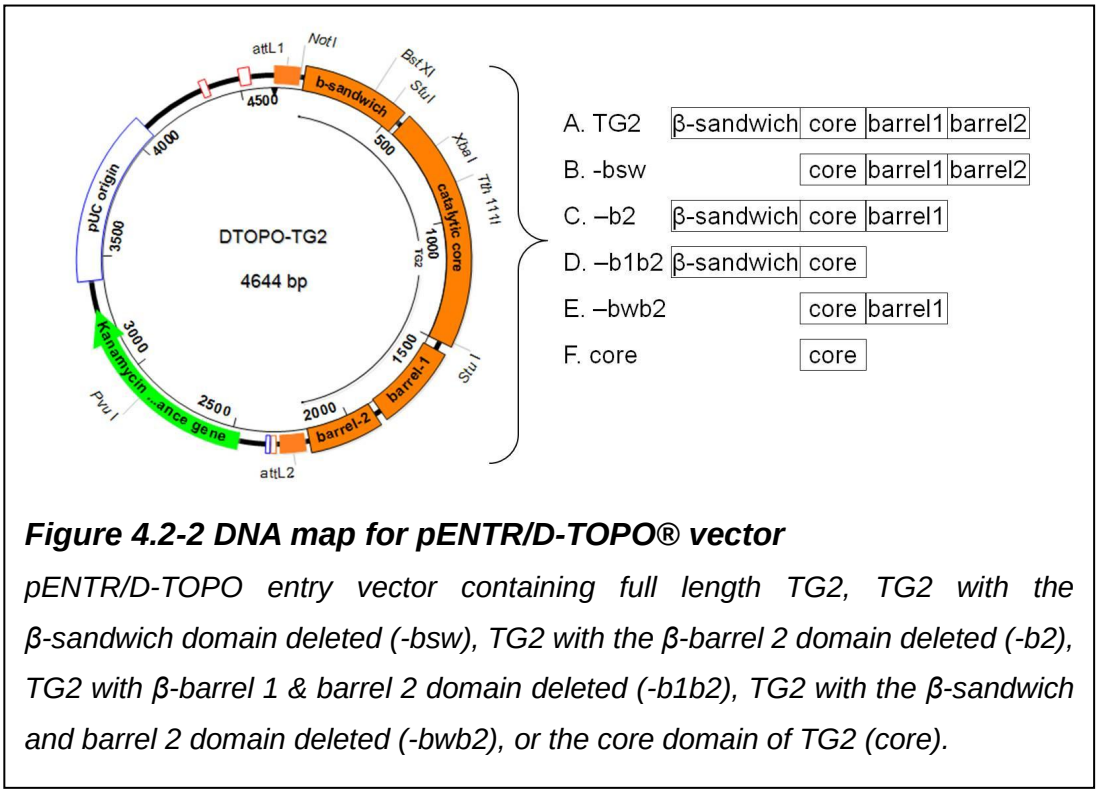

Figure 4.2-2 DNA map for pENTR/D-TOPO® vector

pENTR/D-TOPO entry vector containing full length TG2, TG2 with the β-sandwich domain deleted (-bsw), TG2 with the β-barrel 2 domain deleted (-b2), TG2 with β-barrel 1 & barrel 2 domain deleted (-b1b2), TG2 with the β-sandwich and barrel 2 domain deleted (-bwb2), or the core domain of TG2 (core).

4.3 Deletion Analysis - Total TG by activity and antigen in the cell lysate

To establish if all the TG2 domain deletion mutants were both equally transfected into the cell and had equal TG activity, the total TG activity in the cell lysates and total TG2 antigen was measured 48 hours post transfection.

TG2 protein in each cell lysate was determined by western blot (Figure 4.3-1 A-C) using β-actin as a loading control. TG2 was probed for using mAb cub7402 (ab2386, Abcam, UK) that targets the catalytic core which is present in each construct. This detected a band of molecular weight 75 kDa for full length TG2 (tg), 61 kDa for TG2 with β-sandwich domain missing (–bsw), 66 kDa for TG2 with β barrel 2 missing (–b2), 52 kDa for TG2 with β barrel 1 & β barrel 2 missing (–b1b2), 51 kDa for TG2 with β-sandwich domain and β barrel 2 missing (–bwb2) and 38 kDa for the core domain (core) in OK (Figure 4.3-1 A), NRK52E (Figure 4.3-1 B) and MDCKII cells (Figure 4.3-1 C) respectively. All constructs appeared to be equally expressed within each cell line.

TG activity in the cell lysates (Figure 4.3-1 D-F) also increased equally (approx 5-fold) for all constructs within each cell line. This confirmed comparable transfection efficiency and that all domain deletions retained TG activity. Subsequently TG2 transport could be tracked using extracellular TG activity assays.

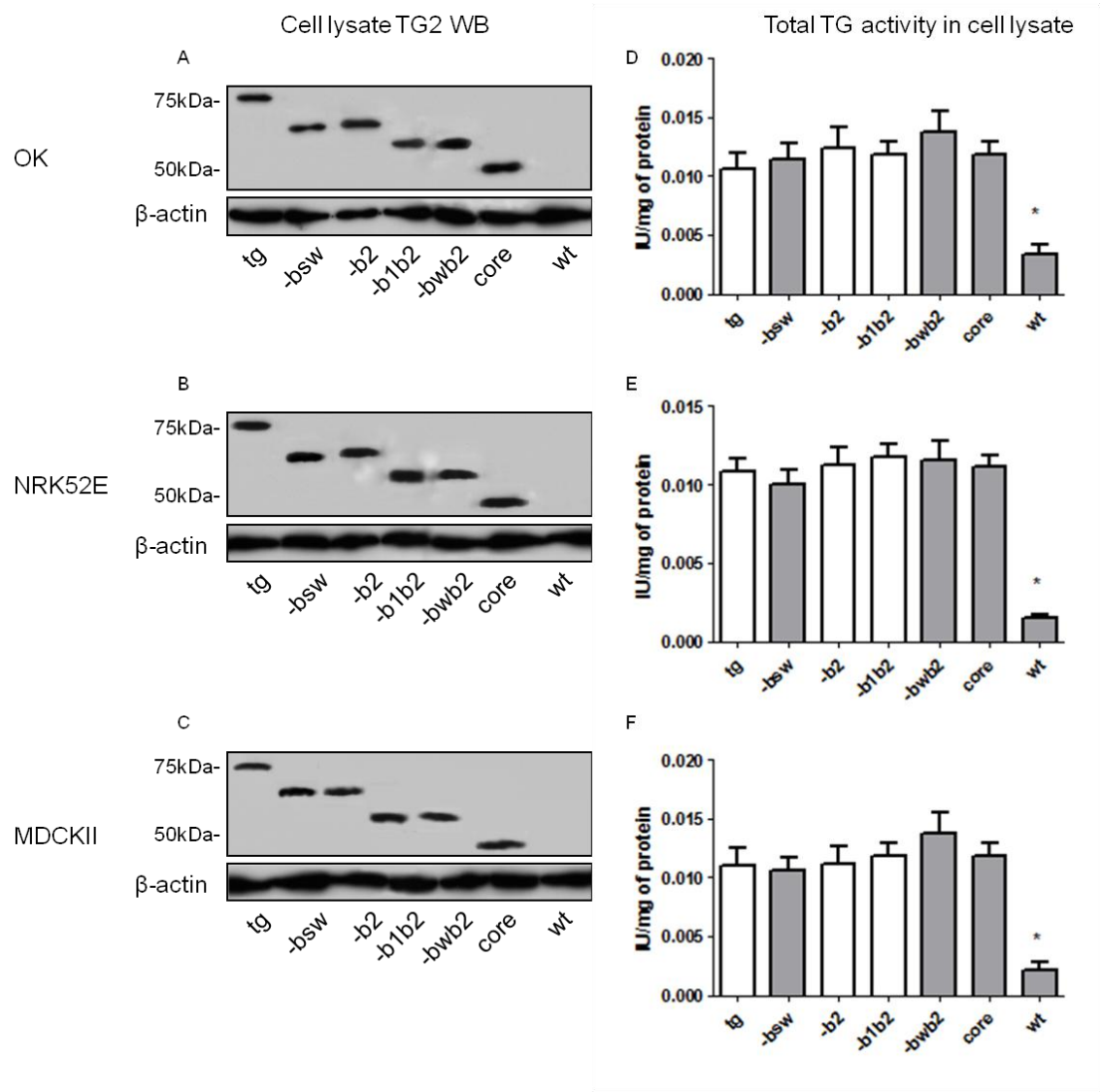

Figure 4.3-1 TG2 levels following domain deletion

*OK, NRK52E and MDCK II renal epithelial cells were transfected with the following constructs 1) full length tissue transglutaminase (tg), 2) TG2 with β-sandwich domain deleted (-bsw), 3) TG2 with the barrel2 deleted (-b2), 4) TG2 with β-barrel 1 and β-barrel 2 domains deleted (-b1b2), 5) TG2 with both β-sandwich and β-barrel 2 domains deleted (-bwb2) and finally 6) TG2 catalytic core (core). Western blots for TG2 in cell lysates post transfection are shown in A-C and total TG activity in cell lysates (D-F). wt: non-transfection control. Data represents mean values ±SEM, n=5, *= p<0.05*

4.4 Deletion analysis – Extracellular TG activity

Extracellular TG2 activity was measured 48 hours post transfection using a biotin-cadaverine incorporation (Section 3.4.7). An increase in extracellular TG activity was readily detectable in the extracellular environment after transfection with full length TG2 (tg, Figure 4.4-1 A-C), with activity increased between 3 & 4 fold in all 3 cell lines transfected. Similarly, cells transfected with TG2 cDNA with β-barrel 2 (-b2) and both β-barrel 1 & β-barrel 2 domains missing (-b1b2) had the same levels of extracellular TG activity to that of full length TG2 in all 3 cell lines suggesting that β-barrel domains played no role in TG2 externalisation. However, when cells were transfected with constructs in which the β-sandwich domain was missing (ie -bsw, -bwb2 , and just core), extracellular TG activity was similar to that in cells that had not been transfected. This suggests that the transfected deletion mutant of TG2 is not being trafficked and that β-sandwich domain is crucial for TG2 transport.

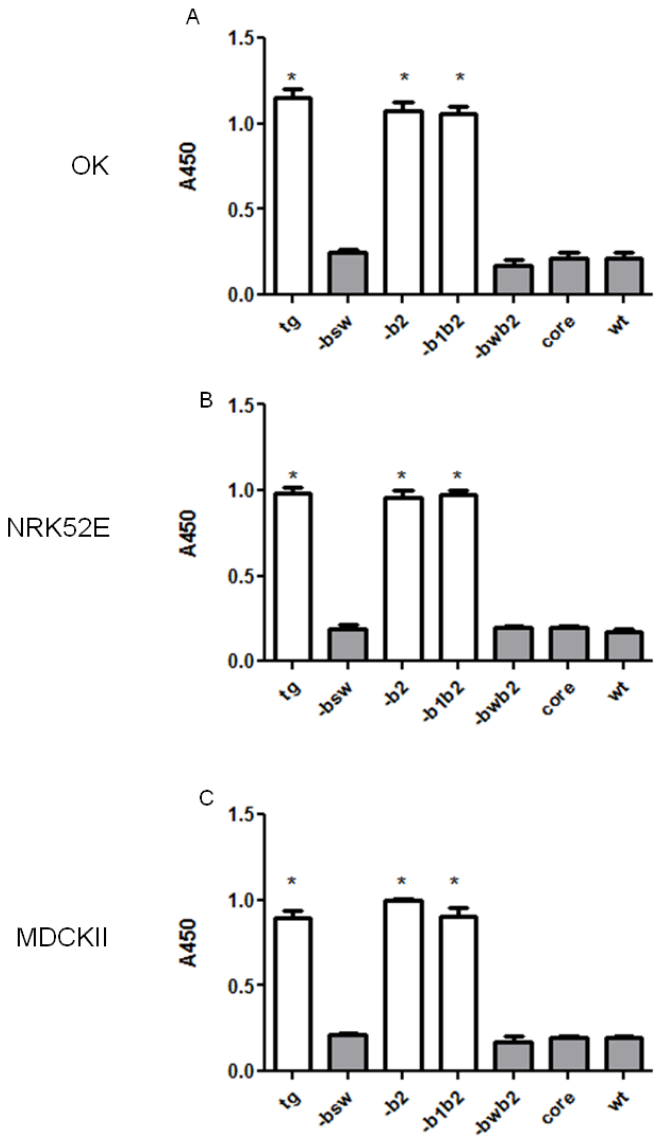

Figure 4.4-1 Extracellular TG activity following domain deletion

*OK, NRK52E and MDCK II renal epithelial cells were transfected with full length TG2 (tg), TG2 mutants including TG2 with β-sandwich domain deleted (-bsw), TG2 with the barrel 2 deleted (-b2), TG2 with β-barrel 1 and β-barrel 2 domains deleted (-b1b2), TG2 with both β-sandwich and β-barrel 2 domains deleted (-bwb2) and TG2 catalytic core only (core).wt: non-transfected control. Extracellular TG activity was measured 48 hour post transfection. Data represents mean values ±SEM, n=5, *= p<0.05*

4.5 Measurement of TG2 in culture medium

It is possible that removing a domain may not be affecting TG2 transport, but simply its ability to localise to the cell surface or extracellular matrix which extracellular TG activity assay used predominantly measure. Experiments were therefore repeated taking measurements of TG antigen using western blot (Figure 4.5-1 A-C) and activity (Figure 4.5-1 D-F) in the culture medium to ensure TG2 was not “floating” away post transport. In all 3 tubular epithelial cells, only the full length TG2 and mutant TG2s with barrel domains had been deleted (-b1 and –b1b2, Figure 4.5-1 A-C) was detected in culture medium with the same molecular weight as in the cell lysate: 66 kDa for TG2 with β barrel 1 missing (–b1) and 52 kDa for both β barrels missing (–b1b2). The TG2 fraction found in the medium (Figure 4.5-1 E-F) mirrored measurements of extracellular TG activity using a modified cell ELISA (Figure 4.4-1 A-C). None of the constructs with β-sandwich domain missing (-bsw, -bwb2 and core) were detected in the medium as constructs with barrel domains missing.

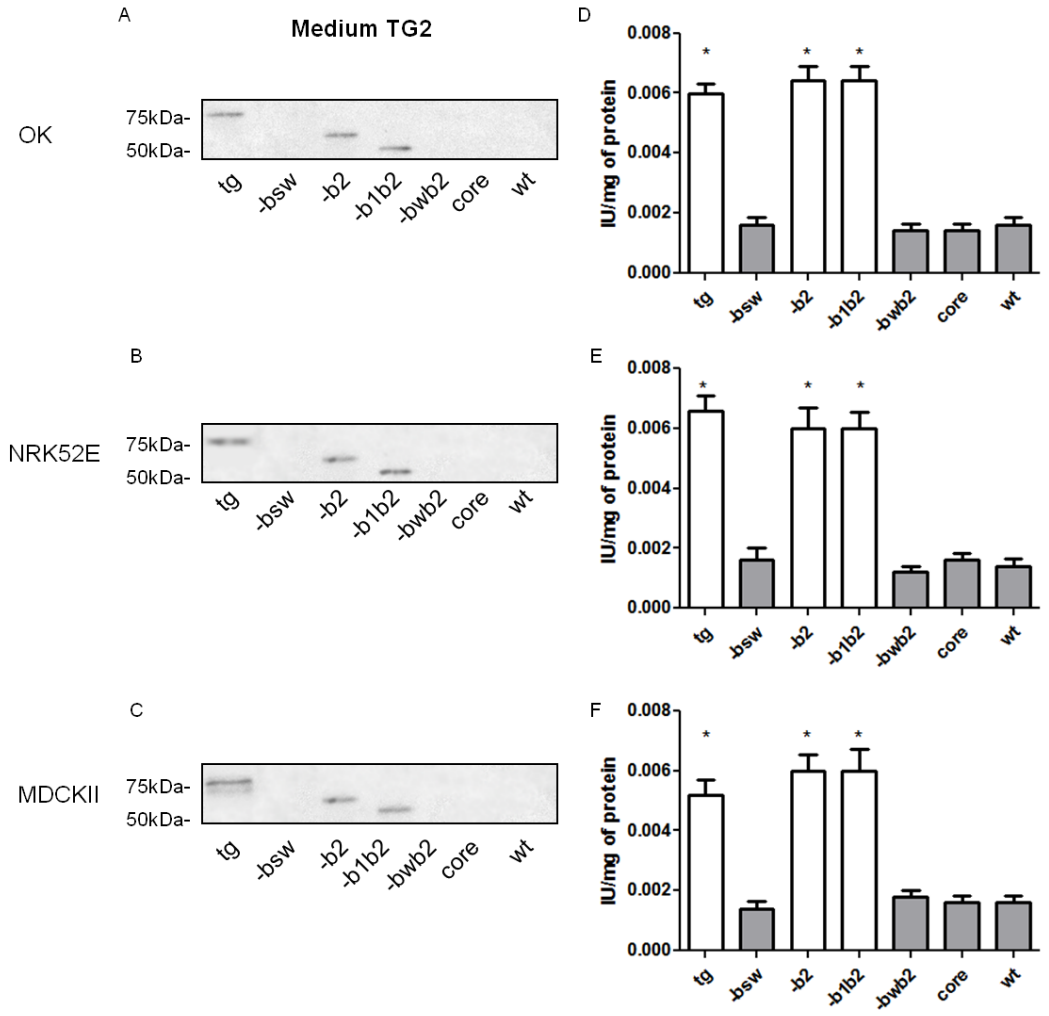

Figure 4.5-1 TG activity and Antigen in culture medium following domain deletion

*OK, NRK52E and MDCK II renal epithelial cells were transfected with full length TG2 (tg), TG2 mutants including TG2 with β-sandwich domain deleted (-bsw), TG2 with the barrel 2 deleted (-b2), TG2 with β-barrel 1 and β-barrel 2 domains deleted (-b1b2), TG2 with both β-sandwich and β-barrel 2 domains deleted (-bwb2) and TG2 catalytic core only (core).wt: non-transfected control. TG2 antigen and TG activity in culture medium was measured 48 hour post transfection pcDNA6.2/cTC-Tag-dest vector containing full length TG2 cDNA or pcDNA6.2/cTC-Tag-dest vector containing TG2 mutants. Data represents mean values ±SEM, n=5, *= p<0.05*

4.6 Proportion of TG2 on cell surface and TG2 in the culture medium

In this study, we measured extra- and intra-cellular TG activity to determine TG2 externalisation. The result showed significant different between TG2 mutants and full length of TG2. However, we do expect this would lead to an increase in intracellular TG activity in cells transfected with the TG2 lacking the β-sandwich domain as it would be retained in the cell. However the data of TG2 in the cell failed to demonstrate this. Subsequently to address this, the total amount of TG2 in each compartment was calculated (Figure 4.6-1), which while not statistically significant, did suggest that TG2 was being retained. This data can be explained by the proportion of TG2 measured on cell surface (extracellular TG activity) and TG activity in the medium which is only 5% of the TG activity in the cell lysate. Thus the differences can be observed by transforming the unit expressed as TG activity IU/mg of protein into TG activity per well. The extracellular TG levels compared to intracellular TG levels are relatively small. So if only 5% of transfected TG2 is retained, it will not have a huge affect on intracellular TG2 as only 5% of the total TG2 transfected, but it has a dramatic affect on TG2 detectable outside of the cells, where TG2 is barely detectable. TG2 in the culture medium was measured up to 16 hours (section 3.4.2) and the half-life of TG2 is 8 hours, the barely detectable TG2 in the culture medium can not be explained by the degradation TG2.

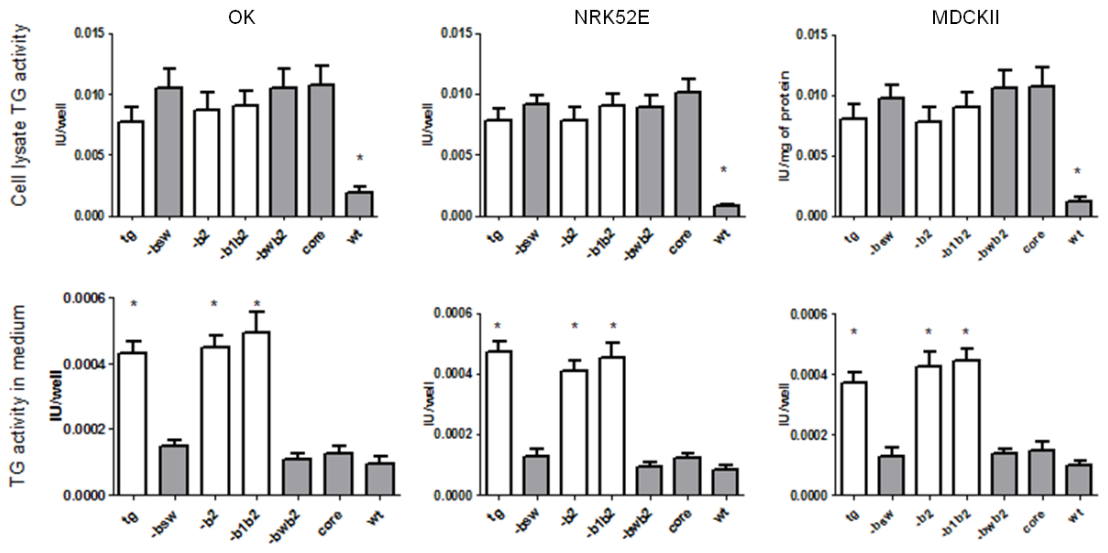

Figure 4.6-1 Total TG activity in cell lysate and medium expressed as TG activity per well

*TG activity in cell lysate and TG activity in culture medium were measured in OK, NRK52E and MDCKII cells 48 hours post transfection with pcDNA6.2/cTC-tag-DEST vector containing full length of TG2 cDNA (tg), TG2 with β-sandwich domain missing (-bsw), TG2 with barrel2 domain missing (-b2), TG2 with barrel 1 and barrel 2 missing (-b1b2), β-sandwich and barrel 2 domain missing (-bwb2) and the core domain of TG2 (core). The unit of TG activity was expressed as Unit per well. wt: non-transfected cells. Data represents mean±SEM, n=5, *:p<0.05.*

4.7 Chronologically labelling of TG2 with time post transfection

TG2 with the β-sandwich domain deleted cannot be externalised. Consequently the differences in TG2 movement in the cell between full length TG2 and mutant TG2 (-bsw) can provide clues to its extracellular trafficking. To visualise TG2 movement, NRK52E cells transfected with pcDNA6.2/cTC-Tag-DEST containing either full length of TG2 or mutant TG2 (-bsw, β-sandwich domain missing) were visualised 24, 48, 72 and 96 hours after transfection by staining with FlAsH reagent. The plasma membrane of the cells was stained red using CellMask^{TM} plasma membrane reagent and the cell nucleus stained blue with DAPI. Most of the synthesised TG2 (green) in 24 hours (tg2) was found around the cell nucleus (Figure 4.7-1 A-C) that is likely

within rough ER and some TG2 localised in the cytosol (Figure 4.7-1 C). The FlAsH stains for mutant TG2 (-bsw) followed the same pattern (Figure 4.7-1 D-F) at 24 hours. Wild type TG2 was accumulated in a vesicle shape structure by 48 hours post transfection with some extracellular TG2 vesicles seen (white arrow, Figure 4.7-1 G-I). In contrast, FlAsH labelled mutant TG2 missing the β-sandwich was also in a vesicle shape structure, but clearly retained within the cytosol, often just inside the plasma membrane (Figure 4.7-1 J-L).

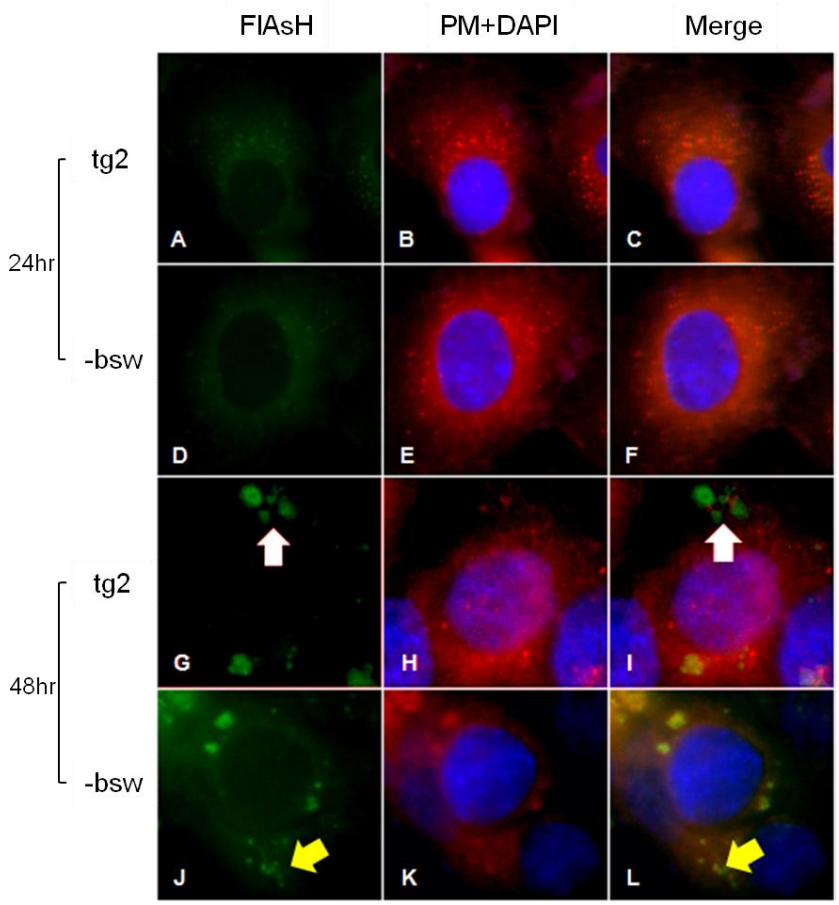

Figure 4.7-1 FlAsH staining for TG2 in NRK52E cells 24 and 48 hours post transfection

NRK52E cells were transfected with pcDNA6.2/cTC-Tag-dest vector containing full length TG2 cDNA (tg2) or mutant TG2 (-bsw, β-sandwich domain missing). FlAsH stains for TG2 (A-C & G-I, tg2) and mutant TG2 (D-F & J-L, -bsw) was carried out at 24 (A-F) and 48 (G-L) hours post transfection. TG2 accumulated extracellularly in a vesicle shape structures are indicated by white arrows at 48 hours post transfection. Mutant TG2 (-bsw) are localised in vesicle shaped structures in the cytosol indicated by yellow arrows (J&L). Plasma membrane (PM) was stained red with CellMask™ plasma membrane and the cell nucleus stained blue with DAPI.

By 72 (Figure 4.7-2 A-C) and 96 hours post transfection (Figure 4.7-2 G-I) most TG2 is on cell surface (white arrows). Little TG2 remains around the cell nucleus or in the cytosol. Mutant TG2 (-bsw) at 72 (Figure 4.7-2 D-F) and 96 hours (Figure 4.7-2 J-L) post transfection accumulated in the peripheral cytosol in the sub-plasma membrane area in a vesicle shape. This is consistent with the finding in section 4.5 that the mutant TG2 with the β-sandwich domain missing) cannot be externalised.

In summary, TG2 is synthesised in the cytosolic ribosomes, accumulated around the cell nucleus within in 24 hours and moved to the peripheral part of the cells. TG2 begins to be exported by 48 hours post transfection. By 72 hours most of the visible TG is outside the cell and appears associated with the cell surface. TG2 without the β-sandwich domain cannot be externalised stays in the cytosol in a sub-plasma configuration.

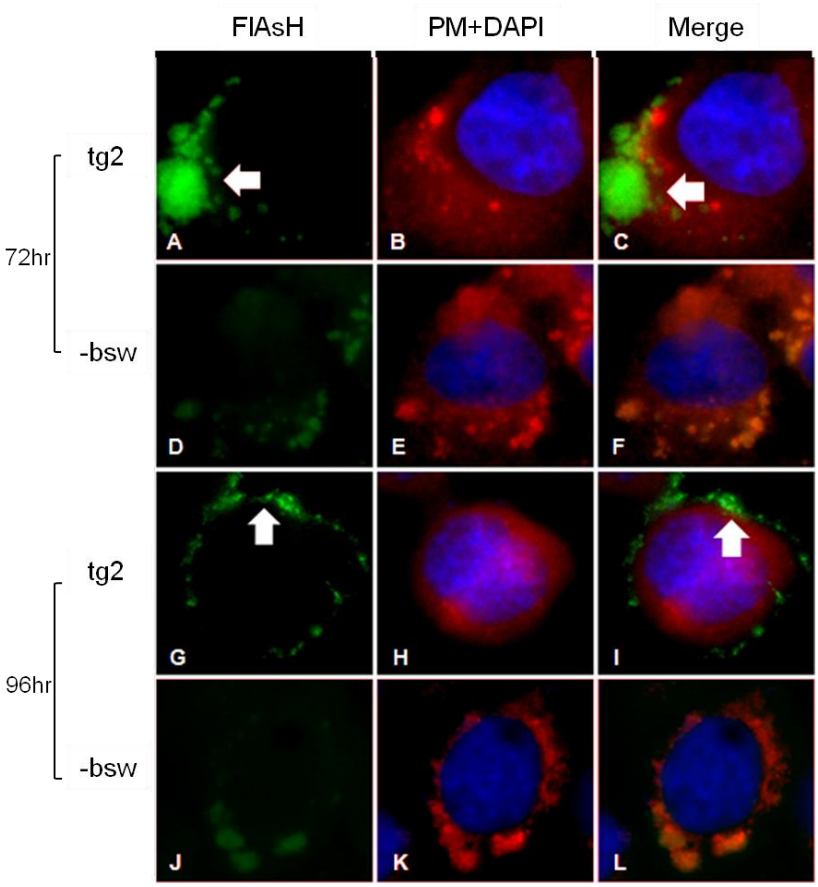

Figure 4.7-2 FlAsH stains for TG2 in NRK52E cells 72 and 96 hours post transfection

NRK52E cells were transfected with tetracysteine tag vector containing either full length TG2 (tg2) or mutant TG2 (-bsw, β-sandwich domain missing). FlAsH labelled TG2 were localised on the plasma membrane surface at 72 & 96 hours post transfection (A & G, white arrows). Mutant TG2 that cannot be externalised was accumulated in the near the plasma membrane (D & J). Plasma membrane (PM) was stained red with CellMask™ plasma membrane and the cell nucleus stained was stained blue (B, E, H, K). The merge images suggested the location of intracellular and extracellular TG2 (C, F, I, L).

4.8 Visualisation of externalised TG2

Given the diffuse nature of the CellMask^{TM} plasma membrane stain, to confirm that full length TG2 was finding its way into the extracellular space, while TG2 missing the β-sandwich domain was unable to do so, the cell periphery was visualised with phase contrast microscopy. This was then merged with FlAsH labelled TG2 as in the previous section at 48 hours post transfection. Two different distribution patterns were observed in the cells transfected with full length TG2 (Figure 4.8-1 A) or mutant TG2 (-bsw, β-sandwich domain deleted) (Figure 4.8-1 B). The green TG2 was found between cells (yellow arrow) for full length TG2, but the mutant TG2 was found just in the cytosol (white arrow, A & B).

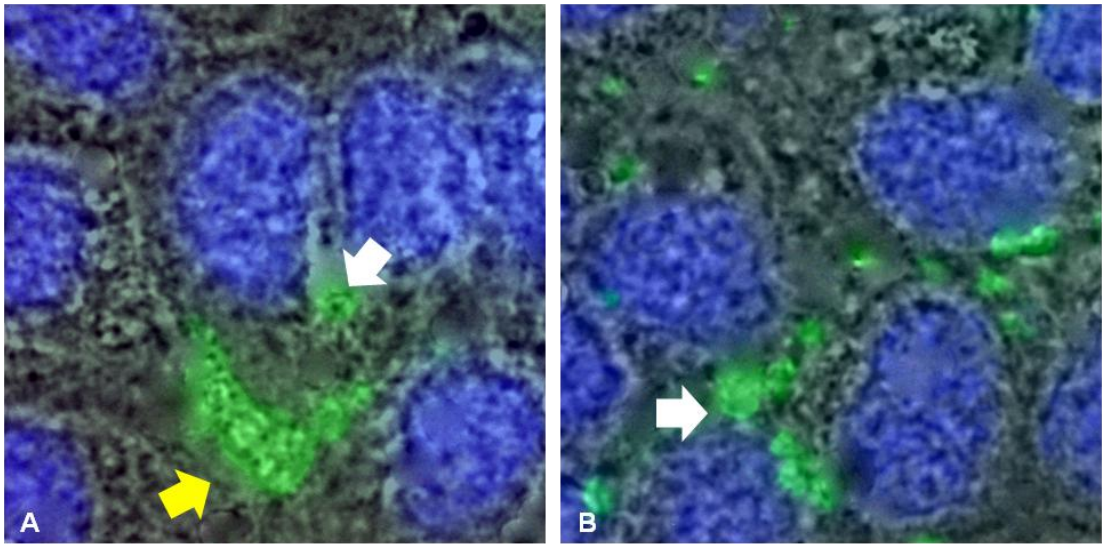

Figure 4.8-1 Extracellular and intracellular TG2 using immunofluorescents

NRK52E cells stained with pcDNA6.2/cTC-Tag-dest vector carrying either full length TG2 cDNA (A) or TG2 with β-sandwich domain deleted (B) were stained with FlAsH (green). The fluorescent images were merged with phase contrast image to show the extracellular and intracellular compartments. The extracellular TG2 is indicated with yellow arrow and intracellular TG2 is indicated with white arrow.

Unfortunately the merging of phase contrast images that have a white background with fluorescent signal in the cytosol raising questions about differences in the amount of TG2 or TG2 lacking the β-sandwich remaining in cells. To address this the plasma membrane was stained red with CellMask^{TM} plasma membrane reagent (Section 3.4.14.10). Wild type cells (wt) picked up no FlAsH stain for TG2 with the plasma membrane staining a deep red (Figure 4.8-2 A). A green TG2 fluorescent signal was found in extracellular space (yellow arrow) and cytosol (white arrow) in cells transfected with full length TG2 (+tg2) (Figure 4.8-2 B) with the plasma membrane being seen as yellow / orange due to the co-localisation of FlAsH labelled TG2 (green) and the red plasma membrane staining. Only intracellular TG2 was found in the cells transfect with TG2 lacking the β-sandwich domain (+tg2-bsw) with the plasma membrane appearing identical to that of the untransfected cells as no TG2 was being exported across the plasma membrane (Figure 4.8-2 C). This clear cell junction for CellMask^{TM} plasma membrane only clearly displayed in very confluent cells, therefore cannot applied to chronological visualisation study.

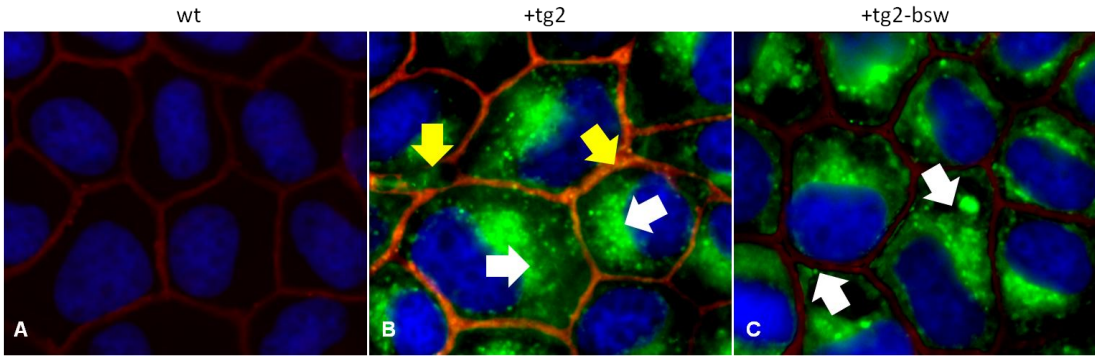

Figure 4.8-2 Visualisation of extracellular TG2

NRK52E cells transfected with tetracysteine tag containing full length TG2 (B, +tg2) or mutant TG2 (C, +tg2-bsw) were visualised 48 hours post transfection. The plasma membrane stained red using CellMask^{TM} plasma membrane reagent. Extracellular green TG2 (yellow arrows) was observed in the cells transfected with full length TG2 (B) but only intracellular TG2 was found in the cells transfected with mutant TG2 (+tg-bsw). The plasma membrane was orange colour because of the co-localisation of green full length TG2 and red plasma membrane stains. In contrast, the plasma membrane was red in wild type NRK52E cells (A, wt) that is similar to the plasma membrane in the cells transfected with mutant TG2 (C). Cell nucleus was stained in blue with DAPI.

4.9 Discussion

In this study, mutant TG2 constructs with each of the 3 non-catalytic domains individually or doubly deleted were generated and transfected into three tubular epithelial cells (TECs). As the catalytic activity of TG2 relies on the core domain alone, all TG2 mutants retained TG activity and thus extracellular TG activity levels, as well as antigen, can be used to access TG2 externalisation. The expression of TG2 was similar across the three different types of TECs used as well as between the different TG2 mutant constructs using the optimised nucleofection protocols.

Measurements of intra- and extra-cellular TG activity can be compared between different TG2 mutants and different cell lines. Despite having the same TG levels inside the cell, TG2 mutants with the β-sandwich domain deleted (either alone or with a barrel domain also deleted), only had the same extracellular TG levels as wild type cells conclusively proving that the β-sandwich is critical to TG2 extracellular trafficking. Cells transfected with TG2 where β-barrel 2 deleted or TG2 with both β-barrel deleted had the same extracellular TG levels as cells transfected with full length TG2 proving that the β-barrels are not required for TG2 cell export. TG2 externalisation was further confirmed by using FlAsH staining of tetracysteine tagged TG2 and mutant TG2. Full length TG2 and TG2 with the β-sandwich domain deleted were synthesised in the ribosomes around the cell nucleus and moved peripherally to the plasma membrane. Full length TG2 can be found both on cell surface and in the extracellular space 48 hours post transfection, whereas TG2 missing the β-sandwich could not be externalised and accumulated under the plasma membrane in vesicle shaped structures.

The β-sandwich domain contains many binding sites including heparin (Verderio *et al.* 2008), integrin (Akimov *et al.* 2000; Telci *et al.* 2008) and fibronectin (Gaudry *et al.* 1999), it is therefore possible that even if TG2 was still exported it can't be measured efficiently using the extracellular TG activity assay as this assay is far less efficient if the TG2 is not on the cell surface or in the ECM. Removal of the β-sandwich could prevent direct ECM or cell surface association. We therefore measured TG activity in the medium and TG2 antigen in the medium to guard against misinterpretation of the data. This

showed that TG activity was not increased in the culture media when the β-sandwich was removed in contrast to full and barrel deletion TG2. This finding confirms that the deletion of β-sandwich domain stops TG2 externalisation. The role of β-sandwich domain in TG2 externalisation has been raised in previous studies (Verderio *et al.* 1998; Gaudry *et al.* 1999; Akimov *et al.* 2000; Herman *et al.* 2006) and thus our findings in renal tubular epithelial cells are consistent with that in Swiss 3T3 fibroblasts (Verderio *et al.* 1998; Gaudry *et al.* 1999), WI-38 fibroblasts, human erythroleukemia cells (Akimov *et al.* 2000), and breast cancer (MCF-7) cells (Herman *et al.* 2006).

Initially TG2 was localised in just the cytosol around the cell nucleus. Despite TG2 having a well described nuclear presence it is likely that early TG2 is just TG2 being synthesised in the cytosolic ribosomes and accumulated around the cell nucleus in 24 hours post transfection. TG2 then moved to the periphery of the cells between 24-48 hours and extracellular TG2 can be visualised 48 hours post transfection. Mutant TG2 that cannot be externalised followed the same pathway – like wild type TG2 it is synthesised in the cytosolic ribosomes at 24 hours post transfection, move to the periphery of the cell and accumulated in a vesicle shape structure 24-48 hours post transfection. More studies such as co-localisation of TG2 and lysosomes or multivesicular bodies (MVBs) (Zemskov *et al.* 2011) may provide information for the involvement of lysosomes or MVBs in TG2 externalisation. So far, no plasma membrane blebbing was observed in images using fixed cells. Plasma membrane blebbing is not likely to be involved in TG2 externalisation based on the plasma membrane stains used in this chapter.

Chapter 5 Which part of the β-sandwich domain is required for TG2 externalisation?

5.1 Introduction

In the previous chapter, it was demonstrated that β-sandwich domain is critical for TG2 externalisation, while β-barrel 1, β-barrel 1 and the core domain are not involved in TG2 externalisation. Extracellular TG2 can be visualised 48 hours post transfection while TG2 missing the β-sandwich domain cannot be externalised and is retained in the cytosol in a vesicle structure. Examination of the literature to assist in identifying the functional sequence within β-sandwich domain responsible for export highlighted a previous report by Griffin and colleagues (Gaudry *et al.* 1999) on TG2 trafficking suggested that a fibronectin site encompassing the first 7 amino acids (Figure 5.1-1) of the TG2 β-sandwich domain was crucial for TG2 presenting on the cell surface. They co-localised TG2 and fibronectin on the cell surface using confocal microscopy in stably transfected Swiss 3T3 cells with a tetracycline induced TG2 expression. The interaction of TG2 and fibronectin was determined using a GTP binding TG2-β-galactosidae fusion protein in transiently transfected COS-7 fibroblasts. However, this study was at odds with data generated in Sheffield were it was noted that renal fibroblasts would accumulate transfected TG2 in the cytosol rather than secreting TG2 into extracellular environment and subsequently the amount of TG2 fibroblasts would export remained constant irrespective of intracellular TG2 levels unless the cells was stressed. There was therefore concern that these studies in 3T3 fibroblasts may be resulting from cell damage and TG2 association with fibroblasts rather than controlled export. As renal tubule cells readily export TG2 with a relationship between TG2 production and that exported, this experiment was repeated in three renal tubule epithelial cells.

Another fibronectin binding site-the sequence 88-106 in β-sandwich domain was reported by Belkin *et al* (Hang *et al.* 2005) using surface plasmon resonance that measured association/dissociation of fibronectin and TG2. However, no studies regarding TG2 externalisation was done in their study on this additional fibronectin binding site and given the link proposed by Griffin and colleagues determine if this site could be involved in TG2 export was a logical progression. To do this, intra- and extra-cellular TG activity was measured following transfection with TG2 containing mutations of this

fibronectin binding site (Asp^{94} from D to A, Asp^{97} from D to A and both Asp^{94}, Asp^{97} from D to A) as in their study (Figure 5.1-1).

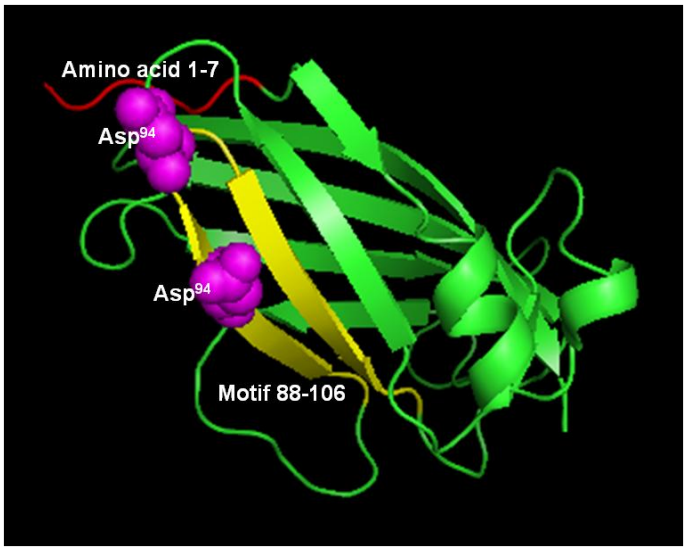

Figure 5.1-1 Location of point mutations in β-sandwich domain of TG2

Point mutation analysis include: removal of first 7 amino acid in N-terminal β-sandwich domain (red) and the motif 88-106 (yellow) with Asp^{94} and/or Asp^{97} to Ala

5.2 Deletion of first 7 amino acids to remove a fibronectin binding site in the β-sandwich domain

The pcDNA 6.2/cTC-tag-DEST vector containing human TG2 cDNA with the first 7 amino acids of β-sandwich domain missing was generated. The mutant TG2 (tg-7a) retained full TG activity (Figure 5.2-1 A & B) and transfected with equal efficiency in 3 different cell lines. As the construct (tg-7a) retained full TG activity, externalisation of TG2 can be tracked using TG activity. The extracellular TG activity and TG activity found in the medium was the same for wild type TG2 (tg) and TG2 lacking the fibronectin binding site at amino acid 1-7 (Figure 5.2-1 D and E). A western blot for TG2 in culture medium was also performed (Figure 5.2-1 C) to confirm this result. This also showed that wild type and TG2 lacking this fibronectin binding site was equally exported from the cell. Therefore the deletion of first 7 amino acids failed to prevent TG2 export and as such this potential fibronectin binding site is not important in TG2 export in tubular epithelial cells.

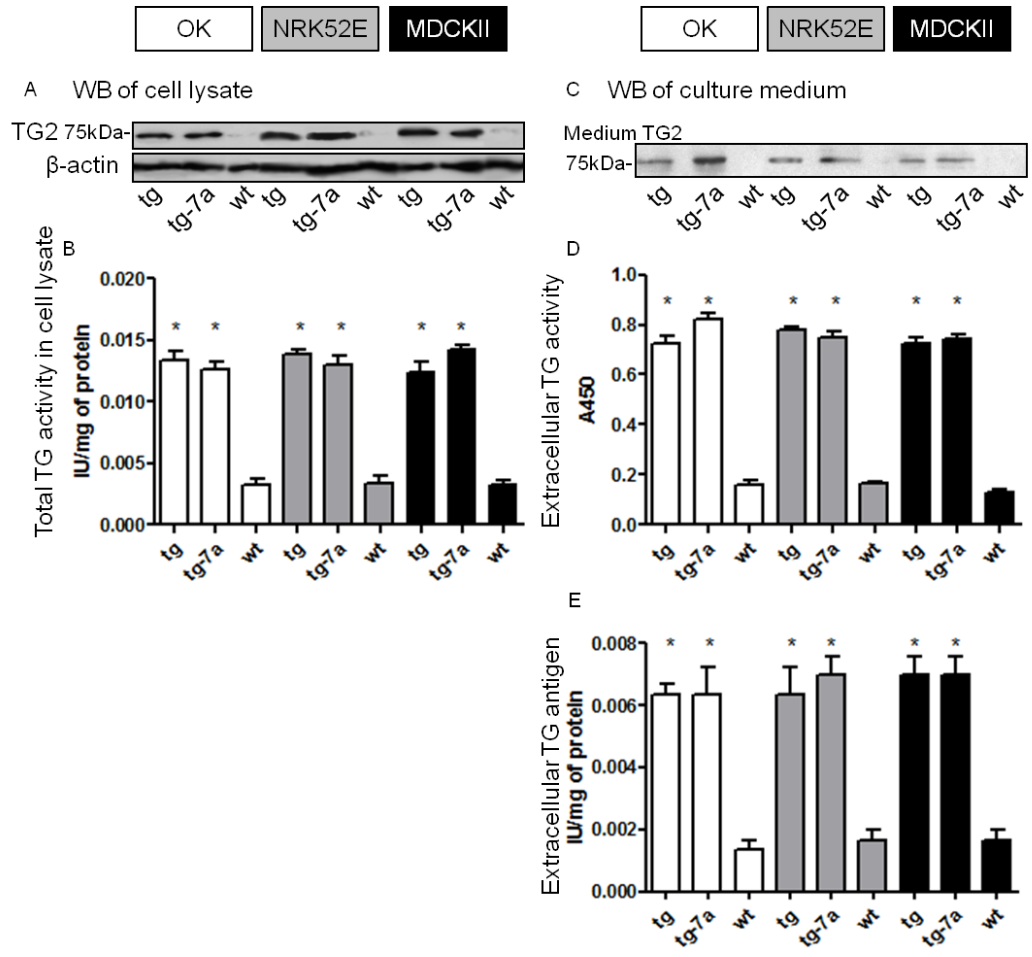

Figure 5.2-1 Intracellular and extracellular TG following the removal of the amino acid 1-7 fibronectin binding site

*OK, NRK52E and MDCK II renal epithelial cells were transfected with full length TG2 (tg) or mutant TG2 lacking the first 7 amino acid of β-sandwich domain missing that constitute a fibronectin binding site (tg-7a,). Western blots for TG2 in cell lysate 48 hours post transfection are shown in A and TG2 in medium are shown in B. Total transglutaminase activity in cell lysates (C), extracellular TG activity (D) and TG activity in culture medium (E) was measured, wt indicates non-transfection control. Data represents mean values ± SEM, n=5, *: p<0.05*

5.3 Affect of mutating a second fibronectin binding site in TG2

The primers for generating point mutation TG2 constructs (Table 3.1-1) were designed as previous described ***(Hang et al. 2005)***. The second fibronectin binding site (^{88}WTATVVDQQDCTLSLQLTT^{106}) in the β-sandwich domain of TG2 reported in the literature (Hang *et al.* 2005), had not been implicated in TG2 trafficking. Given the precious work of Gaudry *et al* (1999) a logical step was to determine if this fibronectin binding site was involved in TG2 extracellular trafficking. Subsequently we introduced a 2 point mutations (Asp^{94} & Asp^{97}) in this binding domain that had previously been shown to disable it's binding to fibronectin (Hang *et al.* 2005). Constructs containing either 1 or both mutations were equally expressed in each of the 3 TECs lines used (Figure 5.3-1 A-C). This construct had the same level of TG activity in the cell lysate to wild type TG2 (Figure 5.3-1 D-F). Therefore TG2 externalisation could be tracked using both extracellular TG activity and antigen.

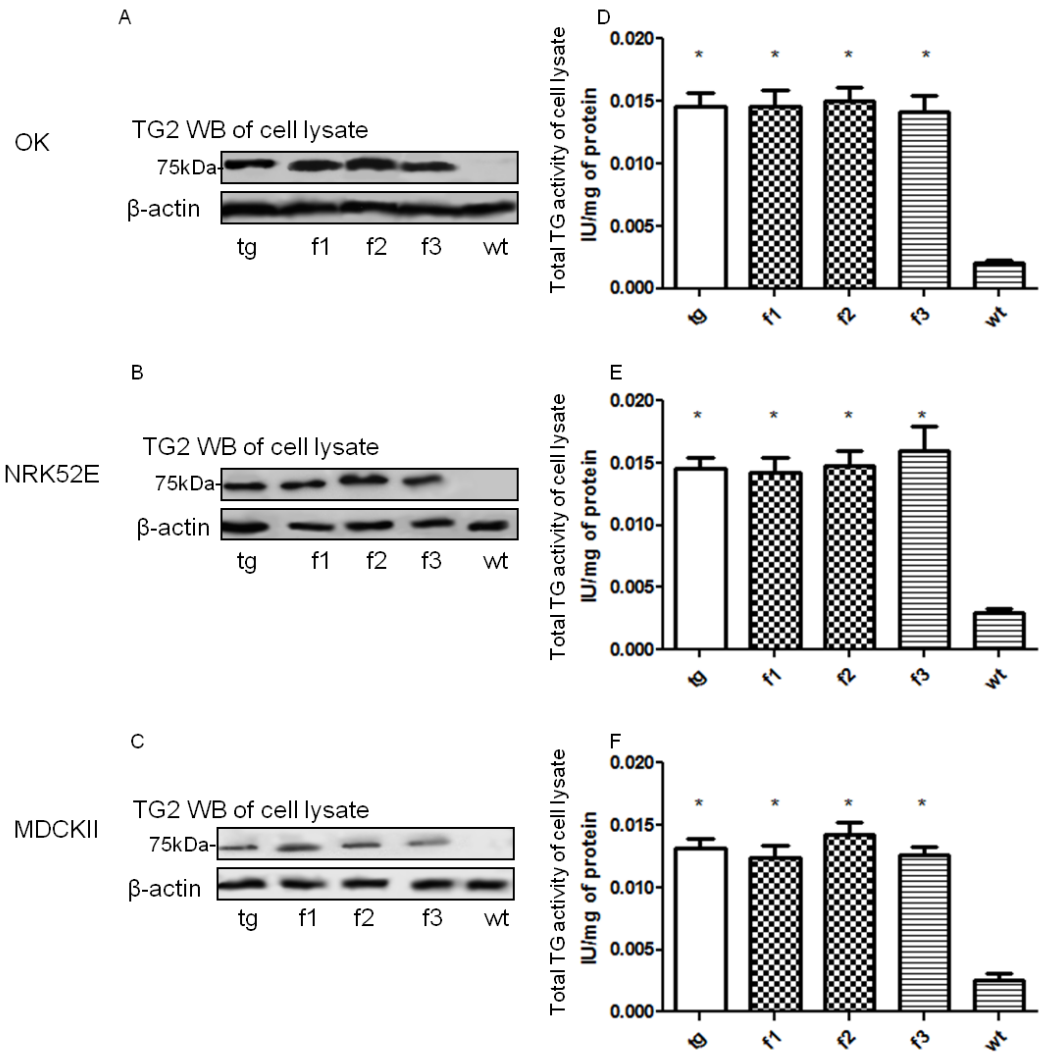

Figure 5.3-1 Intracellular TG2 levels following point mutation

*OK, NRK52E and MDCK II renal epithelial cells were transfected with pcDNA6.2/nTC-tag-DEST vectors containing either 1) full length TG2 (tg), 2) single point mutation of Asp^{94} to Ala (f1), 3) single point mutation of Asp^{97} to Ala (f2), or 4) a two point mutation of TG2 at Asp^{94}& Asp^{97} to Ala (f3), wt indicates non-transfection control. Western blots for TG2 in cell lysate 48 hours post transfection are shown in A-C and TG2 in medium are shown in D-F. Data represents mean values ±SEM. n=5, ** p<0.01, *p<0.05)*

Single mutation of either Asp^{94} (f1)or Asp^{97} (f2) into Ala significantly decreased extracellular TG activity and TG activity in the culture medium by 50% ($p<0.05$), while two point mutation of Asp^{94} and Asp^{97} returned TG2 export to basal levels ($p<0.01$) (Figure 5.3-2 A-C).

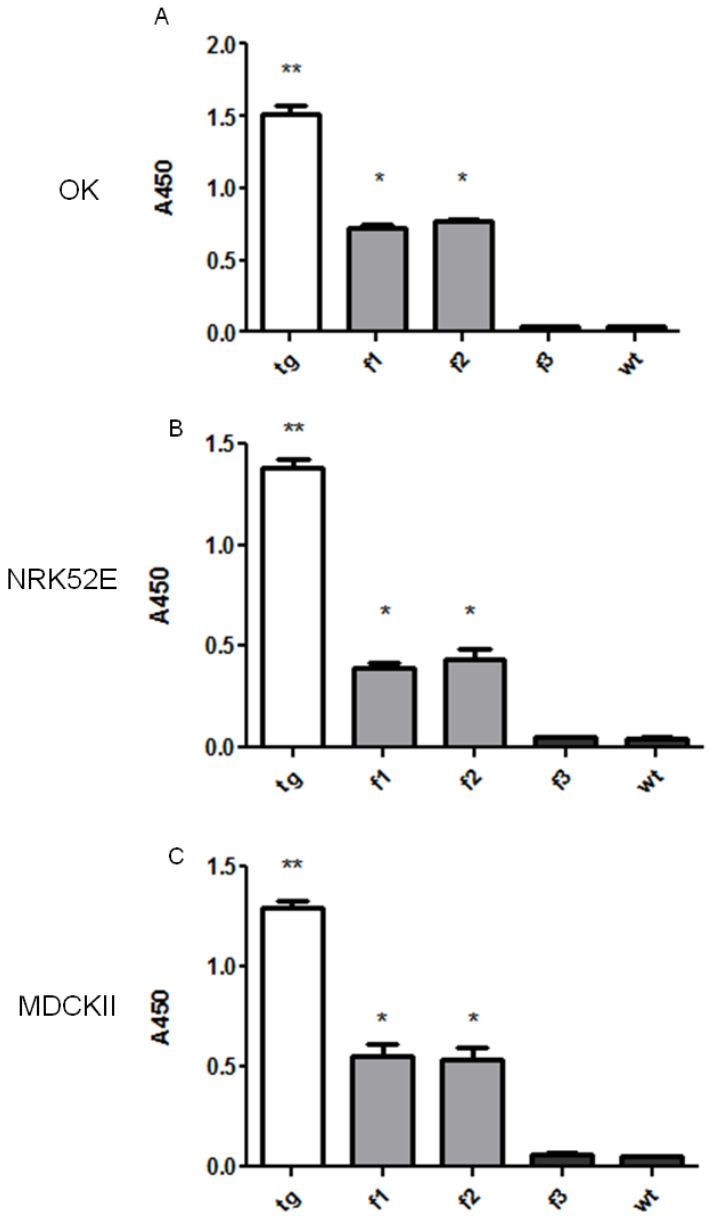

Figure 5.3-2 Extracellular TG activity following point mutation

*Extracellular TG activity was measured using a modified cell ELISA incorporating biotin labelled cadaverine into fibronectin following transfection with pcDNA6.2/cTC-tag-DEST vector containing either 1) full length TG2 (tg), 2) TG2 with a single point mutation of Asp^{94} to Ala (f1), 3) TG2 with a single point mutation of Asp^{97} to Ala (f2), or 4) TG2 with a two point mutation of TG2 at Asp^{94} & Asp^{97} to Ala (f3), wt indicates non-transfection control. Data represents mean values ±SEM. n=5, ** p<0.01, *p<0.05)*

This was further confirmed by measuring extracellular TG2 antigen (Figure 5.3-2 A-C) and TG activity in medium (Figure 5.3-2 D-F). One point mutation of Asp^{94} or Asp^{97} to Ala decreased 50% of TG externalisation and two point mutations completely prevent TG2 externalisation. This indicates this second fibronectin binding domain is critical for TG2 trafficking in tubular epithelial cells.

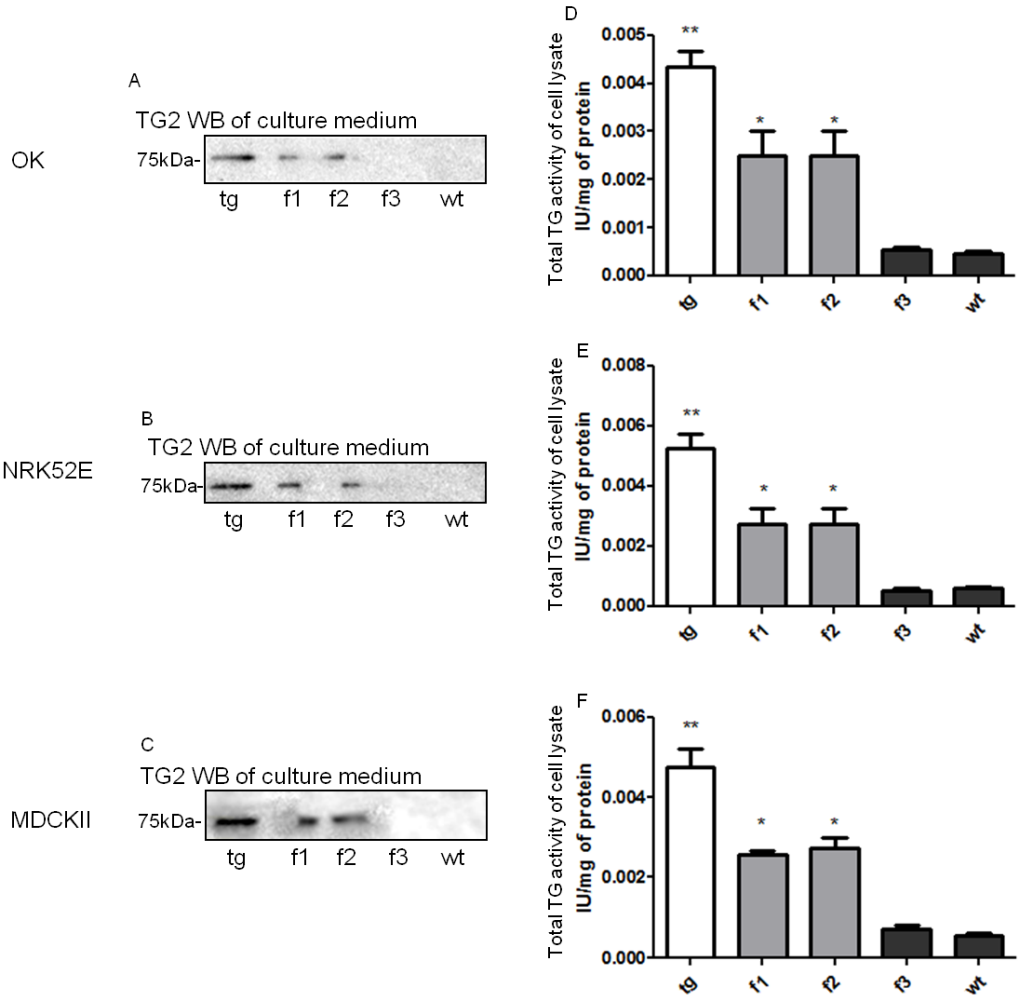

Figure 5.3-3 TG2 in medium following point mutation

*A western blotting immunoprobed for TG2 and measurement of TG activity in the culture medium were measured following transfection with pcDNA6.2/nTC-tag-DEST vector containing either 1) full length TG2 (tg), 2) TG2 with a single point mutation of Asp^{94} to Ala (f1), 3) TG2 with a single point mutation of Asp^{97} to Ala (f2), or 4) TG2 with a two point mutation of TG2 at Asp^{94} & Asp^{97} to Ala (f3), wt indicates non-transfection control. Data represents mean values ±SEM. n=5, ** p<0.01, *p<0.05)*

5.4 TG2 Co-transport with fibronectin

As the sequence 88 to 106 is a fibronectin binding site, it is possible that TG2 in TECs is simply co-transported with fibronectin in the same way as proposed by Griffin in fibroblasts, but with a different fibronectin binding site. To assess this, we knocked down fibronectin using co-transfection of anti-fibronectin siRNA with full length TG2 (tg-f) into three TECs lines. Fibronectin knockdown was in excess of 80% compared to cells transfected with non-sense siRNA (tg-ns) using volume densitometry analysis by western blot analysis (Figure 5.4-1 A) and β-actin was used as a loading control. Fibronectin knockdown had no effect on TG activity in the cell lysate. The cells co-transfected with anti-fibronectin siRNA and TG2 had same TG activity in cell lysate as the cells co-transfected with nonsense siRNA and TG2 did (Figure 5.4-1 B). The measurement of extracellular TG activity, antigen and TG activity in culture medium was identical irrespective of fibronectin knockdown (Figure 5.4-1C-E). Therefore, TG2 externalisation appears to be independent of cell-secreted fibronectin and thus TG2 is not co-transported with fibronectin.

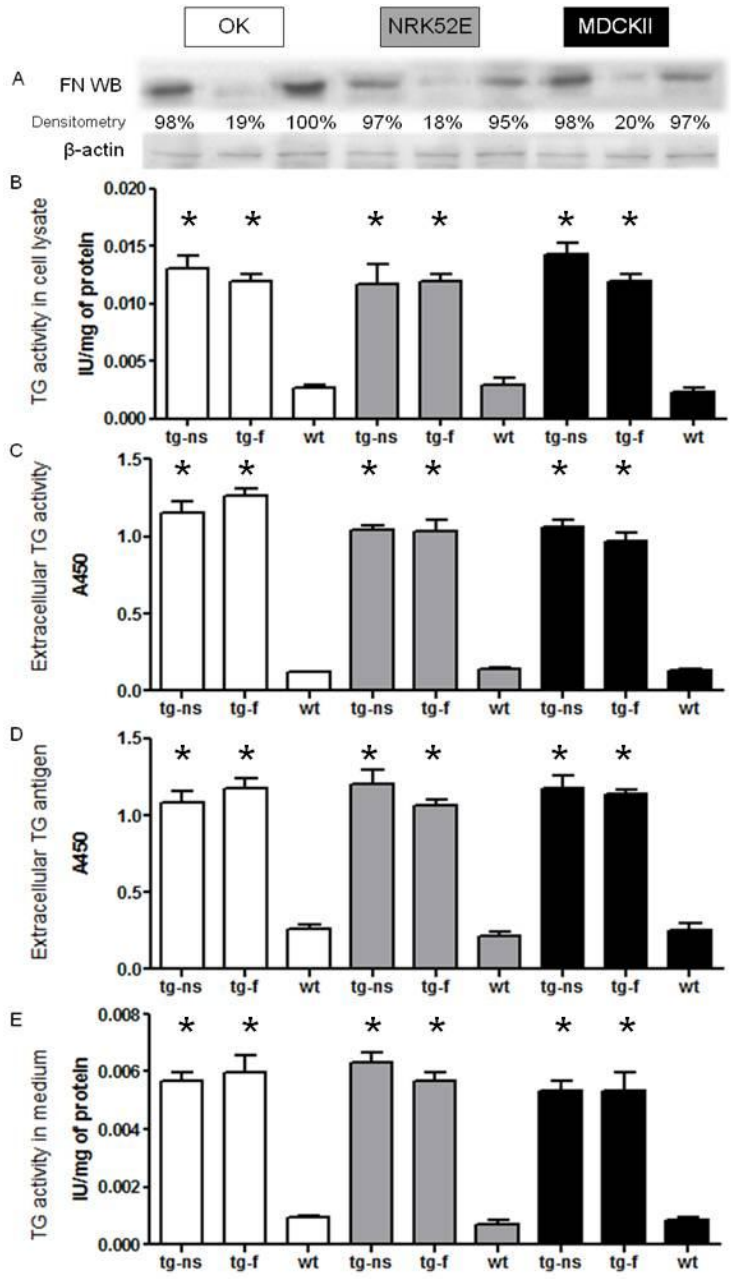

Figure 5.4-1 Intra and extra-cellular TG2 levels following fibronectin knockdown

*OK, NRK52E and MDCK II renal epithelial cells were co-transfected with TG2 plus either anti-fibronectin siRNA (tg-f) or non-sense siRNA (tg-ns). Western blot (WB) was immunoprobed for fibronectin were used to show basal fibronectin level in the cell lysate 48 hours after transfection (A) with β-actin as a loading control. Volume density measurements as a percentage of the fibronectin knockdown against cells transfected with non-sense siRNA are shown below the blot. Total TG activity in cell lysates (B), extracellular TG activity (C), extracellular TG2 antigen (D) and TG activity in culture medium (E) was measured, wt indicates non-transfection control. Data represents mean values ±SEM. n=5, *: p<0.05*

5.5 Dose mutation of the putative TG2 export sequence prevent TG2 export in stably transfected cells

Stably transfection is characteristic by the permanent integrating of the transfected genes into a random position in the genome of mammalian cells and thus ensures long-term protein production. One of the criticisms in studying TG2 externalisation using transient transfected cells is the externalised TG2 can be released because of the cell membrane damage involved in the transfection procedure. To avoid this bias, previous experiments had inbuilt controls, i.e. cells transfected with pcDNA6.2/cTC-tag-DEST vectors containing constructs that were and were not exported in the same experiment. However to provide conclusive proof stably transfected cells were cloned out. This also provide the additional benefits of improved cell imaging and the ability to study protein interactions more closely. NRK52E cells were transfected with pcDNA6.2/cTC-tag-DEST vectors containing full length TG2, TG2 with β-sandwich domain missing and TG2 with a two point mutation (Asp^{94} & Asp^{97}).

Stably transfected NRK52E cells were cloned out by blasticidin resistance and individual clones selected that had comparable TG2 expression between the 3 vectors transfected full length (TG2 cDNA (tg), TG2 with β-sandwich domain missing (-bsw) and two point mutation of Asp^{94} and Asp^{97} (f3) (Figure 5.5-1). The expression of TG2, TG2 with β-sandwich domain missing and TG2 with mutations at amino acid 94 and 97 were measured using western blots immunoprobed for TG2 (Figure 5.5-1 A). Cells expressing both full length TG2 (tg) and point mutant TG2 (f3) showed a clear band at 75 kDa. TG2 with β-sandwich domain missing (-bsw) produced a 60 kDa (-bsw) band (Figure 5.5-1 A). The intracellular total TG activity increased 5 fold compared to wild type cells for full length TG2 and TG2 mutants (Figure 5.5-1 B). Only the full length TG2 was readily secreted extracellularly and can be detected in the culture medium (Figure 5.5-1 C-E). There was no detectable increase in TG2 antigen or activity in the medium for wild type cells and cells transfected with the 2 point mutant TG2 (Figure 5.5-1 D, -bsw and f3). This confirmed studies performed in transiently transfected TECs that TG2 externalisation was prevented once the β-sandwich domain was deleted or Asp^{94} and Asp^{97}

mutation added to the 88-106 amino acid fibronectin binding.

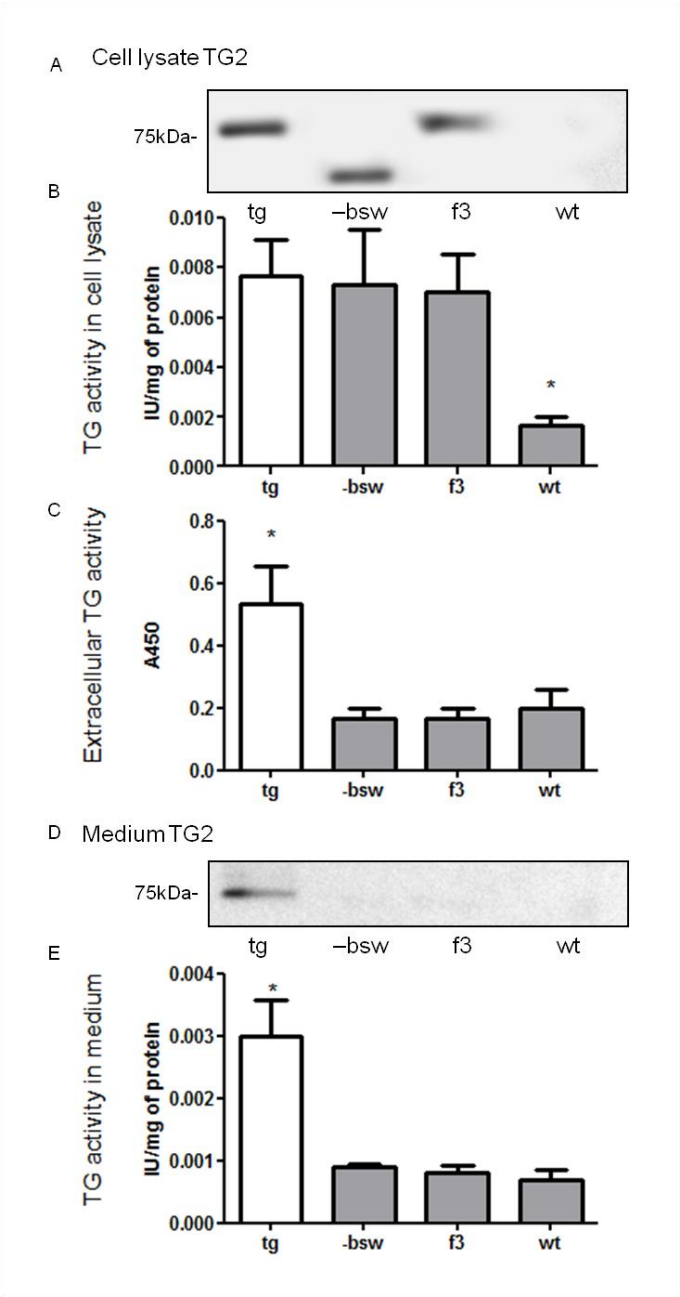

Figure 5.5-1 Measurements of intracellular and extracellular TG in stable transfected NRK52E cells

*Cells were transfected using pcDNA6.2/cTC-tag-DEST vector containing full length TG2 cDNA (tg), TG2 with β-sandwich domain missing (-bsw), two point mutation Asp94 and Asp97 to Ala (f3) and stable clones isolated using blasticidin resistance. Stable clones were selected base the comparable TG2 expression. Wild type NRK52E cells (wt) was used as a non-transfection control. Data represents Mean ± SEM, n=5, * p<0.05*

5.6 Characterisation of the TG2 export motif

A key question to access is if the TG2 export motif (aa 88-106) itself is enough to target TG2 for externalisation in TECs or whether it is required to work with other parts of TG2 to facilitate this process as all our exported constructs previously contained at least the core of TG2 plus the β-sandwich. To address this, theTG2 export motif, the β-sandwich domain and the core domain (not transported, negative control) were inserted in to a HaloTag® vector and the HaloTag® protein (33 kDa) levels measured in the cell lysate and culture medium (Figure 5.6-1). Promega's HaloTag® system utilises has a series of synthetic ligands that forms strong covalent bonds with Halo-tagged protein which can be used in fluorescent imaging, quantification and protein immobilisation studies as well as various customizable ligand approaches.

The HaloTag® protein in the cell lysates was similar between all 3 constructs indicating similar transfection efficiency and production of HaloTag® protein in the cell. However, the HaloTag® protein was only found to be elevated in culture medium when fused to either TG2 export motif aa88-106 and β-sandwich domain construct (Figure 5.6-1), being significantly higher than that of TG2 core domain ($p<0.05$). This clearly indicates that the TG2 export motif aa88-106 is capable of targeting other proteins for externalisation independently of the rest of the β-sandwich or TG2.

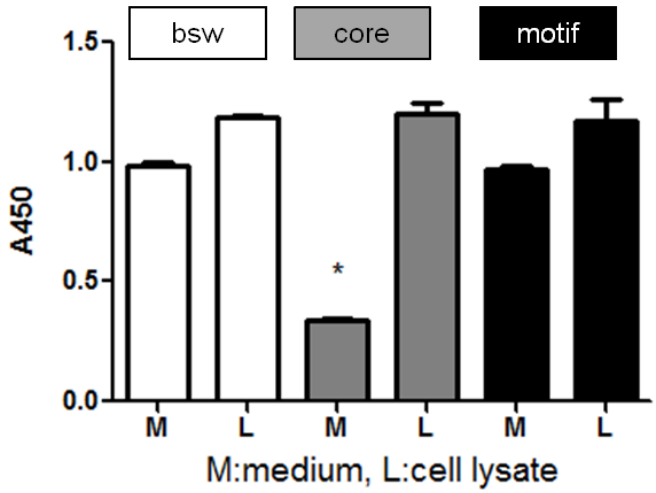

Figure 5.6-1 Can the TG2 export motif target other proteins for cell export?

*NRK52E cells were transfected with pFC14K HaloTag® CMV Flexi® vector containing either the TG2 β-sandwich domain (bsw), TG2 core domain (core), or the TG2 export motif 88-106 (motif). HaloTag® protein levels in culture medium and cell lysate were measured 48 hours post transfection using anti-HaloTag pAb. L: cell lysate, M:culture medium. Data represents mean ± SEM. n=5, *p<0.05*

5.7 Discussion

In this chapter, two function amino acid sequences that are both fibronectin binding site were studied. The first, encompassing the first 7 amino acids of the b-sandwich had previously been linked to TG2 export in fibroblasts, where as the second spanning amino acids88-106 within β-sandwich domain had not been associated with TG2 externalisation. The removal of first 7 amino acids (fibronectin binding site 1) had no effect on TG2 externalisation in TECs. A single point mutation of either amino acid 94 or 97 caused a decrease of 50% in TG2 externalisation while introduction of both point mutations prevented TG2 externalisation suggesting that the amino acid sequence 88-106 is critical for TG2 export and fibronectin is important in this process. This finding was further confirmed using stably transfected NRK52E cells using pcDNA6.2/cTC-tag-DEST vector containing TG2 with β-sandwich domain missing and TG2 with two points mutants (Asp^{94} & Asp^{97}). However, knock

down of fibronectin in cells using co-transfection of anti-fibronectin siRNA and TG2 and no affect on TG2 externalisation suggesting that while this part of TG2 is critical for export, it is not linked directly to fibronectin binding, although one can not exclude it binding to fibronectin like domains in other proteins.

As both amino acid sequences investigated are fibronectin binding sites, caution has to be used in interpreting some of the data as mutations in either could affect the extracellular TG2 antigen ELISA assay that is based on binding to a fibronectin coated plate. However cell lysate from NRK52E cells transfected with TG2 mutants such as TG2 with β-sandwich domain deleted and TG2 with Asp^{94} and Asp^{97} mutated retained a higher level of TG2 antigen than that of wild type cells (data not shown). This suggested the presence of other fibronectin binding site outside β-sandwich domain, most likely within the core domain because the core domain also retained TG2 antigen in the antigen ELISA assay. The gold standard method for studying protein interactions is co-immunoprecipitation (CO-IP); however, CO-IP can be difficult if the protein binding is not strong enough to be pulled down. Cop-IP was not used in these two papers studying the fibronectin binding site (Gaudry *et al.* 1999; Hang *et al.* 2005). In Gaudry *et al*s' work, the fibronectin and TG2 binding was determined by using β-galactosidase activity measurements in a fibronectin coated plate (Gaudry *et al.* 1999). They did not check if other domains of TG2 can interact with fibronectin.

In Hang *et al*s' work, the interaction between TG2 and 42 kDa fibronectin fragment were determined using TG2/factor XIIIa chimeric constructs containing Myc-His tags followed by immobilisation using Sepharose beads (Hang *et al.* 2005). TG2/factor XIIIa chimeras were used because factor XIIIa do not interact with fibronectin and only β-sandwich domain of TG2/factor XIIIa chimera interacted with a 42 kDa fibronectin fragment. A relatively weak interaction or an interaction between TG2 and outside the 42 kDa fibronectin fragment can be missed. Our finding suggested a possibility of novel fibronectin binding site on the core domain of TG2, but more studies are needed to confirm this preliminary observation.

The 86 to 106 amino acid motif we have identified as crucial for TG2 export is an interesting part of the β-sandwich forming a β5/β6 hairpin that is exposed

on the surface of TG2. Asp^{94} and $Asp^{97}$are crucial for the β5/β6 hairpin to form and subsequently the 3 dimensional folding here is also critical TG2 for export (Figure 5.7-2). Simply attaching this amino acid sequence to the C terminal of another protein (e.g. HaloTag protein) seems to target it for export which confirms that it is the part of TG2 required for TG2 trafficking and that no other part of TG2 is used in this process. There have been several hypotheses suggesting that TG2 could be co-transported with fibronectin however our 80% knockdown of fibronectin by siRNA with no effect on TG2 extracellular trafficking not only contradicts these hypotheses but also implies that the amino acid sequence 88-106 must have additional binding partners and/or properties. It is likely that this TG2 export motif can bind to other proteins that contain a fibronectin like domain and that this can act as a transmembrane binding partner. Identifying binding partners is therefore of importance. As most of the unconventional secretory proteins such as FGF-2 and IL-1β need to be recruited by plasma membrane or ER membrane residual proteins before externalised, it is possible the TG2 transport 88-106 binds to other proteins and facilitate TG2 externalisation. Based on the 3D protein structure (Figure 5.7-2) the wideness of β5/β6 hairpin is about the same size of heparan sulfate proteoglycans (HSPGs) side chains. It is possible that the TG2 transport motif binds to HSPGs of syndecan 4 and thus externalised through a direct molecular trap.

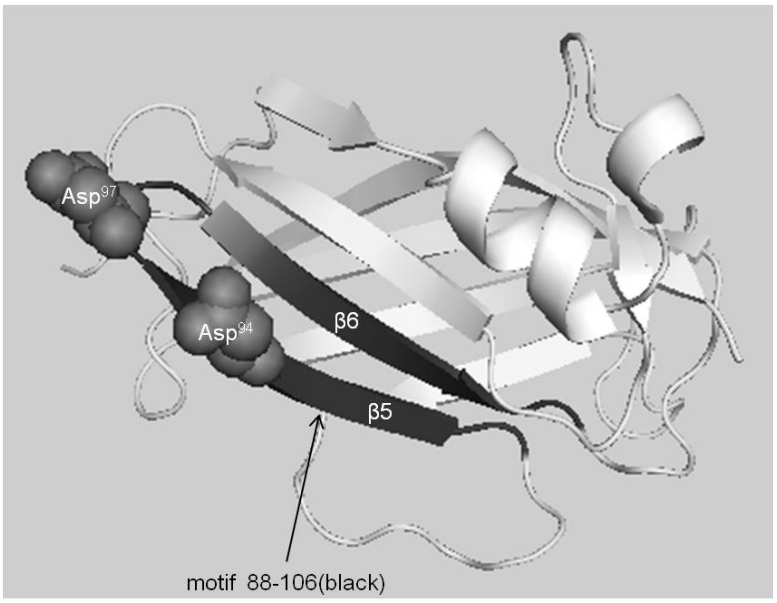

Figure 5.7-2 3D structure of β-sandwich domain and motif 88-106

The structure of β-sandwich domain (white), motif 88-106, β5/β6 (black), Asp^{94} and Asp^{97} are shown as spheres (gray)

Using bio-informatics it has been confirmed that the sequence ^{88}WTATVVDQQDCTLSLQLTT^{106} is specific to TG2. Two very similar sequences were identified in two mammalian cell membrane proteins. The first is the P2X purinoceptors family (15 of 19 amino acids in common with TG2). These are cell membrane ion channels and are activated by ATP (Bo *et al.* 1992; Bo *et al.* 1995; James *et al.* 2002). The other is Semaphorin/CD100 antigen (16 of 19 amino acids in common with TG2). This belongs to a large family of secreted and transmembrane proteins that function as repellent signals during axon guidance (Bougeret *et al.* 1992; Herold *et al.* 1995; Hall *et al.* 1996). Semaphorin, in particular is interesting as it can be secreted and thus may have some common elements with TG2 export. However little is known about Semaphorin export.

Chapter 6 Characterising the process of TG2 extracellular trafficking and the role of the TG2 export motif

6.1 Introduction

In the previous chapter, it was demonstrated that the TG2 export motif consisting of amino acids 88-106 within β-sandwich domain is critical for TG2 extracellular trafficking and this process is independent of fibronectin. In this chapter, physiological characteristics of TG2 extracellular trafficking will be investigated.

In normal renal tubular, tubular epithelial cells are grown surrounding tubular lumen maintained by basement membrane and extracellular matrix of the tubule (Figure 6.1-1). In tissue culture, if the cell is correctly polarised the side cell that sits on the plastic surface represents the basolateral surface and typically will generate a basement membrane between itself and the plastic to aid cell growth and adhesion. The side of the cell that faces upwards into the culture medium is the apical side. Apical side of the cells which typically has a brush border normally forms the tubular lumen facing the urine.

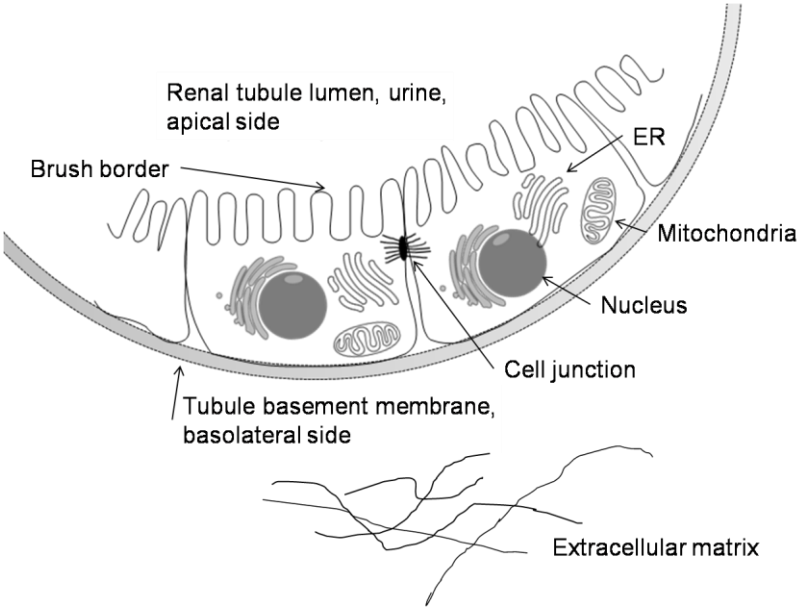

Figure 6.1-1 Diagram of tubular epithelial cells in renal tubule

Renal tubules are formed by renal tubular epithelial cells (TECs).TECs attached to extracellular matrix on the basement membrane that is the basal side of the cell. The surface facing tubular lumen is the apical side of TECs.

6.2 Direction of TG2 secretion

To determine if β-sandwich domain and the motif 88-106 of N-terminal β-sandwich domain can target a protein extracellular trafficking, three pFC14K HaloTag® CMV Flexi® vectors containing β-sandwich domain, the motif 88-106 and the core domain of TG2 were constructed (Table 6.2-1). HaloTag® should be measured in the culture medium in the constructs containing β-sandwich domain and the motif 88-106; however, not in the construct containing core domain. The proteins that bind to the motif 88-106 can be pulled down using HaloTag® magnetic beads and analysed using SDS-PAGE gel with silver stains. The proteins that bind to both β-sandwich domain and the motif 88-106 but not bind to the core domain of TG2 can be the candidate proteins that facilitate TG2 externalisation.

Table 6.2-1 Primers for HaloTag® constructs

	Forward primers	Reverse primers
HaloTag-bsw	AGGAGCGATCGCCATGGCCGAG GAGCTGGTCTTAGAGAGG	GGCGGTTTAAACATCCGCTGGGC ACCAGGCGT
HaloTag-core	TAAAGCGATCGCCATGGCTGTGT ACCTGGACTCGGAA	GTCGGTTTAAACCCCTGTCTCCT CCTTCTCGG
HaloTag-motif	AGCAGCGATCGCCATGTGGACAG CCACCGTGGTGGA	AACTGTTTAAACGGTGGTGAGCT GCAGCGAGAGG

These primer pairs were used to generate cDNA for insertion into pFC14K HaloTag CMV Flexi vector to generate the following plasmids HaloTag-bsw: HaloTag® containing β-sandwich domain, HaloTag-core: HaloTag® containing the core domain of TG2,p HaloTag-motif: HaloTag® containing the motif 88-106 of N-terminal β-sandwich domain of TG2.

To investigate if TG2 was being transported basolaterally (i.e. towards the tubular basement membrane) or apically (i.e. into the lumen), cells were grown in cell culture well inserts (353090 BD, UK) which contain a 0.4μm pore membrane at the bottom which allows free movement of proteins and metabolites. TECs where then grow into a tight monolayer on the insert such that molecules secreted from either the apical or basolateral side of the cell would be compartmentalised. Culture medium inside the insert represented apical secretion of TG2 and had a TG activity below the detection limit of the assay (Figure 6.2-1). In contrast, TG activity was 3 mIU/mg of protein in the culture medium below the cell culture insert indicating basolateral TG secretion to the basement membrane.

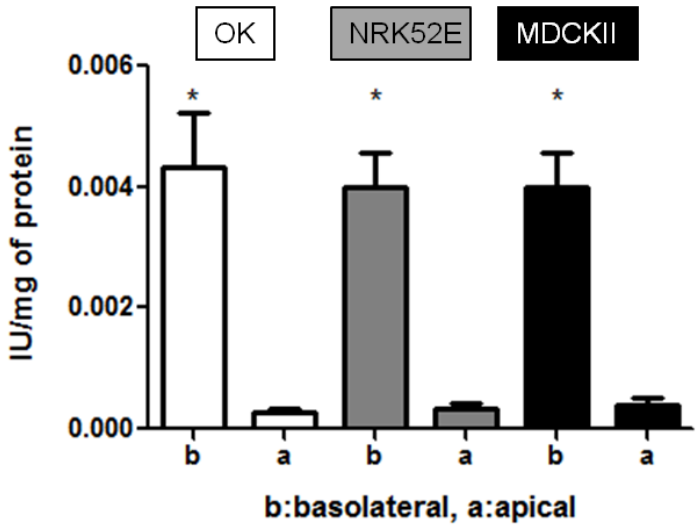

Figure 6.2-1 TG2 is exported across the basolateral membrane

*Total TG activity of culture medium was measured by the incorporation of Biotinylated TVQQEL peptide into casein using a modified ELISA. Cells were transfected with pcDNA6.2/cTC-tag-DEST containing full length TG2 cDNA and culture medium was replaced with serum free medium 48 hours post transfection. Total TG activity was measured after 4 hour of incubation at 37°C. Culture medium from the culture well inserts represent TG2 export to the apical side (a) and culture medium outside of the culture well inserts represent TG2 export to the basolateral side (b).Data represents Mean ± SEM, n=5, *p<0.05*

6.3 Visualisation of basal secretion of TG2

To confirm TG2 was being excreted solely from the basolateral surface of the cell, TG2 export was visualised by immunofluorescence using a combination of deconvolved Z stacks of immunofluorescent images and 3D rendering to generate a complete 3D image of the cell. NRK52E cells transfected with pcDNA6.2/cTC-tag-DEST vector carrying TG2 with a tetracysteine tag were stained with FlAsH. Subsequently cells were stained with a basement membrane marker, collagen IV. Taking a 3D rendered cell image (Figure 6.3-2 A-F) looking directly on the apical surface (ie from above) then the image is almost exclusively green (ie TG2) with the blue nucleus (DAPI) visible (Figure 6.3-2 A). Turning the image side way into a lateral view (Figure 6.3-2 B) clearly shows the red collagen IV under the cell, green TG2 towards the basolateral

membrane with no TG2 at all toward the upper apical membrane with the blue nuclei sitting just above the bulk of the green TG2. Looking at the bottom of the cell, ie a basal view (Figure 6.3-2 C), then all that is visible in some red collagen staining but mainly yellow to white staining which represents co-localisation of TG2 with collagen IV. Cartoons of the 3D images obtained from Figure 6.3-2 A-C are shown in Figure 6.3-2 D-F. Here the volume of the fluorescent signal is calculated based on the threshold of the fluorescent signal and marked as the same colour. The advantage of this is a clearer observation of the fluorescence with middle to low intensity and a calculation of the fluorescent volume.

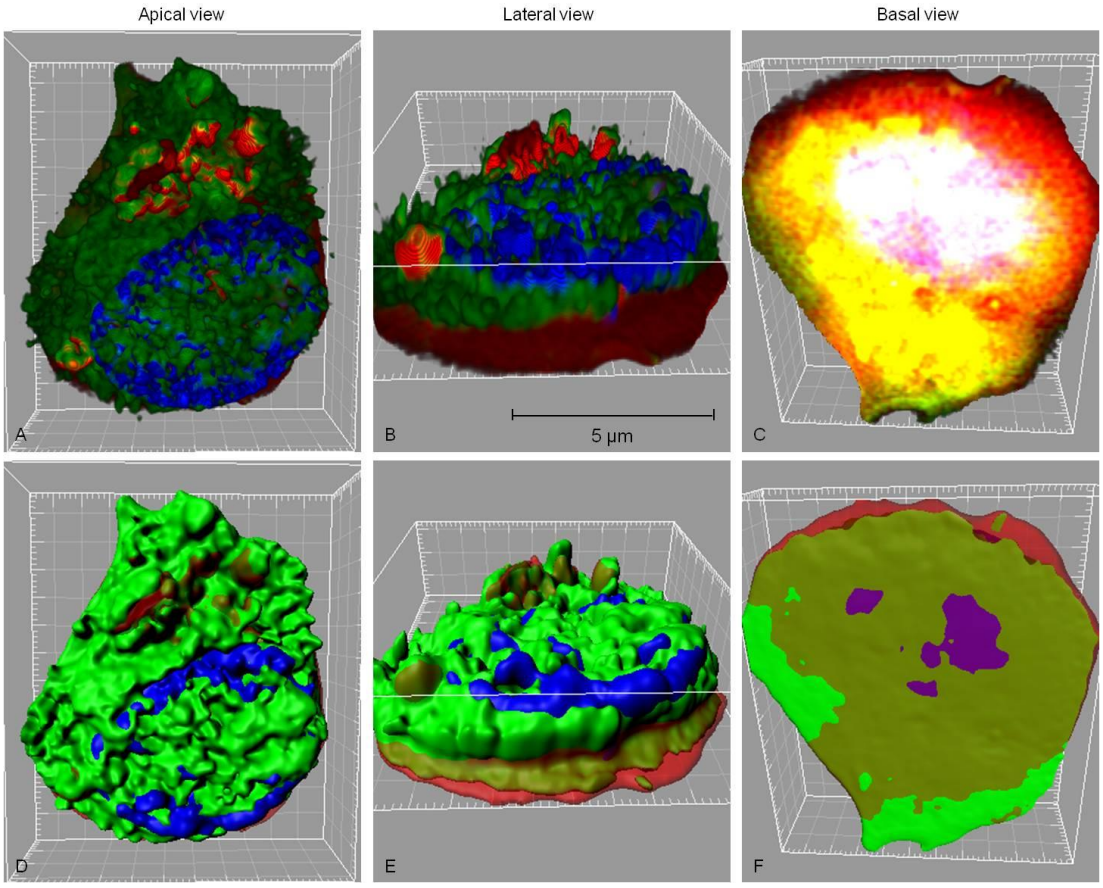

Figure 6.3-2 3 Dimensional imaging for NRK52E cells stained with TG2 (green) and collagen IV (red)

NRK52E cells transfected with pcDNA6.2/cTC-tag-DEST containing full length TG2 were stained with FlAsH green and stained collagen IV red. Z stacks were acquired, deconvolved and 3D rendered. The direct fluorescent signal (A-C) and carton 3D image (D-F) are generated from the same image based on the area and intensity of the fluorescent stain. Apical or top (A, D) , lateral or side (B, E) and basal or bottom (C, F) views are shown. The co-localisation for TG2 and collagen IV is represented by yellow.

To confirm the basal externalisation for TG2, NRK52E cells were also stained with an apical marker-phalloidin. TG2 was again introduced using a tetracysteine tag vector stained green with FlAsH and phalloidin stained red. Three dimensional rendered fluorescent images (Figure 6.3-1 A-F) are again shown as true images (Figure 6.3-1 A-C) and 3D cartoon models. Phalloidin primarily stained the apical surface of the cell and cell junctions, appearing in

the apical view to be floating above the green TG2 and blue nuclear stain (Figure 6.3-1 A, D). It is clear in the lateral view (Figure 6.3-1 B, E) that the red phalloidin is concentrated at the apical surface of the cell with no red present at the basal membrane. In contrast, TG2 in green was exclusively found at the basal side of the cell and no co-localisation was found at the basal side of the cell. The basal view (Figure 6.3-1 C, F) shows exclusively TG2 and the bottom of the nucleus. This further confirms that TG2 is exclusively externalised at the basal side of the cell.

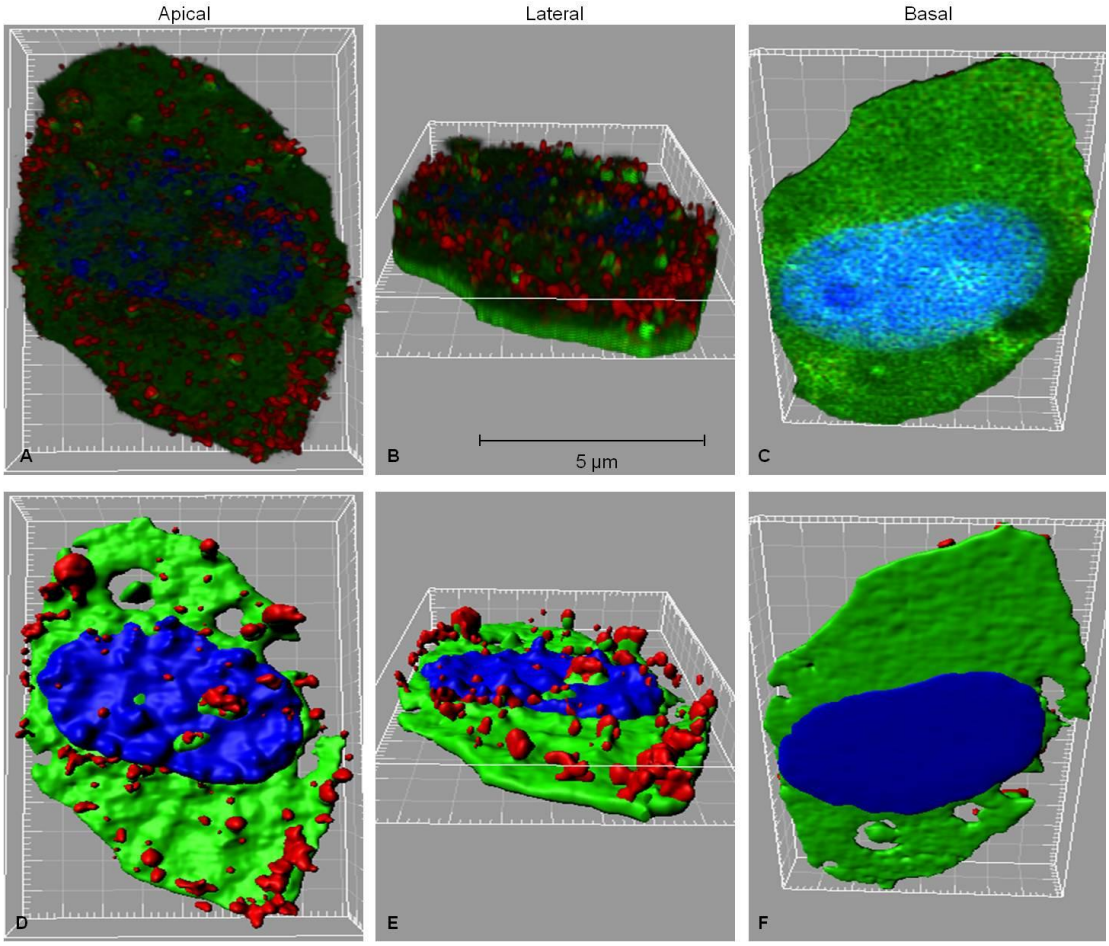

Figure 6.3-1 Three dimensional imaging of NRK52E cells stained for TG2 and phalloidin

NRK52E cells transfected with pcDNA6.2/cTC-tag-DEST containing wild type TG2 were stained with FlAsH to show TG2 as green and then co-stained with phalloidin red to mark the apical membrane. Z stacks were acquired and using deconvolution and 3D rendering apical (A), lateral (B) and basal views (C) were obtained. 3D rendered image was then transformed into volume cartoons based on the area and intensity of the fluorescent stain to generate a clearer picture of where the stains were residing in the cell (D-F).

6.4 Discussion

Perhaps unsurprisingly, we found that TG2 is transported basolaterally into what would be the tubular basement membrane *in vivo*. This finding is consistent with TG2s function in cell adhesion process and its role in ECM deposition and stabilisation (Fisher *et al.* 2009) that becomes pathological in

fibrosis (Johnson *et al.* 2007). In terms of understanding the process of TG2 trafficking then this may help if differences can be identified between the basal and apical membranes in terms of potential transmembrane proteins or channels (Fisher *et al.* 2009). The basolateral externalisation of TG2 can be further visualised using deconvolution microscopy and 3D rendering. The apical and basal side of the cell can be clearly distinguished in the 3D rendering imaging using basement membrane marker (ie collagen IV) and apical membrane marker (ie phalloidin).

As TG2 is solely externalised through basement membrane of the cells, it is possible that TG2 is carried through basement membrane by a trans-membrane proteins. This trans-membrane protein should be dominantly expressed at the basement membrane side of the cell. Heparan sulfate proteoglycans (HSPGs) is one of the trans-membrane proteins that localised at the basement membrane side of the cell. Basement membrane-type HSPGs are the main proteoglycans synthesised by glomerular epithelial cells (Stow *et al.* 1989) and other types of epithelial cells (David *et al.* 1985; Mohan *et al.* 1991). Cell surface HSPGs are co-localised with TG2 and TG2 has a high affinity to heparan sulfate (Scarpellini *et al.* 2009). It is possible that TG2 is externalised through a HSPGs-mediate molecular trap.

Chapter 7 Identify possible transport binding partners for TG2 externalisation

7.1 Introduction

In chapter 5, the amino acid sequence from 88 to 106 has been identified as that responsible for TG2 externalisation. Further proteins tagged with this motif can be externalised from the cell. The aim of this section is to identify the protein or proteins that can bind to the TG2 export motif. To do this the initial approach was to use the TG2 export motif linked to a HaloTag® which can be used to immobilise the tagged protein using magnetic beads or resin. Any protein binding to the motif could then be detected using silver stain. Once a band that is specific to the motif (ie not shown in the core domain construct), the band could be further analysed using mass spectrometry to identified the protein sequence.

A second approach was to use yeast two hybrid screen. The TG2 export motif was inserted into pGBKT7 vector that is an expression vector. This was co-transfected into yeast as “bait” with a human protein library in the pGADT7 vector used as “prey”. Any protein interaction between bait and prey actives the reporter genes and thus yeast is able to synthesis amino acids essential for yeast growth and Aureobasidin A antibiotics resistance. The prey vectors were then recovered from surviving yeast and amplified in E. Coli to identify the protein sequence. The TG2-protein interaction was subsequently confirmed using co-immunoprecipitation (CO-IP). The effect of candidate proteins on TG2 externalisation was determined using intra- and extra-cellular TG2 measurements following the candidate proteins knocked down by siRNA.

7.2 HaloTag pull down of proteins binding to the TG2 export motif

To identify the protein binds to the TG2 export motif, magnetic beads (G9311, Promega) bound to the HaloTag ligand were used to pull down the constructs containing β-sandwich domain, core domain and TG2 export motif from cell lysates of NRK52E cells transfected with pFC14K (HaloTag 7) CMV flex vector containing the β-sandwich domain of TG2 (bsw), core domain of TG2 (core) and TG2 export motif (motif) (Figure 3.1-7).

The proteins-TG2 export motif complex was eluted using Factor Xa and run on a reducing SDS-PAGE followed by sliver stain. Any bands that were presented

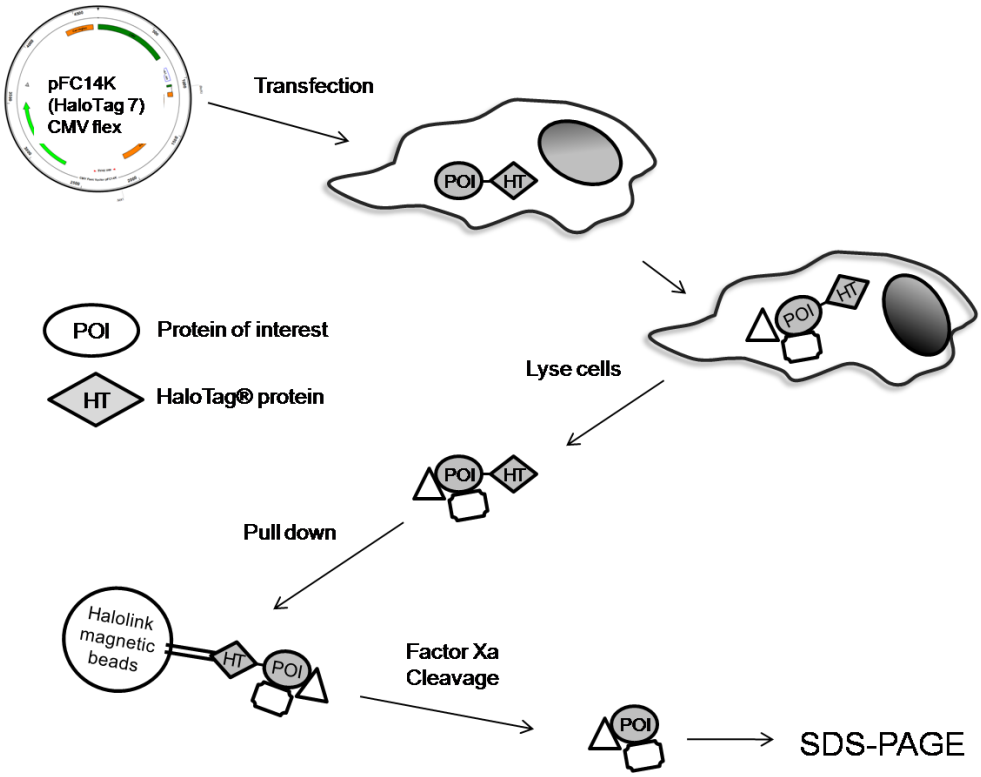

Figure 7.2-1 Schematic for HaloTag protein pull down experiments

Cells were transfected with HaloTag vectors containing protein of interest (POI) (ie TG2 export motif) and allowed to grow for 48 hours to produce an optimal amount of protein synthesised. The cells were lysed and the cell lysate is pulled down using Halolink magnetic beads. POI-HT (HaloTag protein)-proteins complex (ie any protein that binds to the TG2 export motif) bind to Halolink magnetic beads and POI-protein complex was then cleaved from the beads using Factor Xa proteinase. The Factor Xa elution is then run on SDS-PAGE and downstream analysis to identify the interacting protein.

on β-sandwich and TG2 export motif pull downs (ie exported), but not on the pull down from the core domain construct (ie not exported). From a 7.5% gel (Figure 7.2-2), it should be possible to see the β-sandwich domain (15 kDa, bsw), core domain (36 kDa, core) and the TG2 export motif (2 kDa, motif), however, it was not possible to see clear bands at any of these sizes suggesting that either the proteins were too low in abundance, HaloTag harvesting was poor or the HaloTag was not separated from the HaloTag ligand on the magnetic beads. Multiple other bands were visible in the cell lysate pull down from non-transfected cells (wt) indicating a lack of binding to the beads. As the HaloTagged protein can be detected in HaloTag ELISA used

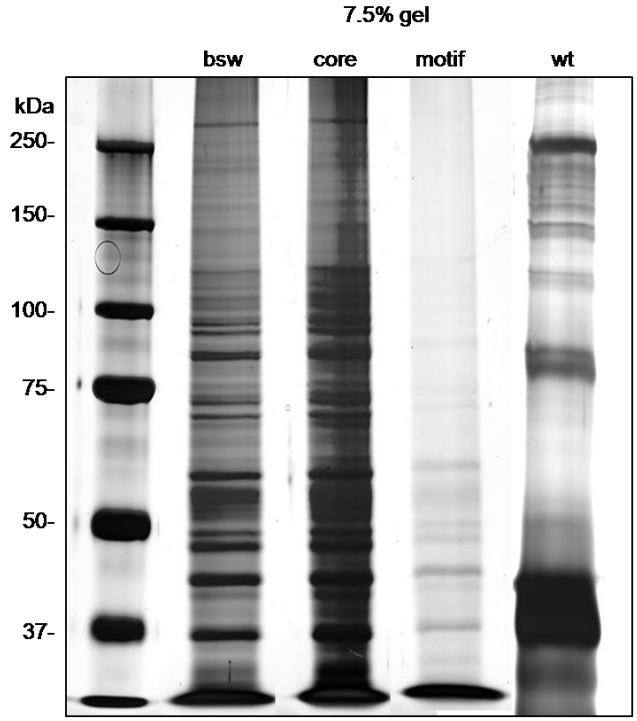

Figure 7.2-2 Silver stain of SDS-PAGE from HaloTag pull down experiments

Cell lysate pull downs from NRK52E cells transfected with pFC14K (HaloTag 7) CMV flex vector containing the β-sandwich domain of TG2 (bsw), core domain of TG2 (core) and TG2 export motif (motif) were run on 7.5% SDS-PAGE followed by silver stain. It should be possible to see any band that is specific to β-sandwich domain and TG2 export motif pull downs but no in core domain construct pull down. However, no specific band was found. Cell lysate from non-transfected NRK52E cells (wt) was used as a negative control.

to measure export in Section 6.2, clearly the labelling and detection system works with the constructs used which makes the lack of identification of the inserted protein surprising. Together this data suggests that HaloTag pull down may be not specific or strong enough to be pulled down by this process. Attention was therefore transferred to a Yeast two hybrid approach to explore the possible binding proteins.

7.3 Potential protein binding partners for TG2 externalisation using yeast two hybrid screen

As HaloTag experiments fail to pull down even the proteins that were transfected into cells, a yeast two hybrid screen was used to identify possible candidate proteins. The TG2 export motif was cloned into bait vector pGBKT7 and two-hybrid library screening with yeast mating using a normalised human protein library was performed (Section 3.5.4). The expression of TG2 export motif in yeast was first tested for autotoxicity and autoactivation. In autotoxicity test, yeasts transfected with pGBKT7 vector containing TG2 export motif had similar numbers and size of colonies as yeasts transfected with empty vector. The expression of TG2 export motif is therefore not toxic to yeast and yeast two hybrid system can be used to study TG2 export motif interacting partners. In autoactivation, no colonies was found in selected culture plate of both yeast transfected with pGBKT7 vector containing TG2 export motif and the yeast mating of pGBKT7 vector containing TG2 export motif and pGADT7 empty vector. This confirms that yeast carrying the TG2 export motif expressed can be selected with selective culture plate systems and subsequently yeast two hybrid system can be used in studying TG2 export motif binding proteins.

Yeast mating resulted in yeasts diploids containing pGADT7 vector with protein sequence that interact with the TG2 export motif growing in selected culture plate. The yeast diploids were picked and the yeasts containing pGADT7 were grown on selected culture plate. A total of 152 positive colonies were identified in two-hybrid screening using normalised human library. 34 pGADT7 vector containing candidate protein sequences were extracted and amplified using JM109 E.coli. The candidate protein DNA sequence was identified using DNA sequencing (Core Genomic Facility of the University of Sheffield) using a T7 Promoter

primer.

To confirm genuine protein interactions in yeast two hybrid system, yeasts were co-transfected with the pGADT7 containing candidate protein DNA sequence and the pGBKT7 vector containing TG2 export motif. Yeasts co-transfected with pGADT7 containing the candidate protein DNA sequence and empty pGBKT7 vector were used as negative controls. Positive colonies on selection plates from yeast co-transfected with pGADT7 vector containing the candidate protein DNA sequence and pGBKT7 vector containing TG2 export motif but no colonies of yeast co-transfected with pGADT7 vector containing candidate protein DNA sequence and empty pGBKT7 vector indicating a genuine protein interaction (Section 3.5.5.2). The DNA sequences were identified using BLAST (Basic Local Alignment Search Tool) (Table 7.3-1).

Table 7.3-1 Potential binding protein sequences and BLAST (Basic Local Alignment Search Tool) results ranked in the frequency of appeared

Identified Prey Sequence	Blast result
MPSSDDEATADSQHSTPPKKKRKVEDPKDF PSELLSFLSHAVFSNRTLACFAIYTTKEKAALL YKKIMEKYSVTFISRHNSYNHNILFFLTPHRH RVSAINNYAQKLCTFSFLICKGVNKEYLMYSA LTRDPFSVIEESLPGGLKEHDFNPEEAEETK QVSWKLVTEYAMETKCDDVLLLLGMYLEFQ YSFEMCLKCIKKEQPSHYKYHEKHYANAAIF ADSKNQKTIC	Large T antigen
MYLNEVAGKHGVGRIDIVENRFIGMKSRGIY ETPAGTILYHAHLDIEAFTMDREVRKIKQGLG LKFAELVYTGFWHSPECEFVRHCLSTMRSW	Argininosuccinate synthase
MTPVDVPVTNPAATILPVHVYPLPQQMRVAF SAARTSNLAPGTLDQPIVFDLLLNNLGETFDL QLGRFNCPVNGTYVFIFHMLKLAVNVPLYVN	C1q domain
LXXNEEVLVSAYANDGAPDHETASNHAILQLF QGDQIWXRLHRGAIYGSS	
MQADVRWLYTNMSFYVRDLSILGFLVSVGW GDGPGTNTPWIPRDNCTYLPLLSLQASYGN FIGMKIYMLRRLNIR	Cytochrome oxidase subunit I
MIFTYLVNFVYKNTRQSVLPMETGFRLLCFY C	Translocon-associated protein gamma
MGFYGGLAGGKDQGEMMSDGGYVVFRRM QL	Neurobeachin-like protein 2
MHHQLWVFMGVWQVERTRER	Ubiquitin-like protein ATG12
MDTKGQLYLFTFIVIASFLWKLYRNENIHVKEI KH	Sodium-dependent dopamine transporter
MEASEFXPSSGINAEWPLRPGHLLYLYYSICT FPGTRNTKLTFLCTEAQTSREQLGTPLIIN	Tapasin
MYLGLKILLSTPLAVCLTVFSYGDYCLFLMGI SDSKCI	Voltage-dependent L-type calcium channel subunit alpha-1C
MAYGLINEFMDSWTTFIDDHISRDVVDPHTAL RYIIETVLFPFFLFPDNKCI	Dynein heavy chain 1
MFFLQLESFFFKRKRYQMPAATTLFNCYLLK GTSMCFRLISLFQGNHGQ	Ganglioside-induced differentiation-associated protein 2
MKTSASPFFLAVGYHKPHIPFRYPKEFQKLY PLENITLAPDPEVPDGLPPVAYNPWMDIRRR EDVQALNISVPYGPIPVDFQRKIRQSYFASVS YLDTQVGRLLSALDDLQLANSTIIAFTSDHGF LMRTNT	Isoform 2 of Iduronate 2-sulfatase
MNITCKAVKIHNFSARDFVTYFLMCVGGVNK SLALHLLIVSFTISKEHSYILSRKSSNLILNSDY NLQLYFECTSISFN	HUMAN Netrin receptor UNC5C precursor
MSRELMRLVLLLGSTLKNFLINEXSKTINICQK FMPXYXQ	S45A4_HUMAN Solute carrier family 45 member 4
MLVWSFHDRIYTFCKSVLFSNIECLIFEFFRFL NWRKALKVFYI	LAT1_HUMAN Large neutral amino acids transporter
MTREKCLKADWLLALPQWRKPRNLQ	Heparan sulfate glucosamine 3-O-sulfotransferase 3A1
MTSCRTSASQKRTRKKTWHFWKKPSW	MDN1_HUMAN Midasin

MHYIERIWVFKEILKVRYCKCS	Dermatan-sulfate epimerase-like protein
MLTLRSVFFSLYLKIVNILISS	Integrin alpha-X
MGDIVMLCLYFFFLTHLXS	Anoctamin-6 (Ca^{2+} channel)
MQWPSVPSARSTTTAKGT	Aflatoxin B1 aldehyde reductase member 4
MSDFKELSLILIYSKM	Alpha1A-voltage-dependent calcium channel
MSFTLRQAYTGTWL	TOM70_HUMAN Mitochondrial import receptor subunit TOM7
MSMKDADTCINSLKNTTPSLK	KCNB1_HUMAN Potassium voltage-gated channel
MVNGFWILTVQAQFLLKIFYLSHL	SYT16_HUMAN Synaptotagmin-16
MTXYTHFVNLYFFQILNALFLNSLXF	MEP1A protein
MHYLLLKLYLLRFHSWHFCHEQRTDATCFAAW	Toll interacting protein variant
MSRELMRLVLLLGSTLKXFLINEESKTINICQNSCPSISXELXALV	KCND3_HUMAN Potassium voltage-gated channel subfamily
MLVWSFHDXIYTFCKSVLFSNIECLIFEFFXFLNWRKALKVFYI	CAN7L_HUMAN Calpain-7-like protein
MCTYSPFQREEALQ	UBR4_HUMAN E3 ubiquitin-protein ligase UBR4
MLCLYFFFLTHLAS	WLS_HUMAN Protein wntless homolog precursor
MGDIVMLCLYFFFLTHLAS	O52E4_HUMAN Olfactory receptor 52E4

Based on this protein list, a literature search was undertaken to identify potential functions of each protein paying particular attention to proteins that may be involved in protein secretion or presented on plasma membrane. Secondly we wanted to identify if these proteins were actually present in the cells exporting TG2 as otherwise they were irrelevant. This was undertaken by reverse transcription polymerase chain reaction (RT-PCR). The candidate proteins identified to be present in NRK52E cells by RT-PCR (Section 3.5.6) were Iduronate 2-sulfatase, large neutral amino acids transporter small subunit 1, neurobeachin-like protein 2, voltage-dependent calcium channel subunit alpha-1A, voltage-dependent L-type calcium channel subunit alpha-1C, tapasin, translocon-associated protein gamma.

Tapasin and translocon-associated protein gamma showed a particularly strong band at the corresponding size in 1% agarose gel (Figure 7.3-1) suggesting the expression of tapasin and translocon-associated protein gamma in mRNA levels in NRK52E cells.

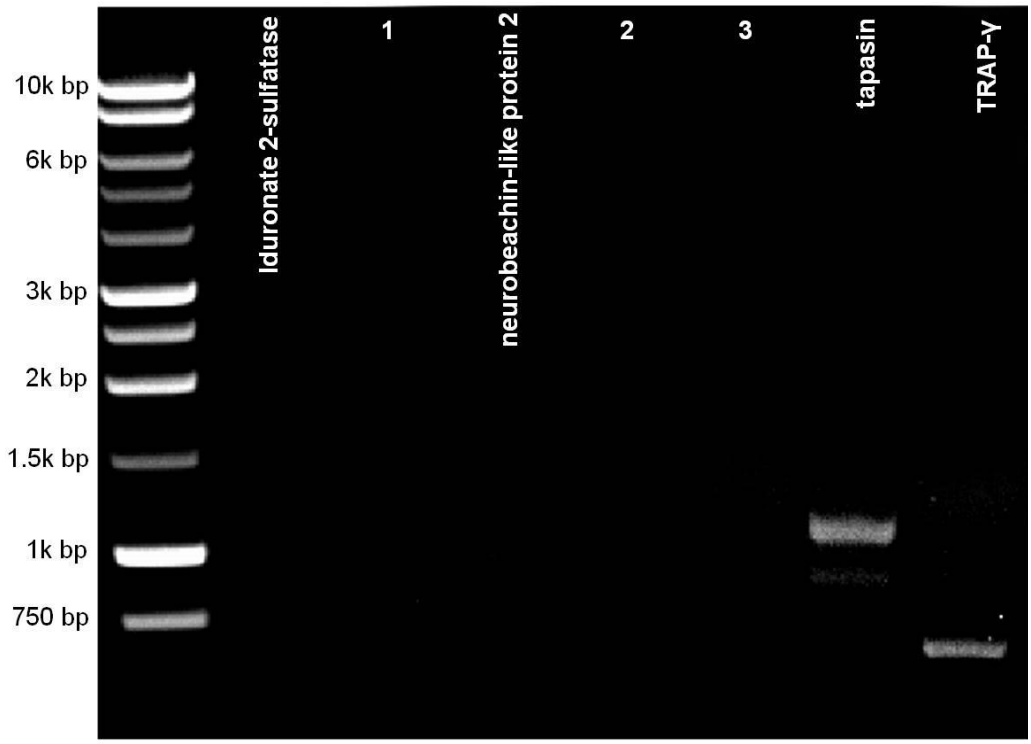

1. large neutral amino acids transporter small subunit 1
2. voltage-dependent calcium channel subunit alpha-1A
3. voltage-dependent L-type calcium channel subunit alpha-1C

Figure 7.3-1 Analysis of reverse transcription polymerase chain reaction (RT-PCR) products from NRK52E cells in 1% agarose gel

RT-PCR products with RNA extract from NRK52E cells using specific primers for detecting the following proteins in order Iduronate 2-sulfatase, large neutral amino acids transporter small subunit 1, neurobeachin-like protein 2, voltage-dependent calcium channel subunit alpha-1A, voltage-dependent L-type calcium channel subunit alpha-1C, voltage-dependent L-type calcium channel subunit alpha-1C, tapasin and translocon-associated protein gamma. Tapasin and translocon-associated protein gamma showed a clear band at the corresponding size in an 1% agarose gel.

antigen (LTA), tapasin and translocon-associated protein γ was selected. Tapasin and translocon-associated protein γ were presented in NRK52E cells analysed using RT-PCR. Tapasin is involved in the assembly of MHC class I and presented peptides at the cell surface and therefore seemed a possible

partner in moving TG2 to the cell surface. Translocon-associated protein γ is a glycosylated endoplasmic reticulum (ER) membrane receptor associated with protein translocation across the ER membrane and therefore one could hypothesise a similar role at the plasma membrane. LTA while not an endogenous mammalian protein was by far the most frequent sequence pulled out by this technique (eg 3 out of 22 colonies in run 1) and for this reason alone warranted investigation. Further there is a link between the BK virus that produces the LTA and the development of chronic allograft nephropathy and we hypothesised that this may cause inappropriate export of TG2 by interacting with the TG2 export motif.

7.4 Confirmation of protein-protein interaction using co-immunoprecipitation

To confirm that these proteins interacted at the cellular levels, a 2 stage set of immunoprecipitation experiments was put in place. Firstly by introducing exogenous TG2 by transfection and then secondly if the former was positive, using endogenous cell levels of the protein.

7.4.1 Large tumour antigen (LTA)-TG2 co-immunoprecipitation in TECs

The expression of LTA was initially confirmed in our TEC lines using western blot (WB) of lysates from wild type NRK52E, OK, MDCKII cells immunoprobed for LTA. NRK49F was used as a positive control because NRK49F was transformed using SV40 virus and should produce LTA. The WB of positive control (NRK49F) showed a band at 100 kDa that is the correct size for LTA (Figure 7.4-1 A). Similarly, NRK52E, OK and MDCKII cells all showed a band at the same molecular weight suggesting the expression of LTA in all TECs (Figure 7.4-1 A). Duel co-immunoprecipitation was performed using cell lysate from NRK52E cells transfected with pcDNA6.2/cTC-Tag-DEST vector containing full length TG2 cDNA and PBS was used as a negative control. A WB of a TG2 immunoprecipitation was probed with an anti-LTA antibody (Figure 7.4-1 B). This demonstrated a band at 100 kDa that corresponds to LTA confirming that TG2 interact. No band was found in the negative control (+v with anti-TG2 antibody). An anti-LTA pulldown was subsequently

fractionated by SDS-PAGE and western blotted before being probed with an antibody to TG2 (cub 7402). This gave a 75 kDa that is TG2 (Figure 7.4-1 C) and no band was found in PBS negative control (Figure 7.4-1 C, +v). These duel co-immunoprecipitation studies confirmed a protein-protein interaction between LTA and TG2 at exogenous TG2 levels in NRK52E cells. Duel co-immunoprecipitation using wild type NRK52E cells clearly showed a band in both anti-TG2 pulldown (Figure 7.4-1 D) and anti-LTA pulldown (Figure 7.4-1 E) at the corresponding molecule weight. No band was found in the PBS negative control pulldown with either an anti-TG2 antibody or anti-LTA antibody. These duel co-immunoprecipitation studies confirmed a LTA-TG2 interaction in endogenous levels of protein in TECs.

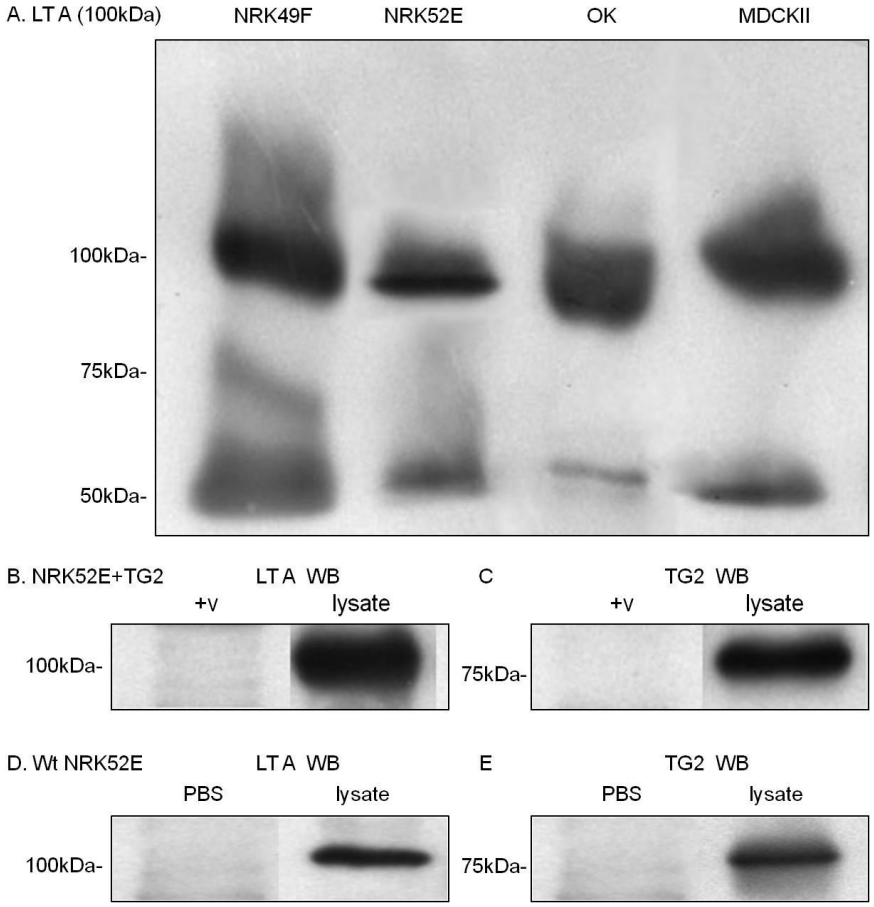

Figure 7.4-1 Co-immunoprecipitation of large tumour antigen (LTA) and TG2

A Western blot (WB) immunoprobed with an anti-LTA antibody using cell lysate from wild type NRK52E, NRK49F, OK and MDCKII cells confirmed the expression of LTA (A). A WB of cell lysate from NRK52E cells transfected with pcDNA6.2/cTC-Tag-dest vector containing full length TG2 cDNA immunoprecipitated using an anti-TG2 antibody (cub7402) was immunoprobed for LTA giving a band at 100 kDa that corresponds to LTA (B). Immunoprobing a WB for TG2 from a LTA pulldown showed a band at 75 kDa that corresponds to TG2 (C). LTA-TG2 interaction at endogenous protein levels was determined using cell lysates from wild type NRK52E cells. This gave a band corresponding to LTA (100 kDa) from a TG2 pulldown (D) and a band corresponding to TG2 at 75 kDa (E) from a LTA pulldown suggesting a protein-protein interaction at endogenous protein levels in NRK52E cells.

7.4.2 Tapasin-TG2 co-immunoprecipitation in TECs

The endogenous expression of tapasin in TECs was analysed by immunoprobing WBs of cell lysate obtained from wild-type cells (Figure 7.4-2 A). A band of 50 kDa which would correspond to the tapasin was seen in all three cell lines confirming there production of tapasin at the protein level. Tapasin-TG2 interaction was firstly investigated using duel co-immunoprecipitation studies using cell lysate from NRK52E cells transfected with pcDNA6.2/cTC-Tag-dest vector containing full length TG2 cDNA and PBS was used as a negative control. Cell lysates were initially incubated with an anti-TG2 antibody to pulldown TG2. This was then fractionated by reducing SDS-PAGE western blotted and immunoprobed with an anti-tapasin antibody. A band at 50 kDa that corresponds to tapasin was clearly visible (Figure 7.4-2 B). No band was found in the negative control (+v with an anti-TG2 antibody). This was then reversed using an anti-tapasin antibody pulldown with a subsequent WB immunoprobed for TG2 giving a band at 75 kDa that corresponds to TG2 (Figure 7.4-2 C). No band was found in the PBS negative control. Tapasin-TG2 interaction in an endogenous protein levels was determined using cell lysate from wild type NRK52E cells and PBS was used as a negative control. A Tapasin WB for TG2 pulldown (Figure 7.4-2 D) and TG2 WB for tapasin pulldown (Figure 7.4-2 E) resulted in a clear band at the corresponding size. This data clearly demonstrates a protein-protein between tapasin and TG2 in TECs in both exogenous and endogenous protein levels.

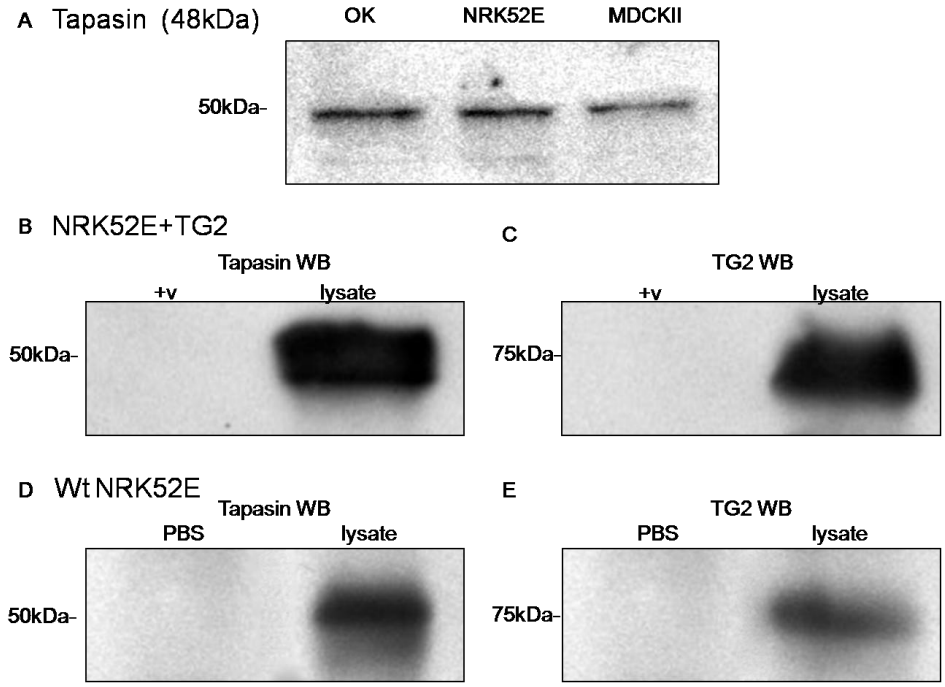

Figure 7.4-2 Co-immunoprecipitation for tapasin and TG2

A Western blot (WB) immunoprobed with an anti-tapasin antibody using cell lysate from wild type NRK52E, OK and MDCKII cells confirmed the expression of tapasin protein in these cells (A). A WB of cell lysate from NRK52E cells transfected with pcDNA6.2/cTC-Tag-dest vector containing full length TG2 cDNA immunoprecipitated using an anti-TG2 antibody (cub7402) was immunoprobed for Tapasin, giving a band at 50 kDa that is the correct size for tapasin (B). A WB of tapasin pulldown immunoprobed for TG2 showed a band at 75 kDa that is the correct size for TG2 (C). Cell lysate from wild type NRK52E cells was used to determine protein-protein interaction at endogenous protein levels. TG2 pulldown and tapasin pulldown generated a clear band at the corresponding molecule weight when immunoprobing WB for tapasin (D) and TG2 (E). PBS was used as a negative control.

7.4.3 Translocon-associated protein γ-TG2 interaction

The protein expression of translocon-associated protein γ (TRAP-γ) in TECs was determined using WB as in the previous 2 sections. OK, NRKE and MDCKII all showed a 20 kDa band in response to an anti- TRAP-γ antibody (Figure 7.4-3 A). Duel co-immunoprecipitation studies were then performed using cell lysate from NRK52E cells transfected with pcDNA6.2/cTC-Tag-dest vector containing full length TG2 cDNA and PBS was used as a negative

control. Initially using an anti-TG2 antibody pulldown (Figure 7.4-3 B) it was not possible to detect any band when this was fractionated by SDS-PAGE and the WB immunoprobed with an anti-TRAP-γ antibody (Figure 7.4-3 B). However, when an anti-TRAP-γ pulldown was subsequently fractionated by SDS-PAGE, western blotted and immunoprobed with an anti-TG2 antibody, a band at 75 kDa that would correspond to TG2 is clearly visible (Figure 7.4-3 C). The protein-protein interaction in endogenous protein levels was determined by repeating the same experiment. No band was detected in a TRAP-γ immunoprobed WB from a TG2 pulldown using cell lysate from wild type NRK52E cells (Figure 7.4-3D). A clear band was seen in TG2 immunoprobed WB from a TRAP-γ pulldown (Figure 7.4-3 E). No band was seen in pulldown experiments using PBS as a negative control. Although the co-immunoprecipitation only works in Anti-TRAP-γ pulldown, this result still suggested a protein-protein between translocon-associated protein γ and TG2 in both exogenous and endogenous protein levels.

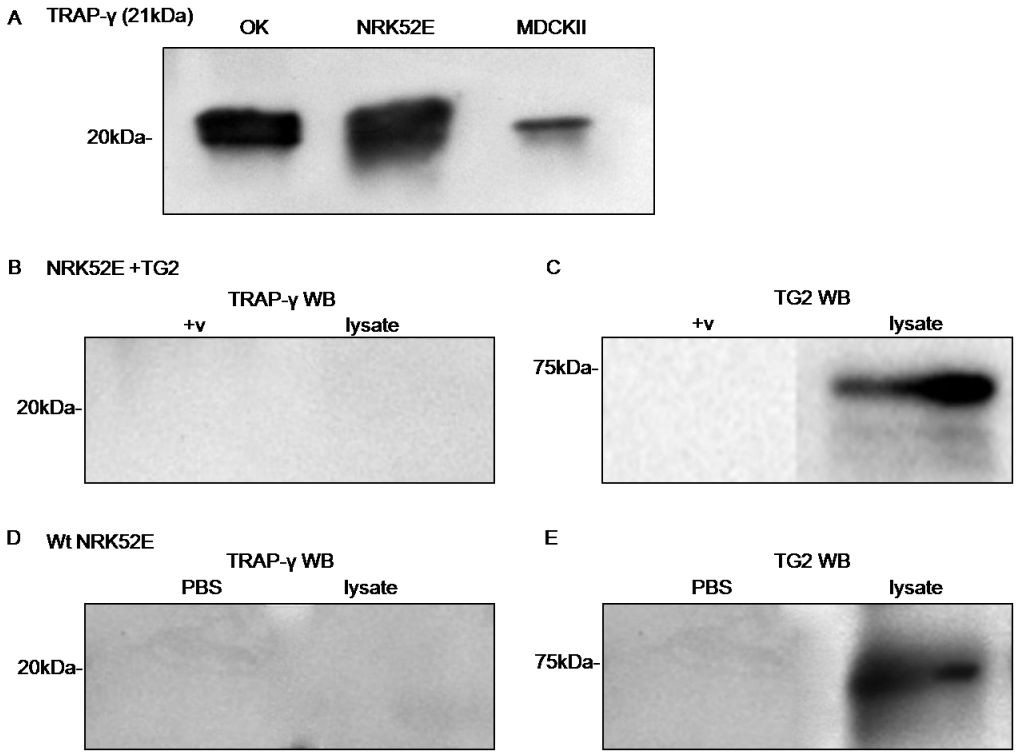

Figure 7.4-3 Co-immunoprecipitation for translocon-associated protein γ (TRAP-r) and TG2

A Western blot (WB) immunoprobed with an anti-TRAP-r antibody using cell lysate from wild type NRK52E, OK and MDCKII cells confirmed the expression of TRAP-r in protein levels (A). TRAP-r immunoprobing of a WB of cell lysate from NRK52E cells transfected with pcDNA6.2/cTC-Tag-dest vector containing full length TG2 cDNA immunoprecipitated using an anti-TG2 antibody (cub7402) showed no band at 20 kDa for TRAP-r (B) and TG2 immunoprobing of a WB from a TRAP-γ pulldown of the same cell lysate showed a band at 75 kDa that corresponds to TG2 (C). TRAP-γ immunoprobing of a WB from a TG2 pulldown of a wild type NRK52E lysate (D) showed no band, while TG2 immunoprobing of a WB from a TRAP-γ pulldown (E) showed a band at 75 kDa for TG2. PBS pulldown with an anti-TG2 antibody (D) and anti-tapasin antibody (E) was used as negative controls.

7.4.4 The motif 88-106 binds to origin binding domain of Large T antigen

The sequence indentified in yeast two hybrid screen is the origin binding domain of LTA. To determine if the binding of LTA and TG2 is dependent on the TG2 export motif and origin binding domain of LTA, the TG2 export motif

containing HA-tag and origin binding domain of LTA containing Myc-tag was cloned into pcDNA 3 (Invitrogen, UK) vector between BamH I and Xho I multiple cloning site as described in section 3.1.7. The primers for PCR products are listed in Table 7.4-1. The digestion and ligation reaction was performed as described in section 3.5.1 and confirmed using DNA sequencing.

Table 7.4-1 Primers for pcDNA 3 vector containing HAtag-moitif and MycTag-LTA origin binding domain

	Forward primers	Reverse primers
HA-motif	GGTCGTGGATCCGCCACCATGTGGACA	CTCGTACTCGAGTTAAGCGTAATCTGGTACGTCGTAGGAGGA
Myc-LT	GGTCGTGGATCCGCCACCGGAACT	CTCGAGTCACAGGTCCTCCTCTGAGATCAGCTTCTGCTCCTCGCAGAG

HA-motif: pcDNA 3 vector containing HA Tag and the TG2 export motif, Myc-LT: pcDNA 3 vector containing Myc Tag and the origin binding domain of large tumour antigen

Duel co-immunoprecipitation studies using an anti-HA-Tag antibody and anti-Myc-Tag antibody was performed to determine the exogenous protein interaction. The pcDNA3 vector containing TG2 export motif with HA-Tag and pcDNA 3 vector containing origin binding domain of LTA and Myc-Tag was co-transfected into NRK52E cells. Cells co-transfected with the HA tagged TG2 export motif and empty vector or Myc tagged origin binding domain of LTA and empty vector was used a negative control. The expression of HA tagged TG2 export motif was analysed using the cell lysate from NRK52E cells transfected with pcDNA3 vector containing TG2 export motif with HA-Tag and the expression of Myc tagged origin binding domain of LTA was analysed using the cell transfected with pcDNA 3 vector containing origin binding domain of LTA and Myc-Tag. HA tagged immunoprobing of a WB from an anti-Myc antibodies pulldown (Figure 7.4-4 A) showed a strong band at 6 kDa that would represent the TG2 export motif-HA tag construct. The co-transfection of Myc-tagged origin binding domain of LTA and empty vector (LTM+V) had no antigen detected. Correspondingly, immunoprobing for Myc tag of a WB from an anti-HA antibody pulldown (Figure 7.4-4 B) gives a band at 25 kDa that is compatible with the Myc tagged origin binding domain of LTA construct. No

antigen detected in the co-transfection of LTM with empty vector (LTM+V). This suggested that origin binding domain of LTA binds to the TG2 export motif aa88-106. The origin binding domain of LTA also binds to cellular DNA and transits to DNA helicase (Paucha *et al.* 1986). The finding may explain the co-localisation of TG2 in cell nucleus that will be detailed in the next section and the role of TG2 in cell proliferation (Barone *et al.* 2007).

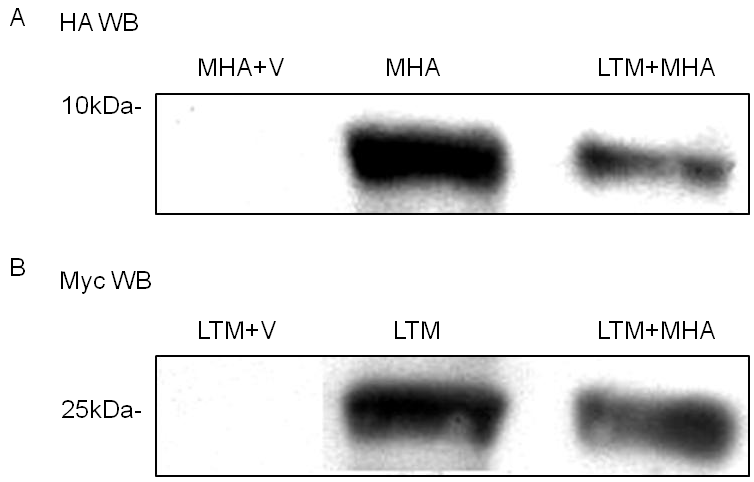

Figure 7.4-4 Co-immunoprecipitation for origin binding domain of large tumour antigen (LTA) and TG2 export motif

Cells lysate from NRK52E cells co-transfected with pcDNA 3 vector carrying the origin binding domain of large tumour antigen and Myc Tag (LTM) and the TG2 export motif aa 88-106 and HA Tag (MHA) were immunoprecipitated by anti-Myc antibodies or anti-HA antibodies. HA immunoprobing of a WB from Myc Tag pulldown (A. LTM+MHA) displayed a band at 6 kDa that corresponds to the TG2 export motif aa 88-106 and HA Tag construct. Myc immunoprobing of a WB from HA Tag pulldown (B. MTA+MHA) displayed a band at 25 kDa that corresponds to the origin binding domain of large tumour antigen and Myc Tag construct. Cells co-transfected with pcDNA 3 vector carrying carrying origin binding domain of large tumour antigen and Myc Tag or the TG2 export motif and empty vector was used as negative controls (A: MHA+V, B: LTM+V). The expression of MHA and LTM construct in NRK52E cells (A: MHA & B: LTM).

7.5 Discussions

In this section, it has been demonstrated that the large tumour antigen (LTA), tapasin and translocon-associated protein γ (TRAP-r) interact with TG2 at both exogenous and endogenous protein levels in TECs. LTA is a virus protein produced by polyomavirus that is involved in cancer and cell transformation such as SV40 in tissue culture (Ewen *et al.* 1989). LTA can be also produced by BK and JC virus in human allograft rejection in kidney recipients (Binet *et al.* 1999). Cell transformation by SV40 in tissue culture may be related to the LTA-p53 (Deppert *et al.* 1989) and LTA-retinoblastoma binding protein (Rb protein) (Ali *et al.* 2001) interactions. TG2 can modify Rb protein in the cell nucleus via transamindation and provide protection against apoptotic insults to ensure that cells remain viable during differentiation (Boehm *et al.* 2002; Milakovic *et al.* 2004). TG2-LTA interaction might be involved in the nuclear-targeted TG2 and the role of TG2 in cell apoptosis. A small portion of LTA a high affinity to plasma membrane can be expressed on cell surface (Lange-Mutschler *et al.* 1983; Lange-Mutschler *et al.* 1984). Based on this observation, It is possible that the plasma membrane-associated LTA carried TG2 to plasma membrane and released it into extracellular space, however whether LTA has a role in TG2 externalisation will be determined using measurements of extra- and intra-cellular TG activity levels following knockdown of LTA by co-transfection of anti-LTA siRNA and TG2 cDNA in TECs. Co-localisation analysis of LTA by co-transfection of anti-LTA siRNA and TG2 cDNA in TECs in the next chapter.

Beforehand, it was not expected to find the expression of LTA in TECs because OK (Malstrom *et al.* 1987), NRK52E (de Larco *et al.* 1978) and MDCK II cells (Richardson *et al.* 1981) were not transformed using SV40. The incidence of polyomavirus infection among animal is unknown and thus it is possible that the animals used to construct the cell lines were infected with polyomavirus. This is logical as TECs with LTA expression would have a higher chance to escape cell apoptosis and be selected in the process of establishing immortal cell lines.

Tapasin is an ER membrane protein that is essential for the appropriate antigen peptide loading assembly and folding of major histocompaliblity

complex (MHC) class I. In tapasin knockout mouse, the peptides have a low affinity in MHC class I receptor on cell surface MHC class I molecules and the expression of MHC class I molecular is decreased on cell surface (Ortmann *et al.* 1997). Subsequently hosts are immunocompromised in tapasin knockout mice and bare lymphocyte syndrome in human (Touraine 1981). The major role of tapasin is to assemble the antigen peptide on MHC class I molecule in ER and tapasin is responsible for the antigen peptide pass through the ER membrane. Based on the observation i.e. TG2 synthesised in the cytosol and accumulated around the cell nucleus in ER membrane-formed vesicles (Section 4.8 & Section 9.2.1), it is possible that tapasin recruited TG2 in the ER-membrane formed vesicles. It will be determined in the next chapter if tapasin in involved in TG2 externalisation using measurements of extra- and intra-cellular TG activity following co-transfection of anti-tapasin siRNA and TG2 cDNA. Visualisation and co-localisation analysis will be needed to determine the possible role of tapasin in TG2 externalisation. TRAP-r is a glycosylated ER membrane receptor associated with protein translocation across the ER membrane (Wang *et al.* 1999). It is possible that TRAP-r may responsible for transport TG2 from rough ER after TG2 synthesised to cytosol or other organelles that is involved in TG2 externalisation. TRAP-γ knockdown will be performed using siRNA technique to determine the role of TRAP-γ in TG2 externalisation in the following chapter.

Chapter 8 The effect of knock down of Large Tumour Antigen, Tapasin and Translocon-associated protein γ on TG2 externalisation in TECs

8.1 Introduction

In Chapter 7 the interaction of large tumour antigen (LTA), tapasin and translocon-associated protein γ with the TG2 export motif was described at the protein level. However, the fact that these 3 proteins interact with the TG2 export motif does not prove that these proteins are involved in TG2 export from the cell and thus determining their significance to the extracellular trafficking of TG2 is critical if that are to be implicated in an export pathway. The aim of this chapter is to knockdown LTA, tapasin and translocon-associated protein-γ (TRAP-γ) using siRNA technology and determine the effect of this on TG2 externalisation. To undertake this, intra- and extra-cellular TG levels were measured 48 hours following the co-transfection of pcDNA6.2/cTC-Tag-dest vector containing full length TG2 cDNA with anti-LTA, anti-tapasin or anti-TRAP-γ siRNA.

8.2 Intracellular and extracellular TG activity following knockdown Large T-antigen

OK, NRK52E and MDCKII cells were co-transfected with pcDNA6.2/cTC-Tag-dest vector containing full length TG2 cDNA and either non-sense siRNA (tg+ns) or anti-LTA siRNA (tg+lt) (siRNA ID: ABGJPMF, applied Biosystems). Wild type cells were used as a negative control (wt). The normal expression of LTA (wt, tg+ns) in all 3 cell lines was knocked down by approximately 50% when transfected with siRNA (Figure 8.2-1 A, tg+lt) when measured by densitometry. Total TG activity in the cell lysates increased by 5 fold for the cells co-transfected with TG2 cDNA and siRNA (Figure 8.2-1 B, tg+ns and tg+lt) compared to wild type cells (wt). Extracellular TG activity (Figure 8.2-1 C) and extracellular TG2 antigen (Figure 8.2-1 D) showed a significant decrease in extracellular TG levels following LTA knock down ($p<0.05$). This result is consistent with measurements of TG activity in culture medium (Figure 8.2-1 E) that is also reduced. This data clearly suggests that large tumour antigen is involved in TG2 externalisation.

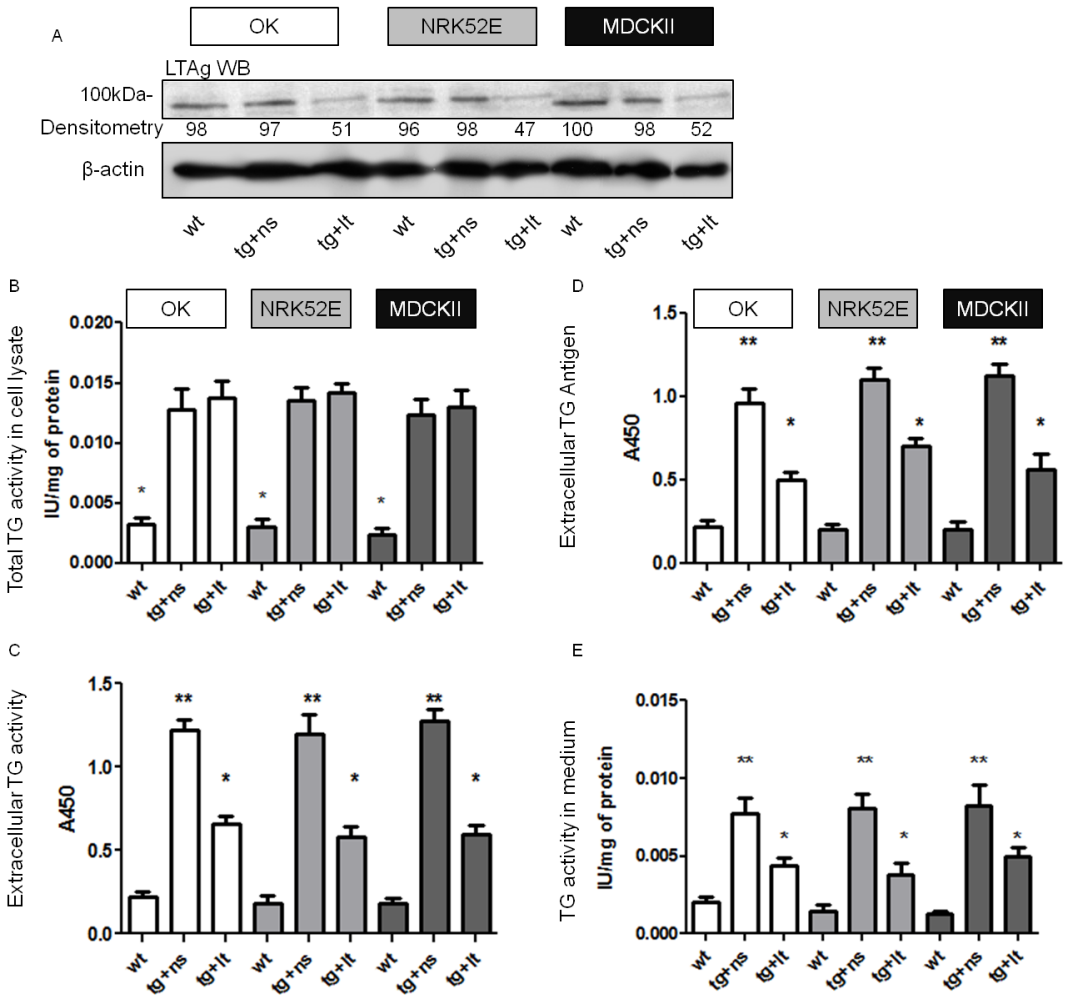

Figure 8.2-1 Extracellular and intracellular TG activity following large T-antigen (LTA) knockdown

*OK, NRK52E and MDCKII cells were co-transfected with pcDNA6.2/cTC-tag-DEST expression vector containing TG2 cDNA (tg) with either non-sense siRNA (tg+ns) or anti-LTA siRNA (tg+lt). Non-transfected cells (wt) were used as a negative control. Western blots from cell lysates were immunoprobed for LTA (A) and densitometry used to quantify LTA expression. The intracellular TG activity was determined by a peptide incorporation assay (B). The extracellular TG activity (C), extracellular TG antigen (D) and TG activity in medium (E) were assayed as previously described. Data represents: Mean ± SEM, n=5, *p<0.05, **p<0.01.*

8.3 Extracellular and intracellular TG activity following Tapasin knockdown

Intra- and extra-cellular TG activity was measured in TECs after being co-transfected with TG2 plus either anti-tapasin siRNA (tg+tap) (siRNA ID: s129197, applied Biosystems) or non-sense siRNA (tg+ns). Non-transfected cells (wt) were used as a negative control. TECs all contain a strong tapasin expression as shown by Western blot analysis (Figure 8.3-1 A). Densitometry demonstrated that the expression of tapasin was knocked down by 70% by siRNA (Figure 8.3-1 A). The co-transfection of TG2 cDNA resulted in a 5-fold increase of total TG activity in the cell lysate compared to wild type cells (Figure 8.3-1 B). The cells co-transfected with TG2 and non-sense siRNA had a corresponding 5-fold increase of extracellular TG activity (Figure 8.3-1 C) and extracellular TG antigen (Figure 8.3-1 D) compared to wild type cells. Despite having the same level of total TG activity in the cell lysate, cells co-transfected with TG2 and anti-tapasin siRNA (tg+tap) had an extracellular TG activity (Figure 8.3-1 C), antigen (Figure 8.3-1 D) and TG activity in culture medium (Figure 8.3-1 E) 5 fold lower than cells transfected with non-sense siRNA constructs. This data indicates that tapasin is linked to TG2 externalisation with almost a compete prevention of TG2 export.

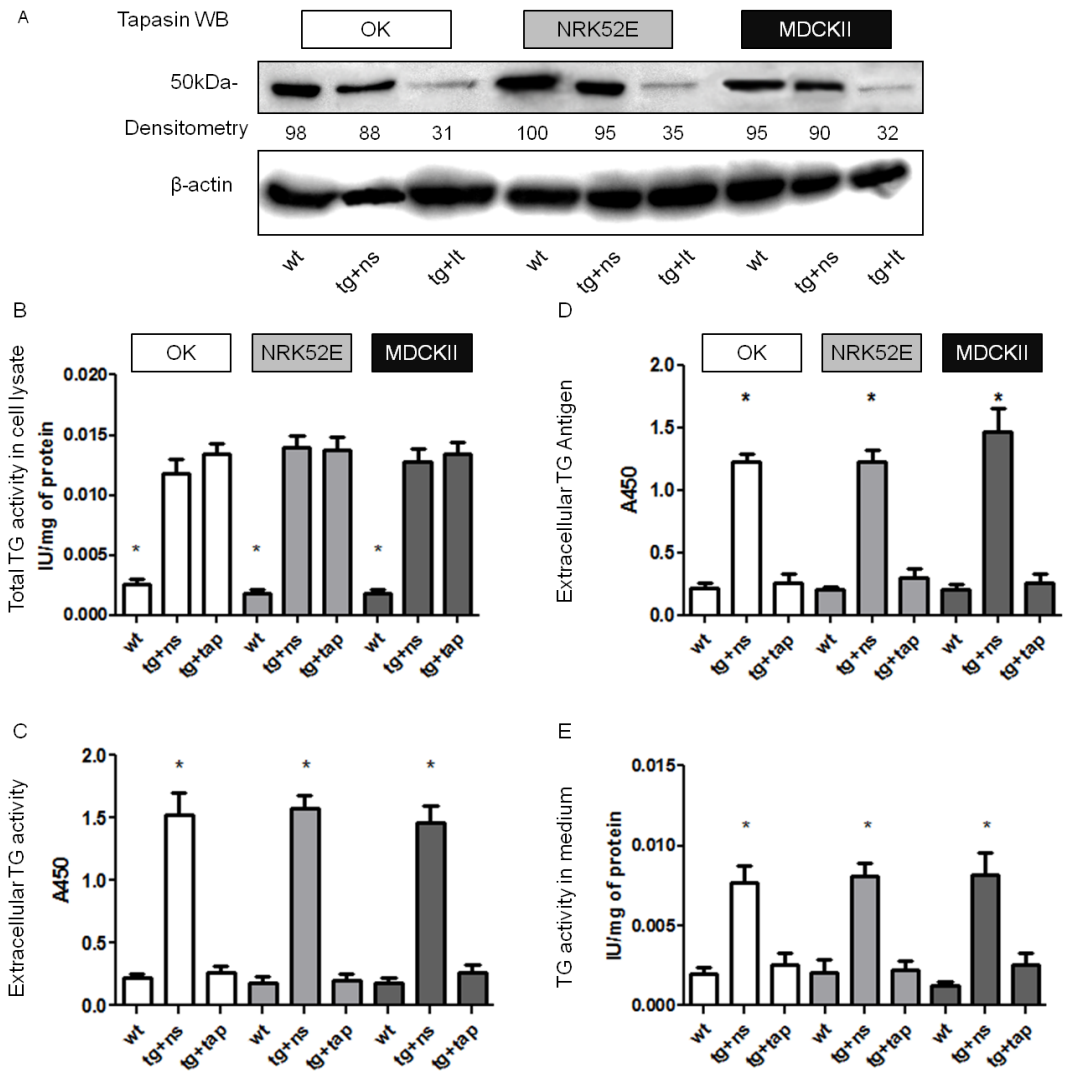

Figure 8.3-1 Extracellular and intracellular TG activity following Tapasin knockdown

*OK, NRK52E and MDCKII cells were co-transfected with pcDNA 6.2/cTC-tag-DEST expression vector containing TG2 cDNA plus either non-sense siRNA (tg+ns) or anti-tapasin siRNA (tg+tap). Non-transfected cells (wt) were used as a negative control. Western blots of cell lysates were immunoprobed for tapasin and densitometry used to quantify the reduction of tapasin expression (A). TG activity in the cell lysate was measured by peptide incorporation assay (B), with extracellular TG activity (C), extracellular TG antigen (D) and TG activity in medium (E) used to measure TG2 externalisation as described in previous chapters. Data represents: Mean ± SEM, n=5, *p<0.01.*

8.4 Extracellular and intracellular TG levels following translocon-associated protein γ (TRAP-γ) knockdown

Measurement of intra- and extra-cellular TG activity following TECs co-transfected with TG2 plus either anti-TRAP-γ siRNA (tg+trap) (siRNA ID: s135754, applied Biosystems) or non-sense siRNA (tg+ns) was performed. The tapasin expression was measured using western blot with densitometry (Figure 8.4-1 A) and the expression of TRAP-γ was knocked down by 80% using anti-TRAP-γ siRNA. The co-transfection of TG2 cDNA and anti-TRAP-γ siRNA or non-sense siRNA both had a 5-fold increase of total TG activity (Figure 8.4-1 A) in the cell lysate compared to wild type cells (wt). The extracellular TG activity (Figure 8.4-1 C), extracellular TG antigen (Figure 8.4-1 D) and TG activity in medium (Figure 8.4-1 E) mirrored the intra-cellular measurement. This suggested that TRAP-γ knock down had no effect on TG2 externalisation.

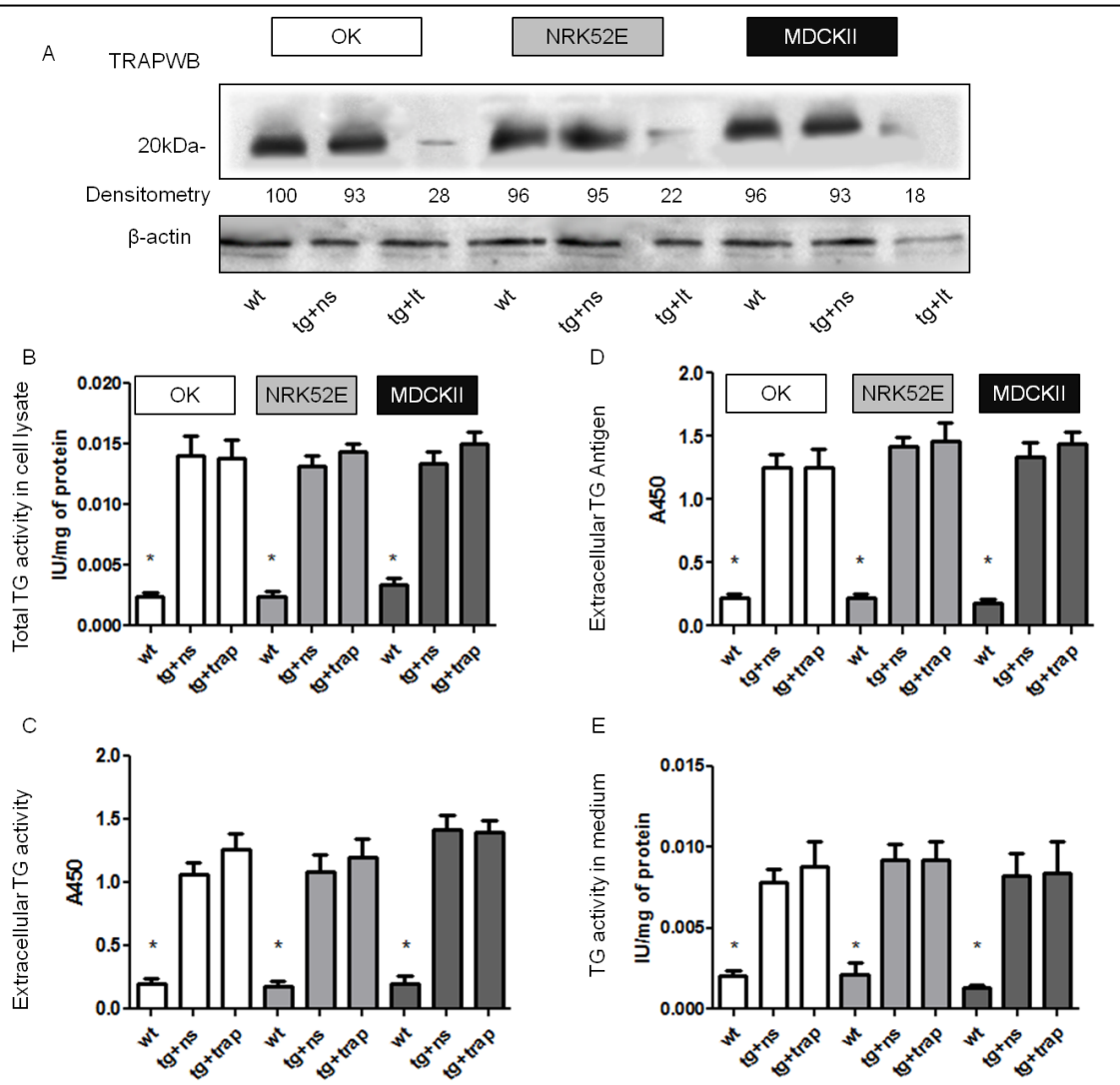

Figure 8.4-1 Intracellular and extracellular TG levels following translocon-associated protein γ (TRAP-r) knockdown

*OK, NRK52E and MDCKII cells were co-transfected with pcDNA 6.2/cTC-tag-DEST vector containing TG2 cDNA plus either non-sense siRNA (tg+ns) or anti-TRAP-γ siRNA (tg+trap). Non-transfected cells (wt) were used as a negative control. Western blots of cell lysates were immunoprobed for TRAP-r and densitometry used to quantify the reduction of tapasin expression (A). TG activity in the cell lysate was measured by peptide incorporation assay (B), with extracellular TG activity (C), extracellular TG antigen (D) and TG activity in medium (E) used to measure TG2 externalisation as described in previous chapters. Data represents: Mean ± SEM, n=5, *p<0.01.*

8.5 Discussion

8.5.1 Possible sequence that binds to TG2 export motif

It is reported that the TG2 export motif covering amino acids 88-106 in the TG2 β-sandwich domain is a fibronectin binding site. However, we identified that both tapasin and LTA also binds to this motif. It is possible that there are similar domains or sequence within these three proteins associate with this TG2 export motif. If the amino acid sequences for human fibronectin, BK virus large T antigen and human tapasin are aligned (Figure 8.5-1), then similar sequence between fibronectin 1, tapasin from human and LTA from BK virus can be

Figure 8.5-1 Amino acid sequence alignment for candidate proteins that binds to the TG2 export motif aa88-106

*Amino acid sequence alignment for Human tapasin (TPSNR_HUMAN, top), human fibronectin 1(FINC_HUMAN, middle) and BK virus large T-antigen (LT_POVBK, bottom). The red box demonstrate a potential key sequence *C*G* that bind may be common to binding TG2 export motif.*

highlighted. Unfortunately there is no clear consensus sequence; however, *C*G* is held across the three proteins (red box) and could possibly be importance. The sequences (red box, amino acid sequence 109-118) of tapasin located in N-terminal β-barrel (Dong *et al.* 2009) that is the cytoplasmic side on ER membrane. This supports the hypothesis that TG2 synthesised in the cytosol can be recruited by the vesicles formed by the ER membrane containing tapasin around the cell nucleus. We showed TG2 export motif binds to origin binding domain of LTA (Section 7.4.4) and this amino acid sequences 185-194 is part of DNA binding domain of LTA (Kim *et al.* 2001) that is facing the cytosol for the plasma membrane associated LTA (Klockmann *et al.* 1984). It is possible that the plasma membrane associated LTA binds TG2 at the periphery of the cells and externalised through plasma membrane blebbing (Section 9.3.1). The TG2 export motif may have the ability to interact with multiple sequences or any interaction could be conformational meaning it would not be possible to link to any linear amino acid sequence.

Chapter 9 Determining possible TG2 externalisation pathways using co-localisation analysis and live cell imaging

9.1 Introduction

In the previous chapter, it was demonstrated that the TG2 export motif in the TG2 β-sandwich domain (88-106) that is critical to TG2 extracellular trafficking binds to large tumour antigen (LTA), tapasin and translocon-associated protein γ. Further a 50% knock down of LTA using anti-LTA siRNA decreased 50% of TG2 externalisation and an 80% knock down of tapasin using anti-tapasin siRNA decreased 80% of TG2 externalisation. According to the sequential visualisation (described in Section 4.6) of TG2 with tie post transfection, TG2 was synthesised around the cell nucleus on the surface on the ER and then moved peripherally to the plasma membrane amassing in vesicular structures within the cytoplasm.

We hypothesise that TG2 follows one of the 4 recognised unconventional externalisation pathways (Figure 9.1-1). These are by inclusion in secreted

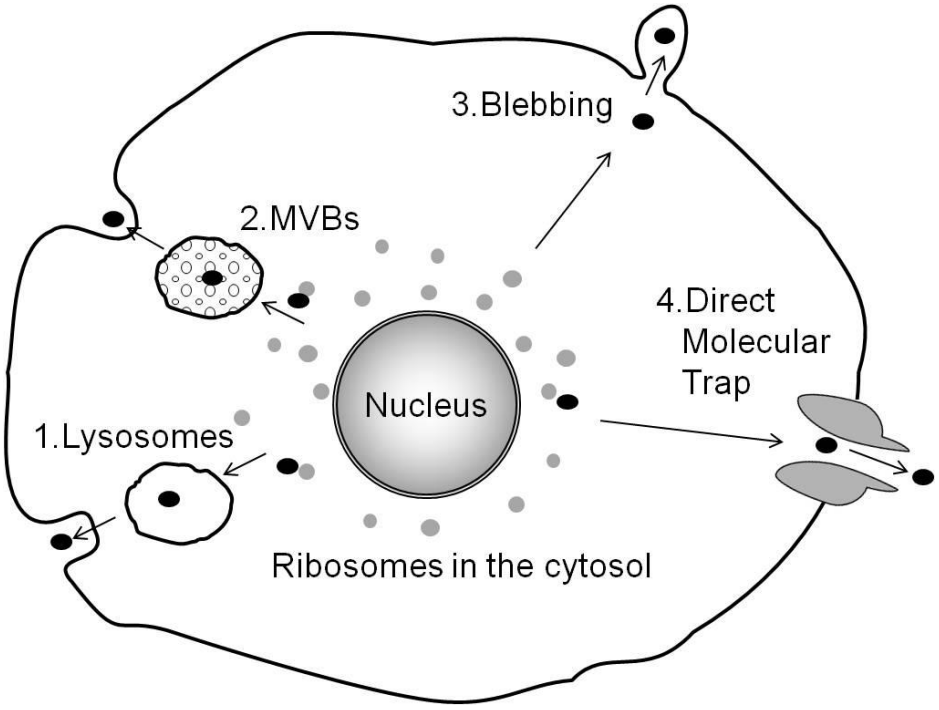

Figure 9.1-1 Possible for unconventional protein externalisation processes

Proteins without leader sequence that are not externalised through endoplasmic reticulum and Golgi apparatus network can be externalised through 1) Lysosomes, 2) multivesicular bodies (MVBs), 3) plasma membrane blebbing and 4) Direct molecular trap by plasma membrane-resident transporters. ○: secretory protein (Nickel 2005)

lysosomes; by inclusion in exosomes; via plasma membrane blebbing; and using a direct molecular trap approach using plasma membrane-resident transporters.

Therefore in this chapter, the initial aim is to use co-localisation studies with various cell organelles to determine where, if and a what stage in the cell TG2 co-localises with cell organelles and if this can yield clues as to how TG2 export from the cell is facilitated. Further if the data would be consistent with 1 of the unconventional export pathways.

To demonstrate this, fluorescent image co-localisation analysis of FlAsH labelled TG2 and organelle light stains was used to determine the involvement of organelles including ER, Golgi apparatus and lysosomes in the TG2 externalisation pathway. The second aim is to use live cell imaging to see how TG2 moves in the cell with time. To do this NRK52E cells transfected with pcDNA6.2/cTC-tag-DEST expression vector containing full length TG2 cDNA. 48 hours post transfection cells were visualised to determine possible morphological changes that could be link to TG2 externalisation in TECs.

9.2 Determination of possible TG2 externalisation pathways

To determine possible TG2 externalisation pathway, cells were transfected with the pcDNA6.2/cTC-Tag-dest vector carrying full length TG2 cDNA with a tetracysteine tag which was subsequently revealed using FlAsH staining. Cells were co-stained for organelles including endoplasmic reticulum (ER), Golgi apparatus and lysosome.

On commencing this work some assumptions were made. Firstly, as TG2 does not have a leader sequence and shoulder not be transported through ER/Golgi network. It was expected that TG2 would have very limited co-localisation with ER and Golgi staining. If TG2 is externalised through the vesicles ER derived vesicles (ie MVBs) then there would be some co-localisation of TG2 and ER membrane stains in the cytosol. Secondly, if TG2 is externalised through recruitment to lysosomes, some of TG2 fluorescent signal should be co-localised with lysosome staining.

9.2.1 Co-localisation of TG2 and endoplasmic reticulum

NRK52E cells transfected with full length TG2 (green) and ER stain (red) were visualised 48 hour post transfection. The ER stain using organelle light ER (Figure 9.2-1 A) appears throughout the cell as punctuate staining that is concentrated around the periphery of the cell nucleus. The greatest amount of TG2 also appears to be around the cell nucleus (Figure 9.2-1 B, yellow arrows) indicated by a considerable amount of co-localise with the ER stain around the cell nucleus (Figure 9.2-1 C, yellow arrows). The peripheral TG2 indicated by white arrows is not co-localised with the ER stain suggesting that TG2 is not externalised through exosomes derived from ER. In co-localisation analysis, 23.7% of the TG2 fluorescent signals are co-localised with ER overall.

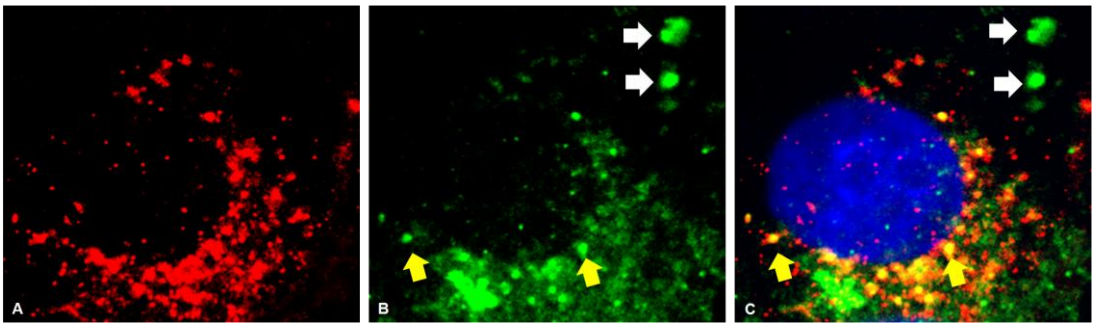

Figure 9.2-1 Fluorescent co-localisation of TG2 and endoplasmic reticulum (ER)

NRK52E cells were transfected using pcDNA6.2/cTC-tag-DEST containing full length TG2. 48 hours post transfection ER was stained red using organelle light ER (A) and TG2 was stained green using FlAsH reagent (B). The cell was stained blue using DAPI and ER, TG2 and nuclear images merged (C). The co-localisation of TG2 and ER is yellow. TG2 co-localised around the cell nucleus with the ER stain is indicated by yellow arrows. Peripheral TG2 are indicated by white arrows. The cell nucleus was stained blue with DAPI.

To obtain more information as to the spatial positioning of TG2 and ER in the cell, a 3D image was rendered from a deconvolved Z stack of images (Figure 9.2-2). The direct fluorescent signals displayed on a grey background can be seen in apical view (Figure 9.2-2 A), lateral view (Figure 9.2-2 B) and basolateral (bottom) view (Figure 9.2-2 C). After the light had been tracked to its origin by deconvolution, most of the ER (red) is clearly around the nucleus (blue) with TG2 concentrated toward the basolateral membrane. The co-localisation of TG2 and ER spots can be only seen around the cell nucleus. By converting the 3D rendered image to a 3D cartoon the ER and TG2 stain can be displayed as blocks between certain thresholds (Figure 9.2-2 D-F). Green and red fluorescent signals above the set threshold are labelled as the same colour. Low red and green fluorescent signals below the selected threshold were ignored to generate a clearer image. Using this approach, the apical view (ie from above the cell) shows the ER (red) is concentrated around the nucleus while the TG2 (green) is located at the bottom of the cell where it is attached to the cover-slip (Figure 9.2-2 D). The accumulation of TG2 at the bottom of the cells is more clearly shown in the bottom, basal view (Figure

9.2-2 F). In the 3D co-localisation analysis, only 15.1% of TG2 (green) volume within the cell is co-localised with ER while 34% of ER around the cell nucleus is co-localised with TG2. All co-localisation is around the cell nucleus.

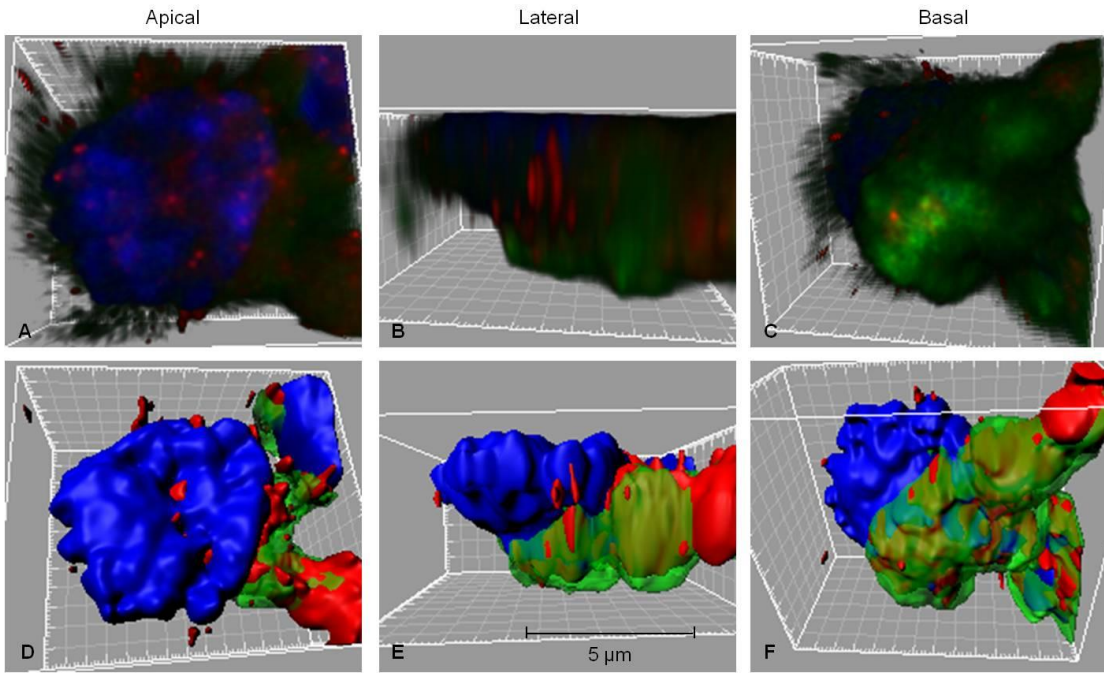

Figure 9.2-2 Three dimensional imaging of a cell co-stained for TG2 (green) and ER (red)

NRK52E cells were transfected using pcDNA6.2/cTC-tag-DEST containing full length TG2. 48 hours post transfection ER was stained red using organelle light ER and TG2 was stained green using FlAsH reagent. A Z stack images acquired at 200nm separation was acquired using cell F and F-view camera. The Z stack images were deconvolved using Autoquant software and 3D rendered using Imaris software to produce a 3D model of the cell. A direct fluorescent signal 3D image blending all 3 colours is seen in apical view (A), lateral (B) and basal (C) views which related to top side and bottom views of the cell respectively. Images A to C were re-mapped into corresponding 3D cartoon models using Imaris (D-F) in which the fluorescent signals above a set threshold are marked as the same colour with the same intensity. The cell nucleus was stained blue with DAPI.

9.2.2 Co-localisation of TG2 and Golgi apparatus

To determine if TG2 is trafficked to the cell exterior via the Golgi apparatus, NRK52E cells transfected with pcDNA6.2/cTC-Tag-dest vector containing full length TG2 cDNA were stained with Golgi apparatus using organelle light Golgi

(red) and TG2 (green) 48 post transfection. Golgi apparatus appeared as vesicle shape around the cell nucleus (Figure 9.2-3 A), TG2 staining was throughout the cell cytoplasm (Figure 9.2-3 B). Merging TG2 and Golgi staining (Figure 9.2-3 C) demonstrated some co-localisation (white arrows) of TG2 and Golgi apparatus. The construction of a 3D cartoon image of the same cell (Figure 9.2-3 C) as described above demonstrates that in apical (Figure 9.2-3 D), lateral (Figure 9.2-3 E) and basal (Figure 9.2-3 F) views the Golgi apparatus form discrete punctuate structures while TG2 concentrates at the base of the cell. It is clearer in 3D images that majority of Golgi and TG2 were not in the same focal plane and some co-localisation of TG2 and Golgi apparatus is displayed in yellow colour (white arrows). There is less than 0.5% of TG2 stain that co-localise with Golgi apparatus. The negligible co-localisation between TG2 and Golgi apparatus suggests TG2 externalisation is independent of the Golgi apparatus.

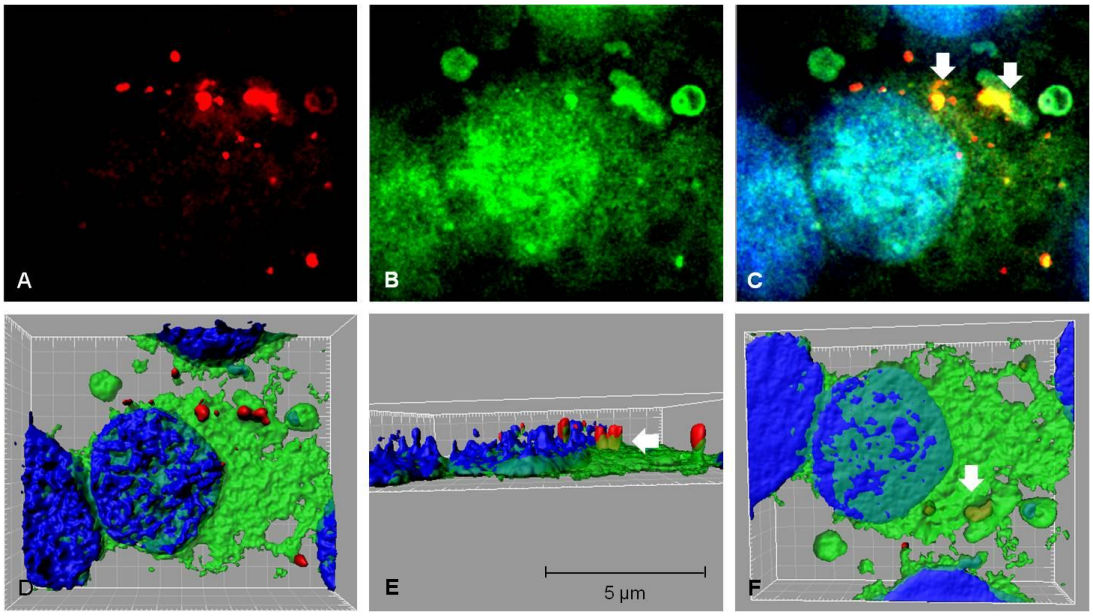

Figure 9.2-3 Fluorescent and 3D images of NRK52E cells stained for Golgi apparatus and TG2

NRK52E cells were transfected using pcDNA6.2/cTC-tag-DEST containing full length TG2. 48 hours post transfection ER was stained red using organelle light ER (A), TG2 was stained green using FlAsH reagent, (B) and the merged image (C) of ER, TG2 and the cell nucleus (blue, DAPI) generated. Co-localisation of ER and TG2 are seen in yellow and indicated by white arrows. A Z stack of images acquired at 200nm separation was acquired using cell F and F-view camera. The Z stack images were deconvolved using Autoquant software and 3D rendered using Imaris software to produce a 3D model of the cell. A 3D image blending all 3 colours is seen in apical view (D), lateral (E) and basal (F) views which related to top side and bottom views of the cell respectively. The cell nucleus was stained blue with DAPI.

9.2.3 Co-localisation of TG2 and lysosomes

To determine if lysosomes are implicated in TG2 extracellular trafficking, NRK52E cells transfected with tetracysteine pcDNA6.2/cTC-Tag-dest vector containing full length TG2 cDNA were co-stained with lysosomes using organelle light lysosomes (red) and TG2 with FlAsH (green) 48 hours post transfection. Lysosomes were visualised as small high density spots throughout the cytoplasm (Figure 9.2-4 A), with TG2 appearing in variable density patches within the cytoplasm (Figure 9.2-4 B). Merging TG2, lysosomes (Figure 9.2-4 C) and the cell nucleus (DAPI) yields very little yellow

co-localisation by eye suggesting that TG2 is not co-localised with lysosomes. Using a Z stack and 3D rendering as described above, cartoon 3D images shown in apical (Figure 9.2-4 D), lateral (Figure 9.2-4 E) and basal (Figure 9.2-4 F) views demonstrate that most of the lysosomes are in different planes from the TG2 stains confirming there is little co-localisation (0.002%).

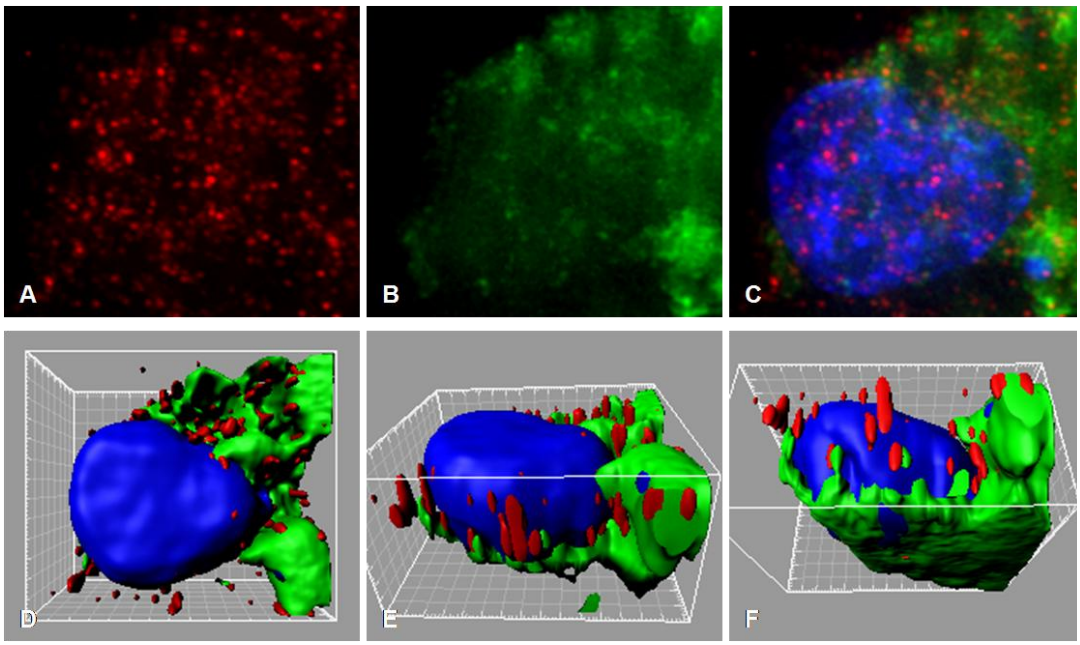

Figure 9.2-4 Fluorescent and 3D images of NRK52E cells stained with Lysosomes and TG2

NRK52E cells were transfected using pcDNA6.2/cTC-tag-DEST containing full length TG2. 48 hours post transfection ER was stained red using organelle light lysosome (A), TG2 was stained green using FlAsH reagent, (B) and the image of lysosome, TG2 and the cell nucleus (blue, DAPI) merged (C). A Z stack images was acquired at 200nm separation using cell F software controlling a F-view camera. The Z stack images were deconvolved using Autoquant software and 3D rendered using Imaris software to produce a 3D model of the cell. A 3D image blending all 3 colours is seen in apical view (D), lateral (E) and basal (F) views which related to top side and bottom views of the cell respectively. The cell nucleus was stained blue with DAPI.

9.3 Live cell imaging

Plasma membrane blebbing can be seen with phase contrast microscopy. Therefore the aim here is to use live cell imaging under phase contrast microscopy to identify plasma membrane blebbing while tracking TG2 movement by transfecting cells with TG2 carrying a tetracysteine tag. If TG2 is externalised through plasma membrane blebbing, TG2 fluorescence co-localised with plasma membrane derived blebs should be seen. If TG2 is externalised through a direct molecular trap mechanism, fluorescent TG2 should pass through the plasma membrane without any morphological changes of the plasma membrane.

9.3.1 Visualisation of plasma membrane blebbing

Two different types of plasma membrane blebbing can be seen using live cell imaging in NRK52E cells at 100 x magnification (ie low power). If 48 hours post transfection of TG2 is taken as time zero for imaging purpose in this particular field (Figure 9.3-1 A), then at 45 minutes (Figure 9.3-1 B) a cell in the right corner of the field showed the appearance of typical plasma membrane blebbing (white arrow). At higher magnification using digital zoom (ie 400 x) the cell has multiple cell blebs into which the green TG2 appears to be packed (Figure 9.3-1 C). As these images were taken on an inverted microscope the visible surface is in fact the basal (underside) surface of the cell. These multiple small vesicles are therefore being generated at basolateral side of the cell. Intestinally, under high power magnification (Figure 9.3-1 C), the blebs directly under the cell appear clear and have either released TG2 or do not contain it. However, some vesicles that have moved away from the periphery of the cell are darker green than the background suggesting they may still contain TG2.

In addition to this type of blebbing, many cells only generate 1-2 large vesicles at the basal surface that are indicated by a red arrow at 45minutes (Figure 9.3-1 B) that are clearly not present 45 minutes before this (Figure 9.3-1 A). Investigation of these cells at 400 x magnification (Figure 9.3-1 D), these blebs/vesicles contain TG2 as the fluorescent signal of these vesicles is greater than the background cytoplasmic TG2 stain. When watched as a

movie it can be seen that the cell concentrates the green TG2 into these blebs prior to colour release as the blebs burst (Low power view, High power view).

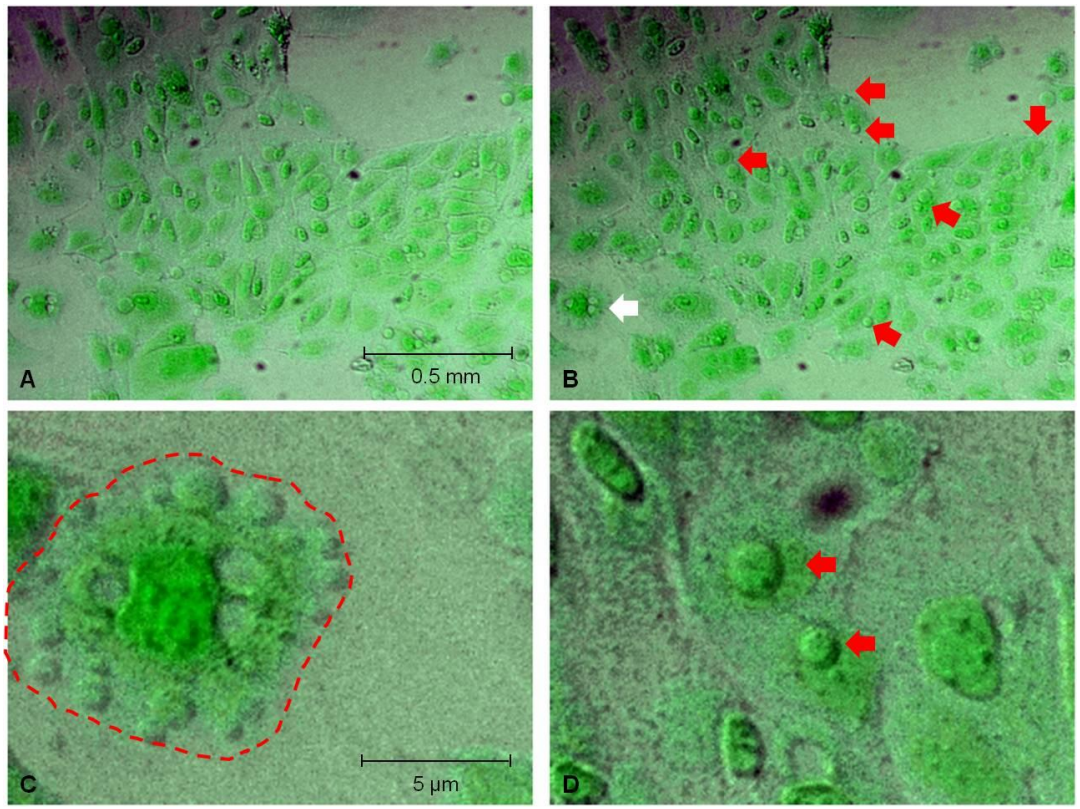

Figure 9.3-1 Visualisation of plasma membrane blebbing by live cell imaging

NRK52E cells transfected with pcDNA6.2/nTC-tag-DEST vector containing full length TG2 were visualised 48 hours post transfection. TG2 was stained green with FlAsH and the images were merged with phase contrast images to show the peripheral of the cells. Sequential images were acquired with an interval of 1 minutes at 100x magnification on an inverted microscopy such that imaging represents the basal surface of the cell. Images are shown at time 0 (A) then at 45 minutes (B). Cells developing multiple blebs that are present over the 45 minutes are indicated by a white arrow and displayed at a high magnification using digital zoom. The cell with plasma blebbing was marked with red dot circle (C). Other cells indicated by red arrows generate 1-2 TG2 containing vesicles (ie green) at the basal side over the 45 minutes and displayed at a high magnification using digital zoom (D).

From live imaging every 2 minutes with 100 x magnification, the time interval was decreased to 20 seconds and magnification increased to 400 x. Starting with a cell that had no plasma membrane blebs visible at time 0 (Figure 9.3-2 A). At 45 minutes, the cell generated plasma membrane blebs at lateral side (Figure 9.3-2 B) with the blebs visible between cells (white arrows). Blebs continually enlarge and move across the basal membrane (Figure 9.3-2 C) with some blebs fusing into one bleb (Figure 9.3-2 D, red arrow). It is therefore possible to conclude that there are two different morphological changes of the plasma membrane seen in 100 x magnification that are both plasma membrane blebbing. The blebs developed at the basal side fuse with another bleb and generate 1 or 2 single big bleb that is visualised in low power view. The detailed changes can be missed using 100 x magnification or a long time interval such as 2 min. As the blebs contain high levels of TG2 (green) and decreased with blebs size, it is likely that plasma membrane is involved in TG2 externalisation.

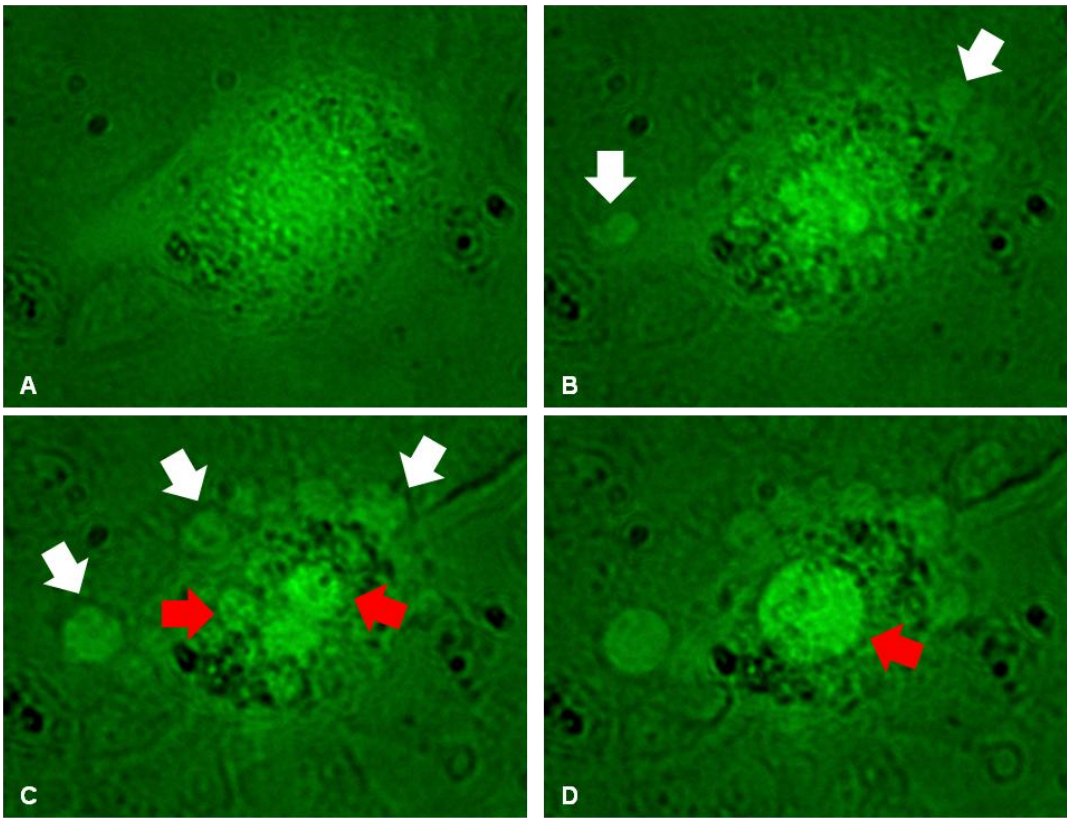

Figure 9.3-2 Visualisation of plasma membrane blebbing by live cell imaging

NRK52E cells were visualised 48 hours post transfection with pcNDA6.1/cTC-tag-DEST vector containing full length TG2. TG2 was stained green with FlAsH and the fluorescent images were merged with phase contrast image to show the periphery of the cells. Single cell imaging was performed at 400x magnification every 20 seconds for 60 minutes starting with a cell showing no blebs at time 0 (A). At 45 minutes blebs start to visualise on the surface (B) and became pronounced after 45 minutes (C). At the centre of the cell blebs fused into a big bleb that containing a high level of fluorescence (D).White arrows indicate blebs and red arrows indicate merging blebs.

9.3.2 A comparison by live cell image of cells transfected with full length TG2 and TG2 with a mutation in the export sequence

To further explored the mechanism of TG2 cell export and the role of the TG2 export motif in this process, cells transfected with full length TG2 and a mutant TG2 that is not externalised were compared using live cell imaging. NRK52E cells transfected with full length TG2 or a mutant TG2 (Asp^{94} and Asp^{97} to Ala)

were visualised 48 hours after transfection. The green fluorescent images showing TG2 were merged with phase contrast images. The morphology of the cells was similar at time 0 (Figure 9.3-3 A, B). By 45 minutes, the full length TG2 showed some vesicle blebs at the basal side of the cell (Figure 9.3-3 C, indicated by yellow arrow). However, with cells transfected with the TG2 with mutation of the export motif there was some accumulation of green fluorescence at the periphery of the cell in sub-plasma membrane area (Figure 9.3-3 D, indicated by white arrow) without its entry into plasma membrane blebs. Therefore, the major difference for mutant TG2 from full length TG2 is the lacking of plasma membrane blebbing.

The differences between cells that performed plasma membrane blebbing and the cells that did not perform plasma membrane blebbing are easier to appreciate when placed into a time laps video for NRK52E cells transfected with TG2 was shown in (video 1) and NRK52E transfected with mutant TG2 (mutation of export motif) was shown in (video 2).

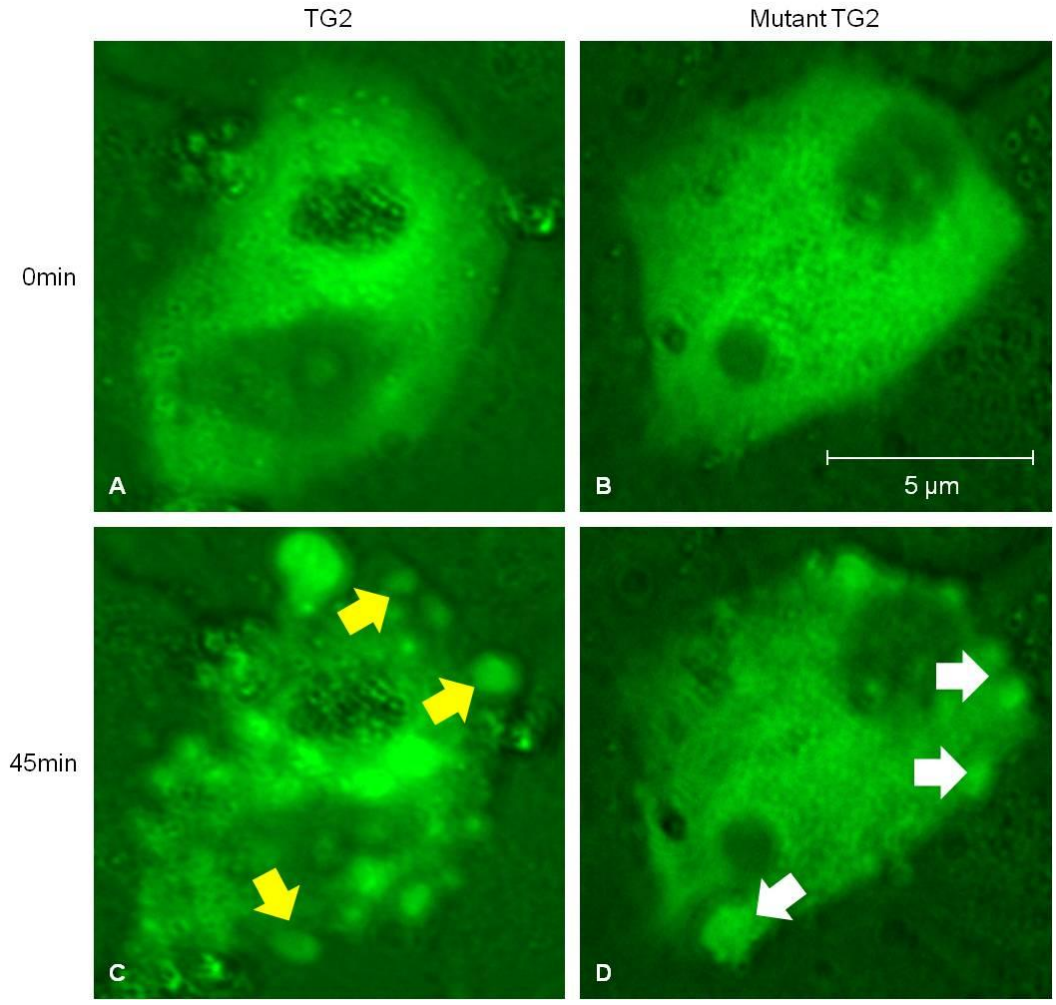

Figure 9.3-3 Live cell images for NRK52E cells transfected with full length TG2 and mutant TG2

NRK52E were visualised 48 hours post transfection with pcDNA6.2/cTC-tag-DEST vector containing either full length TG2 (A and C) or mutant TG2 (mutation of export motif) (B and D) for 1 hour at a magnification of 400x with images acquired every 20 seconds. The green fluorescence for TG2 and mutant TG2 was merged with phase contrast images. Images are shown at 0 minute for full length TG2 (A) and mutant TG2 (B) and 45 minutes (C and D). The yellow arrows (C) indicate TG2 in plasma membrane blebs and white arrows (D) indicate accumulation of TG2 at the periphery of the cells in a vesicle shape in a sub-plasma membrane location.

9.4 Discussion

The aim of co-localisation studies for TG2 and cell organelles was to determine possible TG2 externalisation pathways. Four un-conventional protein externalisation pathways have been described via lysosomes secretion, exosomes secretion, plasma membrane blebbing and a direct molecular trap (Nickel 2005). Very few lysosomes are co-localised with TG2 and thus TG2 is not likely to be externalised through lysosomes. In the exosomes secretion pathway, the exosomes are derived from ER membrane and as such should express ER markers such as calnexin. As the mutant TG2 that is not able to be exported from the cell, it accumulates in vesicle shapes in the sub-plasma membrane area. Co-localisation of TG2 and ER was found around the cell nucleus only rather than towards the plasma membrane. Therefore TG2 is not likely to be externalised through exosomes secretion pathway. To date the morphological characteristics expected for a direct molecular trap secretion pathway have not been described, however the accumulation of TG2 in the sub-plasma membrane area when the export motif is mutated would likely be consistent with this mechanism. Equally the visualisation of TG2 containing plasma membrane blebs suggests that TG2 could be exported through a cell blebbing route.

The co-localisation of TG2 and Golgi apparatus was less than 0.3% of the fluorescent signal for TG2 is co-localised with Golgi apparatus stain. This confirms that TG2 does not follow the classical export pathway for secreted proteins. The fact there was some co-localisation can be explained by the presence of ribosomes (at which proteins can be synthesised) on Golgi apparatus. Therefore typically a small portion of un-conventionally secreted proteins can be co-localised with Golgi apparatus, although not transported through the Golgi apparatus route. This was described previously for FGF-2 (Ko *et al.* 2005). Electron microscopy images were used in early work for studying un-conventional protein secretion to determine if Golgi apparatus was involved (Rubartelli *et al.* 1990; Andrei *et al.* 1999) or which organelles the protein associated with. We also tried ReAsH photoconversion of diaminobenzidine (DAB) (Gaietta *et al.* 2002), however, no electron dense particles could be identified in the cytosol possibly because of inadequate DAB

oxidised from ReAsH fluorescent in the cytosol and thus it has been impossible to identify more accurately TG2 location in the cell.

Recent studies looking at the direct molecular trap mechanism of cell export for FGF-2 secretion clearly showed that FGF-2 accumulated as a vesicle shape at the sub-plasmic membrane area before being secreted (Taverna *et al.* 2003; Seelenmeyer *et al.* 2008). The formation of vesicle shapes in the plasma membrane for TG2 suggests a direct molecular trap pathway may be a possibility. The proposed direct molecular trap mechanism for FGF-2 is based on the expression FGF-2/HSPG complex on cell surface. The mutation of FGF-2 binding to HSPG as and knockdown of HSPG decrease cell surface FGF-2 when measured by flow cytometry. No direct visualisation of the protein interaction that lead to protein secretion has been reported in the literature (Zehe *et al.* 2006). Before starting this study, it was thought possible to visualise protein secretion at basal side of the cell using deconvolution microscopy. Deconvolution microscopy does have some of the advantages of confocal microscopy such as the identification of apical and basal surface of the cell using Z-stack image acquisition. However, the factor that limits the visualisation of protein externalisation at the basal side of the cell is plasma membrane stain. Unsurprisingly, plasma membrane staining generates better fluorescent signals at lateral side of the cell than the apical side. When the cells were incubated with plasma membrane dye, the apical surface of the cell has more chance exposure to the dye than the basal side of the cell. However, simply increasing the incubation time resulted in a high background and did not generate a clear plasma membrane at the apical side. In addition, the difference in strength of fluorescent signals for the plasma membrane at the basal side of the cells produced punctuate and discrete signals after deconvolution. Consequently it was not possible to produce a convincing plasma membrane image at the basal side of the cell using plasma membrane staining. Electron microscopy or atomic force microscopy (Chen *et al.* 2000) may provide a better visualisation at the basement membrane of the cells, although these techniques were not readily available for this study.

Live cell imaging showed that TG2 can be secreted through basolateral plasma blebbing because the live cell image was taken from an inverted

microscopy. FlAsH stains was applied to live cells and generated little back ground. Importantly plasma membrane blebs only occurred in the cells transfected with full length TG2, with no blebs (containing TG2 or not) visible in the cells transfected with TG2 with mutation of the export motif. This strongly suggests that the export motif must trigger some type of blebbing either directly or via its interaction with a partner protein. However, plasma membrane blebbing is more likely to occur in apical side than basolateral side because of the differences in cytoskeleton support (reviewed in Aumuller *et al.* 1999) and thus TG2 entering blebs on the basal surface is unusual. In the literature, most of the studies that supports plasma membrane blebbing as a protein secretion pathway came from tissue culture (Bellomo *et al.* 1988; Keller *et al.* 1998) and microparticles from plasma membrane blebbing in the circulation (Furie *et al.* 2004; Chironi *et al.* 2006). *In vivo* the basal side of the cells are supported by basement membrane such that the formation of blebs may need to overcome the resistance of basement membrane and extracellular matrix pressure (reviewed in Hagmann *et al.* 1999; Fackler *et al.* 2008). However, for proteins involved in ECM regulation as TG2 is believed to do direct delivery to the underlying basement membrane by basolateral blebbing makes sense from efficiency and targeting perspectives. In this study, we showed that TECs can perform basal plasma membrane blebbing using live cell imaging *in vitro* only. Further studies are subsequently needed to determine if TECs can export TG2 *in vivo* against the resistance of the basement membrane and perform basal plasma membrane blebbing.

Chapter 10 Possible TG2 externalisation pathways related to the interaction of the TG2 export motif with large tumour antigen and tapasin

10.1 Introduction

In the previous chapter, it was demonstrated that Golgi apparatus and ER derived exosomes and lysosomes are not involved in TG2 externalisation. No co-localisation of TG2 and Golgi apparatus was found between the rough ER and the plasma membrane where typically ER-Golgi carried classical secretory proteins are found. No co-localisation of lysosomes or MVBs derived exosomes with TG2 was observed in the cytosol. In chapter 5 the TG2 export motif was identified in the TG2 β-sandwich domain, while Chapter 7 and 8 it was demonstrated that LTA and tapasin bind to this motif and both are critical for TG2 export. In Chapter 9, plasma membrane blebbing in cells with elevated TG2 was observed and TG2 containing vesicles were released at the basal surface of the cells. Mutant TG2 that is not externalised accumulated in the cytosol and no plasma membrane blebbing was observed. Given all this knowledge regarding TG2 export, it still remains unclear as to how do all this information fits together into a coherent export pathway for TG2. Therefore in this chapter the aim is to demonstrate how tapasin and LTA are involved in TG2 externalisation. To do this both co-localisation analysis and live cell imaging studies will be undertaken. Live cell imaging will be applied both cells transfected with labelled full length TG2 and mutant TG2 with mutation of the TG2 export motif.

10.2 Co-localisation of TG2 and large tumour antigen (LTA)

The knock down of LTA in TEC cells is associated with a decrease in TG2 externalisation. However, it is unclear how the interaction of LTA and TG2 is linked to TG2 externalisation. To determine the distribution of LTA in the cell and the possible location of TG2 and LTA interaction in the cytosol, wild-type cells were subjected to immunofluorescent co-localisation studies for LTA and TG2.

NRK53E cells were stained with LTA using a Texas red conjugated secondary antibody (red) (Figure 10.2-1 A) and TG2 using a FITC conjugated secondary antibody (green) (Figure 10.2-1 B). By merging LTA and TG2 images (Figure 10.2-1C), some co-localisation can be identified at the peripheral of the cytosol indicated by the white arrow. Some fluorescent signals (Figure 10.2-1 B) are

on top of the cell nucleus that could be TG2 synthesised on the ER. NRK52E cells incubated with TRITC secondary antibodies (Figure 10.2-1 D) and FITC antibodies (Figure 10.2-1 E) are used as negative controls showing that staining is not non-specific binding of the secondary antibodies.

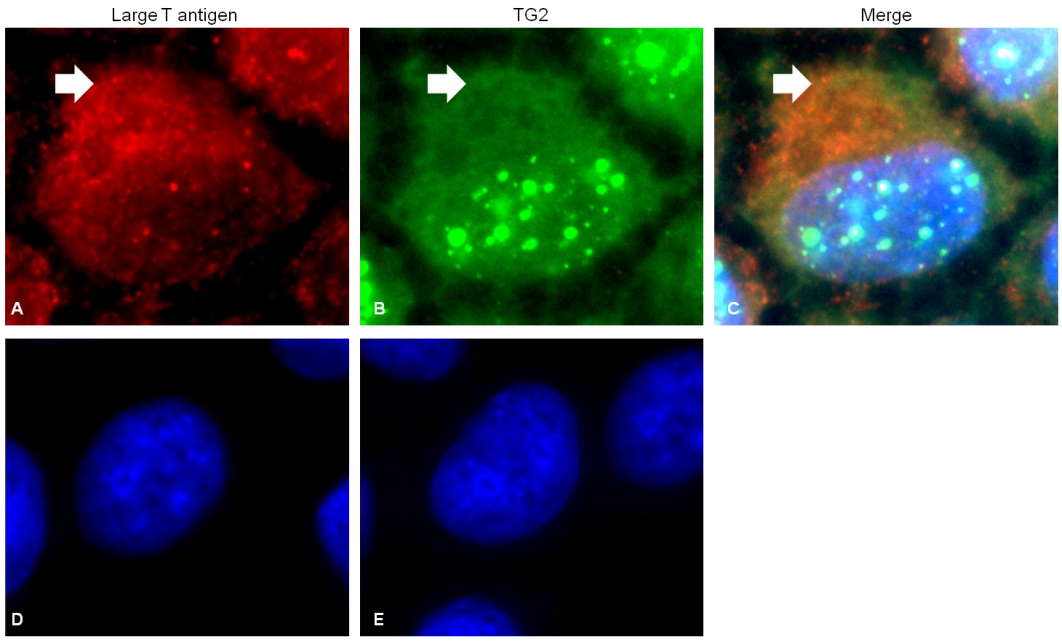

Figure 10.2-1 Co-localisation of large tumour antigen (LTA) and TG2 in NRK52E cells

Wild type NRK52E cells were grown to 80% confluency and fixed with 4% PFA. LTA was stained red with a rat anti-LTA antibody (ab18187, Abcam) followed by an anti-rat IgG-TRITC (ab7094, Abcam) (A). TG2 was stained green with a Mouse anti-transglutaminase 2 antibodies cub7402 (ab2386, Abcam) and an anti-mouse IgG FITC (ab7064, Abcam) (B). Co-localisation of TG2 and LTA was observed merging the images (C). Omission of anti-LTA antibody (D) and an anti-TG2 antibody (E) was used as controls for secondary antibody non-specific binding. Peripheral co-localisation of TG2 and LTA is indicated with white arrows. The cell nucleus was visualised with DAPI (blue).

Most TG2 is externalised via the basal surface which is not easily visible by conventional microscopy as it is the apical (top) surface that is visible from above. Therefore Z stacks of the cell were taken, the image deconvolved and a 3D image of a NRK52E cell stained for endogenous TG2 (green) and LTA (red) generated (Figure 10.2-1). The direct fluorescent signals obtained are shown in apical (Figure 10.2-1 A), lateral (Figure 10.2-1 B) and bottom views (Figure 10.2-1 C). LTA (red) was distributed throughout the cytosol with some expression at the periphery of the cell that could be plasma membrane and TG2 was localised in the cytosol especially in the basal side of the cell. Co-localisation of LTA and TG2 is displayed in yellow, however no co-localisation can be seen in the apical and lateral views. When the cell inverted and viewed from the underside, co-localisation for LTA and TG2 can be clearly seen at the basal side of the cell indicating TG2 and LTA associate towards the basal membrane only. A 3D cartoon between set thresholds of staining was generated as previously described (Figure 10.2-1 D-F) from the same image. The co-localisation of TG2 and LTA is clearly seen at the basal side of the cell (Figure 10.2-1 F) as by white arrows confirming the direct fluorescent imaging. A72% of plasma membrane LTA was co-localised with TG2 at the basal side of the cell.

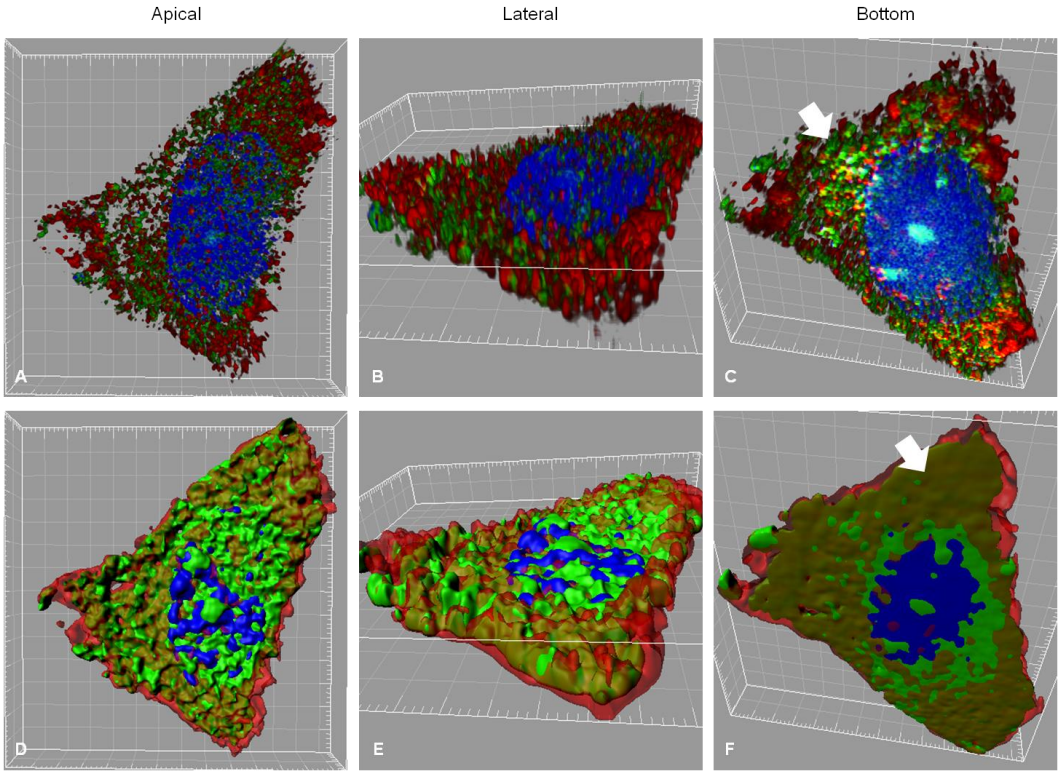

Figure 10.2-2 Three dimensional imaging of NRK52E cells stained with large tumour antigen (LTA) and TG2

Wild type NRK52E cells were grown to 80% confluency and fixed with 4% PFA. LTA was stained red with a rat anti-LTA antibody (ab18187, Abcam) followed by an anti-rat IgG-TRITC (ab7094, Abcam). TG2 was stained green with a Mouse anti-transglutaminase 2 antibodies cub7402 (ab2386, Abcam) and an anti-mouse IgG FITC (ab7064, Abcam).A Z stack images acquired at 200nm separation was acquired using Cell F and F-view camera. The Z stack images were deconvolved using Autoquant software and 3D rendered using Imaris software to produce a 3D model of the cell. A image using direct fluorescent signals is shown in apical (A), lateral (B) and bottom (C). A cartoon model image based on the fluorescent density (D-F) in the same views. Co-localisation of TG2 and LTA is indicated by white arrows. The cell nucleus was visualised with DAPI (blue).

10.3 Co-localisation of TG2 and tapasin

Knockdown of tapasin in the cell is linked to a proportional decrease in TG2 externalisation and thus co-localisation of native TG2 and tapasin was used to determine the possible location of TG2/tapasin interaction in the cytosol. NRK52E cells stained with tapasin (red, Figure 10.3-2 A), TG2 (green, Figure 10.3-2 B) and the two images merged (Figure 10.3-2 C). Tapasin and TG2 had very good co-localisation around the cell nucleus and at the periphery of the cytosol. As most of the tapasin was expressed on the ER membrane that might represent co-localisation with TG2 around the cell nucleus. A small portion of tapasin can be presented on cell surface that might represent the periphery co-localisation of TG2 with tapasin. To confirm the fluorescent signal is specific to tapasin and TG2 antibodies, cells were put through the immunofluorescent

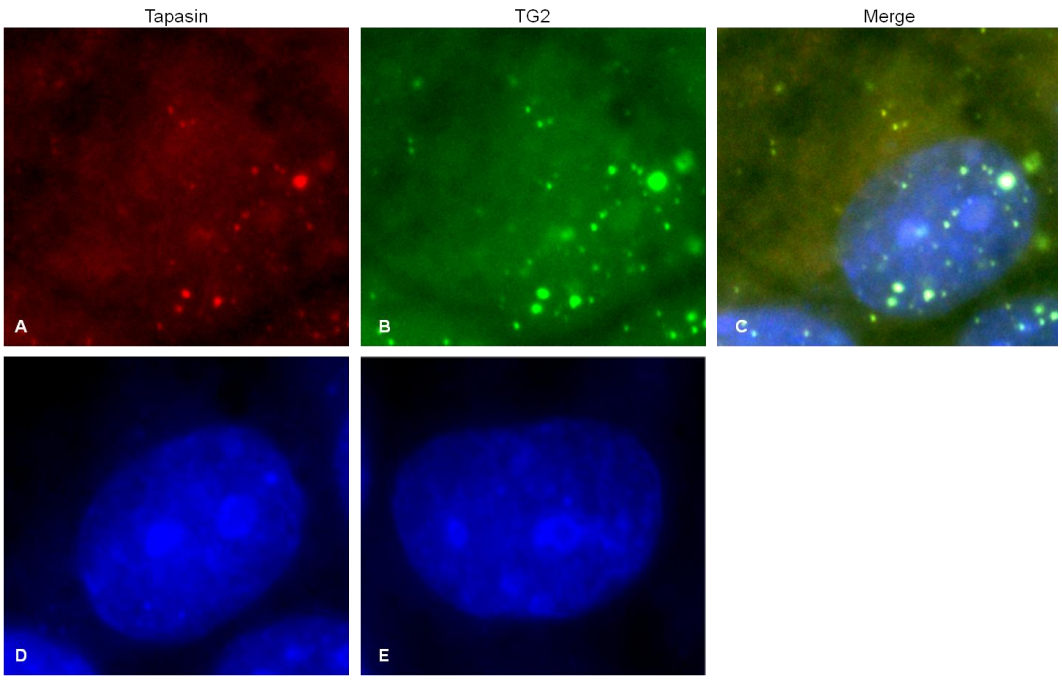

Figure 10.3-1 Co-localisation of tapasin and TG2 in NRK52E cells

Wild type NRK52E cells were grown to 80% confluency and fixed with 4% PFA. Tapasin was stained red with a goat anti-tapasin antibody (sc11473, Santa Cruz biotechnology) followed by an anti-goat IgG TRITC (T7028, Abcam). TG2 was stained green with a Mouse anti-transglutaminase 2 antibodies cub7402 (ab2386, Abcam) and an anti-mouse IgG FITC (F0257, Sigma) (B). Co-localisation of TG2 and tapasin was displayed by merging the images (C). Omission of anti-tapasin antibody (D) and anti-TG2 antibody (E) were used as controls for secondary antibody non-specific binding. The cell nucleus was visualised with DAPI (blue).

procedure with omittion of the primary antibody (Figure 10.3-2 D, E).

To assist with the determining the spatial co-localisation of tapasin and TG2, a Z stacks of cell was obtained, the images were deconvolved to trace the source of light for the staining and the data used to construct a 3D rendered image of NRK52E cells stained for TG2 (green) and tapasin (red) (Figure 10.3-3 A-F). The direct fluorescent signal in apical (Figure 10.3-3 A), lateral (Figure 10.3-3 B) and bottom view (Figure 10.3-3 C) shows no co-localisation in the apical and lateral views. However, like LTA, by inverting the cell co-localisation of tapasin and TG2 can be clearly seen at the basal side of the cell. Subsequent generation of the 3D cartoon model (Figure 10.3-3 D-F) clarifies co-localisation occurring predominantly on the basal membrane although there are clear associations of TG2 and tapasin completely through the cell cytoplasm suggesting that it is tapasin that may “carry” TG2 to the basal membrane.

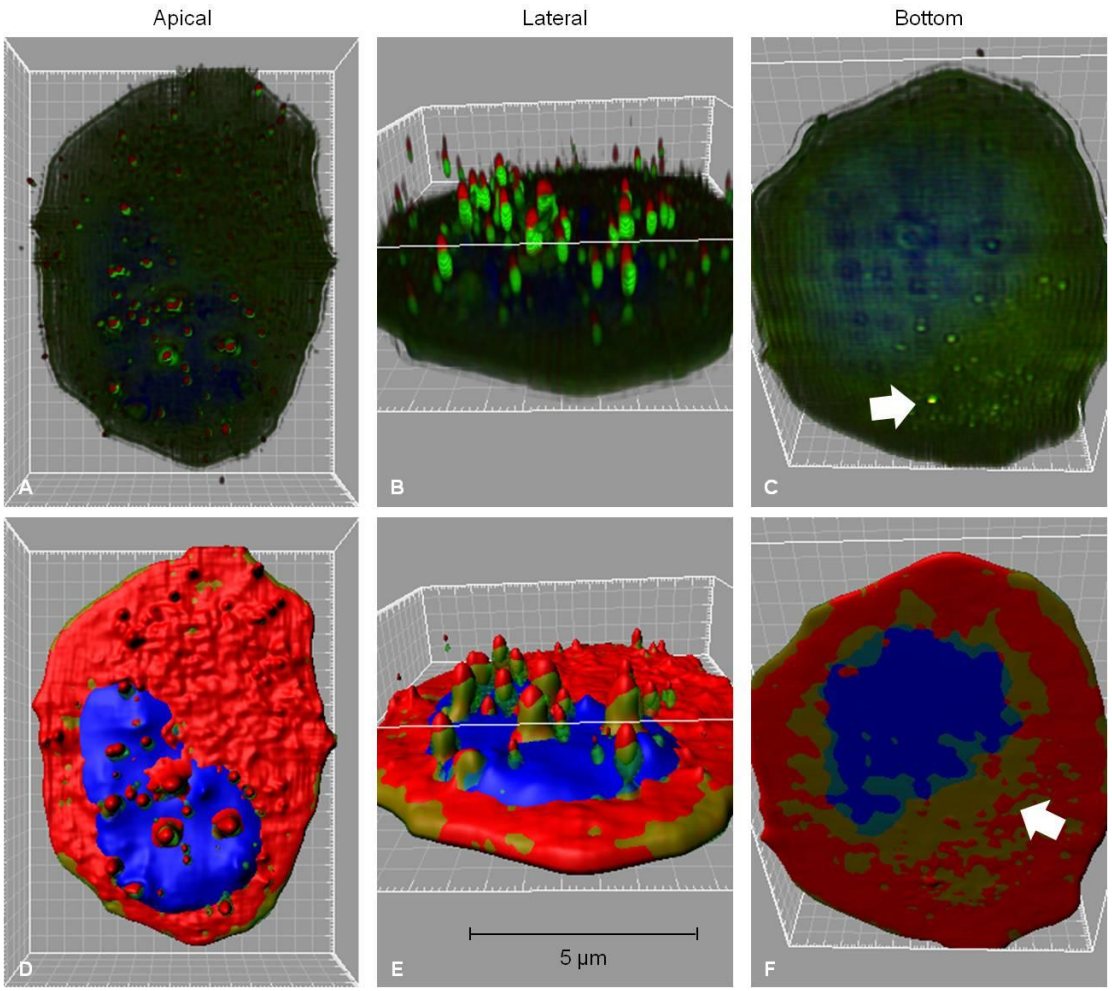

Figure 10.3-2 Three dimensional imaging of NRK52E cells stained with tapasin and TG

Wild type NRK52E cells were grown to 80% confluence and fixed with 4% PFA. Tapasin was stained red with a goat anti-tapasin antibody (sc11473, Santa Cruz biotechnology) followed by an anti-goat IgG TRITC (T7028, Abcam). TG2 was stained green with a Mouse anti-transglutaminase 2 antibodies cub7402 (ab2386, Abcam) and an anti-mouse IgG FITC (F0257, Sigma). A Z stack images acquired at 200nm separation was acquired using cell F and F-view camera. The Z stack images were deconvolved using Autoquant software and 3D rendered using Imaris software to produce a 3D model of the cell. A 3D model of the cell was generated using direct visualisation of the fluorescent in apical (A), lateral (B) and basal (C) views. A cartoon model of the cell using the same image (A-C) based on a set of threshold for fluorescent signals (D-F). Co-localisation of TG2 and tapasin is displayed in yellow colour. The cell nucleus was visualised with DAPI (blue).

10.4 Live cell imaging of TG2 externalisation in NRK52E cells following siRNA Knock down of large tumour antigen (LTA) & Tapasin

In Chapter 9, it was demonstrated that TECs transfected with full length TG2 underwent plasma membrane blebbing with fluorescent TG2 being concentrated within these blebs before being released as the bleb perforated. TECs transfected with TG2 with mutation of the export motif did not performed plasma membrane blebbing.

To determine the effect of LTA and tapasin knock down on TG2 extracellular trafficking, NRK52E cells were co-transfected with TG2 expression vector pcDNA6.2/cTC-Tag-dest containing full length TG2 cDNA and either anti-LTA or anti-tapasin siRNA. Cells were imaged 48 hours post co-transfection in serum free medium. NRK52E cells transfected with TG2 expression vectors alone were used as negative controls. In cells transfected with full length TG2 cDNA alone, once TG2 reached a suitable intensity in the cell image acquisition was started at 20 second intervals for 45 minutes. Initially the ell would appear green and quiescent (Figure 10.4-1 A), but in most cells, a period of plasma membrane blebbing would frequently commence (Figure 10.4-1 B). These blebs would grow, contain highly fluorescent material (ie TG2) then perforate releasing the contents into the extracellular space. When this was repeated in NRK52E cells co-transfected with anti-tapasin siRNA along with the TG2 vectors, the plasma membrane blebs in the same way as the cell transfected with full length TG2 (Figure 10.4-1 D). However, in these cells with tapasin knock down the plasma membrane blebbing did not appear to burst, but rather the green TG2 was pulled back into the cytoplasm and re-condensed in the cytosol (Figure 10.4-1 E). Following co-transfection with anti-LTA siRNA and full length TG2, the cell failed to bleb (Figure 10.4-1 F). Therefore the LTA is associated with plasma membrane blebbing into which TG2 is moved, while the tapasin is related to the bleb being pinched and the TG2 released from the blebs (video3, video4, video5).

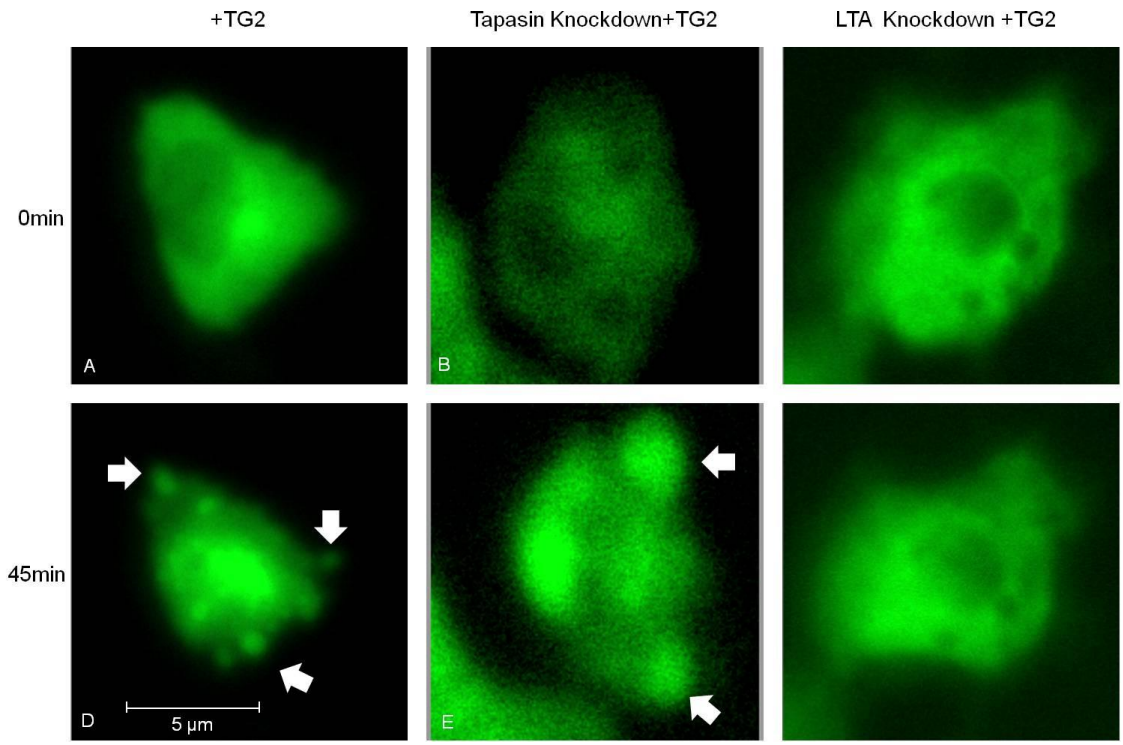

Figure 10.4-1 Live cell imaging of TG2 cell export in NRK52E cells with knockdown of large tumour antigen (LTA) or tapasin

NRK52E cells were imaged 48 hours post co-transfection with pcDNA6.2/cTC-tag-DEST vector containing full length of TG2 plus either anti-tapasin siRNA or anti-LTA siRNA. At time zero cells were stained with FlAsH to stain tetracysteine tagged TG2 green and images were then acquired every 20 seconds for up to one hour for cells just transfected for TG2 (A,D), for cells having addition tapasin knockdown (B, E) or LTA knockdown (C, F). Still images are shown at time zero (A, B, C) and at 45 minutes (B, D, F). The video for each of these are shown as video 3, 4, 5.

10.5 Discussion

Using live cell imaging, it is clearly possible to demonstrate plasma membrane blebbing into which TG2 is concentrated and released from the cell. The removal of LTA in NRK52E cells stops the blebbing process and TG2 masses under the plasma membrane. The removal of tapasin still allows blebs to form, however the TG2 seems to be dragged back into the cytoplasm and the blebs do not appear to perforate or release. Of particular note is that when NRK52E cells transfected with either mutant TG2 that cannot be exported or following LTA knock down, many cells undergo a process that looks very similar to apoptosis with cell shrinkage and detaching from the culture plate. Interestingly both these actions would lead to an elevated intracellular level of TG2. High cellular TG2 has been associated with both apoptosis (Oliverio *et al.* 1999) and a transglutaminase mediate cell death process (Johnson *et al.* 1998) that is very similar to apoptosis but lacking DNA condensation and fragmentation.

The duration of episodes of plasma membrane blebbing is very short lasting about 2-3 minutes and thus unless a large field is viewed on a continual basis cell instigating this event are easily missed. Further, we believe that this process is difficult to see on fixed cells as the process is very dynamic and the fixation process itself seems to lessen the contour of the bleb on the cell making then hard to see. These reasons may explain the failure to visualise TG2 export process previously as well in other novel export routes described such as that for FGF-2 externalisation (Seelenmeyer *et al.* 2008). It is important to consider that the blebbing could be triggered in some way by either the transfection procedure or serum starvation, however, these are conditions used throughout the study under various experimental regimes and thus it seems unlikely they may play a role.

In determining the possible protein secretion pathway for TG2, live cell imaging has provided some compelling but not conclusive information. Firstly, fluorescence generated by FlAsH to track TG2 movement can only be used for detection for about 1hour or around 150 images at 300ms exposure time before it becomes bleached. Unfortunately anti-fade reagents are toxic to cells

and cannot be used in live cell imaging. We therefore believe that the fading fluorescence intensity between 40-60 minutes of the visualisation is more likely due to photo bleaching of the fluorescence than the complete externalisation of TG2 into the culture medium. Secondly, we noticed that cells were visualised for more than 2 hours they tended to die, photo or heat insult to the cells may be responsible for this and thus we tried to use only brief periods of imaging to avoid artefacts resulting from cell damage. Overall the export process we report occur very quickly and intermittently indicating that TG2 builds to a determined cell level at which point the export process is activated.

Chapter 11 Discussion

In this study, we demonstrated that extracellular trafficking of TG2 is dependent of the N-terminal β-sandwich domain of TG2 using deletion analysis. The TG2 export motif (aa 88-106) was identified to be critical in extracellular trafficking of TG2 and no TG2 exported if Asp^{94} and Asp^{97} mutated (Chou *et al.* 2011). Although the TG2 export motif has been reported to be a fibronectin binding site, TG2 extracellular trafficking is independent of fibronectin and no decrease in TG2 export was observed following an 80% knockdown of intracellular fibronectin in TECs. Meanwhile, TG2 was solely externalised through the basolateral side of the plasma membrane using measurement of TG activity in culture medium from cell monolayer grown in culture inserts and deconvolution microscopy imaging. The TG2 export motif binds to large tumour antigen (LTA), tapasin and translocon-associated protein γ using yeast two hybrid screen. Knockdown of intracellular LTA or tapasin proportionally decreased TG2 export suggesting that TG2-LTA and TG2-tapasin interaction is linked to TG2 extracellular trafficking. Using chorological imaging, it was shown that TG2 was synthesised in rough ER around the cell nucleus and moved to periphery of the cells and extracellular accumulation of TG2 could be maximally visualised 48 hours post transfection. In contrast, mutant TG2 that does not undergo extracellular export tented to accumulate in sub-plasma membrane area in a vesicle shape. The main morphological change related to TG2 extracellular trafficking seemed to be plasma membrane blebbing. This was more frequently observed in cells with elevated TG2 levels and much less in cells transfected with mutant TG2 that does not get exported. This suggests that plasma membrane blebbing could be involved in TG2 extracellular trafficking. Plasma membrane blebbing was seen in the cells with tapasin knockdown but the TG2 containing blebs were retracted to the centre of the cell rather than the TG2 containing bleb being pinched and released. Knockdown of LTA in TECs prevented cells displaying plasma membrane blebs (or at least ones that were visible containing “green” TG2) suggesting that LTA and tapasin are both involved in TG2 extracellular trafficking.

As knockdown of tapasin and LTA both decrease extracellular TG2 export, we therefore hypothesise the potential TG2 externalisation pathways: TG2 could be carried by the vesicles formed by the tapasin associated ER membrane to sub-plasmic membrane area, binding to plasma membrane associated LTA and then released to extracellular space through plasma membrane blebbing (Figure 10.5-1). TG2 associated plasma membrane blebbing was also noted in an early study by Gentile et al (1992) showing extensive plasma membrane blebbing in fibroblasts with a high TG2 expression. A recently study by Belkin *et al* showed the recruitment of TG2 by perinucleus recycling endosomes and VAMP3, SNAP23 SNAREs mediated plasma membrane-endosome fusion prior TG2 externalisation (Zemskov *et al.* 2011). Although plasma membrane blebbing was not observed in their study, this suggests a possible route of TG2 externalisation via plasma membrane blebbing as SNAREs on late endosomes membrane could mediate the fusion of endosome with the plasma membrane. It is possible that plasma membrane blebbing was not observed in

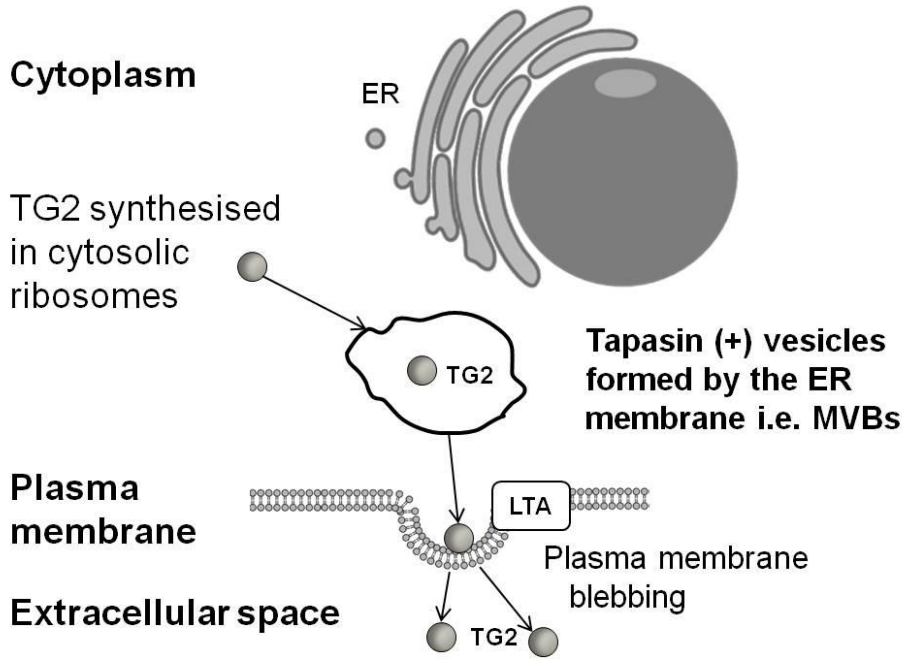

Figure 10.5-1 Possible TG2 externalisation pathways

After TG2 synthesised in the cytosolic ribosomes, tapasin on the membrane of vesicles (the membrane came from ER membrane) recruited TG2 in to the secretary vesicles i.e. multiple vesicular bodies (MVBs) and carried TG2 to the periphery of the cells i.e. sub-plasma membrane. The large tumour antigen (LTA) on plasma membrane binds to TG2 and TG2 was released following plasma membrane blebbing.

their study due to the lack of live cell imaging, spotting blebs is extremely difficult on still images and indeed it was only in this study when live cell imaging was attempted were blebs noticeable despite extensive immunofluorescent studies prior to this.

Previous work has shown that the ability of TG2 to bind fibronectin is important for TG2 trafficking (Gaudry *et al.* 1999; Verderio *et al.* 2003; Telci *et al.* 2008). However work presented here contradicts this suggesting that fibronectin is not essential for TG2 externalisation, at least in TECs. The TG2 export motif spanning aa 88-106 is crucial for TG2 externalisation in TECs is still a fibronectin binding site (Hang *et al.* 2005). The TG2 Antigen assay used in this study (Section 3.4.7) is based on fibronectin binding, and as such, constructs that remove or mutate the either of the described fibronectin binding sites should lower TG2 binding to fibronectin. However if either or both of the known fibronectin sites are altered, TG2 still binds to fibronectin (cell lysate analysed using biotin-cadaverine incorporation showed in section 3.4.7). This finding raises the suspicion that there might be other fibronectin binding site in TG2 molecule most likely on core domain of TG2 because core domain was still able to bind to fibronectin. Early works looking at TG2 extracellular trafficking focused on the co-localisation of TG2 with fibronectin (Martinez *et al.* 1994; Jones *et al.* 1997; Sechler *et al.* 1998; Verderio *et al.* 1998; Gaudry *et al.* 1999) or integrin (Gaudry *et al.* 1999; Akimov *et al.* 2000; Janiak *et al.* 2006) on cell surface. Subsequently fibronectin and integrin were considered as co-transport partners for TG2. The role of extracellular TG2 in cell adhesion is associated with fibronectin and integrin which may be one of the major reasons to link fibronectin and integrin also with TG2 export. Fibronectin and integrin are both externalised through classical ER-Golgi networks. If TG2 is carried by fibronectin or integrin to the plasma membrane, TG2 should be observed in ER-Golgi networks. TG2 extracellular trafficking is independent of the function of ER-Golgi networks because the inhibition of ER-Golgi networks with agents such as brefeldin and tunicamycin did not interfere with TG2 extracellular trafficking (Zemskov *et al.* 2011). In this study, it was demonstrated that knocking down 80% of intracellular fibronectin did not decrease TG2 extracellular trafficking (Chou *et al.* 2011). Based on the

available data, it is not likely that fibronectin or integrin can be the extracellular trafficking partners of TG2. In the four possible unconventional protein transport mechanisms (Figure 9.1-1), binding partners are always need for the extracellular trafficking. For example, FGF2 is recruited by $PI(4,5)P_2$ on the inner side of the plasma membrane. Ist2 is recruited by the COPI coat on the cortical ER membrane. A mannose 6-phosphate moiety is added to IL-1β such that it can be recognized by mannose 6-phosphate receptor on lysosomes and imported into secretary lysosomes. According to our data, it is possible that the TG2 export motif binds to tapasin that presenting on the membrane of the vesicles formed by ER membrane *i.e.* MVBs and carried TG2 to the periphery of the cell by an unknown process. The plasma membrane associated LTA then recruited TG2 and TG2 can be externalised through plasma membrane blebbing. This pathway dose associated well with mechanisms related to other novel pathways. It is possible that other protein can be involved in the TG2 externalisation process.

Fibroblast growth factor 2 (FGF-2) is one of the most expensively studied unconventionally secreted protein. It is suggested to be secreted through a direct molecular trap system via heparan sulfate proteoglycans (HSPGs) on cell surface. The FGF-2 extracellular trafficking route may provide some clues for unravelling TG2 extracellular trafficking pathway more completely. The hypothesis for a direct molecular trap is derived from data showing FGF-2 is being secreted through a ternary complex with high-affinity FGF receptors and HSPGs, mutants defective for HSPG binding and cells with impaired HSPG biosynthesis have defective FGF-2 export (Zehe *et al.* 2006). An early study suggested that FGF-2 can be secreted from plasma membrane blebbing/shedding (Taverna *et al.* 2003). This was contradicted by a later study that showed that FGF-2 is not secreted through plasma membrane derived vesicles and subsequently lead to the hypothesis of a direct molecular trap mechanism (Seelenmeyer *et al.* 2008). In both plasma membrane blebbing and direct molecular trap, the secretion of FGF-2 relies on the binding to another protein such as HSPGs to recruit FGF-2 in the sub-plasmic area. This equates to the current hypothesis for TG2 export where tapasin and LTA are implicated as both bind to the TG2 export motif and both prevent export when

knocked down. As TG2 also had some affinity to HSPGs (Scarpellini *et al.* 2009), it is also hypothesised that TG2 can be secreted through the HSPGs associated direct molecular trap mechanism. The TG2 export motif is composed of the β5/β6 hairpin in the N-terminal β-sandwich domain of TG2. The size of this hairpin is about the same size of the HSPGs side chain. When beginning of yeast two hybrid screens, it was expect that HSPGs or fibronectin would be on the list of potential binding proteins. However, neither fibronectin nor HSPGs was appeared on the list. Dynein is another protein that identified in Y2H screening (section 7.3) and may be interesting to look into its role in TG2 externalisation. Dynein is a motor protein that able to move cellular cargos along the cytoskeletal microtubules. Dynein was not selected because no co-localisation of TG2 and cytoskeleton stain (actin, data not shown) was found in our work.

Although plasma membrane blebbing is the only morphological finding that we found different between cells transfected with full length of TG2 and mutant TG2, it is difficult to confirm conclusively that TG2 is externalised through plasma membrane blebbing. Further experiments will be needed to confirm if plasma membrane blebbing is responsible for TG2 externalisation. For example if inhibition of plasma membrane blebbing stops TG2 externalisation using ROCK inhibitor (Emre *et al.* 2010), this would strongly link blebbing as part of the mechanism. In the case of FGF-2, inhibition of plasma membrane blebbing using a ROCK inhibitor did not decrease FGF-2 extracellular trafficking (Seelenmeyer *et al.* 2008) leading to description of the molecular trap mechanism.

Microparticles (MPs) are small vesicles released from the plasma membrane blebbing / shedding and can carry specific markers from the derived cells such as platelet and endothelial cells. As platelet derived MPs contains Factor XIII (Garcia *et al.* 2005), it is possible that epithelial cells derived MPs contains TG2. A recent study also suggested that TG2 can be found in the microparticles from smooth muscle cells (van den Akker *et al.* 2011). The microparticles can be formed from plasma membrane blebbing suggesting the association between plasma membrane blebbing and TG2 extracellular trafficking. So far no study has suggested that TECs produce MPs, therefore,

the role of MPs in fibrosis comes from the studies regarding circulating MPs and atherosclerosis. MPs in the circulation are extensively studied in the association with various diseases (Furie *et al.* 2004; Chironi *et al.* 2006). Circulating MPs derived from endothelial cells and platelets are linked to acute coronary syndromes (Mallat *et al.* 2000). Granulocytic origin MPs are linked to metabolic syndrome (Diamant *et al.* 2002). Platelet MPs are linked to atherosclerosis and peripheral arterial disease (van der Zee *et al.* 2006). Circulating MPs bear tissue factor on the surface that is critical for thrombus spreading and fibrin formation (Chou *et al.* 2004). The circulating MPs can be captured by thrombus-associated-platelets and initiate blood coagulation and fibrin formation (Hrachovinova *et al.* 2003). Circulating MPs can also stimulate the release of pro-inflammatory endothelial cytokines such as interleukin (IL)-6 and IL-8 and induce expression of the adhesion molecules including ICAM-1, VCAM-1 and E-selectin (Nomura *et al.* 2001). Nitric oxide is an important mediator for endothelial cells in control vascular tone and the impairment of nitric oxide release indicate vascular dysfunction. MPs can impair the release of nitric oxide from vascular endothelial cells in patients with end-stage renal disease (Amabile *et al.* 2005) and patients with myocardial infarction (Boulanger *et al.* 2001) but not the MPs from normal individuals. In addition, MPs can stimulate angiogenesis medicated by vascular endothelial growth factor or sphingomyelin (Kim *et al.* 2002; Brill *et al.* 2005). It is not clear if renal epithelial cells produced MPs from plasma membrane blebbing and what is the function of MPs on extracellular matrix. As shown in a recent study, endothelial origin MPs can interact with extracellular matrix through the activation of MMP-2 (Lozito *et al.* 2011), it is possible that tubular epithelial cells produce TG2 containing MPs that adhere to the tubular basement membrane, TG2 would thus be released into the extracellular matrix (ECM) and thus instigating ECM remodeling. Further studies are needed to determine if TECs can produce MPs and the role of MPs in kidney fibrosis *in vivo*. The live cell images shown in the final results chapter suggest that TECs can product MPs at the basal side of the cells and the MPs fused into 1-2 big vesicles in tissue culture plates. It would be interesting to visual this process *in vivo* and if MPs attach to the ECM and release MPs containing protein in the ECM.

In the literature, autophagy had been suggested as another unconventional protein secretion pathway. As mentioned in Section 1.3.1.2, autophagy is a cell self-eating process that occurs in normal and stimulated condition such as starvation. Cellular components including damaged or redundant organelles are packed into double-membrane vesicles called autophagosomes (Manjithaya *et al.* 2010). Although autophagy is not listed in the four potential unconventional protein externalisation pathways (Figure 9.1-1), autophagy can be considered as a combination of lysosomes and exosomes secretion. Autophagosomes usually fuse with lysosomes in autophagy and thus the contents are degraded and recycled. However, more and more evidences have shown that autophagy can be an unconventional protein secretion pathway (reviewed in Todde *et al.* 2009). Multivehicle bodies (MVBs) are essential for protein externalised in autophagy (reviewed in Piper *et al.* 2007). The exported proteins are transported into MVBs (i.e. from the ribosomes in cytosol or rough ER), the contents of MVBs moved to autophagosomes and released into extracellular space while autophagosomes fused with the plasma membrane. MVBs express markers such as LAMPs that is used for lysosome identification (LAMP-2). As no co-localisation of TG2 and lysosomes at the peripheral of the cells was found, this suggests that TG2 is not externalised through autophagy. However, it is worth further study if autophagosomes using microtubule-associated protein 1 light chain 3 (LC3) (Kabeya *et al.* 2000) could be co-localised with TG2.

In this study, we explored TG2 externalisation using TG2 cDNA or mutant TG2 transfected into TECs followed by the measurements of total cellular TG activity and extracellular TG. One disadvantage for this approach is the TG2 externalisation measurement is in an overloaded environment compared to the native TG2 synthesised in the cell. We believed that the approach is valid to determine TG2 externalisation based on following reasons. Firstly, the TG2 level that we measured in transfected cell was increased by just 5-10 fold compared to wild type TECs in culture. TECs when placed in primary culture use 99% of their TG2 activity by passage 3. In vivo TEC have a lot more TG2 and was below what is seen in post transfection. This increase of TG2 levels was much less than that (30-100 fold increase) of TG2 levels measured in

patients with chronic kidney disease (Johnson *et al.* 2003). Therefore, the increase of TG2 levels after transfection was at best 5% of the TG2 levels *in vivo* and thus the cells were not overloaded. Secondly, the basal levels of TG2 in the cell are at the lowest end of the assay and are very difficult to be detected by western blotting, it is more difficult to measure the intracellular and extracellular TG levels after knockdown endogenous TG2 using specific siRNA. Therefore the transient expression of exogenous TG2 was needed to study TG2 extracellular trafficking. Therefore, the approach that we took could be the most suitable approach for studying TG2 extracellular trafficking.

It was demonstrated that a 50% knock down of intracellular LTA was linked to a 50% decrease of TG2 export (Section 8.2). This indicated LTA is crucial for TG2 extracellular trafficking in TECs. The leading question is therefore how LTA, a viral protein, can facilitate TG2 extracellular trafficking. LTA is known for the binding to tumour suppressor gene such as p53 (reviewed in Pipas *et al.* 2001) and retinoblastoma susceptibility gene pRB (reviewed in Stiegler *et al.* 1998) that may be related to tumorgenesis in human and cell transformation. A small portion (5%) of LTA can be presented on cell surface but the function for the plasma membrane form LTA protein is unknown (Deppert *et al.* 1982). The expression of plasma membrane associated LTA is positively correlated to cells growth rate and cells with a loss of plasma membrane associated LTA expression precede growth arrest (Santos *et al.* 1985). The plasma membrane associated LTA has a higher affinity to antibodies and p53 (Soule *et al.* 1979) than LTA that target the cell nucleus. The transport of plasma membrane associated LTA to the cell surface is a rapid process (Santos *et al.* 1984; Santos *et al.* 1984) and is independent of Golgi networks (Tartakoff 1983). Thus the plasma membrane associated LTA might mimic a growth factor that generate a growth signal transmitting to the cell nucleus and phenotypic changes characteristic of complete transformation. Knock down of LTA is linked to a decrease of TG2 externalisation and prevents of plasma membrane blebbing in TECs. Our findings i.e. co-localisation of LTA and TG2, live cell imaging, lead to the hypothesis that plasma membrane associated LTA might recruit TG2 at the sub-plasma membrane area and subsequently TG2 was externalised through a LTA dependent plasma membrane blebbing mechanism.

This find was also supported by a previous study (Birckbichler *et al.* 1978) that intracellular TG activity is significantly lower for the cells transformed by SV40 virus that theoretically this could be caused by an increase of externalised TG2. As cells without LTA should export TG2, this LTA mediated externalisation pathway may be an extra-pathway from a native TG2 externalisation pathway as if this was the only mechanism then TG2 externalisation would not occur unless an individual is infected by polyomavirus. However, it is unknown if TG2 can be exported without LTA simply because the association between TG2 and LTA has never been found. Subsequently a major question is what is the relevance to TG2 export in healthy individuals or in fact those with CKD. If this is of true biological importance then LTA is expressed in humans and consequently can be related to disease progression in man. LTA is a protein produced by polyomavirus such as Simian Vacuolating Virus 40 (SV40), BK and JC virus in human. BK virus in particular is more prevalent in human in the literature and thus LTA produced by BK virus might be linked to the role of TG2 in CKD. BK virus was first identified from the urine of a kidney transplantation patient (Gardner *et al.* 1971). The infection source for BK virus infection in human is not clear and the infection of BK virus is not needed to treat because of the mild symptom and sign in normal individuals. In immune-compromised host the activation of BK virus is linked to the underlying immuno-supression status such as overuse of immunosuppressant. The treatment for organ transplant recipients is straight forward that is reducing immunosuppressant dosage. About 80% of the general population in UK, US and EU are infected by the BK virus without clinical symptoms (Gardner 1973; Mantyjarvi *et al.* 1973; Portolani *et al.* 1974; Egli *et al.* 2009). BK virus infection only develops symptoms and signs such as viruria and viremia, ureteral ulceration and stenosis and hemorrhagic cystitis in immunocompromised hosts (Mylonakis *et al.* 2001). The reactivation of BK virus in patients with kidney transplantation is associated with progressive loss of graft function (Hogan *et al.* 1980). The chance for human cells with LTA expression without viremia can be even higher because up to 85% of human normal tissue samples or tumour tissues had wild-type LTA coding analysed by PCR (De Mattei *et al.* 1995).

SV40 is a potent DNA tumour virus that can induce tumour in rodent and

transformed cell in culture. SV40 infection also occurred in human. Millions of people were inadvertently exposed to live SV40 from 1955 through early 1963 when they were administered SV40-contaminated virus vaccines that are mostly polio vaccines (Fraumeni *et al.* 1963). Although individuals exposed to SV40-contaminated vaccines are not more at risk for developing cancer than those who received SV40-free vaccines (Shah *et al.* 1976; Strickler *et al.* 1998; Strickler *et al.* 2003). SV40 DNA can be detected in tumour samples obtained from some types of human cancer such as pediatric and adult brain tumours, mesotheliomas, osteosarcomas, bronchopulmonary carcinomas, pituitary tumours and papillary thyroid carcinomas (reviewed in Butel *et al.* 1999) with a frequency of 35%. The expression of LTA can be detected in approximately 50% of tumour samples. Therefore, LTA not only presents in tissue culture but also presents in human with a very high prevalence.

SV40 is wildly used for cell transformation in tissue culture; however, OK (Koyama *et al.* 1978), NRK52E (Huu *et al.* 1966) and MDCKII cells (Richardson *et al.* 1981) are not transformed using SV40. However, OK, NRK52E and MDCKII cells do express LTA by western blot. The incidence of polyomavirus infection in animals is unknown and it is possible that the animal from which the primary cell culture was obtained had been infected by polyomavirus and consequently the cells expressed LTA protein. It is also possible that spontaneously immortal cells also expressed LTA. In mouse embryo fibroblasts or rat embryo fibroblasts, the expression of LTA drive the cell into S-phase and the cell becomes immortal. This is more complicated in other cells. For example, human fibroblast expressing LTA can be propagated for an extended period but eventually senesced. An active telomerase is therefore required to escape senesce in human fibroblasts (Ahuja *et al.* 2005). The interaction between LTA and p53 (Deppert *et al.* 1989) or retinoblastoma (Rb) family of tumour supressor proteins (Ludlow *et al.* 1989) is clearly contribute to the SV40 transformation. It is less clear, LTA associated cell transformation also involved other transcriptional proteins and mechanisms such as SEN6 (Jha *et al.* 1998), TEF-1, Nbs1 and Fbw7 that may be also modulated by LTA that contribute to cell transformation (Ahuja *et al.* 2005). As expression of LTA on the cell surface is a critical step in determining a

successful transformation, this suggested that the plasma membrane associated LTA plays an important role in cell transformation.

TG2 has a diverse biologic function including differentiation, receptor-mediated endocytosis, cell adhesion, and induction of apoptosis (Mehta *et al.* 2006). Early studies suggested that the interaction between importin-3 and TG2 may be linked to TG2 nucleus translocation (Peng *et al.* 1999; Milakovic *et al.* 2004). TG2 staining is frequently found to be co-localised with the cell nucleus as is also seen in this study. The nucleus localisation of TG2 plays a key role in its protective function against cell death in HEK293 cells (Gundemir *et al.* 2009). The expression of TG2 can be associated with chemotherapeutic drugs resistance in human breast cancer cells (Ai *et al.* 2008). The cell nucleus localisation for TG2 may be related to the expression of genes related to neutrophil functions and may be involved in several intracellular and extracellular functions of extravagating neutrophil (Balajthy *et al.* 2006). The interaction between large tumour antigen (LTA) and TG2 may explain how TG2 is transported to the cell nucleus because of the nucleus origin sequence on LTA. It is known that LTA can enter the cell nucleus and serve as a helicase (Titolo *et al.* 2003), subsequently it is possible that the interaction between TG2 and LTA is involved in the function of TG2 in the cell nucleus. The major function of LTA on cell surface is not clear and is generally considered to be involved in complete cell transformation (Butel *et al.* 1986). Based on our finding, the plasma membrane associated LTA might be able to carry proteins cross the plasma membrane. As LTA also interacts with p53 and RB protein that may be related to cell apoptosis. LTA also has a nuclear localization signal (LXCXE) located before the origin-binding domain that is the domain that interact with the TG2 export motif. LTA therefore can be a potential player in process of TG2 nucleus localisation and possibility the role of TG2 in the cell nucleus. It would be interesting to explore the association between LTA and specific TG2 functions according to TG2 expression in different component of the cell i.e. the cell nucleus, cytoplasm, and the plasma membrane.

Based on the fact that a viral protein is related to TG2 externalisation raises the question as to whether the level of LTA expression within an individual is related to the development of TG2 extracellular trafficking and thus tissue

fibrosis in general. Since LTA is a virus protein and may not be part of the native TG2 secretion pathway in mammalian cells, LTA related TG2 externalisation can be considered as a pathological TG2 externalisation pathway compared to the normal TG2 secretion. Abolish of LTA expression can be harmless for mammalian cells and has minimal effect on normal cell physiology but potentially a dramatic affect on TG2 export. It is possible to prevent cells from expressing LTA protein by virus vaccination and thus the data generated within this thesis strongly suggests that this may be a way of mitigating TG2 export that is so tightly linked to the development of CKD.. More epidemiological studies are initially needed to support the clinical application of this finding. For example, if individuals with BK virus infection have a higher incidence of CKD and those without a history of BK virus infection had a lower risk of CKD. Further if CKD patients have a high incidence of LTA expression in kidney tissue and a high viral titter.

Tapasin is a transmembrane protein that tethers empty class I molecules to the peptide transporter associated with antigen processing (reviewed in Grandea *et al.* 2001). The structure of tapasin is composed of a short cytoplasmic tail containing an ER retention signal, a transmembrane region and a large N-terminal intraluminlar part (Li *et al.* 1997). The assembly of MHC class I molecules is a series of coordinated and regulated interactions with ER-resident chaperones. Tapasin is majorly involved in the assembly of MHC class I molecules and peptide-loading complex interaction. Proteins associated with the assembly of peptide-loading complex with tapasin include β2-microglobulin, calreticulin, MHC class I heavy chain, ERp57, protein disulphide isomerise and transporter associated with antigen-processing proteins (reviewed in Cabrera 2007). The major function of tapasin is to enhance peptide loading in peptides loading complex (Figure 10.5-2). The mature MHC class I molecular is transported to Golgi apparatus and externalised to cell surface through the classical ER-Golgi network. In the process, tapasin interact with transporter associated with antigen-processing proteins and is responsible for an optimal peptides load in MHC class I molecules (Sadasivan *et al.* 1996). Tapasin is related with quality control of peptides loading complex. Deficiency of a functional tapasin results in a

low-affinity peptides loaded in MHC class I molecules (Garbi *et al.* 2000). Unstable MHC class I molecules on cell surface (Grandea *et al.* 2000) and consequently severe immune-deficiency (reviewed in Grandea *et al.* 2001). As unstable MHC I molecules can present on the cell surface suggesting, tapasin is not essential for the MHC I molecule extracellular trafficking, the MHC class I molecule externalisation pathway may not apply to the tapasin dependent TG2 externalisation. Tapasin predominately resides on ER membrane, retains immature class I molecules in the ER and transports the mature class I molecular to Golgi apparatus. Approximately 10% of tapasin can be presented

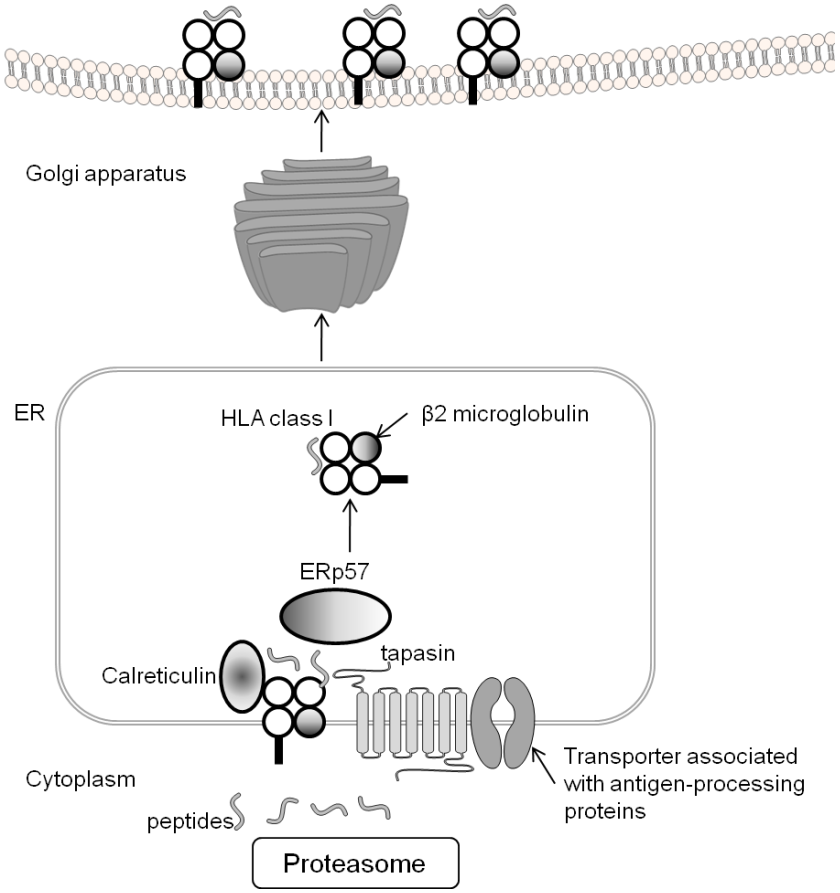

Figure 10.5-2 Tapasin related MHC class I molecular antigen presenting process

Mature MHC class I complex that is composed of a MHC class I molecule and β2-microglobulin heterodimers and is expressed on the cell surface. The mature MHC class I molecule is externalised through Golgi apparatus after interaction with tapasin, ERp57, calrecitulin, transporter associated with antigen-processing proteins in ER.

on plasma membrane (Teng *et al.* 2002), but the function for these plasma membrane associated tapasin is unknown. The plasma membrane-associated tapasin may be also related to TG2 externalisation based on the data generated in this study. TG2 was still seen at the plasma membrane following knockdown of tapasin (Section 10.4) with accumulation into vesicles shaped structure in the sub-plasma membrane area. Fluorescent microscopy co-localised TG2 and tapasin around the cell nucleus that is mostly likely in the ER as well as at the cell periphery in the sub-plasma membrane area. Both these locations are consistent with tapasin know cellular location (Teng *et al.* 2002). Interestingly plasma membrane blebbing was observed in TECs following tapasin knock down suggesting that while tapasin is essential for TG2 externalisation it is not part of the plasma membrane blebbing machinery. In live cell imaging of TECs following tapasin knockdown, TG2 was retracted back to the centre of the cell while cell shrinkage and formed vesicle in the centre of the cell. We therefore proposed that TG2 is carried by tapasin from ER to the periphery of the cell and released to extracellular space following LTA-associated plasma membrane blebbing. As both knockdown of tapasin and LTA resulted in a proportional decrease of TG2 externalisation, this suggests that tapasin and LTA may be involved in the same externalisation route. It is possible that LTA replace another normal protein in TG2 export. Compared to the LTA related TG2 externalisation, the tapasin pathway for TG2 externalisation seems to be a physiological TG2 externalisation mechanism. Tapasin is one of ER residual protein in normal condition and is associated with MHC class I molecules expressed on cell surface. The MHC class I molecules are transported to the cell surface through the ER-Golgi network. As TG2 is not exported through the ER-Golgi network, it is likely that tapasin carried TG2 to the cell surface through a different mechanism such an exosomal secretion, plasma membrane blebbing or a direct molecular trap. As tapasin deficiency is linked to severe immune dysfunction, therefore targeting TG2 export motif or LTA may have more potential in fibrosis treatment under pathological condition.

It is not clear whether TG2 externalisation is limited to one of the unconventional protein secretion pathways or is involved in more than one

pathway. As knock down of LTA and tapasin both decrease TG2 externalisation, it is likely that the extracellular trafficking of TG2 is involved in one pathway that needs both LTA and tapasin to work. As TG2 is a multiple function protein, it would be beneficial to clinical application if we can target pathological TG2 externalisation without affecting its normal cellular physiological functions as well. Based on the findings of this study i.e. tapasin carried TG2 to the periphery of the cell and TG2 is secreted via LTA related plasma membrane blebbing. Targeting LTA could be a potential treatment target to prevent TG2 externalisation.

It is possible to avoid the cells expression LTA in human disease. Vaccination is an effective treatment for virus infection in clinical practice. The infection by BK virus and SV40 do not cause acute illness and thus has not been a major concern, however, the development of a LTA vaccine started because of the association between LTA and some types of human cancers (reviewed in Butel *et al.* 1999). A modified SV40 LTA has been cloned into a vaccine virus vector and tested in animal tumour model systems (Bright *et al.* 1994) with the transforming domains removed. The vaccine is effective against both subsequent tumour challenge and pre-existing tumours (Imperiale *et al.* 2001). As it is possible to develop vaccine against LTA, the expression of LTA can be abolished using vaccination and consequently decrease pathological TG2 externalisation that is related to the accumulation of ECM proteins and accelerate fibrosis formation. This approach can potentially be a treatment target in atherosclerosis, liver, lung, kidney fibrosis, Coeliac disease, cancer and Alzheimer's disease where TG2 externalisation is a key event in driving the pathology.

Although autophagy was not involved in TG2 externalisation in this study, autophagy has an import role in kidney injury (reviewed in Anders *et al.* 2010) and glomeronephritis (Hartleben *et al.* 2010). Autophagy allows stressed cells to reduce intracellular microorganisms, protein aggregates, and cellular organelles by moving and digesting them in autophagolysosomes. In the autophagolysosome, endogenous molecules and danger-associated molecules may be presented to Toll-like receptors. Toll-like receptors are part of immune receptor families that detect danger signals in extracellular and

intracellular compartments. Toll-like receptors loaded the molecules digested in autophagolysosomes onto the major histocompatibility complex and presented as autoantigens (Anders *et al.* 2010). As TG2 is also wildly involved in cell proliferation, antigen presenting process and apoptosis, it would be interesting to explore the association between autophagy and TG2. In our study, LAMP-2 was used as a marker for autophagolysomes. As autophagy is involved in a series of vesicles formation during the digestion process, microtubule-associated protein 1 light chain 3 (LC3) is also a maker for autophagosome (Kabeya *et al.* 2000). It would be interesting to explorer the co-localisation between LC3 and TG2.

Some questions regarding the proposed TG2 extracellular trafficking pathway (Figure 10.5-1) remains un-answered and thus more studies are needed. Firstly, where is tapasin-TG2 interaction occurred while tapasin carried TG2 to the periphery of the cells (ie rough ER, cortical ER). Secondly, is tapasin interacted with LTA? Therefore tapasin can transfer TG2 to LTA on the plasma membrane and another protein may be also involved to release TG2 from tapasin. Thirdly, if TG2 extracellular trafficking is dependent on plasma membrane blebbing. Fourthly, is there other organelles are involved in TG2 extracellular trafficking (ie late endosomes or MVBs). We believe these questions can be answered using live cell imaging with co-localisation analysis or fluorescence resonance energy transfer.

Chapter 12 References

(2002). "K/DOQI clinical practice guidelines for chronic kidney disease: evaluation, classification, and stratification." Am J Kidney Dis 39(2 Suppl 1): S1-266.
Achyuthan, K. E., R. J. Goodell, et al. (1995). "Immunochemical analyses of human plasma fibronectin-cytosolic transglutaminase interactions." J Immunol Methods 180(1): 69-79.
Achyuthan, K. E. and C. S. Greenberg (1987). "Identification of a guanosine triphosphate-binding site on guinea pig liver transglutaminase. Role of GTP and calcium ions in modulating activity." J Biol Chem 262(4): 1901-1906.
Aeschlimann, D., M. K. Koeller, et al. (1998). "Isolation of a cDNA encoding a novel member of the transglutaminase gene family from human keratinocytes. Detection and identification of transglutaminase gene products based on reverse transcription-polymerase chain reaction with degenerate primers." J Biol Chem 273(6): 3452-3460.
Aeschlimann, D. and V. Thomazy (2000). "Protein crosslinking in assembly and remodelling of extracellular matrices: the role of transglutaminases." Connect Tissue Res 41(1): 1-27.
Ahuja, D., M. T. Saenz-Robles, et al. (2005). "SV40 large T antigen targets multiple cellular pathways to elicit cellular transformation." Oncogene 24(52): 7729-7745.
Ai, L., W. J. Kim, et al. (2008). "The transglutaminase 2 gene (TGM2), a potential molecular marker for chemotherapeutic drug sensitivity, is epigenetically silenced in breast cancer." Carcinogenesis 29(3): 510-518.
Akar, U., B. Ozpolat, et al. (2007). "Tissue transglutaminase inhibits autophagy in pancreatic cancer cells." Mol Cancer Res 5(3): 241-249.
Akimov, S. S., D. Krylov, et al. (2000). "Tissue transglutaminase is an integrin-binding adhesion coreceptor for fibronectin." J Cell Biol 148(4): 825-838.
Ali, S. H. and J. A. DeCaprio (2001). "Cellular transformation by SV40 large T antigen: interaction with host proteins." Semin Cancer Biol 11(1): 15-23.
Amabile, N., A. P. Guerin, et al. (2005). "Circulating endothelial microparticles are associated with vascular dysfunction in patients with end-stage renal failure." J Am Soc Nephrol 16(11): 3381-3388.
Anders, H. J. and D. O. Schlondorff (2010). "Innate immune receptors and autophagy: implications for autoimmune kidney injury." Kidney Int 78(1): 29-37.
Andrei, C., C. Dazzi, et al. (1999). "The secretory route of the leaderless protein interleukin 1beta involves exocytosis of endolysosome-related vesicles." Mol Biol Cell 10(5): 1463-1475.
Andrei, C., P. Margiocco, et al. (2004). "Phospholipases C and A2 control lysosome-mediated IL-1 beta secretion: Implications for inflammatory processes." Proc Natl Acad Sci U S A 101(26): 9745-9750.
Annes, J. P., J. S. Munger, et al. (2003). "Making sense of latent TGFbeta activation." J Cell Sci 116(Pt 2): 217-224.
Antonyak, M. A., J. E. Boehm, et al. (2002). "Phosphoinositide 3-kinase activity is required for retinoic acid-induced expression and activation of the tissue transglutaminase." J Biol Chem 277(17): 14712-14716.
Antonyak, M. A., C. J. McNeill, et al. (2003). "Activation of the Ras-ERK pathway inhibits retinoic acid-induced stimulation of tissue transglutaminase expression in NIH3T3 cells." J Biol Chem 278(18): 15859-15866.
Aronov, S., R. Gelin-Licht, et al. (2007). "mRNAs encoding polarity and exocytosis factors are cotransported with the cortical endoplasmic reticulum to the

incipient bud in Saccharomyces cerevisiae." Mol Cell Biol 27(9): 3441-3455.
Atkins, R. C. (2005). "The epidemiology of chronic kidney disease." Kidney Int Suppl(94): S14-18.
Aumuller, G., B. Wilhelm, et al. (1999). "Apocrine secretion--fact or artifact?" Ann Anat 181(5): 437-446.
Bakker, E. N., C. L. Buus, et al. (2005). "Small artery remodeling depends on tissue-type transglutaminase." Circ Res 96(1): 119-126.
Balajthy, Z., K. Csomos, et al. (2006). "Tissue-transglutaminase contributes to neutrophil granulocyte differentiation and functions." Blood 108(6): 2045-2054.
Barone, M. V., I. Caputo, et al. (2007). "Humoral immune response to tissue transglutaminase is related to epithelial cell proliferation in celiac disease." Gastroenterology 132(4): 1245-1253.
Bartlett, J. M. and D. Stirling (2003). "A short history of the polymerase chain reaction." Methods Mol Biol 226: 3-6.
Basile, D. P., D. R. Martin, et al. (1998). "Extracellular matrix-related genes in kidney after ischemic injury: potential role for TGF-beta in repair." Am J Physiol 275(6 Pt 2): F894-903.
Beaglehole, R. and D. Yach (2003). "Globalisation and the prevention and control of non-communicable disease: the neglected chronic diseases of adults." Lancet 362(9387): 903-908.
Bednarek, S. Y., M. Ravazzola, et al. (1995). "COPI- and COPII-coated vesicles bud directly from the endoplasmic reticulum in yeast." Cell 83(7): 1183-1196.
Begg, G. E., L. Carrington, et al. (2006). "Mechanism of allosteric regulation of transglutaminase 2 by GTP." Proc Natl Acad Sci U S A 103(52): 19683-19688.
Belkin, A. M., S. S. Akimov, et al. (2001). "Matrix-dependent proteolysis of surface transglutaminase by membrane-type metalloproteinase regulates cancer cell adhesion and locomotion." J Biol Chem 276(21): 18415-18422.
Bellomo, G., F. Mirabelli, et al. (1988). "Oxidative stress-induced plasma membrane blebbing and cytoskeletal alterations in normal and cancer cells." Ann N Y Acad Sci 551: 128-130.
Berg, J. M. T., John L.; Stryer, Lubert (2002). Biochemistry.
Bernfield, M., M. Gotte, et al. (1999). "Functions of cell surface heparan sulfate proteoglycans." Annu Rev Biochem 68: 729-777.
Binet, I., V. Nickeleit, et al. (1999). "Polyomavirus disease under new immunosuppressive drugs: a cause of renal graft dysfunction and graft loss." Transplantation 67(6): 918-922.
Birckbichler, P. J. and M. K. Patterson, Jr. (1978). "Cellular transglutaminase, growth, and transformation." Ann N Y Acad Sci 312: 354-365.
Bishop, J. R., M. Schuksz, et al. (2007). "Heparan sulphate proteoglycans fine-tune mammalian physiology." Nature 446(7139): 1030-1037.
Blott, E. J. and G. M. Griffiths (2002). "Secretory lysosomes." Nat Rev Mol Cell Biol 3(2): 122-131.
Bo, X., J. Simon, et al. (1992). "Solubilization and molecular size determination of the P2x purinoceptor from rat vas deferens." J Biol Chem 267(25): 17581-17587.
Bo, X., Y. Zhang, et al. (1995). "A P2X purinoceptor cDNA conferring a novel pharmacological profile." FEBS Lett 375(1-2): 129-133.
Boehm, J. E., U. Singh, et al. (2002). "Tissue transglutaminase protects against apoptosis by modifying the tumor suppressor protein p110 Rb." J Biol Chem

277(23): 20127-20130.
Bohle, A., G. Kressel, et al. (1989). "The pathogenesis of chronic renal failure." Pathol Res Pract 185(4): 421-440.
Bougeret, C., I. G. Mansur, et al. (1992). "Increased surface expression of a newly identified 150-kDa dimer early after human T lymphocyte activation." J Immunol 148(2): 318-323.
Boulanger, C. M., A. Scoazec, et al. (2001). "Circulating microparticles from patients with myocardial infarction cause endothelial dysfunction." Circulation 104(22): 2649-2652.
Bowness, J. M., A. H. Tarr, et al. (1988). "Increased transglutaminase activity during skin wound healing in rats." Biochim Biophys Acta 967(2): 234-240.
Brian Henderson, A. G. P. (2005). Molecular Chaperones and Cell Signalling, Cambridge University Press.
Bright, R. K., M. H. Shearer, et al. (1994). "SV40 large tumor antigen associated synthetic peptides define native antigenic determinants and induce protective tumor immunity in mice." Mol Immunol 31(14): 1077-1087.
Brill, A., O. Dashevsky, et al. (2005). "Platelet-derived microparticles induce angiogenesis and stimulate post-ischemic revascularization." Cardiovasc Res 67(1): 30-38.
Butel, J. S. and D. L. Jarvis (1986). "The plasma-membrane-associated form of SV40 large tumor antigen: biochemical and biological properties." Biochim Biophys Acta 865(2): 171-195.
Butel, J. S. and J. A. Lednicky (1999). "Cell and molecular biology of simian virus 40: implications for human infections and disease." J Natl Cancer Inst 91(2): 119-134.
Cabrera, C. M. (2007). "The double role of the endoplasmic reticulum chaperone tapasin in peptide optimization of HLA class I molecules." Scand J Immunol 65(6): 487-493.
Campisi, A., D. Caccamo, et al. (2003). "Glutamate-induced increases in transglutaminase activity in primary cultures of astroglial cells." Brain Res 978(1-2): 24-30.
Candi, E., S. Oddi, et al. (2001). "Transglutaminase 5 cross-links loricrin, involucrin, and small proline-rich proteins in vitro." J Biol Chem 276(37): 35014-35023.
Cao, L., D. N. Petrusca, et al. (2008). "Tissue transglutaminase protects epithelial ovarian cancer cells from cisplatin-induced apoptosis by promoting cell survival signaling." Carcinogenesis 29(10): 1893-1900.
Charras, G. T., M. Coughlin, et al. (2008). "Life and times of a cellular bleb." Biophys J 94(5): 1836-1853.
Charras, G. T., C. K. Hu, et al. (2006). "Reassembly of contractile actin cortex in cell blebs." J Cell Biol 175(3): 477-490.
Chen, C. H. and H. G. Hansma (2000). "Basement membrane macromolecules: insights from atomic force microscopy." J Struct Biol 131(1): 44-55.
Chironi, G., A. Simon, et al. (2006). "Circulating leukocyte-derived microparticles predict subclinical atherosclerosis burden in asymptomatic subjects." Arterioscler Thromb Vasc Biol 26(12): 2775-2780.
Cho, B. R., M. K. Kim, et al. (2008). "Increased tissue transglutaminase expression in human atherosclerotic coronary arteries." Coron Artery Dis 19(7): 459-468.
Chou, C. Y., A. J. Streets, et al. (2011). "A crucial sequence for transglutaminase type 2 extracellular trafficking in renal tubular epithelial cells lies in its N-terminal

{beta}-sandwich domain." J Biol Chem.
Chou, J., N. Mackman, et al. (2004). "Hematopoietic cell-derived microparticle tissue factor contributes to fibrin formation during thrombus propagation." Blood 104(10): 3190-3197.
Chung, S. I. and J. E. Folk (1970). "Mechanism of the inactivation of guinea pig liver transglutaminase by tetrathionate." J Biol Chem 245(4): 681-689.
Connellan, J. M. and J. E. Folk (1969). "Mechanism of the inactivation of guinea pig liver transglutaminase by 5,5'-dithiobis-(2-nitrobenzoic acid)." J Biol Chem 244(12): 3173-3181.
D'Eletto, M., M. G. Farrace, et al. (2009). "Transglutaminase 2 is involved in autophagosome maturation." Autophagy 5(8): 1145-1154.
David, G. and H. Van den Berghe (1985). "Heparan sulfate-chondroitin sulfate hybrid proteoglycan of the cell surface and basement membrane of mouse mammary epithelial cells." J Biol Chem 260(20): 11067-11074.
de Larco, J. E. and G. J. Todaro (1978). "Epithelioid and fibroblastic rat kidney cell clones: epidermal growth factor (EGF) receptors and the effect of mouse sarcoma virus transformation." J Cell Physiol 94(3): 335-342.
De Mattei, M., F. Martini, et al. (1995). "High incidence of BK virus large-T-antigen-coding sequences in normal human tissues and tumors of different histotypes." Int J Cancer 61(6): 756-760.
Deppert, W., T. Steinmayer, et al. (1989). "Cooperation of SV40 large T antigen and the cellular protein p53 in maintenance of cell transformation." Oncogene 4(9): 1103-1110.
Deppert, W. and G. Walter (1982). "Domains of simian virus 40 large T-antigen exposed on the cell surface." Virology 122(1): 56-70.
Diamant, M., R. Nieuwland, et al. (2002). "Elevated numbers of tissue-factor exposing microparticles correlate with components of the metabolic syndrome in uncomplicated type 2 diabetes mellitus." Circulation 106(19): 2442-2447.
Dieterich, W., T. Ehnis, et al. (1997). "Identification of tissue transglutaminase as the autoantigen of celiac disease." Nat Med 3(7): 797-801.
Dong, G., P. A. Wearsch, et al. (2009). "Insights into MHC class I peptide loading from the structure of the tapasin-ERp57 thiol oxidoreductase heterodimer." Immunity 30(1): 21-32.
Dubbink, H. J., L. de Waal, et al. (1998). "The human prostate-specific transglutaminase gene (TGM4): genomic organization, tissue-specific expression, and promoter characterization." Genomics 51(3): 434-444.
Dudek, S. M. and G. V. Johnson (1994). "Transglutaminase facilitates the formation of polymers of the beta-amyloid peptide." Brain Res 651(1-2): 129-133.
Duran, J. M., C. Anjard, et al. (2010). "Unconventional secretion of Acb1 is mediated by autophagosomes." J Cell Biol 188(4): 527-536.
Egli, A., L. Infanti, et al. (2009). "Prevalence of polyomavirus BK and JC infection and replication in 400 healthy blood donors." J Infect Dis 199(6): 837-846.
El Nahas, M. (2005). "The global challenge of chronic kidney disease." Kidney Int 68(6): 2918-2929.
Emre, N., J. G. Vidal, et al. (2010). "The ROCK inhibitor Y-27632 improves recovery of human embryonic stem cells after fluorescence-activated cell sorting with multiple cell surface markers." PLoS One 5(8): e12148.
Ewen, M. E., J. W. Ludlow, et al. (1989). "An N-terminal transformation-governing sequence of SV40 large T antigen contributes to the binding of both p110Rb and

a second cellular protein, p120." Cell 58(2): 257-267.
Fackler, O. T. and R. Grosse (2008). "Cell motility through plasma membrane blebbing." J Cell Biol 181(6): 879-884.
Fan, J. M., Y. Y. Ng, et al. (1999). "Transforming growth factor-beta regulates tubular epithelial-myofibroblast transdifferentiation in vitro." Kidney Int 56(4): 1455-1467.
Fesus, L. and M. Piacentini (2002). "Transglutaminase 2: an enigmatic enzyme with diverse functions." Trends Biochem Sci 27(10): 534-539.
Fesus, L. and Z. Szondy (2005). "Transglutaminase 2 in the balance of cell death and survival." FEBS Lett 579(15): 3297-3302.
Fesus, L. and E. Tarcsa (1989). "Formation of N epsilon-(gamma-glutamyl)-lysine isodipeptide in Chinese-hamster ovary cells." Biochem J 263(3): 843-848.
Filmus, J. and S. B. Selleck (2001). "Glypicans: proteoglycans with a surprise." J Clin Invest 108(4): 497-501.
Fisher, M. (1973). The role of tissue transglutaminase in the extracellular matrix changes associated with kidney scarring. Ph.D, University of Sheffield.
Fisher, M., R. A. Jones, et al. (2009). "Modulation of tissue transglutaminase in tubular epithelial cells alters extracellular matrix levels: a potential mechanism of tissue scarring." Matrix Biol 28(1): 20-31.
Fok, J. Y., S. Ekmekcioglu, et al. (2006). "Implications of tissue transglutaminase expression in malignant melanoma." Mol Cancer Ther 5(6): 1493-1503.
Folk, J. E. and J. S. Finlayson (1977). "The epsilon-(gamma-glutamyl)lysine crosslink and the catalytic role of transglutaminases." Adv Protein Chem 31: 1-133.
Fraumeni, J. F., Jr., F. Ederer, et al. (1963). "An evaluation of the carcinogenicity of simian virus 40 in man." JAMA 185: 713-718.
Freyssinet, J. M. (2003). "Cellular microparticles: what are they bad or good for?" J Thromb Haemost 1(7): 1655-1662.
Fukuda, K., M. Kojiro, et al. (1994). "Differential regulation of tissue transglutaminase in rat hepatoma cell lines McA-RH7777 and McA-RH8994: relation to growth rate and cell death." J Cell Biochem 54(1): 67-77.
Furie, B. and B. C. Furie (2004). "Role of platelet P-selectin and microparticle PSGL-1 in thrombus formation." Trends Mol Med 10(4): 171-178.
Gaietta, G., T. J. Deerinck, et al. (2002). "Multicolor and electron microscopic imaging of connexin trafficking." Science 296(5567): 503-507.
Garbi, N., P. Tan, et al. (2000). "Impaired immune responses and altered peptide repertoire in tapasin-deficient mice." Nat Immunol 1(3): 234-238.
Garcia, B. A., D. M. Smalley, et al. (2005). "The platelet microparticle proteome." J Proteome Res 4(5): 1516-1521.
Gardner, S. D. (1973). "Prevalence in England of Antibody to Human Polyomavirus (B.K.)." Br Med J 1(5845): 77-78.
Gardner, S. D., A. M. Field, et al. (1971). "New human papovavirus (B.K.) isolated from urine after renal transplantation." Lancet 1(7712): 1253-1257.
Gaudry, C. A., E. Verderio, et al. (1999). "Cell surface localization of tissue transglutaminase is dependent on a fibronectin-binding site in its N-terminal beta-sandwich domain." J Biol Chem 274(43): 30707-30714.
Gaudry, C. A., E. Verderio, et al. (1999). "Tissue transglutaminase is an important player at the surface of human endothelial cells: evidence for its externalization and its colocalization with the beta(1) integrin." Exp Cell Res 252(1): 104-113.
Gentile, V., M. Saydak, et al. (1991). "Isolation and characterization of cDNA clones to

mouse macrophage and human endothelial cell tissue transglutaminases." J Biol Chem 266(1): 478-483.
Gentile, V., V. Thomazy, et al. (1992). "Expression of tissue transglutaminase in Balb-C 3T3 fibroblasts: effects on cellular morphology and adhesion." J Cell Biol 119(2): 463-474.
Glenner, G. G. and C. W. Wong (1984). "Alzheimer's disease: initial report of the purification and characterization of a novel cerebrovascular amyloid protein." Biochem Biophys Res Commun 120(3): 885-890.
Godar, S., V. Horejsi, et al. (1999). "M6P/IGFII-receptor complexes urokinase receptor and plasminogen for activation of transforming growth factor-beta1." Eur J Immunol 29(3): 1004-1013.
Grandea, A. G., 3rd, T. N. Golovina, et al. (2000). "Impaired assembly yet normal trafficking of MHC class I molecules in Tapasin mutant mice." Immunity 13(2): 213-222.
Grandea, A. G., 3rd and L. Van Kaer (2001). "Tapasin: an ER chaperone that controls MHC class I assembly with peptide." Trends Immunol 22(4): 194-199.
Grant, F. J., D. A. Taylor, et al. (1994). "Molecular cloning and characterization of a novel transglutaminase cDNA from a human prostate cDNA library." Biochem Biophys Res Commun 203(2): 1117-1123.
Grenard, P., M. K. Bates, et al. (2001). "Evolution of transglutaminase genes: identification of a transglutaminase gene cluster on human chromosome 15q15. Structure of the gene encoding transglutaminase X and a novel gene family member, transglutaminase Z." J Biol Chem 276(35): 33066-33078.
Grenard, P., S. Bresson-Hadni, et al. (2001). "Transglutaminase-mediated cross-linking is involved in the stabilization of extracellular matrix in human liver fibrosis." J Hepatol 35(3): 367-375.
Gressner, A. M., R. Weiskirchen, et al. (2002). "Roles of TGF-beta in hepatic fibrosis." Front Biosci 7: d793-807.
Gross, S. R., Z. Balklava, et al. (2003). "Importance of tissue transglutaminase in repair of extracellular matrices and cell death of dermal fibroblasts after exposure to a solarium ultraviolet A source." J Invest Dermatol 121(2): 412-423.
Grundmann, U., E. Amann, et al. (1986). "Characterization of cDNA coding for human factor XIIIa." Proc Natl Acad Sci U S A 83(21): 8024-8028.
Gundemir, S. and G. V. Johnson (2009). "Intracellular localization and conformational state of transglutaminase 2: implications for cell death." PLoS One 4(7): e6123.
Hagmann, J., M. M. Burger, et al. (1999). "Regulation of plasma membrane blebbing by the cytoskeleton." J Cell Biochem 73(4): 488-499.
Hall, K. T., L. Boumsell, et al. (1996). "Human CD100, a novel leukocyte semaphorin that promotes B-cell aggregation and differentiation." Proc Natl Acad Sci U S A 93(21): 11780-11785.
Halstensen, T. S., H. Scott, et al. (1993). "Gluten stimulation of coeliac mucosa in vitro induces activation (CD25) of lamina propria CD4+ T cells and macrophages but no crypt-cell hyperplasia." Scand J Immunol 38(6): 581-590.
Hanahan, D. and R. A. Weinberg (2000). "The hallmarks of cancer." Cell 100(1): 57-70.
Hang, J., E. A. Zemskov, et al. (2005). "Identification of a novel recognition sequence for fibronectin within the NH2-terminal beta-sandwich domain of tissue transglutaminase." J Biol Chem 280(25): 23675-23683.
Haroon, Z. A., J. M. Hettasch, et al. (1999). "Tissue transglutaminase is expressed,

active, and directly involved in rat dermal wound healing and angiogenesis." FASEB J 13(13): 1787-1795.
Haroon, Z. A., T. Wannenburg, et al. (2001). "Localization of tissue transglutaminase in human carotid and coronary artery atherosclerosis: implications for plaque stability and progression." Lab Invest 81(1): 83-93.
Harrison, C. A., C. M. Layton, et al. (2007). "Transglutaminase inhibitors induce hyperproliferation and parakeratosis in tissue-engineered skin." Br J Dermatol 156(2): 247-257.
Hartleben, B., M. Godel, et al. (2010). "Autophagy influences glomerular disease susceptibility and maintains podocyte homeostasis in aging mice." J Clin Invest 120(4): 1084-1096.
Herman, J. F., L. S. Mangala, et al. (2006). "Implications of increased tissue transglutaminase (TG2) expression in drug-resistant breast cancer (MCF-7) cells." Oncogene 25(21): 3049-3058.
Herold, C., G. Bismuth, et al. (1995). "Activation signals are delivered through two distinct epitopes of CD100, a unique 150 kDa human lymphocyte surface structure previously defined by BB18 mAb." Int Immunol 7(1): 1-8.
Hill, G. S., D. Heudes, et al. (2003). "Morphometric study of arterioles and glomeruli in the aging kidney suggests focal loss of autoregulation." Kidney Int 63(3): 1027-1036.
Hirschberg, R. (2005). "Wound healing in the kidney: complex interactions in renal interstitial fibrogenesis." J Am Soc Nephrol 16(1): 9-11.
Ho, G. J., E. J. Gregory, et al. (1994). "Cross-linking of beta-amyloid protein precursor catalyzed by tissue transglutaminase." FEBS Lett 349(1): 151-154.
Hoffner, G. and P. Djian (2005). "Transglutaminase and diseases of the central nervous system." Front Biosci 10: 3078-3092.
Hogan, T. F., E. C. Borden, et al. (1980). "Human polyomavirus infections with JC virus and BK virus in renal transplant patients." Ann Intern Med 92(3): 373-378.
Hrachovinova, I., B. Cambien, et al. (2003). "Interaction of P-selectin and PSGL-1 generates microparticles that correct hemostasis in a mouse model of hemophilia A." Nat Med 9(8): 1020-1025.
Huang, L., M. Fisher, et al. (2004). "Tubular epithelial cells exposed to high glucose levels continue to export transgluatminase (Tg) once normal glucose levels are restored." Proceedings of the spring Renal Association meeting, Aberdeen, UK. Published on-line abstracts via www.renal.org Poster 4.
Huang, L., J. L. Haylor, et al. (2009). "Transglutaminase inhibition ameliorates experimental diabetic nephropathy." Kidney Int 76(4): 383-394.
Hughes, R. C. (1999). "Secretion of the galectin family of mammalian carbohydrate-binding proteins." Biochim Biophys Acta 1473(1): 172-185.
Huu, D.-N., E. N. Rosenblum, et al. (1966). "Persistent infection of a rat kidney cell line with Rauscher murine leukemia virus." J Bacteriol 92(4): 1133-1140.
Hwang, K. C., C. D. Gray, et al. (1995). "Interaction site of GTP binding Gh (transglutaminase II) with phospholipase C." J Biol Chem 270(45): 27058-27062.
Ichinose, A., L. E. Hendrickson, et al. (1986). "Amino acid sequence of the a subunit of human factor XIII." Biochemistry 25(22): 6900-6906.
Iismaa, S. E., M. J. Wu, et al. (2000). "GTP binding and signaling by Gh/transglutaminase II involves distinct residues in a unique GTP-binding

pocket." J Biol Chem 275(24): 18259-18265.
Ikura, K., T. Nasu, et al. (1988). "Amino acid sequence of guinea pig liver transglutaminase from its cDNA sequence." Biochemistry 27(8): 2898-2905.
Imperiale, M. J., H. I. Pass, et al. (2001). "Prospects for an SV40 vaccine." Semin Cancer Biol 11(1): 81-85.
Inada, R., M. Matsuki, et al. (2000). "Facilitated wound healing by activation of the Transglutaminase 1 gene." Am J Pathol 157(6): 1875-1882.
Isaka, Y., Y. Fujiwara, et al. (1993). "Glomerulosclerosis induced by in vivo transfection of transforming growth factor-beta or platelet-derived growth factor gene into the rat kidney." J Clin Invest 92(6): 2597-2601.
Ishida, F., K. Okubo, et al. (2010). "Spontaneous regression of the inhibitor against the coagulation factor XIII A subunit in acquired factor XIII deficiency." Thromb Haemost 104(6): 1284-1285.
Issa, R., X. Zhou, et al. (2004). "Spontaneous recovery from micronodular cirrhosis: evidence for incomplete resolution associated with matrix cross-linking." Gastroenterology 126(7): 1795-1808.
James, G. and A. M. Butt (2002). "P2Y and P2X purinoceptor mediated Ca2+ signalling in glial cell pathology in the central nervous system." Eur J Pharmacol 447(2-3): 247-260.
Janiak, A., E. A. Zemskov, et al. (2006). "Cell surface transglutaminase promotes RhoA activation via integrin clustering and suppression of the Src-p190RhoGAP signaling pathway." Mol Biol Cell 17(4): 1606-1619.
Jeong, J. M., S. N. Murthy, et al. (1995). "The fibronectin-binding domain of transglutaminase." J Biol Chem 270(10): 5654-5658.
Jha, K. K., S. Banga, et al. (1998). "SV40-Mediated immortalization." Exp Cell Res 245(1): 1-7.
Johnson, G. V., T. M. Cox, et al. (1997). "Transglutaminase activity is increased in Alzheimer's disease brain." Brain Res 751(2): 323-329.
Johnson, T. S., A. F. El-Koraie, et al. (2003). "Tissue transglutaminase and the progression of human renal scarring." J Am Soc Nephrol 14(8): 2052-2062.
Johnson, T. S., M. Fisher, et al. (2007). "Transglutaminase inhibition reduces fibrosis and preserves function in experimental chronic kidney disease." J Am Soc Nephrol 18(12): 3078-3088.
Johnson, T. S., M. Griffin, et al. (1997). "The role of transglutaminase in the rat subtotal nephrectomy model of renal fibrosis." J Clin Invest 99(12): 2950-2960.
Johnson, T. S., C. R. Knight, et al. (1994). "Transfection of tissue transglutaminase into a highly malignant hamster fibrosarcoma leads to a reduced incidence of primary tumour growth." Oncogene 9(10): 2935-2942.
Johnson, T. S., C. I. Scholfield, et al. (1998). "Induction of tissue transglutaminase by dexamethasone: its correlation to receptor number and transglutaminase-mediated cell death in a series of malignant hamster fibrosarcomas." Biochem J 331 (Pt 1): 105-112.
Johnson, T. S., N. J. Skill, et al. (1999). "Transglutaminase transcription and antigen translocation in experimental renal scarring." J Am Soc Nephrol 10(10): 2146-2157.
Jones RA, F. M., Griffin M, and Johnson TS (2005). "Tissue Transglutaminase knockout mesangial cells show alterations in extracellular matrix deposition." Renal Association meeting 2005.
Jones, R. A., P. Kotsakis, et al. (2006). "Matrix changes induced by transglutaminase 2

lead to inhibition of angiogenesis and tumor growth." Cell Death Differ 13(9): 1442-1453.
Jones, R. A., B. Nicholas, et al. (1997). "Reduced expression of tissue transglutaminase in a human endothelial cell line leads to changes in cell spreading, cell adhesion and reduced polymerisation of fibronectin." J Cell Sci 110 (Pt 19): 2461-2472.
Jung, S. A., H. K. Lee, et al. (2007). "Upregulation of TGF-beta-induced tissue transglutaminase expression by PI3K-Akt pathway activation in human subconjunctival fibroblasts." Invest Ophthalmol Vis Sci 48(5): 1952-1958.
Kabeya, Y., N. Mizushima, et al. (2000). "LC3, a mammalian homologue of yeast Apg8p, is localized in autophagosome membranes after processing." EMBO J 19(21): 5720-5728.
Keller, H. and P. Eggli (1998). "Protrusive activity, cytoplasmic compartmentalization, and restriction rings in locomoting blebbing Walker carcinosarcoma cells are related to detachment of cortical actin from the plasma membrane." Cell Motil Cytoskeleton 41(2): 181-193.
Kim, C. W., H. M. Lee, et al. (2002). "Extracellular membrane vesicles from tumor cells promote angiogenesis via sphingomyelin." Cancer Res 62(21): 6312-6317.
Kim, D. S., S. S. Park, et al. (2006). "Reversal of drug resistance in breast cancer cells by transglutaminase 2 inhibition and nuclear factor-kappaB inactivation." Cancer Res 66(22): 10936-10943.
Kim, H. Y., B. Y. Ahn, et al. (2001). "Structural basis for the inactivation of retinoblastoma tumor suppressor by SV40 large T antigen." EMBO J 20(1-2): 295-304.
Klahr, S., G. Schreiner, et al. (1988). "The progression of renal disease." N Engl J Med 318(25): 1657-1666.
Kleeff, J., T. Ishiwata, et al. (1998). "The cell-surface heparan sulfate proteoglycan glypican-1 regulates growth factor action in pancreatic carcinoma cells and is overexpressed in human pancreatic cancer." J Clin Invest 102(9): 1662-1673.
Klockmann, U., M. Staufenbiel, et al. (1984). "Membrane interactions of simian virus 40 large T-antigen: influence of protein sequences and fatty acid acylation." Mol Cell Biol 4(8): 1542-1550.
Ko, M. K. and E. P. Kay (2005). "Regulatory role of FGF-2 on type I collagen expression during endothelial mesenchymal transformation." Invest Ophthalmol Vis Sci 46(12): 4495-4503.
Koli, K., J. Saharinen, et al. (2001). "Latency, activation, and binding proteins of TGF-beta." Microsc Res Tech 52(4): 354-362.
Kopp, J. B., V. M. Factor, et al. (1996). "Transgenic mice with increased plasma levels of TGF-beta 1 develop progressive renal disease." Lab Invest 74(6): 991-1003.
Kotsakis, P. and M. Griffin (2007). "Tissue transglutaminase in tumour progression: friend or foe?" Amino Acids 33(2): 373-384.
Koyama, H., C. Goodpasture, et al. (1978). "Establishment and characterization of a cell line from the American opossum (Didelphys virginiana)." In Vitro 14(3): 239-246.
Laiho, E., J. Ignatius, et al. (1997). "Transglutaminase 1 mutations in autosomal recessive congenital ichthyosis: private and recurrent mutations in an isolated population." Am J Hum Genet 61(3): 529-538.
Lan, H. Y. (2003). "Tubular epithelial-myofibroblast transdifferentiation mechanisms in proximal tubule cells." Curr Opin Nephrol Hypertens 12(1): 25-29.

Lange-Mutschler, J. and R. Henning (1983). "A subclass of simian virus 40 T antigen with a high cell surface binding affinity." Virology 127(2): 333-344.
Lange-Mutschler, J. and R. Henning (1984). "Cell surface binding simian virus 40 large T antigen becomes anchored and stably linked to lipid of the target cells." Virology 136(2): 404-413.
Leavitt, B. R., J. A. Guttman, et al. (2001). "Wild-type huntingtin reduces the cellular toxicity of mutant huntingtin in vivo." Am J Hum Genet 68(2): 313-324.
Li, S., H. O. Sjogren, et al. (1997). "Cloning and functional characterization of a subunit of the transporter associated with antigen processing." Proc Natl Acad Sci U S A 94(16): 8708-8713.
Liu, Y. (2004). "Epithelial to mesenchymal transition in renal fibrogenesis: pathologic significance, molecular mechanism, and therapeutic intervention." J Am Soc Nephrol 15(1): 1-12.
Liu, Y. (2006). "Renal fibrosis: new insights into the pathogenesis and therapeutics." Kidney Int 69(2): 213-217.
Lodish, H. F. (2007). Molecular cell biology. New York, W.H. Freeman.
Lorand, L. and R. M. Graham (2003). "Transglutaminases: crosslinking enzymes with pleiotropic functions." Nat Rev Mol Cell Biol 4(2): 140-156.
Lozito, T. P. and R. S. Tuan (2011). "Endothelial cell microparticles act as centers of Matrix Metalloproteinsase-2 (MMP-2) activation and vascular matrix remodeling." J Cell Physiol.
Ludlow, J. W., J. A. DeCaprio, et al. (1989). "SV40 large T antigen binds preferentially to an underphosphorylated member of the retinoblastoma susceptibility gene product family." Cell 56(1): 57-65.
MacKenzie, A., H. L. Wilson, et al. (2001). "Rapid secretion of interleukin-1beta by microvesicle shedding." Immunity 15(5): 825-835.
Maiuri, L., C. Ciacci, et al. (2005). "Unexpected role of surface transglutaminase type II in celiac disease." Gastroenterology 129(5): 1400-1413.
Mallat, Z., H. Benamer, et al. (2000). "Elevated levels of shed membrane microparticles with procoagulant potential in the peripheral circulating blood of patients with acute coronary syndromes." Circulation 101(8): 841-843.
Malstrom, K., G. Stange, et al. (1987). "Identification of proximal tubular transport functions in the established kidney cell line, OK." Biochim Biophys Acta 902(2): 269-277.
Mangasser-Stephan, K. and A. M. Gressner (1999). "Molecular and functional aspects of latent transforming growth factor-beta binding protein: just a masking protein?" Cell Tissue Res 297(3): 363-370.
Manjithaya, R. and S. Subramani (2010). "Autophagy: a broad role in unconventional protein secretion?" Trends Cell Biol.
Mann, A. P., A. Verma, et al. (2006). "Overexpression of tissue transglutaminase leads to constitutive activation of nuclear factor-kappaB in cancer cells: delineation of a novel pathway." Cancer Res 66(17): 8788-8795.
Mantyjarvi, R. A., O. H. Meurman, et al. (1973). "A human papovavirus (B.K.), biological properties and seroepidemiology." Ann Clin Res 5(5): 283-287.
Martinez-Salgado, C., A. B. Rodriguez-Pena, et al. (2008). "Involvement of small Ras GTPases and their effectors in chronic renal disease." Cell Mol Life Sci 65(3): 477-492.
Martinez, J., D. G. Chalupowicz, et al. (1994). "Transglutaminase-mediated processing of fibronectin by endothelial cell monolayers." Biochemistry 33(9): 2538-2545.

Martinez, M. C., A. Tesse, et al. (2005). "Shed membrane microparticles from circulating and vascular cells in regulating vascular function." Am J Physiol Heart Circ Physiol 288(3): H1004-1009.
Matlung, H. L., H. C. Groen, et al. (2009). "Calcification locates to transglutaminases in advanced human atherosclerotic lesions." Am J Pathol 175(4): 1374-1379.
McNeil, P. L., L. Muthukrishnan, et al. (1989). "Growth factors are released by mechanically wounded endothelial cells." J Cell Biol 109(2): 811-822.
McNew, J. A., F. Parlati, et al. (2000). "Compartmental specificity of cellular membrane fusion encoded in SNARE proteins." Nature 407(6801): 153-159.
Meguid El Nahas, A. and A. K. Bello (2005). "Chronic kidney disease: the global challenge." Lancet 365(9456): 331-340.
Mehta, K. (1994). "High levels of transglutaminase expression in doxorubicin-resistant human breast carcinoma cells." Int J Cancer 58(3): 400-406.
Mehta, K., J. Y. Fok, et al. (2006). "Tissue transglutaminase: from biological glue to cell survival cues." Front Biosci 11: 173-185.
Mehul, B. and R. C. Hughes (1997). "Plasma membrane targetting, vesicular budding and release of galectin 3 from the cytoplasm of mammalian cells during secretion." J Cell Sci 110 (Pt 10): 1169-1178.
Melino, G., M. Annicchiarico-Petruzzelli, et al. (1994). "Tissue transglutaminase and apoptosis: sense and antisense transfection studies with human neuroblastoma cells." Mol Cell Biol 14(10): 6584-6596.
Melk, A. and P. F. Halloran (2001). "Cell senescence and its implications for nephrology." J Am Soc Nephrol 12(2): 385-393.
Milakovic, T., J. Tucholski, et al. (2004). "Intracellular localization and activity state of tissue transglutaminase differentially impacts cell death." J Biol Chem 279(10): 8715-8722.
Milburn, C. C., M. Deak, et al. (2003). "Binding of phosphatidylinositol 3,4,5-trisphosphate to the pleckstrin homology domain of protein kinase B induces a conformational change." Biochem J 375(Pt 3): 531-538.
Miyazaki, T., M. Ise, et al. (1997). "Indoxyl sulfate stimulates renal synthesis of transforming growth factor-beta 1 and progression of renal failure." Kidney Int Suppl 63: S211-214.
Mohan, P. S. and R. G. Spiro (1991). "Characterization of heparan sulfate proteoglycan from calf lens capsule and proteoglycans synthesized by cultured lens epithelial cells. Comparison with other basement membrane proteoglycans." J Biol Chem 266(13): 8567-8575.
Molberg, O., S. McAdam, et al. (2001). "T cells from celiac disease lesions recognize gliadin epitopes deamidated in situ by endogenous tissue transglutaminase." Eur J Immunol 31(5): 1317-1323.
Molberg, O., S. N. McAdam, et al. (1998). "Tissue transglutaminase selectively modifies gliadin peptides that are recognized by gut-derived T cells in celiac disease." Nat Med 4(6): 713-717.
Morgan, M. R., M. J. Humphries, et al. (2007). "Synergistic control of cell adhesion by integrins and syndecans." Nat Rev Mol Cell Biol 8(12): 957-969.
Murthy, S. N., S. Iismaa, et al. (2002). "Conserved tryptophan in the core domain of transglutaminase is essential for catalytic activity." Proc Natl Acad Sci U S A 99(5): 2738-2742.
Mylonakis, E., N. Goes, et al. (2001). "BK virus in solid organ transplant recipients: an emerging syndrome." Transplantation 72(10): 1587-1592.

Nickel, W. (2003). "The mystery of nonclassical protein secretion. A current view on cargo proteins and potential export routes." Eur J Biochem 270(10): 2109-2119.
Nickel, W. (2005). "Unconventional secretory routes: direct protein export across the plasma membrane of mammalian cells." Traffic 6(8): 607-614.
Nickel, W. and M. Seedorf (2008). "Unconventional mechanisms of protein transport to the cell surface of eukaryotic cells." Annu Rev Cell Dev Biol 24: 287-308.
Nijenhuis, A. V., L. van Bergeijk, et al. (2004). "Acquired factor XIII deficiency due to an inhibitor: a case report and review of the literature." Haematologica 89(5): ECR14.
Nomura, S., N. N. Tandon, et al. (2001). "High-shear-stress-induced activation of platelets and microparticles enhances expression of cell adhesion molecules in THP-1 and endothelial cells." Atherosclerosis 158(2): 277-287.
Nunes, I., P. E. Gleizes, et al. (1997). "Latent transforming growth factor-beta binding protein domains involved in activation and transglutaminase-dependent cross-linking of latent transforming growth factor-beta." J Cell Biol 136(5): 1151-1163.
Ohura, N., K. Yamamoto, et al. (2003). "Global analysis of shear stress-responsive genes in vascular endothelial cells." J Atheroscler Thromb 10(5): 304-313.
Oliverio, S., A. Amendola, et al. (1999). "Inhibition of "tissue" transglutaminase increases cell survival by preventing apoptosis." J Biol Chem 274(48): 34123-34128.
Ortmann, B., J. Copeman, et al. (1997). "A critical role for tapasin in the assembly and function of multimeric MHC class I-TAP complexes." Science 277(5330): 1306-1309.
Paucha, E., D. Kalderon, et al. (1986). "Simian virus 40 origin DNA-binding domain on large T antigen." J Virol 57(1): 50-64.
Peng, X., Y. Zhang, et al. (1999). "Interaction of tissue transglutaminase with nuclear transport protein importin-alpha3." FEBS Lett 446(1): 35-39.
Petersen, M., M. Thorikay, et al. (2008). "Oral administration of GW788388, an inhibitor of TGF-beta type I and II receptor kinases, decreases renal fibrosis." Kidney Int 73(6): 705-715.
Pfeffer, S. R. and J. E. Rothman (1987). "Biosynthetic protein transport and sorting by the endoplasmic reticulum and Golgi." Annu Rev Biochem 56: 829-852.
Piacentini, M., M. D'Eletto, et al. (2011). "Transglutaminase 2 at the crossroads between cell death and survival." Adv Enzymol Relat Areas Mol Biol 78: 197-246.
Piacentini, M., M. G. Farrace, et al. (1999). "'Tissue' transglutaminase release from apoptotic cells into extracellular matrix during human liver fibrogenesis." J Pathol 189(1): 92-98.
Piacentini, M., M. G. Farrace, et al. (2002). "Transglutaminase overexpression sensitizes neuronal cell lines to apoptosis by increasing mitochondrial membrane potential and cellular oxidative stress." J Neurochem 81(5): 1061-1072.
Piacentini, M., L. Fesus, et al. (1991). "The expression of "tissue" transglutaminase in two human cancer cell lines is related with the programmed cell death (apoptosis)." Eur J Cell Biol 54(2): 246-254.
Pinkas, D. M., P. Strop, et al. (2007). "Transglutaminase 2 undergoes a large conformational change upon activation." PLoS Biol 5(12): e327.
Pipas, J. M. and A. J. Levine (2001). "Role of T antigen interactions with p53 in

tumorigenesis." Semin Cancer Biol 11(1): 23-30.
Piper, R. C. and D. J. Katzmann (2007). "Biogenesis and function of multivesicular bodies." Annu Rev Cell Dev Biol 23: 519-547.
Pisano, J. J., J. S. Finlayson, et al. (1968). "[Cross-link in fibrin polymerized by factor 13: epsilon-(gamma-glutamyl)lysine.]." Science 160(830): 892-893.
Polymeropoulos, M. H., C. Lavedan, et al. (1997). "Mutation in the alpha-synuclein gene identified in families with Parkinson's disease." Science 276(5321): 2045-2047.
Portolani, M., A. Marzocchi, et al. (1974). "Prevalence in Italy of antibodies to a new human papovavirus (BK virus)." J Med Microbiol 7(4): 543-546.
Qi, W., X. Chen, et al. (2006). "The renal cortical fibroblast in renal tubulointerstitial fibrosis." Int J Biochem Cell Biol 38(1): 1-5.
Remuzzi, G. and T. Bertani (1998). "Pathophysiology of progressive nephropathies." N Engl J Med 339(20): 1448-1456.
Richardson, J. C., V. Scalera, et al. (1981). "Identification of two strains of MDCK cells which resemble separate nephron tubule segments." Biochim Biophys Acta 673(1): 26-36.
Rothman, J. E. (1994). "Mechanisms of intracellular protein transport." Nature 372(6501): 55-63.
Rubartelli, A., F. Cozzolino, et al. (1990). "A novel secretory pathway for interleukin-1 beta, a protein lacking a signal sequence." EMBO J 9(5): 1503-1510.
Russell, D. H. and J. R. Womble (1982). "Transglutaminase may mediate certain physiological effects of endogenous amines and of amine-containing therapeutical agents." Life Sci 30(18): 1499-1508.
Russell, M. R., D. P. Nickerson, et al. (2006). "Molecular mechanisms of late endosome morphology, identity and sorting." Curr Opin Cell Biol 18(4): 422-428.
Sadasivan, B., P. J. Lehner, et al. (1996). "Roles for calreticulin and a novel glycoprotein, tapasin, in the interaction of MHC class I molecules with TAP." Immunity 5(2): 103-114.
Santos, M. and J. S. Butel (1984). "Antigenic structure of simian virus 40 large tumor antigen and association with cellular protein p53 on the surfaces of simian virus 40-infected and -transformed cells." J Virol 51(2): 376-383.
Santos, M. and J. S. Butel (1984). "Dynamic nature of the association of large tumor antigen and p53 cellular protein with the surfaces of simian virus 40-transformed cells." J Virol 49(1): 50-56.
Santos, M. and J. S. Butel (1985). "Surface T-antigen expression in simian virus 40-transformed mouse cells: correlation with cell growth rate." Mol Cell Biol 5(5): 1051-1057.
Sarkar, N. K., D. D. Clarke, et al. (1957). "An enzymically catalyzed incorporation of amines into proteins." Biochimica et biophysica acta 25(2): 451-452.
Scarpellini, A., R. Germack, et al. (2009). "Heparan sulphate proteoglycans are receptors for the cell-surface trafficking and biological activity of transglutaminase-2." J Biol Chem.
Sechler, J. L. and J. E. Schwarzbauer (1998). "Control of cell cycle progression by fibronectin matrix architecture." J Biol Chem 273(40): 25533-25536.
Seelenmeyer, C., C. Stegmayer, et al. (2008). "Unconventional secretion of fibroblast growth factor 2 and galectin-1 does not require shedding of plasma membrane-derived vesicles." FEBS Lett 582(9): 1362-1368.
Seitz, J., C. Keppler, et al. (1990). "Immunohistochemistry of secretory

transglutaminase from rodent prostate." Histochemistry 93(5): 525-530.
Selkoe, D. J. (1991). "The molecular pathology of Alzheimer's disease." Neuron 6(4): 487-498.
Selkoe, D. J. (2000). "The origins of Alzheimer disease: a is for amyloid." JAMA 283(12): 1615-1617.
Shah, K. and N. Nathanson (1976). "Human exposure to SV40: review and comment." Am J Epidemiol 103(1): 1-12.
Shin, D. M., J. H. Jeon, et al. (2004). "Cell type-specific activation of intracellular transglutaminase 2 by oxidative stress or ultraviolet irradiation: implications of transglutaminase 2 in age-related cataractogenesis." J Biol Chem 279(15): 15032-15039.
Siegel, M. and C. Khosla (2007). "Transglutaminase 2 inhibitors and their therapeutic role in disease states." Pharmacol Ther 115(2): 232-245.
Sims, P. J. and T. Wiedmer (2001). "Unraveling the mysteries of phospholipid scrambling." Thromb Haemost 86(1): 266-275.
Skill, N. J., M. Griffin, et al. (2001). "Increases in renal epsilon-(gamma-glutamyl)-lysine crosslinks result from compartment-specific changes in tissue transglutaminase in early experimental diabetic nephropathy: pathologic implications." Lab Invest 81(5): 705-716.
Skill, N. J., T. S. Johnson, et al. (2004). "Inhibition of transglutaminase activity reduces extracellular matrix accumulation induced by high glucose levels in proximal tubular epithelial cells." J Biol Chem 279(46): 47754-47762.
Sollid, L. M. (2002). "Coeliac disease: dissecting a complex inflammatory disorder." Nat Rev Immunol 2(9): 647-655.
Song, H., W. Chang, et al. (2007). "Tissue transglutaminase is essential for integrin-mediated survival of bone marrow-derived mesenchymal stem cells." Stem Cells 25(6): 1431-1438.
Soule, H. R. and J. S. Butel (1979). "Subcellular Localization of simian virus 40 large tumor antigen." J Virol 30(2): 523-532.
Spurgeon, K. R., D. L. Donohoe, et al. (2005). "Transforming growth factor-beta in acute renal failure: receptor expression, effects on proliferation, cellularity, and vascularization after recovery from injury." Am J Physiol Renal Physiol 288(3): F568-577.
Stetler-Stevenson, W. G. (1999). "Matrix metalloproteinases in angiogenesis: a moving target for therapeutic intervention." J Clin Invest 103(9): 1237-1241.
Stiegler, P., M. Kasten, et al. (1998). "The RB family of cell cycle regulatory factors." J Cell Biochem Suppl 30-31: 30-36.
Stinchcombe, J., G. Bossi, et al. (2004). "Linking albinism and immunity: the secrets of secretory lysosomes." Science 305(5680): 55-59.
Stow, J. L., C. J. Soroka, et al. (1989). "Basement membrane heparan sulfate proteoglycan is the main proteoglycan synthesized by glomerular epithelial cells in culture." Am J Pathol 135(4): 637-646.
Strickler, H. D., J. J. Goedert, et al. (2003). "Trends in U.S. pleural mesothelioma incidence rates following simian virus 40 contamination of early poliovirus vaccines." J Natl Cancer Inst 95(1): 38-45.
Strickler, H. D., P. S. Rosenberg, et al. (1998). "Contamination of poliovirus vaccines with simian virus 40 (1955-1963) and subsequent cancer rates." JAMA 279(4): 292-295.
Strutz, F. and G. A. Muller (1995). "On the progression of chronic renal disease."

Nephron 69(4): 371-379.
Tartakoff, A. M. (1983). "Perturbation of vesicular traffic with the carboxylic ionophore monensin." Cell 32(4): 1026-1028.
Taverna, S., G. Ghersi, et al. (2003). "Shedding of membrane vesicles mediates fibroblast growth factor-2 release from cells." J Biol Chem 278(51): 51911-51919.
Telci, D., Z. Wang, et al. (2008). "Fibronectin-tissue transglutaminase matrix rescues RGD-impaired cell adhesion through syndecan-4 and beta1 integrin co-signaling." J Biol Chem 283(30): 20937-20947.
Temmerman, K., A. D. Ebert, et al. (2008). "A direct role for phosphatidylinositol-4,5-bisphosphate in unconventional secretion of fibroblast growth factor 2." Traffic 9(7): 1204-1217.
Teng, M. S., R. Stephens, et al. (2002). "A human TAPBP (TAPASIN)-related gene, TAPBP-R." Eur J Immunol 32(4): 1059-1068.
Thomas-Ecker, S., A. Lindecke, et al. (2007). "Alteration in the gene expression pattern of primary monocytes after adhesion to endothelial cells." Proc Natl Acad Sci U S A 104(13): 5539-5544.
Thomazy, V. and L. Fesus (1989). "Differential expression of tissue transglutaminase in human cells. An immunohistochemical study." Cell Tissue Res 255(1): 215-224.
Titolo, S., E. Welchner, et al. (2003). "Characterization of the DNA-binding properties of the origin-binding domain of simian virus 40 large T antigen by fluorescence anisotropy." J Virol 77(9): 5512-5518.
Todde, V., M. Veenhuis, et al. (2009). "Autophagy: principles and significance in health and disease." Biochim Biophys Acta 1792(1): 3-13.
Tomasek, J. J., G. Gabbiani, et al. (2002). "Myofibroblasts and mechano-regulation of connective tissue remodelling." Nat Rev Mol Cell Biol 3(5): 349-363.
Touraine, J. L. (1981). "The bare-lymphocyte syndrome: report on the registry." Lancet 1(8215): 319-321.
Trigwell, S. M., P. T. Lynch, et al. (2004). "An improved colorimetric assay for the measurement of transglutaminase (type II) -(gamma-glutamyl) lysine cross-linking activity." Anal Biochem 330(1): 164-166.
Turner, P. M. and L. Lorand (1989). "Complexation of fibronectin with tissue transglutaminase." Biochemistry 28(2): 628-635.
USRDS (2009). U.S. Renal Data System, USRDS 2009 Annual Data Report: Atlas of Chronic Kidney Disease and End-Stage Renal Disease in the United States.
van de Wetering, J., C. H. Weimar, et al. (2006). "The impact of transforming growth factor-beta1 gene polymorphism on end-stage renal failure after heart transplantation." Transplantation 82(12): 1744-1748.
van den Akker, J., A. van Weert, et al. (2011). "Transglutaminase 2 is secreted from smooth muscle cells by transamidation-dependent microparticle formation." Amino Acids.
van der Zee, P. M., E. Biro, et al. (2006). "P-selectin- and CD63-exposing platelet microparticles reflect platelet activation in peripheral arterial disease and myocardial infarction." Clin Chem 52(4): 657-664.
Verderio, E., B. Nicholas, et al. (1998). "Regulated expression of tissue transglutaminase in Swiss 3T3 fibroblasts: effects on the processing of fibronectin, cell attachment, and cell death." Exp Cell Res 239(1): 119-138.
Verderio, E. A., T. Johnson, et al. (2004). "Tissue transglutaminase in normal and

abnormal wound healing: review article." Amino Acids 26(4): 387-404.
Verderio, E. A., A. Scarpellini, et al. (2008). "Novel interactions of TG2 with heparan sulfate proteoglycans: reflection on physiological implications." Amino Acids.
Verderio, E. A., D. Telci, et al. (2003). "A novel RGD-independent cell adhesion pathway mediated by fibronectin-bound tissue transglutaminase rescues cells from anoikis." J Biol Chem 278(43): 42604-42614.
Verma, A., H. Wang, et al. (2006). "Increased expression of tissue transglutaminase in pancreatic ductal adenocarcinoma and its implications in drug resistance and metastasis." Cancer Res 66(21): 10525-10533.
Wakshlag, J. J., M. A. Antonyak, et al. (2006). "Effects of tissue transglutaminase on beta -amyloid1-42-induced apoptosis." Protein J 25(1): 83-94.
Wang, L. and B. Dobberstein (1999). "Oligomeric complexes involved in translocation of proteins across the membrane of the endoplasmic reticulum." FEBS Lett 457(3): 316-322.
Wen, C. P., T. Y. Cheng, et al. (2008). "All-cause mortality attributable to chronic kidney disease: a prospective cohort study based on 462 293 adults in Taiwan." Lancet 371(9631): 2173-2182.
Wilhelmus, M. M., S. C. Grunberg, et al. (2009). "Transglutaminases and transglutaminase-catalyzed cross-links colocalize with the pathological lesions in Alzheimer's disease brain." Brain Pathol 19(4): 612-622.
Yang, J., X. Zhang, et al. (2003). "Downregulation of Smad transcriptional corepressors SnoN and Ski in the fibrotic kidney: an amplification mechanism for TGF-beta1 signaling." J Am Soc Nephrol 14(12): 3167-3177.
Yin, G. and J. R. Swartz (2004). "Enhancing multiple disulfide bonded protein folding in a cell-free system." Biotechnol Bioeng 86(2): 188-195.
Yoo, J. O., Y. C. Lim, et al. (2012). "Transglutaminase 2 promotes both caspase-dependent and caspase-independent apoptotic cell death via the calpain/Bax protein signaling pathway." J Biol Chem 287(18): 14377-14388.
Yuan, L., K. Choi, et al. (2005). "Tissue transglutaminase 2 inhibition promotes cell death and chemosensitivity in glioblastomas." Mol Cancer Ther 4(9): 1293-1302.
Zehe, C., A. Engling, et al. (2006). "Cell-surface heparan sulfate proteoglycans are essential components of the unconventional export machinery of FGF-2." Proc Natl Acad Sci U S A 103(42): 15479-15484.
Zemskov, E. A., I. Mikhailenko, et al. (2011). "Unconventional secretion of tissue transglutaminase involves phospholipid-dependent delivery into recycling endosomes." PLoS One 6(4): e19414.
Zemskov, E. A., I. Mikhailenko, et al. (2007). "Cell-surface transglutaminase undergoes internalization and lysosomal degradation: an essential role for LRP1." J Cell Sci 120(Pt 18): 3188-3199.
Zhang, W., B. R. Johnson, et al. (1998). "Immunohistochemical demonstration of tissue transglutaminase in amyloid plaques." Acta Neuropathol 96(4): 395-400.